Evaluation of Remote Sensing for the Detection of Landfill Gas and Leachate in an Urban Environment

Robert John Ellis

Doctor of Philosophy

THE UNIVERSITY OF ASTON IN BIRMINGHAM

January 1997

THE UNIVERSITY OF ASTON IN BIRMINGHAM

Evaluation of Remote Sensing for the Detection of Landfill Gas and Leachate in an Urban Environment

Robert John Ellis

Doctor of Philosophy 1996

Summary

The technique of remote sensing provides a unique view of the earth's surface and considerable areas can be surveyed in a short amount of time. The aim of this project was to evaluate whether remote sensing, particularly using the Airborne Thematic Mapper (ATM) with its wide spectral range, was capable of monitoring landfill sites within an urban environment with the aid of image processing and Geographical Information Systems (GIS) methods.

The regions under study were in the West Midlands conurbation and consisted of a large area in what is locally known as the Black Country containing heavy industry intermingled with residential areas, and a large single active landfill in north Birmingham.

When waste is collected in large volumes it decays and gives off pollutants. These pollutants, landfill gas and leachate (a liquid effluent), are known to be injurious to vegetation and can cause stress and death. Vegetation under stress can exhibit a physiological change, detectable by the remote sensing systems used. The chemical and biological reactions that create the pollutants are exothermic and the gas and leachate, if they leave the waste, can be warmer than their surroundings. Thermal imagery from the ATM (daylight and dawn) and thermal video was obtained and used to find thermal anomalies on the area under study.

The results showed that vegetation stress is not a reliable indicator of landfill gas migration as sites within an urban environment have a cover too complex for the effects to be identified. Gas emissions from two sites were successfully detected by all the thermal imagery with the thermal ATM being the best.

Although the results were somewhat disappointing, recent technical advancements in the remote sensing systems used in this project would allow geo-registration of ATM imagery taken on different occasions and the elimination of the effects of solar insolation.

KEYWORDS: Image Classification, ATM, Thermography, Image Processing, GIS.

for Jane

Acknowledgements

List of Contents

6

List of Figures

List of Tables

1. Introduction

The West Midlands has a considerable industrial past dating back to the first stirrings of the industrial revolution. The region to the west of Birmingham, known locally as the Black Country, was a focus of considerable activity due to the local presence of mineral resources. Such activities create waste and in the region old quarries were used for the disposal of industrial as well as domestic refuse. Historical records are poor and even where tip sites are known, often little or no information is available on the contents.

In the current climate, where the general public has a high level of awareness concerning environmental matters, landfill site operators are often reluctant to allow access for monitoring purposes. Remote sensing techniques provide a unique perspective of the earth's surface and large areas can be surveyed in a fraction of the time than that required for ground based studies, and can view inaccessible areas.

This project was established to evaluate whether remote sensing techniques are a viable alternative to extensive, and consequently expensive, ground based monitoring regimes. It was jointly funded by the West Midlands Hazardous Waste Unit (responsible for overseeing and policing waste disposal in the region), the Black Country Development Corporation (set up in 1985 to rejuvenate the derelict and contaminated areas of the Black Country) and Aspinwall and Company (one of the UK's foremost environmental consultancies).

1.1. Project Objective

The objective of this project was to evaluate the use of remote sensing for monitoring pollution, namely landfill gas and leachate, produced by landfill sites in an urban environment. The evaluation includes a costing of the acquisition of the different types of imagery, the ease of use, an assessment of the image quality and the times taken to complete the various processes involved.

The remote sensing imagery used in this project consisted of:

- vertical aerial photography,
- digital imagery produced by the Daedalus AADS 1268 Airborne Thematic Mapper (ATM); one flight during the day and another at dawn, the latter utilising the thermal band only, and
- airborne thermal video camera imagery produced by the Thermovision 450 thermal infra-red imager.

The principal device used in this project was the ATM. It is a digital line-scanner, capable of sensing multi-spectral radiation far into the infra-red region of the electro-magnetic spectrum. The particular device used is owned and flown by the Natural Environment Research Council (NERC) who also provide an aerial photography service. This study utilised both the ATM and aerial photographs, and, using the NERC facilities, data of both forms was obtained simultaneously for the daylight flight. Only the ATM could be used for the dawn flight as not enough light is available for photography. More details about the ATM can be found in Appendix A.

Airborne video cameras have the capability of giving a real-time view through a visual display monitor and can record the scenes on to video tape, playable immediately following landing. The video camera used for this project was owned by TBV Stangers Ltd. and mounted in a helicopter. This platform has the advantage of allowing the imagery to be gathered from a variety of angles (the sites can be circled) and at a lower altitude (helicopters are allowed to fly at lower altitudes than fixed wing aircraft, particularly in urban areas). On the other hand, less area can be covered in the same time as the ATM and the imagery is difficult to use quantifiably. The camera used and the method of application is described in detail in Appendix B.

Landfilled carbonaceous waste will eventually degrade and give off pollutants, mainly landfill gas and leachate. The two main constituents of landfill gas, methane and carbon dioxide, are known to be injurious to vegetation and when plants are put under stress their leaves often exhibit a change in colour in the visible and infra-red parts of the spectrum. Whilst refuse decays underground a considerable amount of heat is produced and the temperature can reach 55°C underground. If, therefore, leachate or gas escapes to the surface two things may occur: a colour change in the vegetation may be in evidence and/or a heat signature may occur; both of these effects would be detectable by the remote sensors and enhanceable by computerised techniques.

In addition, to supplement the aerial imagery, the following ground surveys were carried out:

- 30cm spike tests for methane, carbon dioxide and oxygen and
- vegetation cover surveys.

These surveys made it possible to verify, on the ground, what the ATM was detecting from the air.

1.2. Landfill Sites and Associated Problems

Landfilling is a method where the large volumes of waste are placed in a depression. Also known as waste disposal sites or sanitary landfills, landfill sites are the major method of disposal for solid waste in the UK, and approximately 90% of the UK's solid waste is disposed of in this manner (DoE, 1992c).

Any waste that has organic components and is deposited in large quantities will eventually decay and give off methane and carbon dioxide (by products of microbial consumption) if the conditions are right. The gases produced will escape from the site in a number of different ways and in some cases will create hazards. Certain instances have been shown that landfill gas can have injurious effects on some plants if present in the root zone. If methane collects in a confined space, such as buildings or culverts it may create an explosion hazard. Landfill sites situated within an urban area pose an increased problem due to the close proximity of residential areas. Buildings provide a multitude of confined spaces and such a hazard was brought poignantly to light in Loscoe, Derbyshire where an entire house was destroyed by migrating methane (Tankard, 1987).

Of the types of waste produced domestic refuse has been identified as being by far the most susceptible to attack by micro-organisms due to the large proportion of organic material (vegetable and food waste). Table 1.1 gives an indication of the scale of the situation showing that almost half of the UK's waste is domestic.

Type of waste	percentage by weight
Domestic	45.90
Inert	26.55
Commercial/Industrial	25.15
Hazardous solids	2.40
Total	100

Table 1.1. Types and respective quantities of waste deposited in 87 UK landfill sites (Croft & Campbell, 1992).

1.3. Choice of Area

The area chosen for this project comprises much of what is known locally as the Black Country. This area has a legacy of intense industrial activity dating back to the 17th century because the raw materials for to iron and steel production - coal, ironstone and limestone - were in close proximity to each other. Due to this industrial past and the associated mining and quarrying, the area is peppered with filled holes and made ground whose locations and contents are often unknown.

There are two separate areas under study. The first is a single active landfill site just on the Birmingham side of its boundary with Walsall and is the discrete area to the east on the lower frame of figure 1.1. The second, and considerably larger, area is within the region known locally as the Black Country. It covers approximately 50km^2 of the Black Country, mainly in the Sandwell region of the West Midlands but also taking in a small portion of Dudley and Wolverhampton. This region is made up of a mix of industrial estates intermingled with residential areas, and is criss-crossed by canals and railways, a large number of which have been since filled in or pulled up. In addition, there are many known areas of 'made ground' (landfills, tips and spoil heaps - landfill operators will emphasise that a landfill is managed in a sanitary manner whilst a tip in merely rubbish thrown into a pile) and possibly many more unknown.

The Black Country region was chosen as a study area because it provided a large area with a historical fill problem. An area of this size, especially in an urban environment, creates a strategic difficulty when monitoring by conventional ground-based methods. The single site in Birmingham was chosen because it was, in a sense, unique by being an active landfill in urban surroundings, which is uncommon. The general idea behind these choices was to provide as wide a range of situations as possible. As well as looking at the area as a whole, a number of sites were highlighted for more detailed study. As the area is residential, and therefore sensitive, the confidentiality of the site operators has been respected and none of the sites are named.
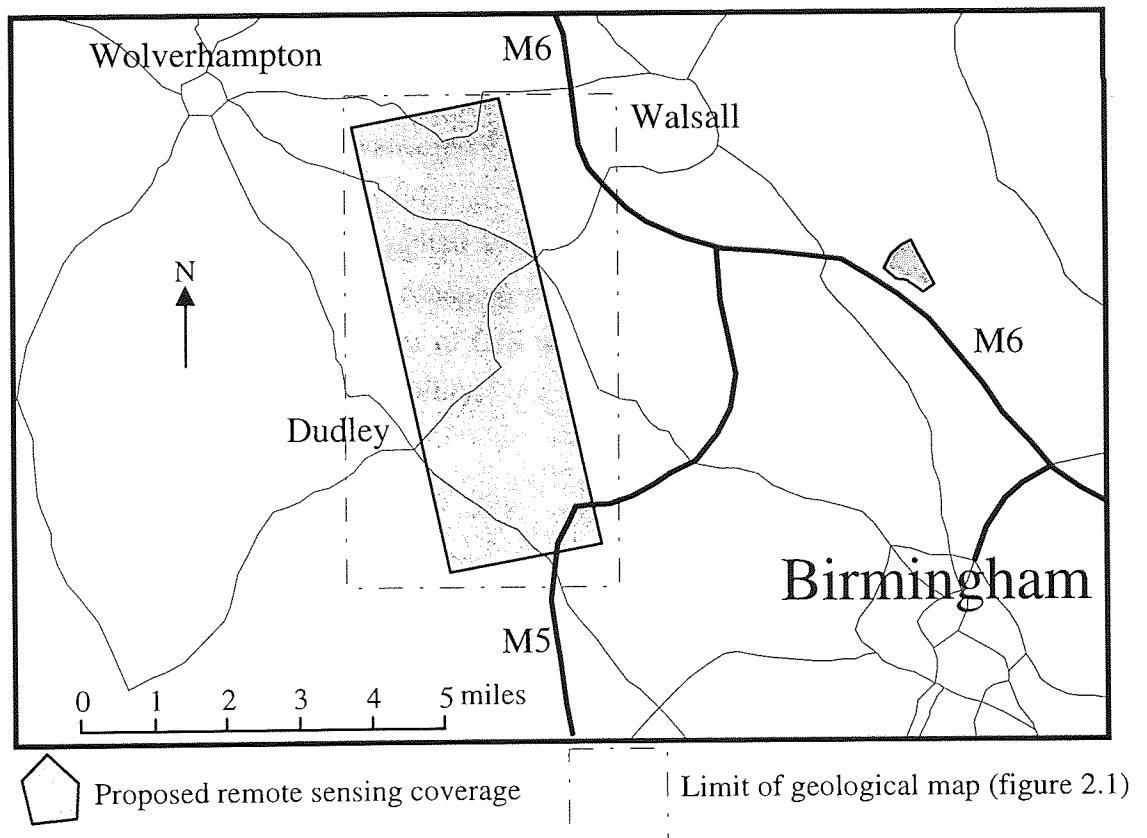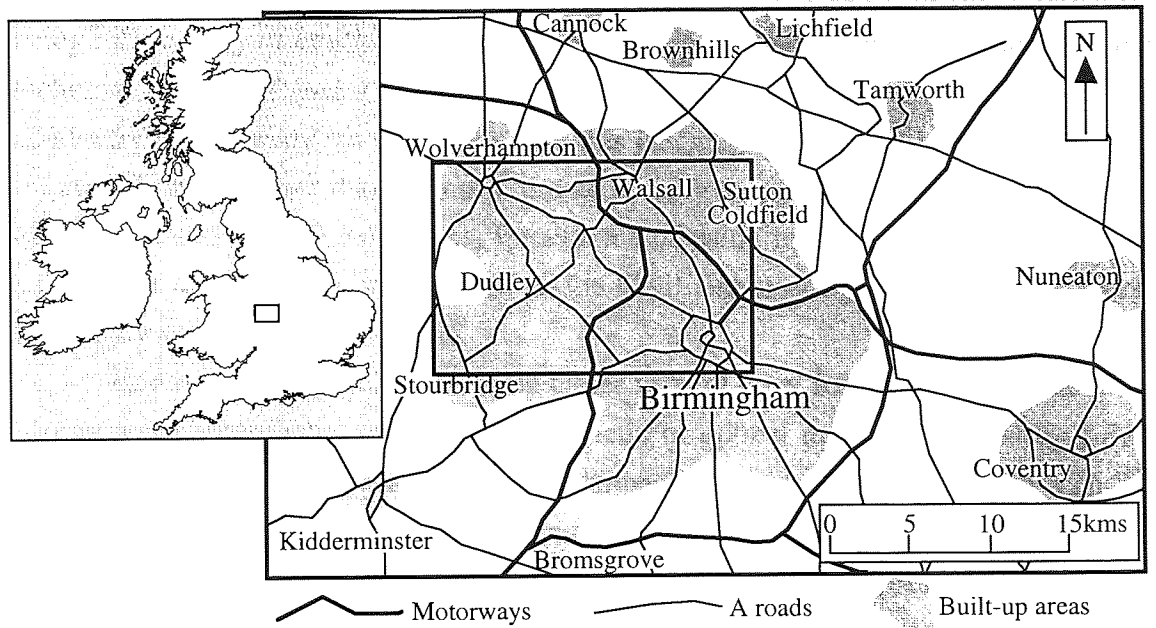
Figure 1.1. Location of the study areas.

1.4. Application of Remote Sensing to this Project

Remote sensing, by definition, is a method of studying objects without being in contact with them. The technique usually makes use of electro-magnetic radiation being reflected by or emitted from the object/s under investigation in question. From a technical point of view many geophysical methods such as seismology or conductivity/resistivity surveys come into this category but as they have been around for considerably longer than the term remote sensing they are very rarely included and remain in the realm of geophysics. Experience of using remotely sensed data (either airborne or satellite) has been gained in the Civil Engineering Department of Aston University over a number of years.

Remotely sensed data can come either in hard copy forms, of which the most common is photography, or stored on magnetic or optical media, produced by either video cameras, digital linescanners or scanned photographs. Photographs can be analysed directly, whilst the digital forms are displayed on a monitor prior to analysis. Digital data can be manipulated using image processing techniques which have the capability to highlight and pin-point the significant areas of interest and are an integral part of dealing with remote sensing imagery. In the current climate of advancing technology, more complex computer operations can be executed. Geographic Information Systems (GIS), the use of temporal and spatial data with the aid of a computer, are one such advancement and often employ remotely sensed imagery as a data source.

The theories to be applied to this project (vegetation colour change due to pollution or heat given off by escaping pollutants) are all detectable by remote sensing methods. In addition, a number of GIS techniques were applied to the ATM imagery to assess their integration capability.

1.5. The Main Hypotheses of the Study

This project was proposed to evaluate whether remote sensing techniques are appropriate for rapidly surveying the landfill sites in an urban area. This problem can be divided into three aspects: i) detection of gas, ii) detection of leachate and iii) detection of unknown sites.

From the literature review presented in chapters 3 and 4 it is possible to propose the following hypotheses that may be applied to this project:

1. Gas detection

Escaping gas may be detected by locating:

a) damaged or lack of vegetation (aerial photographs and ATM),

b) anomalous heat signatures (ATM and thermal video).

2. Leachate detection

Migrating leachate may be detected by locating:

a) damaged or lack of vegetation (aerial photographs and ATM),

b) damp areas (aerial photographs and ATM),

c) colour anomalies (aerial photographs and ATM),

d) anomalous heat signatures (ATM and thermal video).

3. Detecting unknown sites

Unknown sites can also be called 'forgotten' sites as many local authorities may not monitor them unless there has been a complaint by a member of the public. Some of these sites may contain pollutants that are still active after many years have passed. It may be of interest to the local authority to know where possible problem sites are.

Two methods were devised for addressing this problem.

i) Studying multi-temporal aerial photographs to identify the development of a site and areas that have been filled.

ii) Utilising GIS techniques on aerial photographs and ATM imagery to highlight areas that may be old landfill sites using conditions of likelihood (size, type of ground cover).

1.6. Outline of Thesis

The study was sponsored mainly by parties involved in waste management control, land reclamation and development and environmental appraisal and consulting but was carried out in the remote sensing centre at Aston University. Because of this the thesis is designed with a dual approach. It is aimed at: 1) those who are familiar with remote sensing and are interested in its application to landfill sites; and 2) those who know about landfilling and want to know how remote sensing can be applied to their field of expertise.

The study area is described from both a historical viewpoint (including geology) and the current situation giving an idea of the problems that are faced in

chapter 2. The third chapter gives an overview on landfill sites including legislation, operation and the pollutants produced by them. Chapter 4 provides an overview of remote sensing, detailing the principles, devices and applications employed in this project. The fifth chapter describes the image processing and GIS techniques used in the project. Chapter 6 gives details on how the data was collected and assesses the quality of the different forms of imagery. In particular attention has been paid to the spectral rectification of the ATM data to produce a balanced image intensity across the image. The results of the research are presented in chapter 7 with a discussion at the end of each section. Where appropriate, the different remote sensing systems are compared to see how they differ in quality and ease of use. In addition, the ground measurements were integrated with the aerial data. Chapter 8 reviews the economics of the data acquisition and procedures used in the project. Chapter 9 highlights possible improvements that could have been applied to the project and how recent technological advances could help similar projects in the future. Chapter 10 provides conclusions where the success of the various aspects of the project is assessed.

2. Geographical Area Studied

2.1. Location and History

The West Midlands conurbation is unusual for a heavily built-up area because of the lack of any major navigable river. Due to this absence it did not become a centre for manufacturing until the man-made transport systems came into being; the canal and rail networks. Even though the region was late in starting, it became, and still is, a major industrial centre of Britain. At the time of the industrial revolution, most of the growth, industrial and demographic, was taking place in the region known as the Black Country. The following information in this sub-section was obtained from Mallin (1991).

The Black Country is an area of approximately 200 square kilometres covering parts of north Worcestershire and south Staffordshire with the principal towns being Dudley and Wolverhampton. The borders traditionally coincided with the outcrop or near surface occurrence of the coal seam known as the 'thick' or 'ten yard' coal, which has been mined extensively for fuel. Now though, the coal is virtually extinct so the current boundaries are somewhat indistinct.

The area was named the Black Country because of the dreadful air quality experienced during the height of the Industrial Revolution in the 19th Century. The smoke produced from the foundries and furnaces hung in the air and settled on the landscape creating the overall gloomy appearance of the area at that time.

In the 17th and 18th centuries, the region consisted of a number of small hamlets working autonomously and making glass and iron using resources found locally and generally at the surface. At the time, charcoal was the main sources of fuel but, increasingly, coal was being used towards the middle part of the 18th century. The iron production was very small scale, consisting mainly of rough cast-iron nail manufacture. Because the quality of the local coal was not good enough to produce good iron, if it was used it was imported from Russia, Sweden or Spain. The importing of foreign coal no longer became necessary when, in 1766, Abraham Darby, in Coalbrookdale, invented a new process of producing iron that could utilise the local coal. It was also around this time when many canals were being cut. 1772 saw the connection of the rivers Severn and Trent and also the link between Birmingham and Wolverhampton. The industrial potential of the area was just being realised.

There were two main phases of industrial activity in the Black Country. The first phase, 1800-1870, was a period of massive growth during which the population grew by seven times - twice the national average. The second phase, 1870-1945, was a period of gradual decline due to the exhaustion of local resources.

The spur for the rapid industrial development is believed to have been the Napoleonic Wars which took place from 1803-1815 and produced a massive demand for weaponry - a demand that the Black Country had all the necessary resources to meet. Following the wars, all of the building blocks for successful industrial growth were in place. This was progressively helped by the improving transportation network and by 1830 South Staffordshire was at the hub of the national canal network, being at the juncture of canals serving the Thames, the Mersey, the Severn and the Wash. The successful running of the first steam locomotive, 'Rocket', in 1830 by George Stevenson was just another stimulus to expedite the industrial revolution.

By the 1870s the region was overtaken by Scotland, South Wales and Yorkshire as the principal pig iron producers. Part of the reason was that the region's natural resources were running out - only the coal was left in any quantity. The region made a mistake by remaining far too loyal to wrought iron when Bessemer was making his explorations into steel. His experiments were not well received in the region so he took his work to Sheffield, where it flourished. By the time the Black Country had perfected the process the initiative has been lost to South Wales, Lancashire and Yorkshire. The decline continued with a slight resurgence provoked by the First World War.

2.2. Geology

The solid geology of the Black Country region related to this project is shown on figure 2.1. (extracted from British Geological Survey, 1:50000, solid geology, sheets 167 and 168). The precise area of figure 2.1 is shown on the lower frame of figure 1.1 as the dashed box.

From direct map interpretation it is possible to deduce the following information. The oldest rocks in the region are the Wenlock and Ludlow (Silurian) Limestones appearing in the west as inliers. They are present as the hills famous for the Wren's Nest and Dudley Castle and zoo. Many caverns have been bored into the hillsides to mine the limestone used for the local industries. Overlain unconformably onto the Silurian limestones are rocks of Westphalian in age (Upper Carboniferous). The lowest of the Westphalian series are the Middle Coal Measures in which the 'Thick' coal, with other productive seams, is found. These seams are over or near to the surface of the whole region. Over these are the purple and ochreous marls of the Etruria Marl, covering most of the central part of the area. Above these are the olive and buff sandstones of the Halesowen Beds appearing as small outcrops in the south-east part of the region. Following these are the marls and sandstones of the Keele and Enville Beds at the south-eastern edge. During the Carboniferous there was a period of
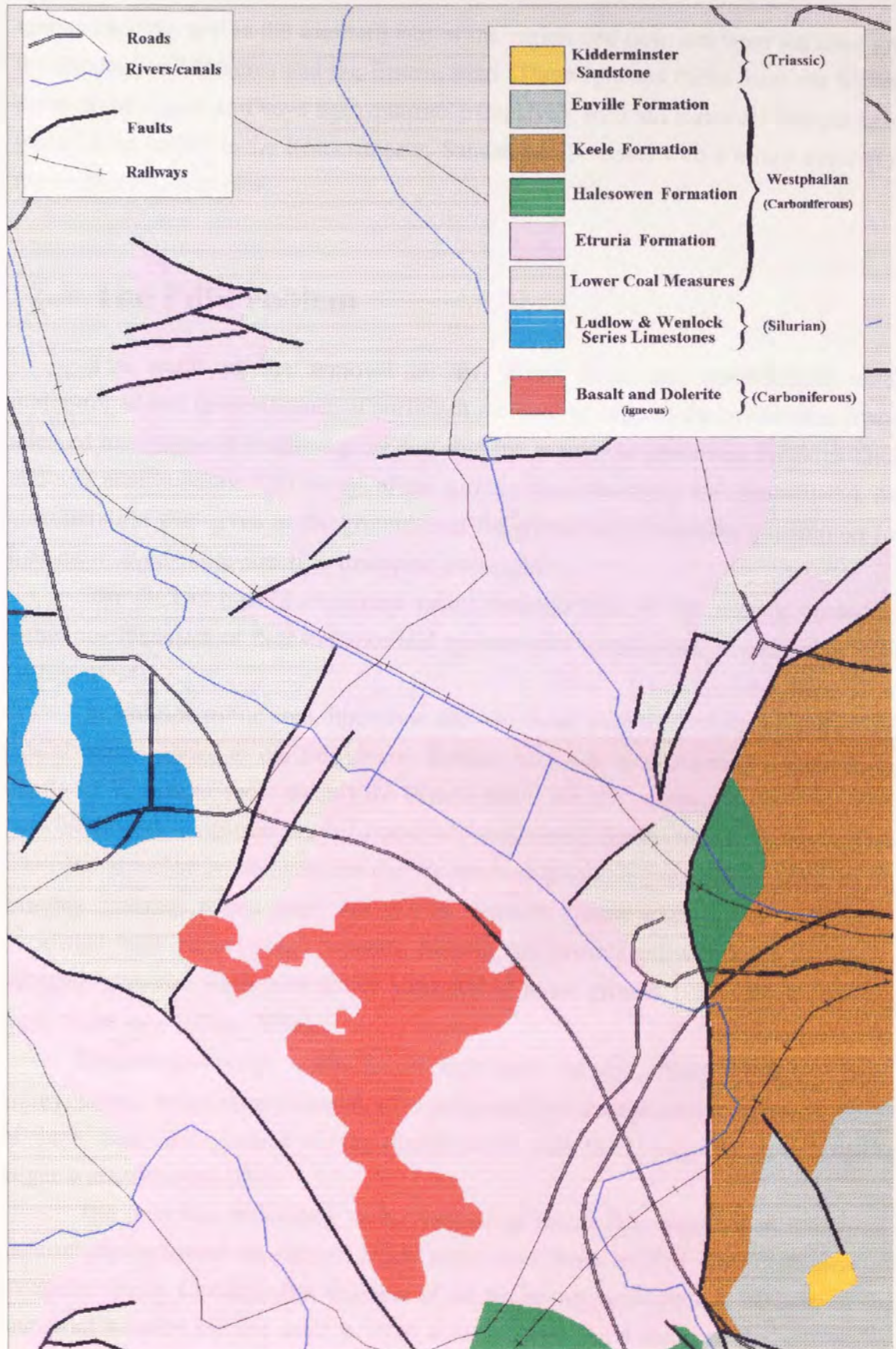
Figure 2.1. Geology of the Black Country project area. (Area relates to dashed box on lower frame of figure 1.1).

igneous activity and in the southern part of the region and dolerites were intruded into the Productive Measures and the Etruria Marl. These igneous rocks form the highest point of the region and have been quarried extensively for road material. The youngest rocks of the region is the Kidderminster Sandstone (Triassic) with a minor outcrop in the south-eastern corner.

2.3. The Fill Problem

The result of the removal of the 'Thick Coal' left considerable voids underground and in the absence of sufficient methods to support the overburden it was allowed to collapse. Considering the fact that the main coal seam was 9 metres thick and was always within 150 metres of the surface, the subsidence was pronounced. No consideration was given to the ground over the mines and it was not uncommon for houses, or even entire streets to disappear overnight.

The BCDC have documented many consequences of the mining, including numerous instances of hole collapse and spontaneous combustion of subsurface coal (Elliot, 1994).

In addition to the coal, limestone and ironstone were worked underground and this also contributed to the subsidence. Surface clay was also quarried sometimes to depths of 30 metres, most notably the Etruria Marl, and the resulting holes were often backfilled with industrial waste, frequently containing heavy metal contamination. Sand and gravel were excavated in the Wednesbury area along what was known as the Moxley Channel where there are glacial deposits. These excavations were often backfilled with contaminated deposits. Mining spoil combined with indiscriminately dumped industrial waste now forms a blanket of made ground 1-15m thick covering most of the area (Elliot, 1994).

Numerous sewage works lie, or have been present, along the River Tame valley leaving many areas covered with contaminated sewage sludge deposits. Many of these works are gradually being closed down with the sewage being directed to larger works (Butler, 1993).

The area was networked with a myriad of canals that were cut in the earlier days of the industrial revolution. Many have since been infilled with contaminated industrial waste. Considerable amounts of silt builds up in canals and because of the industrial location the silt itself is often contaminated. As a result of the subsidence many canals had to have their sides built up, so the depth of silt in some canals can be up to 10m (Elliot, 1994).

In some areas there have been situations where sub-surface gasses were being produced. Carbon Dioxide has been produced by acidic groundwater percolating through colliery spoil and reacting with the carbonaceous material. Concentrations of 8-10% are not unusual. Methane is produced by anaerobic biological reactions with carbonaceous material in landfill sites and shallow coal workings and is occasionally present in explosive concentrations (Elliot, 1994).

Although there are clearly numerous angles that could be examined in consideration of underground pollutants, and particularly methane, it is those specifically related to landfill sites that are of interest to this project.

2.4. Hydrogeology

As the monitoring of leachate is a part of this project it is necessary to address the hydrogeological settings of the area. The main area is situated on mainly Carboniferous sandstones, limestones and marls which are designated in Knipe et al (1993) as regions of no groundwater flow. If leachate is produced, due to the lower likelihood of vertical movement it may be prone to migrate overland and into nearby water courses.

By contrast the single site to the east is located on the Kidderminster sandstone of Triassic age. This sandstone is permeable and along with other associated underlying sandstones is used as an aquifer. Water is abstracted from the sandstone so the effects of leachate production are more important for this site as groundwater pollution may occur. The problems of leachate production from a hydrogeological point of view are discussed specifically for each of the main sites in section 6.5.

3. Landfill Sites

3.1. Introduction

Landfilling is a method of disposing of solid waste by burial. The usual process involves placing the waste in a depression, often a disused quarry, compacting it, building it up in successive layers and eventually capping it off, usually with topsoil, to a prescribed level. In some lowland countries where large voids are rare the waste is built up into a mound and termed 'airfill' or 'land raise'. The final completion and restoration of the site is arguably the most important part of the landfilling process. Whatever the usage following site closure the condition of the completed landfill influences how the whole philosophy of landfilling is perceived as an acceptable method of waste disposal (DoE, 1992c).

Landfill is the main form of waste disposal in the UK today taking 90% of the waste produced (Croft & Campbell, 1992). The remainder is either treated or disposed of in other ways, the most common alternative is incineration with the residues usually disposed of at a landfill. Other disposal methods include using sewage sludge waste as a land fertiliser or dumping it at sea (the latter now almost completely discontinued in the EC).

Until the passing of the Control of Pollution Act 1974 the possession of a licence to dispose of waste to land was not a requirement. The Act stipulated that licences were to be obtained before any disposal could take place, to ensure that:

"the waste disposal and treatment poses no unacceptable risk to public health or the environment."

(HMIP, 1991)

There are a number of problem that arise from the practice of landfilling such as noise, litter, odour and pests but of most concern are the pollutants caused by the biodegradation of the refuse, a toxic and reducing liquid termed leachate and a gas comprising mainly methane and carbon dioxide.

It has been determined that of all the types of waste, those with a domestic origin containing easily putrescible organic matter give off leachate and landfill gas most readily. Croft & Campbell (1992) found that domestic waste comprises almost half of the UK's solid waste as shown in table 1.1.

This chapter will outline the main points in the landfilling process. Full details on the subject are contained in texts such as DoE (1992a, 1992b and 1992c) and Ball & Bell (1994).

3.2. Legislation

Ball & Bell (1994) provide a good description of the legislative history of waste disposal in Chapter 13 of their book 'Environmental Law' form which the information for this section has been obtained.

The first major piece of national legislation relating to waste disposal in the UK was the Deposit of Poisonous Wastes Act 1972, passed following an incident (the dangerous deposition of hazardous waste) in the West Midlands - up until then there was no nation-wide policy regarding waste disposal. The Act was designed to combat the type of incident that had occurred and was consequently too narrow in its perspective. Even so, it was one of the first ever controls over hazardous waste disposal in the world. The 1972 Act led to the Control of Pollution Act 1974 (COPA) being passed, which introduced a comprehensive system requiring that anyone wishing to dispose of waste, either to landfill or incineration, should obtain a licence from an official disposal authority. COPA provided a piece of model legislation that other countries could emulate and in turn led to the EC Framework Directive on Waste (75/442).

As experience was gained in implementing COPA many problems were identified and to rectify these the Environmental Protection Act 1990 (EPA) was passed. EPA is centred on the whole waste cycle, including producers and carriers, altering fundamentally the way that waste is dealt with.

COPA introduced an extensive system of licensing. A waste disposal licence was required from the Waste Disposal Authority (WDA) to deposit 'controlled' waste which is defined as (DoE, 1992c):

i)   household - waste arising from private dwellings, residential homes, universities, schools and educational parts of hospitals;

ii) industrial - waste from factories as defined in the Factory Act 1961;

iii) commercial - waste from trade, business or sports premises.

In addition, the WDA was given the duty of arranging for the disposal of waste, producing a waste disposal plan for the region and operating the licensing system. The prospective disposal operator would apply to the WDA who would then consult with the collection authority and the NRA. The licence could only be refused if it was shown that it would present a danger to public health or a risk of water pollution.

The licence usually has many conditions attached to it which are likely to include:

i) continual monitoring;
ii) stipulation of what type of waste can be accepted;
iii) details of operating principles;
iv) reporting of problems to the authority;
v) accurate record keeping, and submitting to the authority types and volumes of waste deposited;
vi) aftercare procedures and post closure usage;
vii) final topography.

The disposal authority was obliged to check on the sites under licence regularly and if there were a problem it should be remedied, preferably at the cost of the operator of the site. When all work had been completed the operator would then surrender the licence to the WDA, although the operator was allowed to surrender the licence at any time.

COPA, whilst proving to be a groundbreaking piece of legislation was inherently flawed. The WDA, whilst having the responsibility of granting and enforcing licences also had to organise disposal itself. This caused a 'poacher and gamekeeper' situation producing a conflict of interests. In addition, the standard of the licensing and policing system enforced by the WDAs varied enormously across the country as there was no central guidance. Often the standard of enforcement was very low. The licence surrender procedure created much consternation, as well. A site operator was able to surrender the licence at any time thus relinquishing all responsibility to current and future problems that might occur, and therefore was under no obligation to carry out any aftercare programmes agreed in the original licence.

The EPA was drawn up to counter many of these problems and strengthen the control that COPA already gave. The operational and regulatory functions of the authorities were split into two separate bodies, thus avoiding the conflict of interest. The licence coverage has been extended in such a way that greater duties have been imposed on the operator to ensure that waste is dealt with properly by producers and intermediate handlers thus necessitating good waste management within firms. The loophole allowing site operators to surrender their licences has been closed. No surrender can occur without the approval of the Waste Regulation Authority (WRA) who will then grant a Certificate of Completion. Altogether the WRA have increased powers to impose conditions on the licence (including licence refusal) and enhanced

powers of enforcement with greater penalties attached for transgressions. Greater emphasis has also been placed on waste minimisation and recycling.

Waste management legislation and policies have been influenced by many EC Directives. The EC has had a general policy of waste minimisation, recycling, re-use, clean technology and eco-labelling. This was emphasised by the framework Directive on Waste 75/442 which established a general scheme for waste management and has been updated by Directive 91/156. Other relevant EC Directives include those involving hazardous waste (78/319 and 91/689), sewage sludge (86/278) and air pollution and incineration (89/369 and 89/429).

Altogether, with the extra restrictions being applied to waste, the cost of waste disposal will rise considerably provoking economic incentives for waste reduction.

3.3. Landfill Site Operation

The items outlined in this section are described in more detail in DoE (1992c) and are considered as good practice.

3.3.1. Types of Landfill Site

There are two main types of landfill site and they are constructed with consideration to leachate. The first, dilute and disperse, is designed to hold on to leachate for a long time (long enough to reduce the damaging effects) and then release it to the underlying strata. The site is chosen on the grounds of geographical/geological location. The second, containment, attempts to hold on to the leachate indefinitely with the aid of lining materials placed as a layer on the base of the site.

Dilute and disperse

The principle of dilute and disperse sites is to reduce the toxicity of the leachate by physical, chemical and biological processes before they are released into the environment. These processes include dilution, adsorption, absorption, oxidation, reduction and microbial degradation, all of which may occur as the leachate passes through the waste. These reactions may continue as the leachate leaves the site boundaries and passes into the underlying geological strata.

Much care has to be taken in locating these sites when considering groundwater, particularly with respect to potable water abstraction. Only areas with a fairly high clay content in the underlying strata, therefore low permeability, should be

considered. This form of site is only suitable for relatively inert wastes and would probably not currently be accepted for normal landfill, although many already exist.

Many of the older landfill sites in the UK are dilute and disperse sites although that may not have been the original plan. When they were originally planned it usually meant finding a suitable hole and filling it with no consideration taken of what the void was situated upon. Later when more studies were carried out and it was found that merely filling a hole may be detrimental to the environment the term 'dilute and disperse' was used to vindicate the original ides however flawed it may have been. Nowadays the philosophy of this form of landfill is very much discouraged in favour of the 'containment' concept.

Containment

Containment sites are the most usual form of landfill site allowable under the current legislation. The principle is to hold on to the leachate for a considerable time allowing the toxicity to reduce. The designed retention time can vary from decades to hundreds of years before the release of the leachate into the environment. This is achieved by using lining materials situated between the waste and the base and sides of the site. These materials can be natural (i.e. clays) or artificial (i.e. thermoplastic sheeting) and are discussed in more detail in section 3.3.2. This practice is the advised method of filling at present if liquid pollutants are likely to arise.

3.3.2. Lining

Lining materials are essential for containment sites, they can be either natural or artificial and are placed in the base of the hole before any waste is deposited. The intention of a liner is to stop or hinder pollutants from migrating from the site boundaries. The employment of a liner will depend on the waste type (will it produce toxic leachate?) and the underlying strata (is it used for a potable water supply?). Any liner has to be installed under strict quality control as part of a quality assurance programme.

Natural liners

Any suitable natural material considered for a liner should have a permeability of $< 1 \times 10^{-7}$ cm/sec, which translates to 0.0315m/year. Many natural liners have the ability to remove some pollutants from the leachate as it passes through them.

The most common natural material is clay, either found locally or imported, but others may include compacted colliery spoil or Pulverised Fuel Ash (PFA) if they meet the required permeability.

Artificial liners

These liners should be impermeable for at least 30 years and should be resistant to any chemical, physical and biological attack that may result from being in contact with leachate and heat.

Artificial, or synthetic, liners are usually thermoplastics and derived from polyethylene, polypropylene and polyvinyl chloride (PVC) but there are alternatives of which Geosynthetic Clay Liners (GCL), which are a woven fabric filled with bentonite clay, are one.

It has been found that some synthetic liners can swell and lose strength. The seams are the weakest points and are readily attacked by the chemicals found in leachate. Heat sealed seams have been found to last longer than those sealed by adhesives (DoE, 1992c).

A synthetic liner will need a protecting material above and below to prevent puncturing from the underlying bedrock or sharp objects in the waste. The protection can be provided by river silt, colliery spoil, sand, limestone, quarry fines, bentonite, pulverised fuel ash (PFA) or special geotextiles.

3.3.3. Filling Methods

There are three main distinguishable types of filling method but because of individual site operations the differences can become indistinct.

a) Trench method

The trench method involves excavating a trench, depositing the waste in it and using the excavated material as cover. This procedure has found very little use in the UK.

b) Area method

The area method entails simply laying the waste over the available area. There are considerable problems encountered when trying to control leachate unless high waste inputs are sustained providing sufficient absorptive capacity. Although this method used to be common it is no longer favoured in the UK.

c) Cell method

This the most common method used in the UK at the moment so it will be described in greater detail.

The cell method involves depositing the waste in pre-bunded areas and then moving upwards and outwards at the same time so restorative processes (i.e. capping) and filling can at some stage be simultaneously carried out in different parts of the site.

The waste is laid in the prepared areas and compacted by being driven over by special heavy machinery furnished with large cleated (toothed) metal wheels to assist the break-up of larger objects. The wheels are often hollow so they can be filled with water to increase the weight if necessary. The waste is pressed into layers of a specified thickness then an inert layer, often soil or PFA, is laid down. The layering then continues again on top until that area of the site is completed. Figure 3.1 shows how, using the cell method, different thicknesses of waste may occur in different parts of the site. This makes it possible to carry out a number of different operations on the same site simultaneously so at no point is it necessary to wait for another process to completed before the next one can continue.
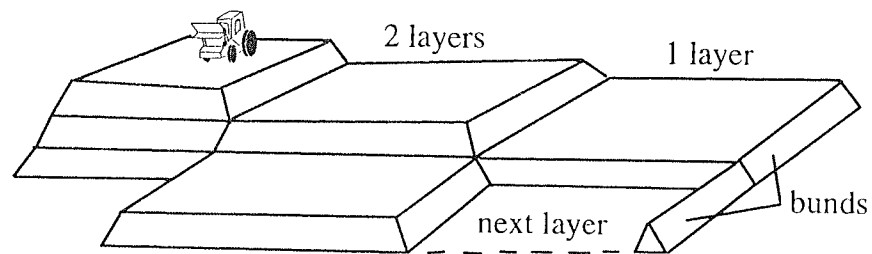
Figure 3.1. Simplified diagram of the cell method (not to scale).

At the end of a working day the exposed waste is covered with inert material which should be stored on site. The cover is to isolate the waste thus discouraging vermin and preventing rubbish from blowing away.

Most household waste undergoes some degree of compaction in the dustwagon when it is collected. Occasionally waste is baled at a transfer station and is merely stacked by fork-lift when it reaches the site.

3.3.4. Capping

When all filling has finished the site has to be restored in accordance with the conditions specified in the licence. The cap is designed to prevent water ingress and encourage run-off, thus reducing the leachate formation within the waste. In addition the site is usually domed which also increases run-off and takes into account the settling of the waste. Waste can settle up to 20% (i.e. occupying 80% of its original volume) but it starts to settle as soon as it is laid down so the amount of settling after capping is greatly reduced. The following thicknesses for the capping components are suggested in DoE (1992c) and are illustrated on figure 3.2.

Buffer layer

The top-most layer of waste is covered with a graded buffer layer, usually gravel, to act as a smoother for subsequent layers. The Buffer layer should be about 0.5m thick.

Capping layer

Over the buffer is arguably the most important part of the cap which is the impermeable capping layer. This is most commonly made of clay but can be of bentonite, colliery shale, PFA, GCL or a synthetic material, as long as the permeability is less than 10^{-7}cm/s. This layer should be about 1m thick. If a synthetic sheeting material or GCL is used in conjunction with the necessary support material (i.e. clay or gravel) this thickness is likely to be less.

Topsoil

The final layer is topsoil, which is necessary if the site is to be vegetated afterwards which is usually the case. This layer should preferably be 1m thick but it depends on the future use. Whatever the use it should not fall below 0.4m in thickness
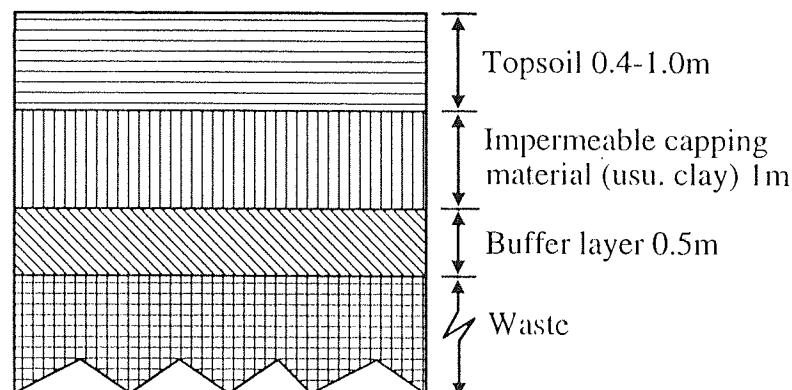
Figure 3.2. Suggested capping for a completed landfill site (values from DoE, 1992c).

3.3.5. Provision for Monitoring

Arrangements to carry out a monitoring strategy for leachate and landfill gas should be written into the disposal licence. The amount and type of monitoring will depend on the size of the site, the underlying geology (with special attention to the presence of underlying aquifers), the proximity of buildings and the type of waste deposited.

The leachate created by the decay of the fill will usually drain to the base of the site. If it is to be pumped to the surface then pipes will have to be laid across the base of the site before any filling takes place. The site should be graded to flow to a collection point (i.e. a leachate well or sump) and if necessary a drainage network should be incorporated.

Boreholes, surrounding the site, should be sunk down to the water table before any filling takes place to check the quality of the groundwater as a background datum level. These boreholes should then be used regularly to sample the groundwater to see if any pollution occurs.

Landfill gas also needs to be monitored. The movement of landfill gas is not governed by gravity so can migrate sideways through the walls of the site. The gas can be monitored with a series of boreholes placed around the perimeter of the site and sampled before any landfilling commences to measure the background levels. The number of monitoring boreholes is usually based on the proximity of buildings, increasing with closeness.

3.4. Landfill Gas and Leachate Production

This section is concerned with the production of leachate and landfill gas and the associated parameters involved. The constituents, migration regimes and treatment of leachate and landfill gas are dealt with in sections 3.5 and 3.6 respectively.

Leachate and landfill gas are the two main polluting substances produced by the waste deposited in landfill sites. Leachate, by definition, is a mobile liquid that is able to seep through the waste and in doing so extracts contaminants from it. The major contributory factor is rain water that enters the waste either whilst filling is in operation or through the cap after filling has been completed. Some leachate is produced by the decay of organic matter, usually from trapped inter-cellular liquids.

Landfill gas is a combination of methane and carbon dioxide in a ratio of approximately 60-65:35-40 respectively along with some other trace components. Before any gas can be produced there has to be some moisture present, either from infiltrated water or the release of inter-cellular moisture, resulting from the primary breakdown of organic matter.

When the circumstances are suitable, gas begins to be generated. Early conditions are aerobic and carbon dioxide is the main component produced. In due time the oxygen is either displaced or consumed and anaerobic conditions prevail. At this point methane begins to be produced in increasing amounts until the reactions

reach an equilibrium where methane and carbon dioxide are the major constituents as described in section 3.6.

Micro-organisms are responsible for the degradation of waste into its liquid and gaseous components. Figure 3.3 shows the typical chemical process of how the organic component of leachate is produced initially, with the subsequent formation of landfill gas.
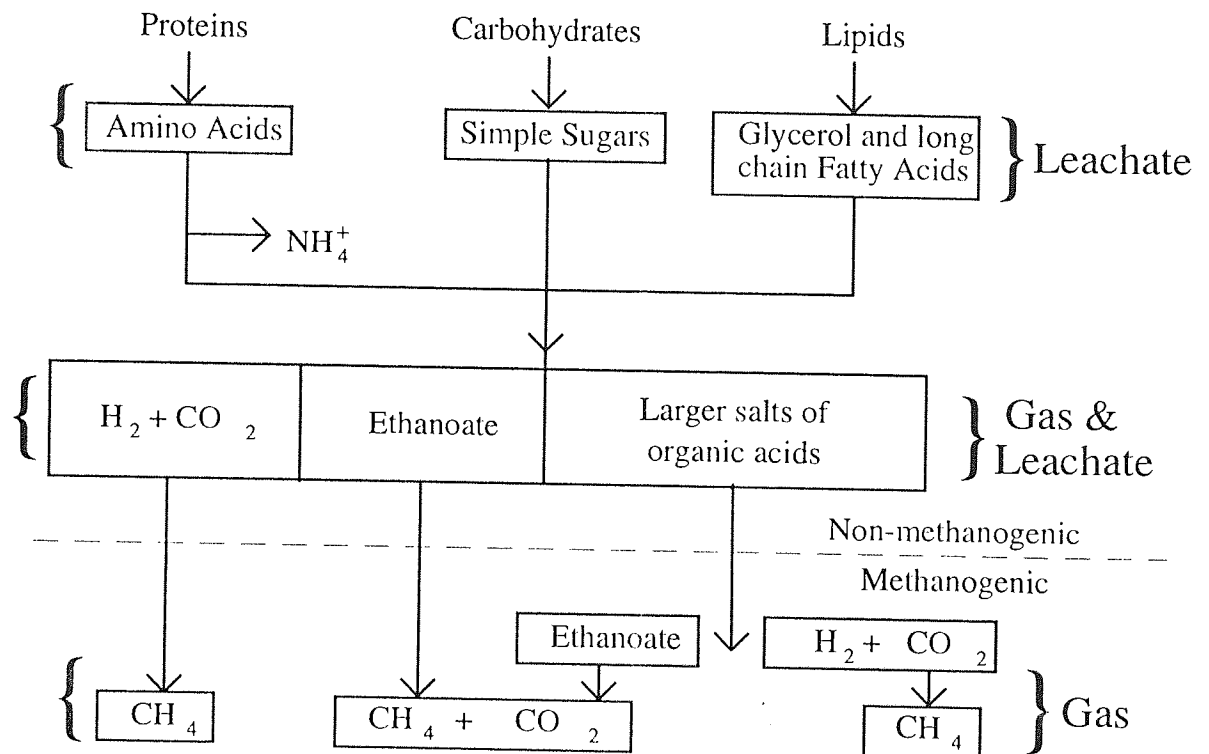
Figure 3.3. Typical production pattern for landfill gas and leachate. Adapted from Farquar & Rover (1973) and DoE (1992c).

The whole process can be divided into a methanogenic stage and a non-methanogenic stage (Flower et al, 1978). The first products formed by the process of degradation are various components of leachate. They are formed by the breakdown of larger organic molecules (proteins, carbohydrates and lipids) into their smaller constituents as shown on figure 3.3 by aerobic bacteria. Further breakdown produces H_2, CO_2, water and small organic acids and salts (usually ethanoic acid and ethanoate (CH_2COOH and CH_2COO^-)). When the oxygen has been depleted by the aerobic (non-methanogenic) bacteria, anaerobic bacteria become the dominant micro-organisms. The anaerobic (methanogenic) bacteria play the major part in the production of landfill gas as a by-product of their metabolism.

During the methanogenic stage, methane producing bacteria are responsible for the production of CH_4 and it does this in two ways. Firstly by reacting CO_2 and H_2 together as shown in equation 3.1.

$$CO_2 + 4H_2 \longrightarrow CH_4 + 2H_2O + heat \qquad (eq\ 3.1)$$
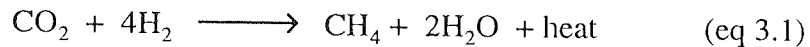
The bacteria in the second reaction utilise the heat produced in the first to break down the organic acid molecules as shown in equation 3.2 creating a chain reaction by producing CO_2 which in turn feeds the reaction in equation 3.1.

$$CH_3COOH \xrightarrow{\ heat\ } CH_4 + CO_2 \qquad (eq\ 3.2)$$

These reactions continue until the supply of organic material is consumed.

3.4.1. Factors Affecting Landfill Gas and Leachate Production

The amount of gas and leachate produced is dependent on a number of factors.

i) **Type of waste.** The micro-organisms that produce leachate and landfill gas predominately feed on carbonaceous material. The types of wastes that produce most gas are domestic wastes because of their high organic content in the form of vegetable and paper matter. Vegetable waste, mainly food and garden refuse is readily degradable and can be consumed by the micro-organisms in 1-5 years dependent on ambient conditions. Paper waste can take 5-20 years to fully deteriorate and woody materials can take 20-100 years because of the more hardy cellulose content of these materials (Bingemer & Crutzen, 1987).

ii) **Moisture content of waste.** Any moisture within the waste will add to the liquid content so increasing the volume of leachate. Often much of the moisture is supplied in the form of trapped liquid in vegetable food waste and garden refuse. At least 30% moisture in the waste (30% of the saturated weight) is necessary to initiate gas production. Gas production increases with moisture content, the peak being at 60-80% moisture (Flower et al, 1978).

iii) **Adsorptive moisture holding capacity of waste.** Leachate is specifically free-flowing liquid produced by decaying refuse. Leachate is produced when the amount of liquid present exceeds the moisture holding capacity of the waste, so if the waste within the landfill has a high moisture retention capacity this can

reduce the amount of leachate leaving the site. The mobile leachate carries nutrients, bacteria and moisture to other parts of the site which may induce more favourable conditions for gas generation if none previously existed.

iv)**Infiltration/impermeability of cover.** The addition of water into a landfill will add to the moisture already present and therefore contribute to the volume of leachate and accelerate its production. Most of the infiltrating water will be from rain, hence the importance of an impermeable capping on the finished site to reduce leachate volume. Many wastes have a fairly low moisture content and will not necessarily degrade in such a way as to produce pollutants. For instance, normal household waste has an average moisture content of 25% (DoE, 1992a) so the additional water from external sources is essential for gas and leachate generation. In regions where rainfall is low (for instance some areas in the USA) almost no gas and leachate is produced because of lack of water ingress (Flower et al, 1978). In the United Kingdom, however, there is ample supply especially from rain. Even if a site has been capped with an impermeable layer it does not necessarily mean that no gas will be produced. Abundant rainwater may have already entered the waste whenever rain fell during the normal filling operations.

v) **Age of waste in the landfill.** As the degradation process reaches equilibrium the gas and leachate production will peak. The time taken for this can be from days to months, but once it reaches this point the levels can remain there for from a few years to decades. (see section 3.6 and figure 3.7).

vi)**Physico-chemical conditions.** The physical assemblage and chemical constituents of the waste can be an important factor and can be described by a number of parameters.

a) Density and porosity of the waste. If the waste is very compressed there are few void spaces and leachate has difficulty moving away from where it is formed thus suppressing both leachate and gas output. If the waste has been shredded it has a greater surface area so more reactions can take place thus increasing gas and leachate production.

b) The pH level in the waste. The pH level can affect methane production and may vary due to the acidity or alkalinity of the waste. The bacteria responsible for methane production (methanogens) prefer a pH of approximately 7 for optimum production. There are slight variations in opinion but all are in general agreement about optimum pH range: 6.4-7.2 (Zimmerman et al, 1982), around 7 (Flower et al, 1978), 6.4-7.4 (DoE, 1992a) and 6.5-8.5 (DoE, 1992c).

c) The temperature of the waste. The temperature inside the landfill is also a very important parameter. There are two main types of methanogenic bacteria: mesophilic and thermophilic. Mesophilic bacteria reach an optimum production rate at between 30 to 40°C and thermophilic bacteria attain peak production from 50-55° C. The mesophilic bacteria appear to be the most important as the temperature range for peak gas production seems to be centred around their optimum range as stated by a number of authors: 30-37°C (Flower et al, 1978), 29-37°C (DoE, 1992c), 35-45°C (DoE, 1992a) and 30-40°C (Pacey & DeGier, 1986).

d) Nutrient availability. Bacteria, as with all organisms, need certain nutrients for growth. Those that are important are carbon, hydrogen, oxygen, nitrogen, phosphorus, potassium, sodium, calcium, magnesium, sulphur and some other trace elements. Again vegetable wastes provide these elements in sufficient quantities to advance gas and leachate production. Waste lacking in these nutrients are termed 'inert'.

e) Size and depth of the landfill. The larger the landfill is the more it will be unaffected by external conditions and be able to regulate itself. The deeper the site is the lower the chance of oxygen being circulated through the bulk of the refuse. If oxygen is present it will interrupt the methanogenic bacteria and reduce the amount of methane being formed and increase the carbon dioxide production by aerobic micro-organisms.

Shallow sites will be more affected by external conditions and may show seasonal variations in gas production with more being generated during the summer months when it is warmer. In addition, shallower sites will be more affected by oxygen circulation as the bulk of the waste will be nearer the surface. Therefore, deeper sites will produce greater quantities of pollutants at a greater rate than shallower ones, but the latter may remain active for much longer.

Attal et al (1992) made a detailed study of a French municipal waste landfill to determine the methane generating potential of the waste. To accomplish this two 25cm boreholes were drilled down to the base of the site to enable temperature, methane and organic content to be measured. Figure 3.4 shows graphs of temperature and methane concentration against depth from a completed landfill (Attal et al, 1992). Both graphs clearly show temperature and methane levels increasing down to about 10-15 metres and then levelling out strongly suggesting a possible relationship between temperature and methane in a landfill. The top 10-15 metres is in the transition stage of degradation and has not reached the equilibrium point. This is probably due to a combination of the waste being younger, so not having had the sufficient time to decay and it being near the surface so external factors are acting to suppress methane production (cool external temperatures and/or oxygen circulation).

Temperature
(°C)

a) Temperature against burial depth

CH₄ (% v/v)

CH_4 (% v/v)

b) Methane against burial depth
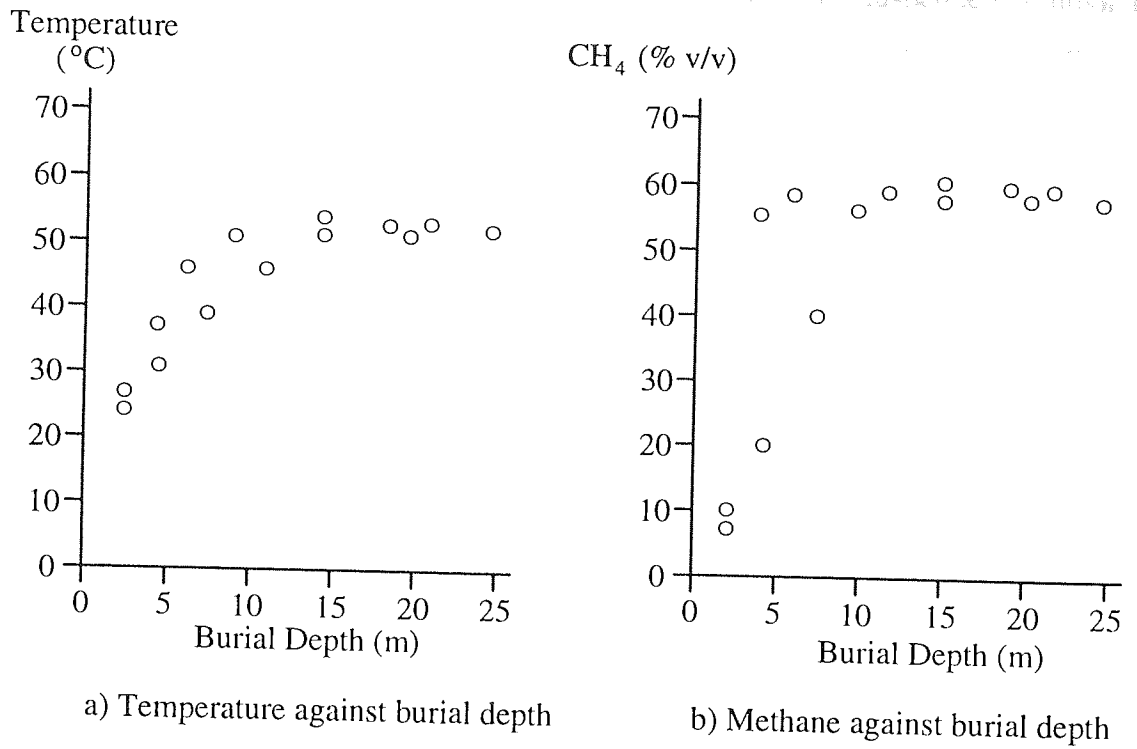
Figure 3.4. Temperature and methane plotted against burial depth for a completed landfill (adapted from Attal et al, 1992).

Volatile Suspended
Solids %
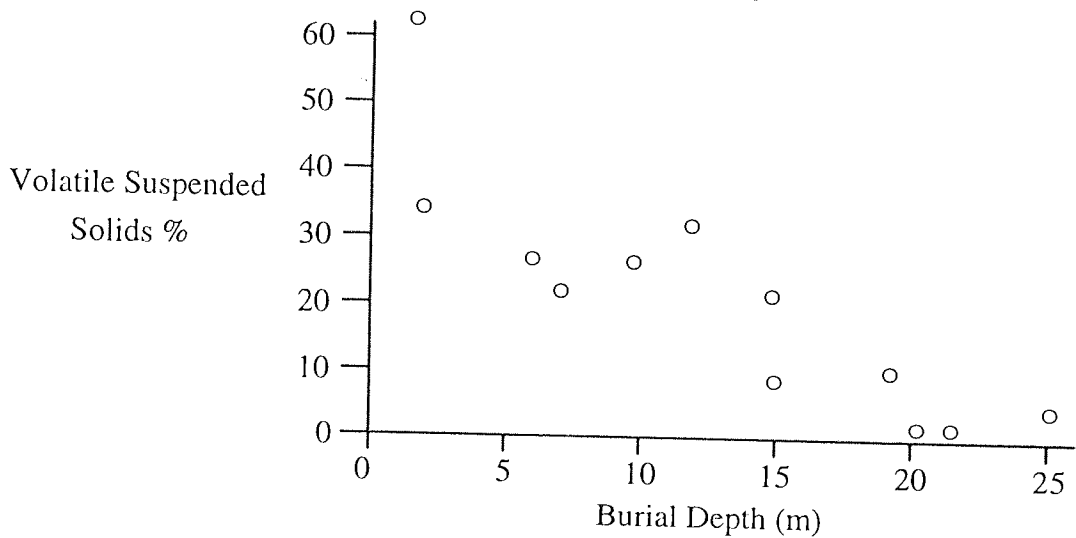
Figure 3.5. Volatile suspended solids (available organic content) against burial depth for a completed landfill (adapted from Attal et al, 1992)

Figure 3.5 shows that the deeper the burial and the older the waste, the lower the available organic content (also expressed as the volatile Suspended Solids). It indicates that how the organic matter depletes over time due to the degradation processes and how the younger waste has a higher methanogenic potential.

Much literature has been devoted to the behaviour and production of landfill gas. Three DoE reports (1992a, 1992b and 1992c) present a comprehensive overview of landfilling including pollution problems and legislation. Scott & Baldwin (1989) state that 4-500m³ of methane can theoretically be produced from one ton of domestic refuse at standard temperature and pressure. Taking into consideration that many landfill sites eventually hold well over a million tons of waste the volume of gas that can be produced is of great significance.

3.5. Leachate

Leachate is one of the two main polluting substances associated with landfill sites and it can be a highly toxic and reducing liquid. Table 3.1 shows how 'strong' leachates can be and how the strength declines with age.

Aston University

Illustration removed for copyright restrictions
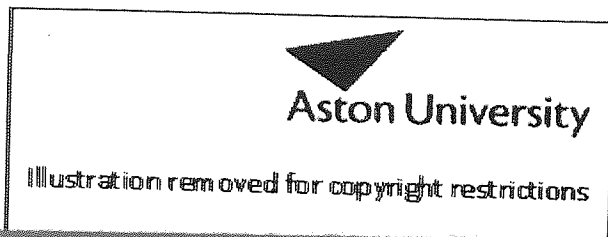
Table 3.1. COD and BOD for recent and aged wastes (DoE, 1992c).

Leachate is specifically a free flowing liquid and is produced by a combination of the breakdown of organic material into fatty acids, amino acids, simple sugars and other light compounds, and infiltrating water from rain or, rarely, groundwater, as described in section 3.4.

As the leachate percolates through the refuse it picks up other substances such as metal ions and soluble organic compounds increasing its toxicity markedly (DoE, 1992a).

3.5.1. Leachate Migration

Leachate is not only the moisture trapped within the waste as it is deposited but has a number of other contributory factors which are shown on figure 3.6.

precipitation

↓ ↓ ↓

Evapo-transpiration

water loss with gas release

surface water infiltration

cover

surface run-off

soil

soil

sub-surface water infiltration

waste

Leachate production ↓ ↓

Water table

Groundwater flow

Migration of leachate into groundwater
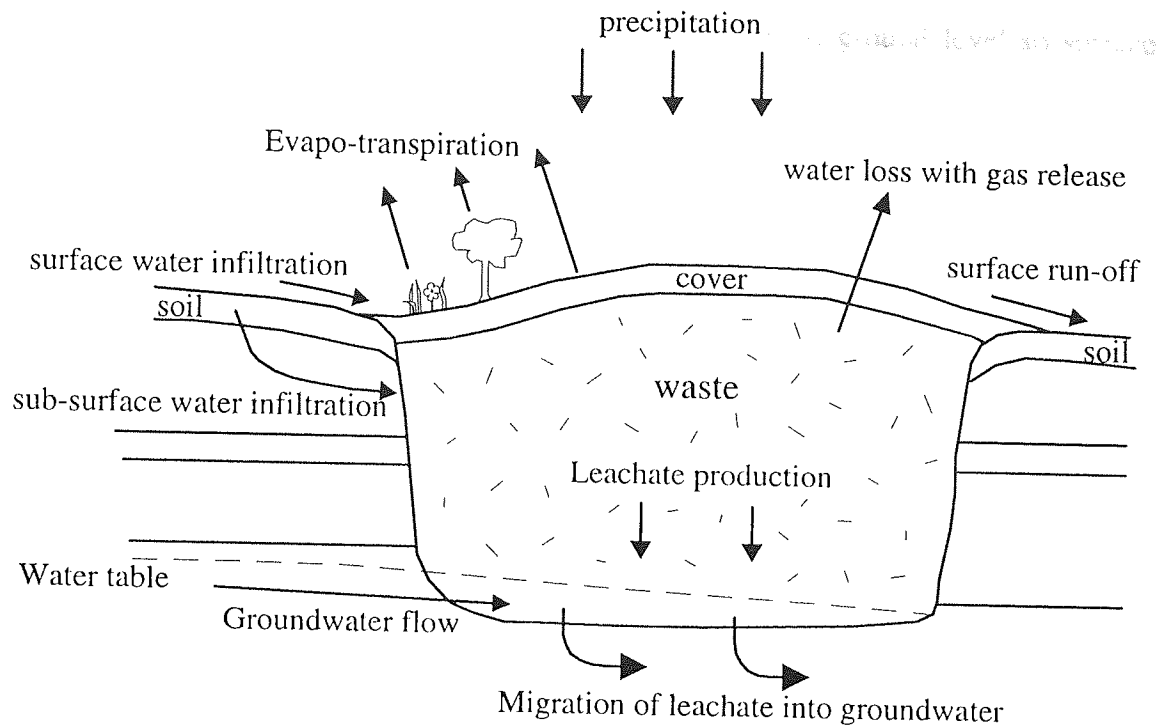
Figure 3.6. Landfill water balance (adapted from DoE, 1992c).

The amount of mobile leachate depends on a number of physical processes, namely infiltration, evapo-transpiration, absorption into and adsorption onto the waste. These factors are summarised in equation 3.3.

$$L_o \propto I - E - A \qquad \text{(eq. 3.3)}$$

Where: L_o = Free mobile leachate [m³/tonne].

I = Infiltration (from precipitation, surface, sub-surface and groundwater infiltration and including water contained in deposited waste) [m³/tonne]

E = Evapo-transpiration (from plants, surface evaporation and water vapour in escaping gases) [m³/tonne].

A = Absorptive and adsorptive capacity of the waste [m³/tonne].

The free mobile leachate can move through the site under the influence of gravity and will make its way down towards the base of the site. Figure 3.6 shows the water table over the base of the site giving leachate an easy pathway out of the site.

As most UK landfill sites are below ground level the major problem for leachate control is movement into groundwater. In lowland countries, such as the Netherlands, where waste is built up in domes because no void spaces are available

('air' fill as opposed to 'land' fill), the base of the site is at ground level so surface leachate is more of a problem.

The amount of leachate actually leaving the site is one of the most important considerations when deciding how polluting a landfill site is. It is dependant on:

a) the presence/absence and integrity of liner. Liners are engineered to hinder or completely stop the egress of leachate from the site.

b) effectiveness of leachate pumping if present. Pumping from the base of the site to the surface can greatly reduce the leachate passing through the base of the site.

The physical nature of a site will influence the path leachate takes if it migrates from the site boundary. It can cause problems in three ways:

i) Surface soil - the toxic components can kill surface vegetation (this is a more common problem for 'airfill' sites since the waste is above the local ground level).

ii) Surface water - if leachate enters a surface water course its reducing nature will deplete the oxygen content of the water. This may cause the extinction of all oxygen dependent life and metals may pass into the food chain.

iii) Groundwater - if leachate passes into the local groundwater in sufficient quantities to pollute it may take many years for the groundwater quality to recover to pre-polluted levels.

3.5.2. Leachate Treatment

Leachate treatment is designed to reduce its polluting effect. The simplest method is leachate recirculation which is basically pumping it from the base of the site and spraying it back over the waste. Spraying has a threefold effect on the strength of the leachate which are:

a) aeration of the leachate, oxidising some of the harmful elements;

b) enhancing evaporation thus reducing the volume of the leachate;

c) increasing the attenuation process by forcing it to pass through the waste once more.

Artificial treatment methods can only be achieved once the leachate has been extracted from the site. A list of treatments are listed below:

i)   biological anaerobic or aerobic systems (effective on the organic components);

ii) chemical oxidation and reduction (for inorganic and organic components);

iii) precipitation (using hydroxides to remove metal ions);

iv) air stripping (for removing ammonia);

v)   carbon adsorption (for organic and inorganic constituents).

The treatment applied at a site, if necessary, will depend on the quality of the leachate present. If no data is available then experience gained at other sites which are depositing a similar wastes should be taken into consideration in the treatment system design. Often the leachate is sent directly to a foul water sewer and dealt with by the receiving wastewater treatment plant. However the leachate must meet certain prescribed discharge criteria to prevent overloading the receiving sewage works.

3.5.3. Leachate Monitoring

It is essential to monitor the build up or migration of the leachate to verify the integrity of the measures taken. Any leachate pumped to the surface should be periodically sampled especially if it is to undergo subsequent treatment to make sure it is not too strong for the receiving system. If the leachate is to go to a foul water sewer it should be sampled to determine whether it meets the discharge consent or licence given by the water authority.

The level of leachate in the site should be measured regularly to ascertain whether it is building up in such quantities that may bring into question the integrity of the liner, if one is present.

During the site preparation stage a number of monitoring boreholes should be sunk around the site. The number and position of the boreholes will vary depending on the site geology, the size of the site, the presence of an aquifer and the proximity of buildings. A background measurement groundwater quality should be taken from the boreholes before landfilling takes place with samples taken on a regular basis.

3.6. Landfill Gas

The main components of landfill gas from mature wastes are methane and carbon dioxide. The process of landfill gas production in a landfill from the moment waste is deposited to the point where all the carbonaceous material has degraded can be separated out in to five distinct stages (Farquar & Rovers, 1973). Figure 3.7 is a graphical representation of the five stages showing gas concentration against time.
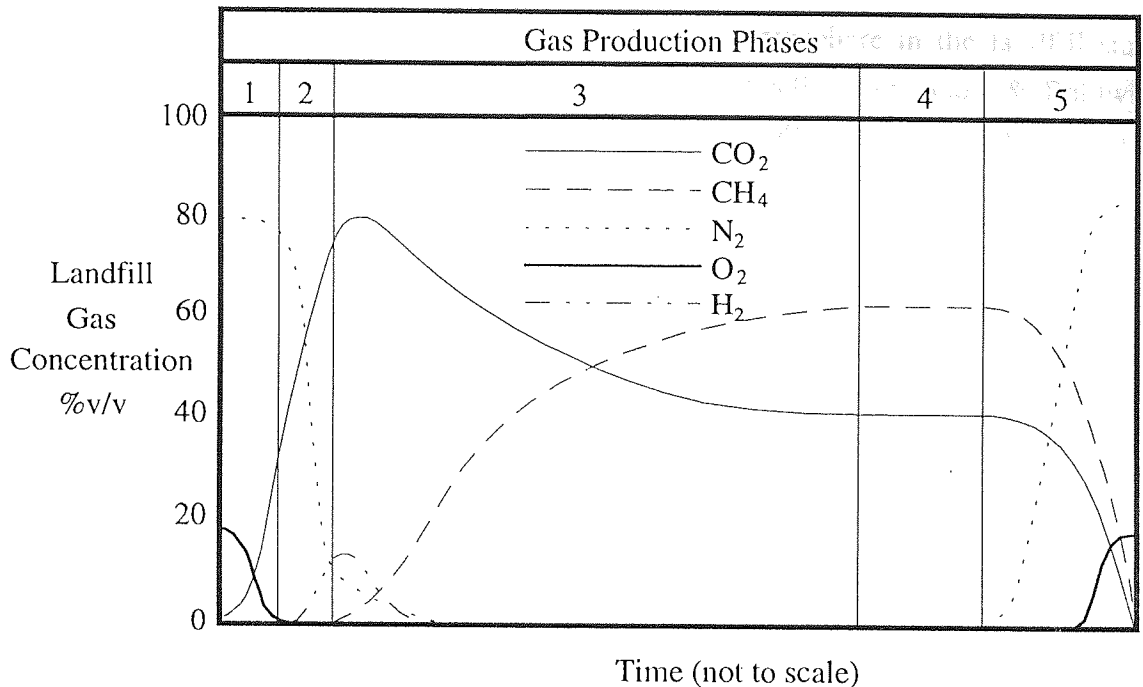
Figure 3.7. Idealised landfill gas composition variation over time (adapted from Farquar & Rovers, 1973).

The five stages shown is figure 3.7 are described in detail as follows.

Stage 1 - Before any decay has taken place the gases present are made up by air. Degradable waste is attacked by aerobic micro-organisms consuming the oxygen in the entrapped air and forming simple organic compounds, CO_2 and H_2O. Heat is generated and the organisms multiply accelerating the degradation and subsequently the oxygen consumption.

Stage 2 - This stage begins when all the oxygen had been consumed by the micro-organisms or displaced by CO_2. The aerobic organisms expire and are superseded by anaerobic ones which start producing hydrogen as a by-product. These are able to break down the larger organic molecules (food, paper etc.) into smaller compounds (CH_4, NH_3, CO_2, H_2O and small organic acids).

Stage 3 - Stage 3 begins with the commencement of CH_4 produced by anaerobic methanogenic bacteria which break down organic acids as in equations 3.1 and 3.2. As the bacteria become prevalent the gas mixture in the waste eventually consists of only CH_4 and CO_2.

The time scale for the first three stages can be from only a few weeks to up to a year depending on prevailing conditions.

46

Stage 4 - An equilibrium occurs where the atmosphere in the landfill stays consistently at 35-40% CO_2 and 60-65% CH_4 (Campbell, 1985, Scott & Baldwin, 1989, Parsons & Smith, 1986, Attal et al, 1992, DoE, 1992a and DoE, 1992c) and at this point the gas is termed 'mature'. Stage 4 is the main gas producing period and can last from five years to decades.

Stage 5 - When all the degradable substances have been exhausted no more landfill gas is produced and gradually the atmosphere reverts back to the original levels at the start of stage 1 - normal air concentration.

Although methane and carbon dioxide are the major components of landfill gas there are a number of minor constituents as listed in table 3.2.

	Typical value	Observed	Reasons for unusually high

Others not included above	0.00005	0.025	deposited

Table 3.2. Observed ranges of components in landfill gas in UK landfill sites. Values are % by volume (DoE 1992c).

3.6.1. Landfill Gas Migration

Gas has a much greater migration potential than leachate as its movement is not governed by gravity. This was brought poignantly to light in Loscoe, Derbyshire, where a house was virtually destroyed when gas migrated over a hundred metres beyond the boundaries of a nearby landfill site and ignited (Tankard. 1987). Figure 3.8 shows a number of ways that landfill gas can migrate from a landfill site.
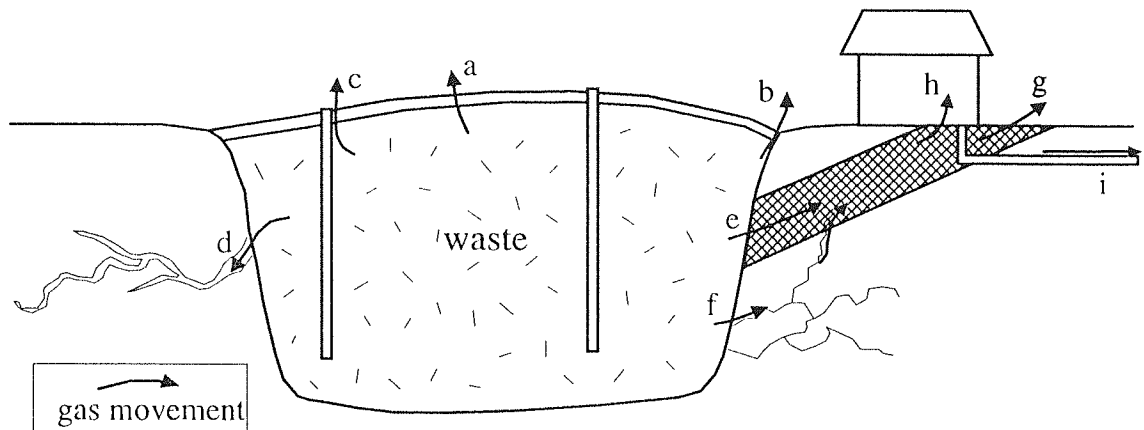
Figure 3.8. Landfill gas migration pathways to the atmosphere (adapted from DoE, 1992a).

Gas can escape from the site in the following manners (letters refer to figure 3.8):

1. through the cover materials via desiccation or other cracks in the cap (a), settlements cracks at the site perimeter (b) or features that provide vertical pathways such as leachate or gas wells (c),
2. through caves/cavities (d),
3. into permeable strata (e),
4. into cracks from explosions related to the previous quarrying etc. (f).

If the gas escapes through subterranean pathways it can reach the surface :

i) straight to the atmosphere (g),
ii) into buildings (h),
iii) along service conduits or culverts (i).

In addition to the to gas directly migrating from the site, gas may be formed by the secondary degradation of leachate which may have itself migrated from the site.

3.6.1.1. Prevention of Gas Migration

Because of the problems that may be encountered with landfill gas, effective measures have been developed to prevent the gas from migrating beyond the boundaries of the site.

There are three main procedures that can be undertaken to minimise the effect of landfill gas migration (from DoE, 1992a and DoE, 1992c) which are shown on figure 3.9.

a) Impermeable barriers

These are the liners as mentioned in section 3.3.4 and are constructed so nothing can pass through them. They are placed between the waste and the outer edge of the site as shown on figure 3.9. If the liner was in place to prevent leachate migration it would lie on the base of the site inhibiting downward movement of mobile fluids.

b) Passive venting

This system uses a porous media placed between the waste and the edge of the site. It provides a route of least resistance to the gas and directs it upwards and into the atmosphere. The media can be large pebbles, gravel, bricks or lumps of concrete as long as there are interconnected void spaces that lead to the surface.
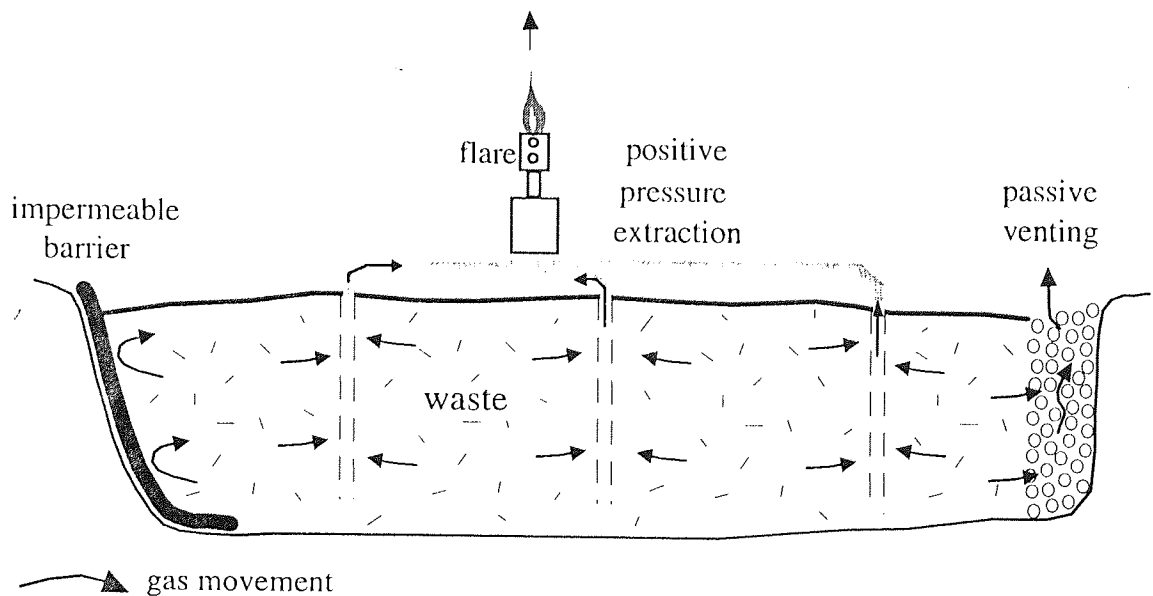
Figure 3.9. Three methods of gas control.

c) Positive pressure extraction

This system requires the greatest resources and needs periodic maintenance. A number of holes are either bored into the waste or are constructed during filling in which perforated pipes are situated with a porous media placed around them. A system of pipes lead from the head of each hole to a pump which physically sucks the gas out. The gas is then often burned and the combustion products are released to the atmosphere.

The alternative to flaring the gas is to utilise it for heating buildings or producing electricity and supplementing the national grid with the added bonus of being a non-fossil fuel (Couth & Rumbold, 1992 and Slim & Jones, 1992). For a successful gas utilisation system experience has shown the following criteria are necessary (from DoE, 1992c):

- minimum depth of 10 metres;
- at least 0.5 million tons of waste;
- waste age between 5 and 10 years;
- the water table should be at least 5 metres below the base of the site - saturated conditions hinder gas collection.

Based on the above criteria, most landfills can not economically utilise the gas and commonly employ passive methods or flaring to control gas. If a positive extraction system is used the pumping rate should be set at the same rate as gas production otherwise air may be drawn in to the landfill. As well as increasing the amount of CO_2 and oxygen in the gas it may reduce the methane content to such a degree that the flare blows itself out and simply vents to the atmosphere untreated (Crutcher et al, 1982).

3.6.2. Monitoring

Current UK legislation requires monitoring for gas (CO_2 CH_4 and O_2) during filling and following completion (DoE, 1992a, DoE, 1992b and DoE, 1992c). This usually takes the form of boreholes on and around the site. The boreholes have to be monitored on a regular basis as gas production has been shown to be erratic (Bagchi & Carey, 1986) and influenced by atmospheric pressure (Bogner, 1986). If a site is using a flare the operators should monitor the gas entering the stack to check the composition in order to adjust input valves and maintain an optimum gas mixture.

3.6.3. Problems Associated with Landfill Gas

The problems that are associated with landfill gas are varied. The two main constituents, methane and carbon dioxide, can pose an asphyxiation risk if they displace the oxygen in a confined space such as culverts, basements or badly ventilated buildings. If methane, specifically, accumulates in concentrations 5-15% by volume with air there is a risk of explosion and the most likely places where this may occur are again culverts, basements or badly ventilated buildings but also voids in the landfill site, which may cause underground fires.

Both CO_2 and CH_4 are greenhouse gasses and contribute to the greenhouse effect and global warming, although methane is by far the most significant. The methane produced by UK landfill sites has been identified as a major portion of the UK's methane budget and measures are to be taken to reduce the current emissions (DoE, 1994).

Some of the minor constituents of landfill gas are odorous (e.g. aromatics, organic acids and esters) and may cause a nuisance if the conditions allow. The odours tend to be greater when aerobic degradation occurs, for instance when the waste is stored above ground prior to deposition. Generally, this can be avoided if the waste is covered immediately on arrival (DoE, 1992b).

More information on the above problems can be found in the standard texts stated in section 3.1 as well as DoE (1994).

Landfill gas has been proven to damage vegetation and because of the significance of this to the project it is dealt with in greater detail in the following sections.

3.6.4. Landfill Gas Effects on Vegetation

Much literature has been devoted to documenting the effects of landfill gas on vegetation (Campbell, 1989, Leone et al, 1977, McRae & Hewitt, 1986, Tankard, 1986 and Pankhurst, 1973) as it can be affected by some of the constituents and subsequent effects of landfill gas. There are four main ways that this can occur:

i)   lack of oxygen;

ii) toxicity of CO_2;

iii) increase in the acidity of the soil due to the dissolution of CO_2; and

iv) anaerobic/reducing conditions of soil permitting the release and build up of metals such as zinc, manganese and iron in toxic quantities.

Plants need oxygen in the root-zone to grow and it is normally supplied by air circulating through the soil. If the oxygen concentration drops below 12% by volume this can prove to be detrimental (Pankhurst, 1973). If oxygen is present in the root-zone but in subnormal amounts this is termed hypoxia and if there is no oxygen at all this is termed anoxia (Levitt, 1980).

CO_2 has proved to be the component in landfill gas that is harmful to plants. Flower et al (1978) found this to be the case when experimenting with tomato plants. In concentrations over 5% by volume CO_2 has adverse toxic effects on vegetation as well as displacing oxygen from the root-zone (Pankhurst, 1973) and also interferes with the water transport mechanisms causing wilting (Pankhurst, 1973 and Levitt, 1980). In addition it impedes respiration which causes the build up of toxins such as pyruvate, ethanol and lactate (Levitt, 1980).

Although methane has been shown to be non-toxic to plants (Flower et al, 1978) it can cause anoxic conditions in two ways. Firstly, if it displaces the oxygen hypoxic conditions are initiated and secondly it can oxidise to CO_2 which has the double effect of depleting oxygen and increasing CO_2 (Flower et al, 1981, Pankhurst, 1973 and McRae & Hewitt, 1986).

CO_2 is known to dissolve in water to produce carbonic acid. Excess acidity can affect the vegetation as well as creating reducing conditions in the root-zone (Pankhurst, 1973). The reducing capability of the soil can mobilise toxic elements such as zinc, manganese and iron (Flower et al, 1981 and McRae & Hewitt, 1986).

Some of the minor constituents of landfill gas also play a part in harming vegetation. Flower et al (1978) measured considerable die-back in barley, rye, oats and wheat with only a few parts per million of ethylene and McRae & Hewitt (1986) have measured ethylene over 30ppm in some affected soils.

The degree of harm is dependent on a number of factors among which are: the susceptibility of the plant to the toxins; the soil characteristics and; the depth of the root penetration into the soil (Sangrey & Philipson, 1979 and Jones, 1991). Plants that are hardier to this particular type of interference will clearly survive better but will eventually succumb at some point. Coarser, better aerated soils will have greater air circulation which will dissipate the harmful elements in the root-zone thus reducing the toxic effects (Jones, 1991). For similar reasons vegetation with shallow root systems will experience considerably more air circulation than those with deeper roots explaining why trees are often more affected than other smaller plants (Flower et al, 1981 and Leone et al, 1977).

This literature review reveals a number of ways that leachate and landfill gas show themselves. Both leachate and landfill gas have toxic components and can damage vegetation. They also are produced in a biochemical reaction system that generates heat. These effects can be detected by remote sensing techniques and the application of such methods to this problem is discussed in chapter 4.

4. Remote Sensing

4.1. Introduction

> "Remote sensing is the science and art of obtaining information about an object, area or phenomenon through the analysis of data acquired by a device that is not in contact with the object, area or phenomenon under investigation."
>
> Lillesand and Kiefer (1986)

This definition of remote sensing can be applied to any process that gathers information about an object without being in contact with it. When remote sensing as a term was coined in 1960 (Curran, 1985) it included aerial photography and some geophysical methods. For any remote sensing method there has to be a phenomenon that conveys the information from the object under investigation to the sensor. Electro-magnetic radiation is the phenomenon that allows aerial photography to work. In the case of the geophysical methods the phenomena can be a magnetic field (magnetometry), an electric field (conductivity/resistivity) or a pressure wave transmission through another medium (seismology or sonar).

Since 1960 the meaning of remote sensing has altered to refer to:

> "...the use of electromagnetic radiation sensors to record images of the environment which can be interpreted to yield useful information."
>
> Curran (1985)

The above streamlined definition now describes more accurately how remote sensing is applied at the moment and was generally adopted with the increased use of artificial satellites for observing the earth, particularly the first of the Landsat series of satellites which was launched in 1972.

Now there are literally dozens of remote sensing satellites currently in orbit along with many more airborne systems and probably thousands of aerial photography cameras in continual use. With the recent developments in video camera technology and the enormous improvements of computers the use of remote sensing is likely to expand further in the future.

This chapter addresses some of the principles of remote sensing focusing on those used in the project, paying particular attention to passive sensors. For more general information the reader is directed to standard texts such as Colwell (1983), Lillesand and Kiefer (1986), Barret and Curtis (1992), Curran (1985), Open University (1989) and Drury (1990).

4.2. The Principles of Remote Sensing

Most remote sensing systems utilise electro-magnetic radiation. However, not all of the spectrum can be put to use. Remote sensing techniques employ only the radiation from ultra-violet to microwaves and figure 4.1 shows this part of the spectrum.

Wavelength

| 100nm | 500nm | 1μm | 5μm | 10μm | 50μm | 100μm | 500mm | 1m |

| ultra violet | visible | near infra-red | thermal infra-red | microwaves | radio waves |

| visible region |
| blue | green | red |

| 400nm | 500nm | 600nm | 700nm |
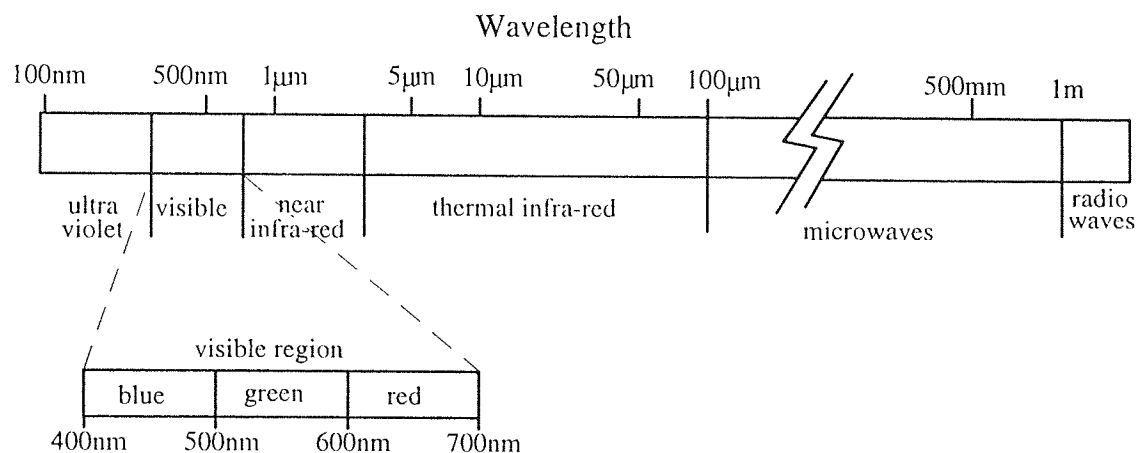
Figure 4.1. The regions of the electro-magnetic spectrum used for remote sensing (adapted from Open University, 1989).

There are two fundamental ways in which remote sensors work; actively or passively. Active sensors generate the radiation themselves, emit a pulse and measure the returning signal when it has reflected off the object under investigation. The most common form is Radar (RAdio Detection And Ranging) which utilises microwaves and was developed in the 1940s. Microwaves are ideal for this purpose because of their lack of attenuation in the atmosphere, the low energy requirements to produce them and their ability to reflect off most solid objects. Active sensors were not used in this project so will not be considered any further. For more information on Radar see Trevett (1986) and also the standard texts cited in section 4.1.

Passive remote sensors utilise the radiation emitted by other sources. They either measure the intensity of solar radiation that has been reflected by the objects under investigation, or the radiation generated by sources on the earth's surface. Passive sensors are the most common type of remote sensor and use radiation from ultra-violet to thermal infra-red for aerial photography, video cameras, and most airborne and satellite scanning systems. The three former systems are used in this project, so are dealt with in some detail.

All objects will emit radiation if they have a temperature greater than absolute zero ($^-273.16°C$ or 0K). The amount they emit depends on their temperature and their

emission characteristics. An object that emits radiation comparable directly with its kinetic temperature (see section 4.2.2.1) is known as a black body although it is an idealised concept. The sun emits radiation as a black body at 6000K as shown in figure 4.2. The peak coincides with the green part of the spectrum (0.5-0.6μm), the region in which the human eye is most sensitive
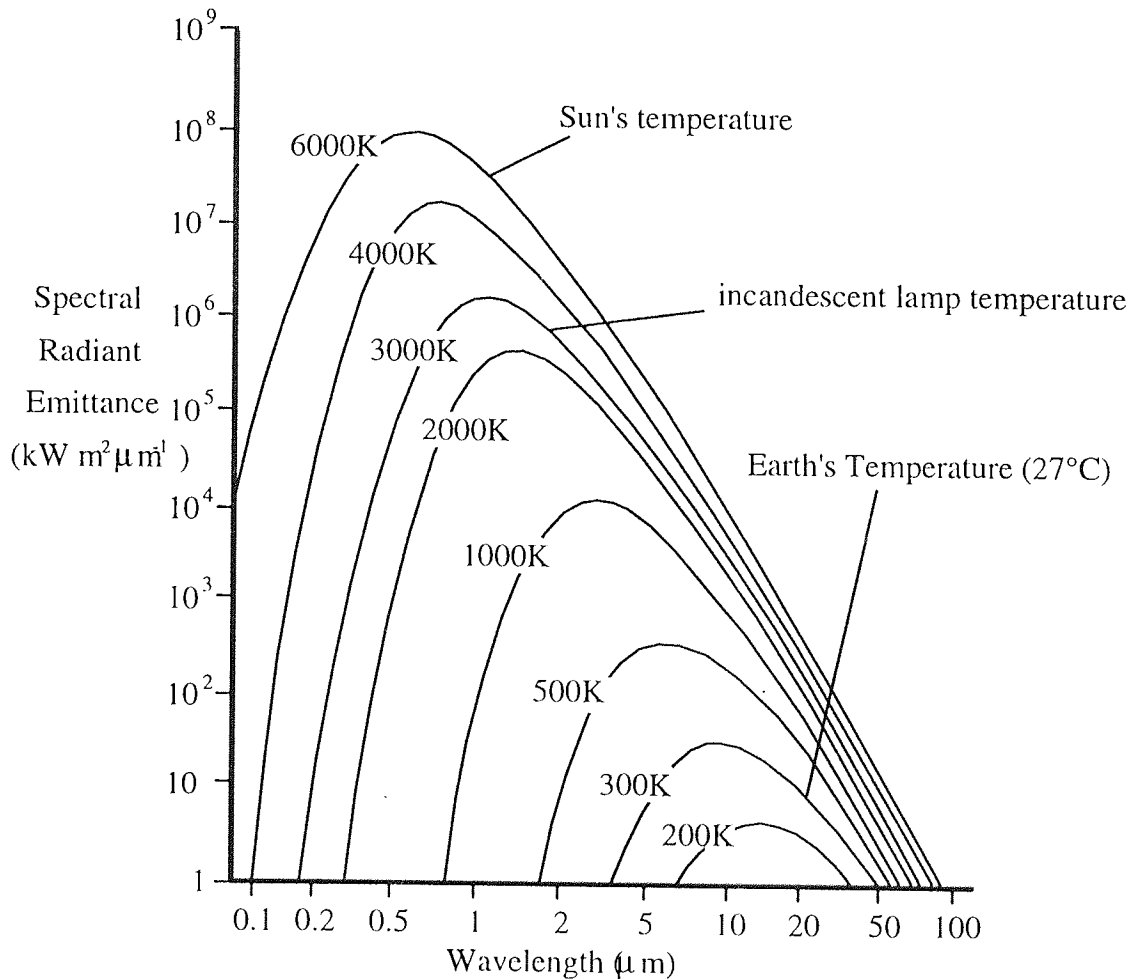
Figure 4.2. Spectral radiant emittance for a black body at a variety of temperatures (adapted from Drury, 1990).

The earth emits radiation consistent with an object at a temperature of approximately 300K (27°C). It is because the earth's emitted radiation is separable from solar radiation, when taking into account the actual values measured at the earth's surface, that the region is important for locating warm areas on the surface of the earth (see section 4.2.2).

4.2.1. Attenuation of Radiation by the Atmosphere

Not all of the incoming solar radiation can be detected by remote sensing techniques due to interactions in the atmosphere. The two main attenuation processes are scattering (re-direction of light energy) and absorption (removal of light energy). Figure 4.3 shows how light is intercepted or interrupted in the atmosphere. Light that arrives at the surface is either sunlight, if directly from the sun, or 'skylight' (Lillesand and Kiefer, 1986) if it has been re-directed by any scattering process. Light that has been re-directed back upwards and does not interact with the ground is termed 'airlight' or 'hazelight' (Lillesand and Kiefer, 1986).

Aston University

Content has been removed for copyright reasons
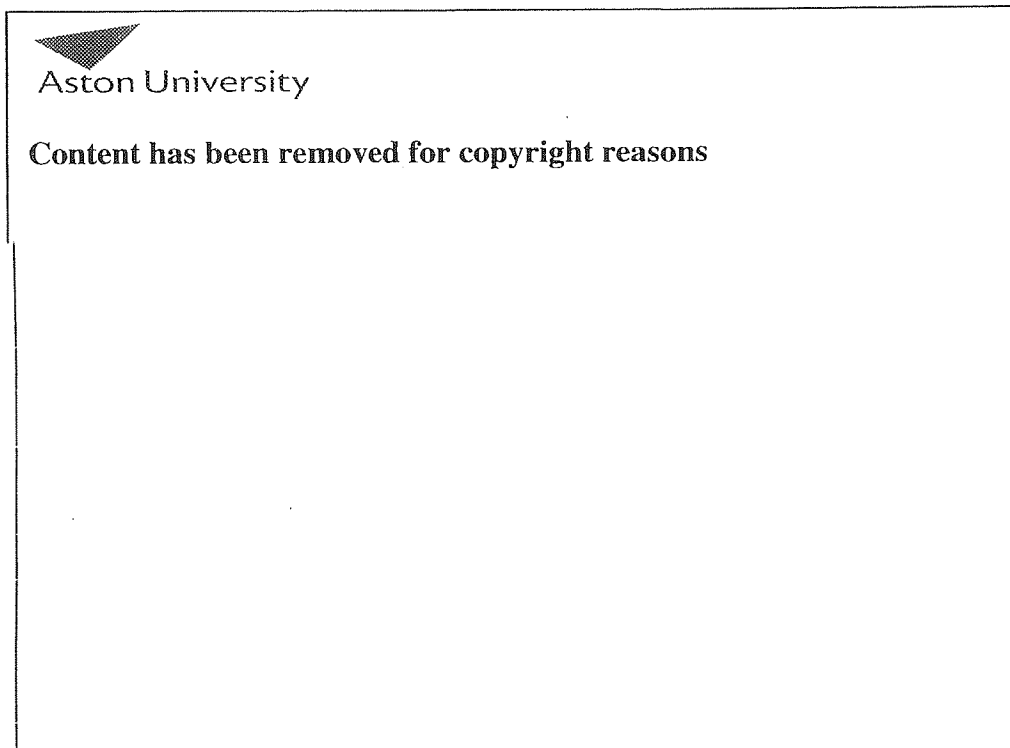
Figure 4.3. The interactions experienced by solar radiation as it passes through the atmosphere. (Open University, 1989).

4.2.1.1. Scattering

Scattering occurs when the incoming radiation is deflected by particles in the atmosphere either causing the radiation not to reach the surface at all or delaying it in such a way that diffuse, non-directional light is produced. There are three main types of scattering that affect visible and near-visible wavelengths: Rayleigh, Mie and non-selective. The form which occurs is a function of the relationship between the wavelength of the radiation and the size of the particles/molecules with which it interacts.

Rayleigh scattering

Rayleigh scattering is the reason why the sky appears blue. The shorter wavelengths of light (as far as the visible spectrum is concerned, the blue portion, see figure 4.1) are scattered in all directions by the molecular particles in air, mainly nitrogen and oxygen. The amount of scattering increases with the reduction in wavelength so in the ultra-violet region the interaction is more pronounced.

Mie scattering

Mie scattering occurs when the incoming radiation interacts with particles that have a similar diameter to the wavelength. In this case the most common culprits are water vapour, smoke particles and fine dust. The scattering occurs at the longer visible wavelengths, mainly the yellow/orange/red part of the visible spectrum, and is often responsible for red sunsets especially after volcanic eruptions or desert storms.

Rayleigh scattering is frequently more pronounced than Mie scattering with the sky usually taking on a blue hue. As Mie scattering gains more influence, by way of an increase in atmospheric particles, the sky can on occasion become almost white.

Non-selective scattering

This form of scattering is produced by particles that are much greater in diameter than the wavelengths they act upon. Water droplets, which can range in size from 5 to 100μm, are the main cause of such scatter. All visible and infra-red light is affected irrespective of wavelength and so this form of scatter is termed non-selective. Red, green and blue light are scattered equally by this mechanism causing fog and clouds to appear white.

4.2.1.2. Absorption

In addition to scattering, there is direct absorption of incoming solar radiation by molecules in the atmosphere. The major components responsible for the absorption are H_2O, CO_2 and oxygen in the form of O_2 and O_3 (ozone).
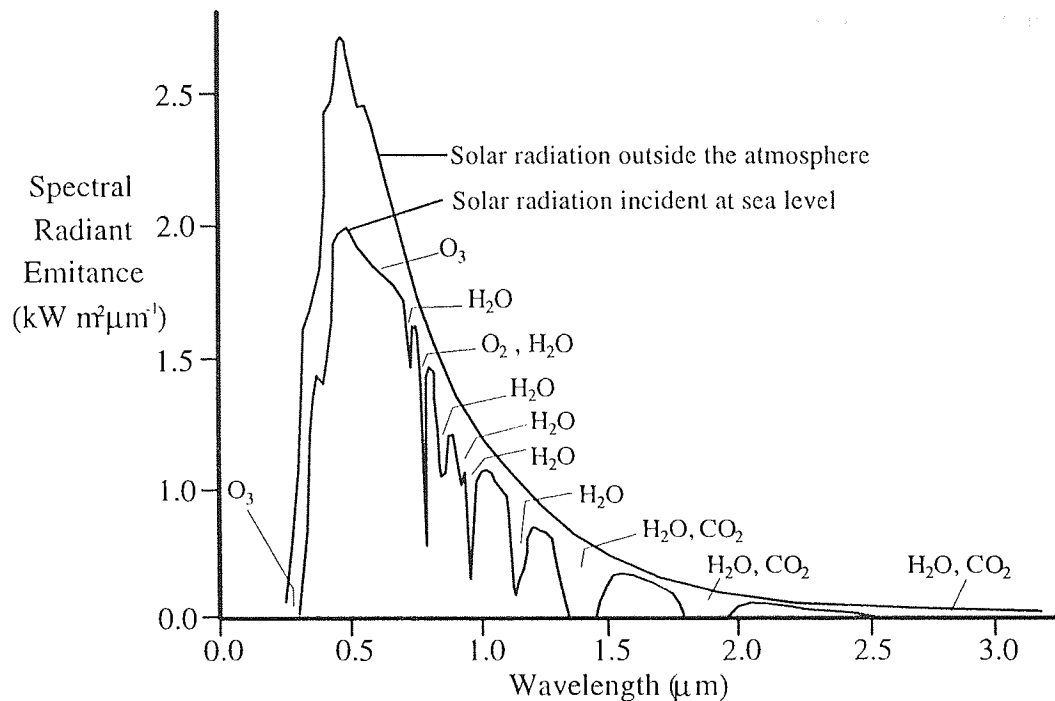
Figure 4.4. Absorbance of radiation by the atmosphere (adapted from Drury, 1990).

Figure 4.4 shows that for certain parts of the spectrum little or no radiation reaches the earth's surface at all because of absorption by the aforementioned atmospheric constituents. Note that the logarithmic vertical scale of figure 4.2 is much greater than the linear vertical scale on figure 4.4. Figure 4.2 shows the radiant emittance at the surface of an ideal emitter whilst figure 4.4 shows the emittance measured at the edge of the earth's atmosphere. The intensity of the sun's radiation experienced at the earth's surface will be considerably less that at the surface of the sun due to the distance between the two It is worth noticing that there is absorption by O_3 in the 0.2-0.4μm portion of the spectrum. The O_3 that absorbs at this point is present as the threatened ozone layer that fends off the harmful ultra-violet rays.

The portions of the spectrum where there is little or no absorption are known as atmospheric 'windows'. In the other regions where there is significant absorbance the amount of radiation reaching the surface is greatly reduced making its detection difficult or impossible. The sensors that are made to detect the reflection of solar radiation are designed to be sensitive in the 'windows'.

4.2.2. The Thermal Region

The far infra-red part of the spectrum (approximately $2\mu m$ to $100\mu m$, see figure 4.1) is known as the thermal infra-red region. This is because the peak output of a black body radiating at 300K (the approximate temperature of the earth) spans this region (see figure 4.2). Of the whole thermal range, only the portion from $2\mu m$ to $15\mu m$ is utilised in remote sensing.

Any energy detected by a remote sensor in the thermal region has a different source from near infra-red and visible radiation. Whilst visible and near infra-red radiation is due to the reflection of solar energy, anything detected beyond $4\mu m$ is due to an object emitting on the earth's surface. Figure 4.5 shows how solar radiation is only measurable at the earth's surface from $0.3\mu m$ to $4\mu m$ and outgoing thermal radiation covers the region $4\mu m$ to $25\mu m$ with practically no overlap between the two.
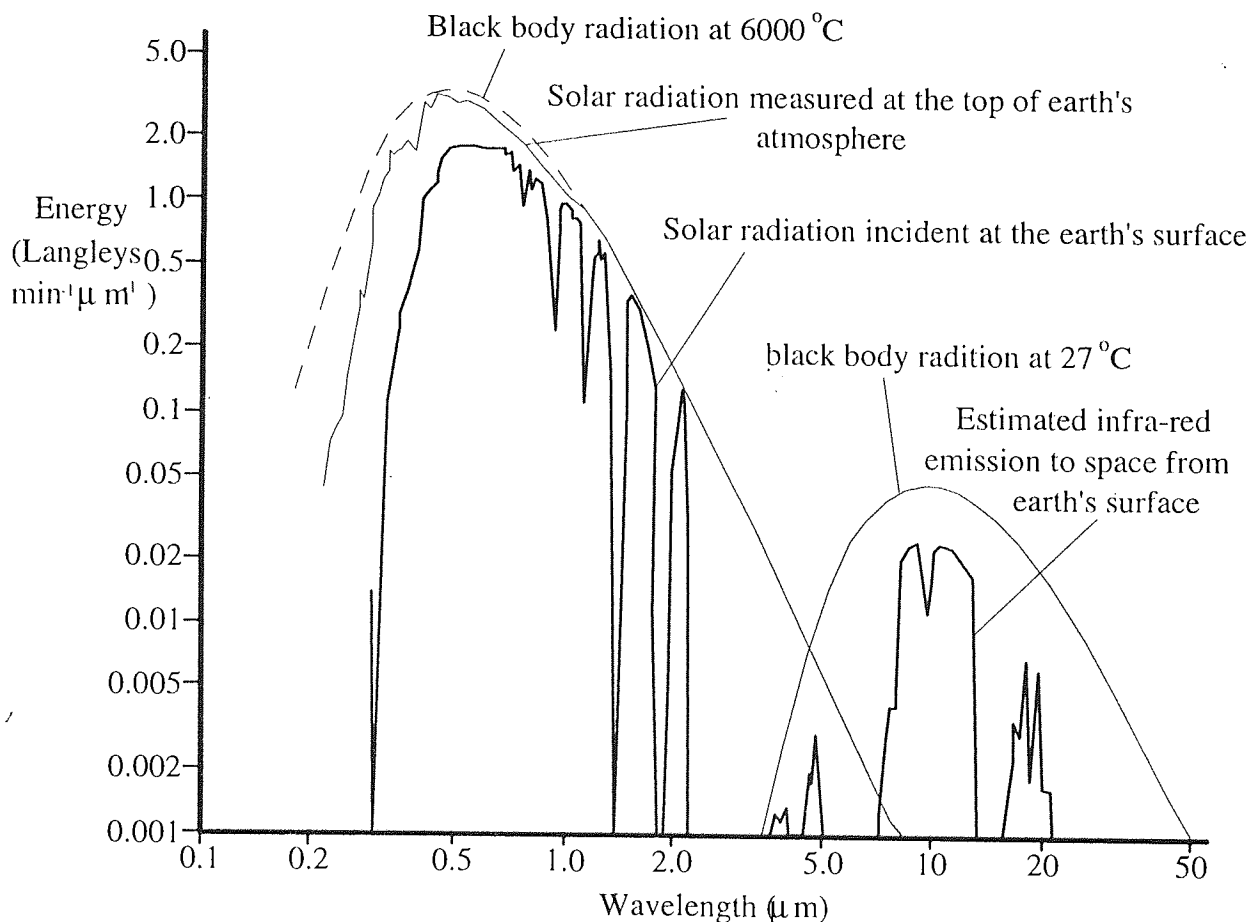
Figure 4.5. Comparison of incoming solar radiation measured at the top of earth's atmosphere to the estimated thermal radiation emitted from the earth's surface (adapted from Sellers, 1965). NB. 1 Langley = the energy needed to raise the temperature of 1g of water from 14.5°C to 15.5°C.)

There are two main reasons behind how an object can gain enough heat to emit radiation in sufficient quantities to be detectable by a thermal infra-red sensing system. The first entails the object absorbing solar radiation, heating up and then emitting thermal radiation at the appropriate wavelength. This effect is significant during the day and the objects that stand out on an image will be those that heat up quicker than their neighbours. The second reason is that the object itself is producing the heat for a reason other than the absorbance of solar radiation (i.e. combustion processes). To differentiate the second form from the first a survey would have to be carried out at night or very early morning. This is to allow as much of the heat from the sun acquired during the day as possible to dissipate, and not to allow any further solar warming by performing the survey prior to sunrise.

4.2.2.1. Emissivity

Every object warmer than absolute zero (0K or $-273.16°C$) contains atoms and molecules that vibrate. The intensity of this vibration determines the kinetic temperature which is measurable by a mercury thermometer or similar contact device. While an object has vibrating constituents it will radiate energy depending on its kinetic temperature. If the object radiated like a black body the radiated temperature would equal the kinetic temperature.

Black body radiators are rare, though, and the relationship between the two kinds of temperature follows equation 4.1:

$$T_{rad} = \epsilon^{¼} T_{kin} \qquad\qquad\text{(eq. 4.1)}$$

T_{rad} = radiant temperature

T_{kin} = kinetic temperature

ϵ = emissivity

The level at which a material emits radiation in relation to its temperature depends on the emissivity (ϵ). It is the radiant temperature that is measurable using remote sensing techniques but to be able to determine the kinetic temperature the emissivity needs to be ascertained first.

Emissivity is a ratio of a material's ability to emit radiation in comparison to that of a black body at equivalent temperature and is defined as:

$$\text{Emissivity } (\epsilon) = \frac{\text{Radiant emittance from an object at a given temperature (K)}}{\text{Radiant emittance from a black body at a given temperature (K)}}$$

where the values of emissivity range between 0 and 1. Some examples of how the emissivity governs the perceived temperature are given in table 4.1. A more comprehensive list of emissivities is tabulated in Appendix C.

Material	Emissivity	Kinetic Temperature	Radiant Temperature

Table 4.1. Four materials at a kinetic temperature of 300K compared to their radiant temperature (values from Lillesand and Kiefer, 1986).

The heat capacity of a material will influence its temperature at varying times of the day. Materials that heat up quickly, whether from increased air temperature or direct absorbance of solar radiation, will also cool down rapidly once the sun sets and the air temperature drops.
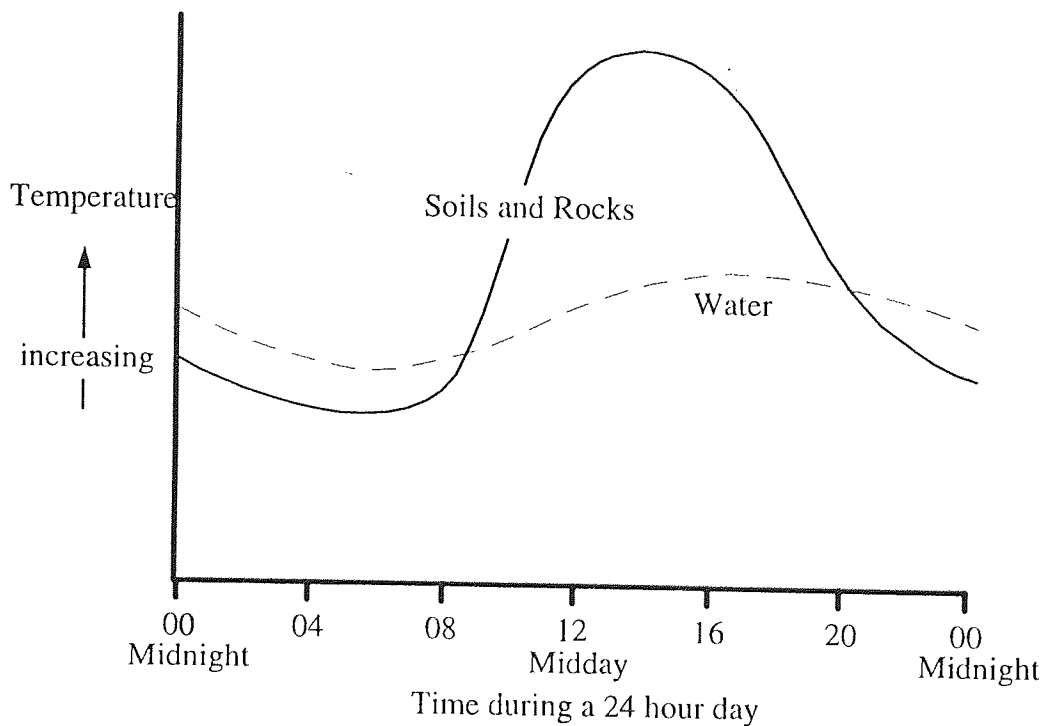
Figure 4.6. A generalised diurnal trace of the temperature of water compared to soils and rocks over a 24 hour period. (adapted from Lillesand and Kiefer, 1986).

Figure 4.6 shows a generalised diurnal temperature variation for water and soil and rocks. Water has a relatively high heat capacity, and consequently a high thermal inertia, so warms up slowly during the day and cools down slowly at night producing a small temperature variation. Soil and rocks, on the other hand, warm up relatively quickly and lose the stored heat rapidly giving rise to a greater temperature variation over a 24 hour period. Vegetation, because of the high water content, has a high thermal inertia and will have a diurnal trace somewhere between the two traces on figure 4.6.

4.3. Remote Sensing Systems

There are a wide variety of remote sensing systems available but only those used in this project are described in detail. The reader is directed to the texts cited in section 4.1 for more information.

There are three systems that are employed in this project; aerial photography, an airborne line-scanner and an airborne video camera. Photographs produce an image through chemical means by utilising light sensitive substances that undergo a permanent chemical change when struck by specific wavelengths of electro-magnetic radiation. Line-scanners and video cameras produce images electronically by measuring the intensity of radiation falling on a detector and converting the response into electrical signals which are then stored on digital media (computer, magnetic disk/tape or optical disk) or analogue media (video tape).

4.3.1. Aerial Photography

Aerial photography is the oldest form of remote sensing and was in use long before the expression was coined. The potential for monitoring the earth from the air was recognised over a century ago, with the first experiments taking place during the 19th century, by suspending cameras from balloons or even arrays of kites.

The advent of powered flight furthered its progress, but it was the First World War that stimulated the development of aerial photography. The combination of the advancement of flight, the rapidly developing photographic technology and the need for reconnaissance provided the opportunity for the technique. Before the First World War most of the aerial photographs taken were in oblique format (taken at an angle from the vertical). It was found that more information could be by obtaining three-dimensional images using stereo pairs of vertical photographs. The use of vertical stereo pairs (see section 4.3.1.3) is now the most widely employed aerial photographic technique and can be tailored to the individual needs by the selection of appropriate lenses, film types and type of aerial platforms.

There are three basic types of photograph: Black and white (or monochrome), normal colour and false colour composite (FCC). If sufficient coverage is achieved then the images can be viewed in three dimensions with the aid of a stereoscope.

For more detailed information on aerial photography the reader is directed to texts such as Avery and Berlin (1992), the Royal Institution of Chartered Surveying (1984) and Graham and Read (1986), Dumbleton (1983) and those cited in section 4.1.

4.3.1.1. Factors Affecting Photographic Quality

Two important factors which determine he quality of a photograph are the ability to discern detail and discrepancies of scale across the image.

The scattering and absorbance of light as it passes through the atmosphere, particularly at shorter wavelengths (the violet region of the spectrum) as described in section 4.2.1, can cause the photograph to appear 'foggy'. To alleviate this effect yellow filters, which block blue light, are placed over the lens reducing the visible haze.

The differences in scale across an image that are experienced are due to inconsistencies in the geometry of flight usually due to turbulence. The deviations in the flight are roll, pitch and yaw with the additional problem of altitudinal variations whether by the aircraft changing altitude of the terrain relief altering rapidly.

Roll and pitch cause the ratio of the distance from the film to the lens and from the lens to the ground to be non-uniform for all parts of the image. If the aircraft tilts in any manner moving the line-of-sight of the camera from the vertical, the ratio becomes inconsistent across the image. The effects of discrete roll and pitch distortion are shown in figures 4.7 and 4.8 respectively. If these two effects combine the distortion is even more pronounced as shown on figure 4.9. Photographs can be assumed to be vertical if the deviation from the vertical does not exceed 3° (Avery and Berlin, 1992).

In general these flight irregularities are almost always present making it difficult to take any quantitative measurements directly from the photographs. Figures 4.7 to 4.9 are exaggerated and customarily actual photographs produced have only subtle distortions. Although the dimensions taken from the photographs cannot be relied upon, the interpretation of ground features is not a problem. Photogrammetric methods do exist that enable accurate measurements to be taken These include the use of an instrument called a parallax bar to devices that have special lenses that can compensate for the distortions experienced. For more information see that standard texts such as Avery and Berlin (1992) and those cited in section 4.1.
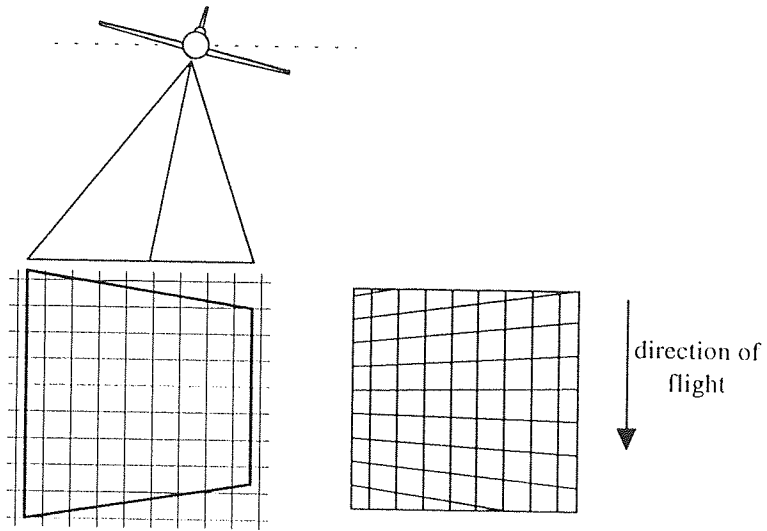
Figure 4.7. The effect of roll distortion on an aerial photograph.

direction of flight
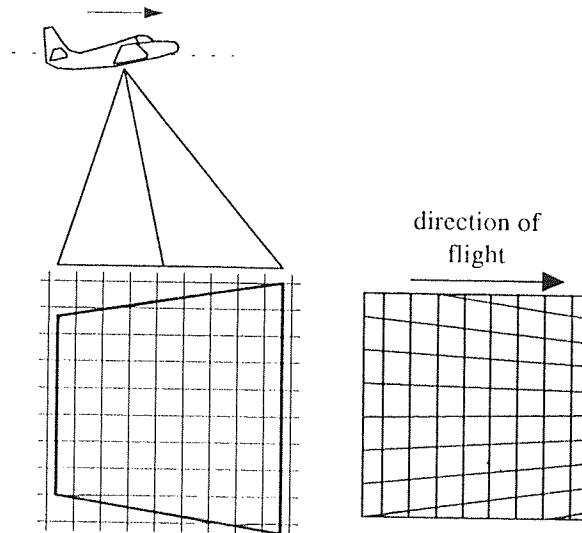
Figure 4.8. The effect of pitch distortion on an aerial photograph.

direction of flight

Area of larger scale

direction of flight

Area of smaller scale
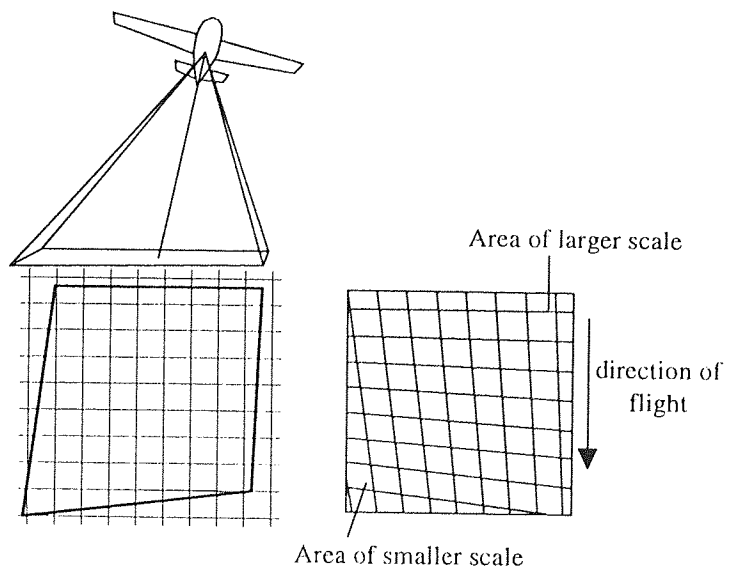
Figure 4.9. The effect of roll and pitch combined distortion on an aerial photograph.

4.3.2. Line-scanners

Line-scanners are the most common form of electronic instrument employed in earth resources remote sensing. As the name suggests, line-scanners view the earth a line at a time, and these are then built up to produce a continuous image. The output is usually in the form of digital data, which is in effect a string of binary numbers that have to be rearranged by computer into a recognisable image.

There are two fundamental types of line-scanner; whisk-broom and push-boom.

4.3.2.1. Whisk-broom Line-scanners

Whisk-broom scanners have a single set of detectors and utilise a rotating mirror which directs the incoming radiation on to the detection array. The rotating mirror enables a single line of ground to be scanned at a time as shown in figure 4.10.
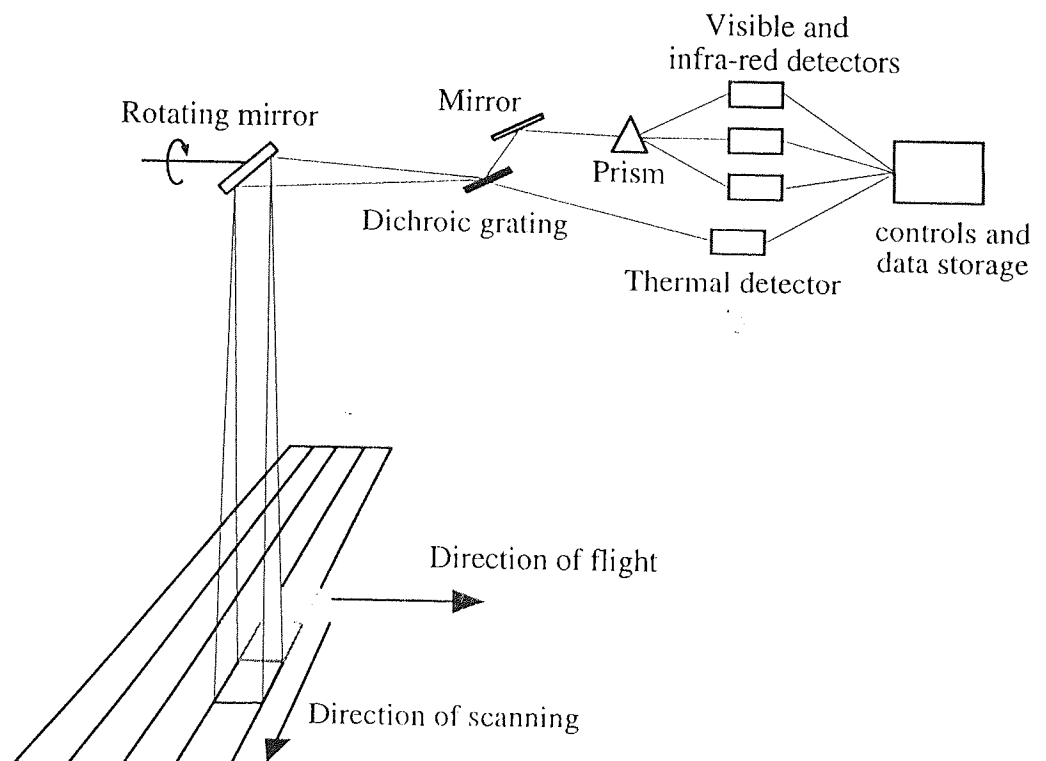
Figure 4.10. The basic workings of a whisk-broom line-scanner (adapted from Curran, 1985).

After the incoming radiation has been reflected off the rotating mirror towards the detectors, the thermal radiation is split from the visible, near and mid infra-red by a dichroic grating (if the line-scanner is manufactured to measure the thermal region).

The thermal radiation is measured immediately but the visible, near and mid infra-red is split further into discrete wavelength groups by a prism. Once the intensity of the incoming radiation has been measured by the detector it is sent to the data storage facility and the next reading is taken.

The number of readings per line depends on the sensor involved. The Airborne Thematic Mapper (detailed in section 4.3.2.3) takes 716 readings per line whilst the Thematic Mapper employed in Landsats 4 and 5 takes 6000 readings per line.

4.3.2.2. Push-broom Line-scanners

Push-broom scanning devices are less common than their whisk-broom counterparts. Instead of having a single detecting head and a moving mirror they use an array of individual sensors covering the whole width of the ground scanned. The most well known sensor of this type is the French satellite SPOT (Système Probatoire de l'Observation de la Terre (Satellite Probation Observation Terrain)) launched in February 1986.

6000 separate detectors

direction of movement

6000 pixels on the ground
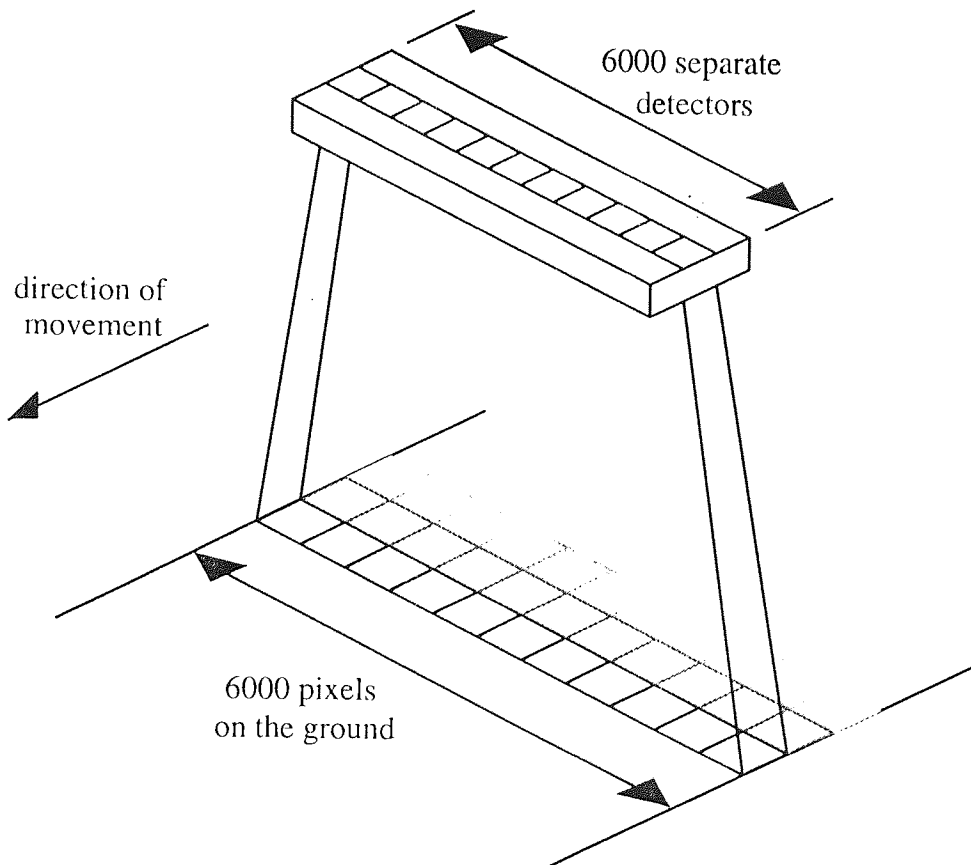
Figure 4.11. A push-broom line-scanner; values relate to the SPOT line-scanner (adapted from Open University, 1989).

The individual detectors are tiny (less than 10mm across) radiation sensitive cells called charged coupled devices (CCDs). A large number of CCDs are placed side-by-side (in the case of SPOT, 6000) and set into a predetermined position as shown on figure 4.11.

Push-broom scanners have a number of advantages over whisk-broom systems. Because the time available for each reading per detector is much longer for CCDs than whisk-broom scanner detectors the signal to noise ratio is greatly improved. Also, there are no moving parts so the possibility of mechanical failure is substantially reduced.

At present it is only possible to detect radiation up to 2.4μm using CCDs so the thermal region is beyond the capability of push-broom sensors.

4.3.2.3.   The Airborne Thematic Mapper

Figure 4.12. The Airborne Thematic Mapper with the scanning head (left) and the control unit (right).

One of the main devices used in this project is the Daedalus AADS 1268 Airborne Thematic Mapper 11 channel multi-spectral whisk-broom line-scanner or ATM for short (shown in figure 4.12). It is described by the manufacturers as the most widely used airborne line-scanner in the world and was developed during the late 1970s following the increased interest in remote sensing due to the Landsat series of satellites.

The 11 bands that the ATM registers in are listed in the table 4.2 along with some applications that the manufacturers suggest.
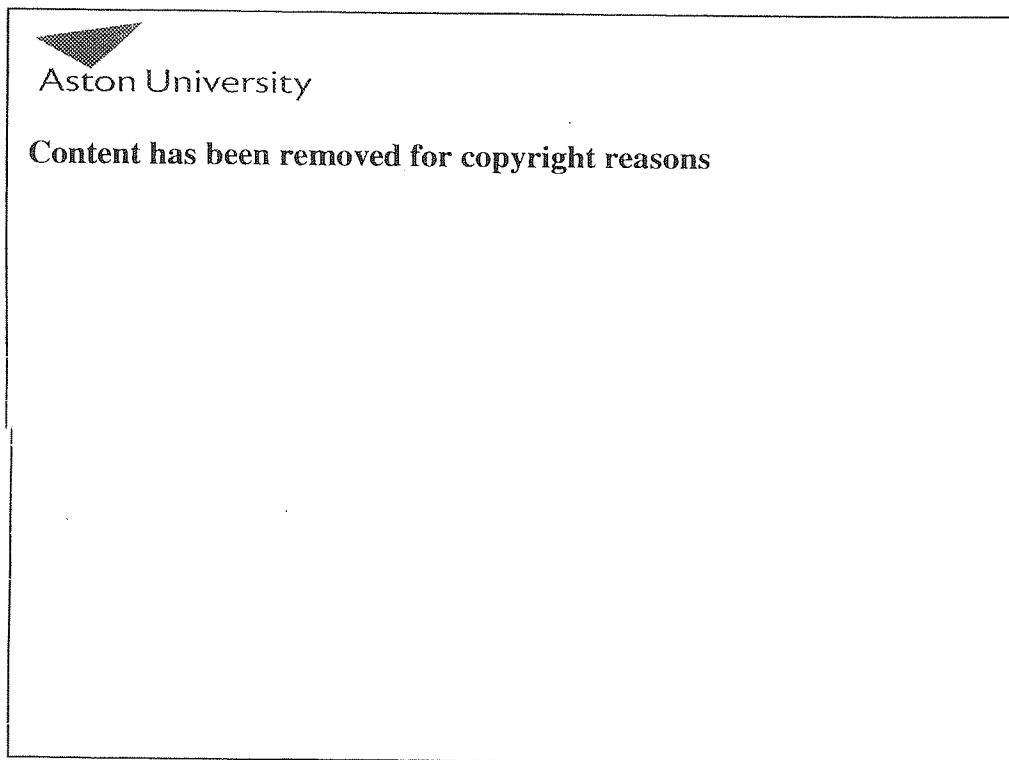
mapping - half amplification of band 11

Table 4.2. Spectral ranges of the ATM and TM (Daedalus Enterprises Inc., 1979)

The ATM was developed as an airborne alternative to the Landsat TM, hence its name. The TM bands were duplicated and additional ones were implemented to increase the spectral range.

4.3.2.3.1. Data Handling

Digital data is basically a string of numbers that represent the intensity of radiation measured by the sensor - usually the greater the intensity the higher the measured value. Each reading that the ATM takes is converted to a number between 0

and 255 inclusive. These values correspond to 8 bits or one single byte per reading with 255 being the largest number that can be contained in one byte. The detectable intensity range is dependent on how the sensor is calibrated. If the intensity of the reading falls outside the calibrated settings it will read it as the highest or lowest possible value. Occasionally, if a reading is well above the highest setting the sensor cannot make sense of it and gives it a reading of 0; this is termed 'burned out'.

To produce a recognisable image the digital numbers have to be read into a computer and organised by placing each value in the corresponding position relative to the original location on the ground. This entails arranging the lines of data adjacent to each other in the order that they are received. As mentioned previously the ATM takes 716 readings per scanned line on the ground so each 716 bytes of image data are displayed in a line on the resultant image. The next 716 bytes are then displayed adjacent to this and so on thereby building up the picture.

The ATM data provided by NERC is supplied in the format called Band Interleaved by Line (BIL). BIL format is where the data from each waveband is supplied in sequence for each given scan line. This is followed immediately by the band data from the next scan line. This is opposed to Band Interleaved by Pixel (BIP) where the band data for each pixel is presented together followed by the data for the next pixel and so on.
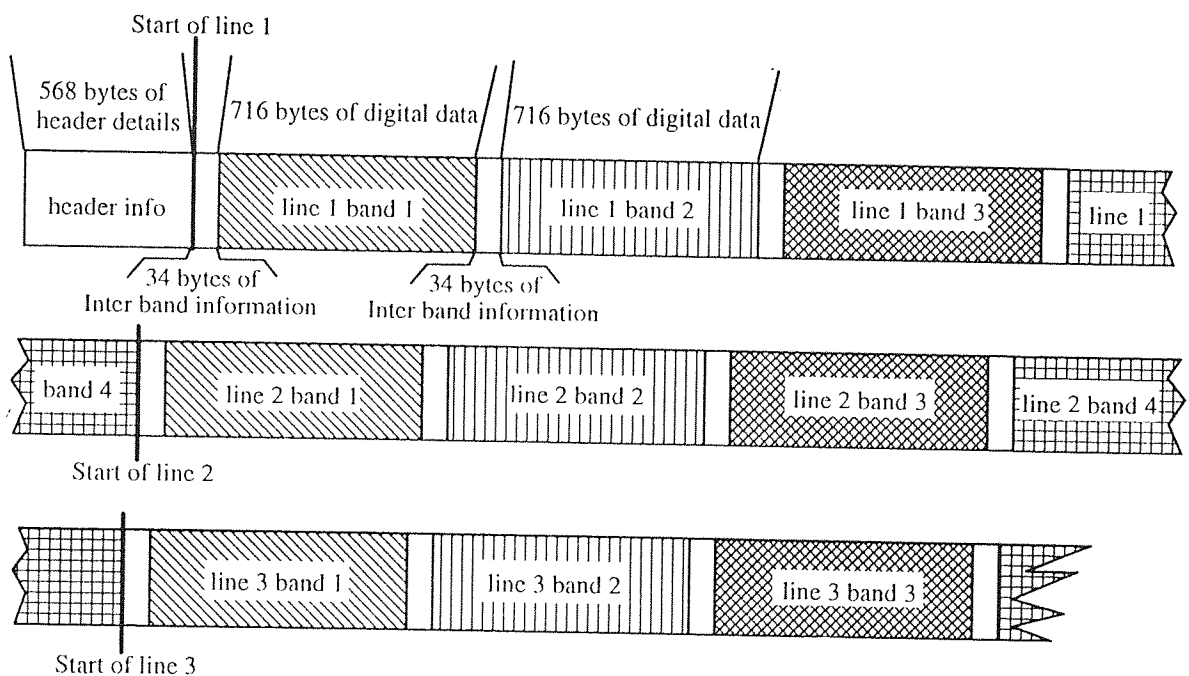
Figure 4.13. Example of Band Interleaved by Line for a 4 channel system (specific data values relate to the ATM).

Each remote sensing device has its own data form. Often there is some 'header' information giving details of data collection time and other necessary facts informing how to organise that data for retrieval. In the case of the ATM data the first 568 bytes are 'header' information and each packet of data per band per line is 750 bytes in size. Figure 4.13 shows a simplified BIL format for the ATM if only four channels were recorded.

Of the 750 bytes of data per band per line 716 of these bytes are the actual imagery data. The remaining 34 bytes being 'housekeeping' data providing information on start-of-frame and end-of-frame codes and black-body calibration sources (for the thermal band).

4.3.2.3.2. Data Extraction

The data from an ATM flight has to be separated out into the 12 recorded bands. With a simple regular structure, data extraction is just a case of reading a specific number of bytes, transferring them to 12 different files and discarding the unwanted non-image data. The procedure is shown in figure 4.14 for four band BIL data.
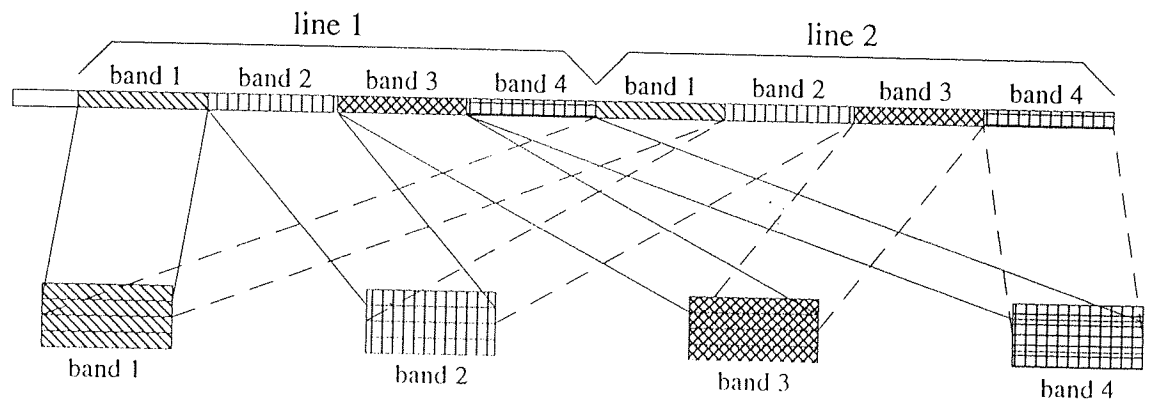
Figure 4.14. The data extraction procedure for BIL formatted data with four channels.

Once the data has been separated out into their discrete bands the separate images are available for processing and interpretation. The computer program to accomplish this was written by Rob Poole, the computer technician in the Civil Engineering Department at Aston.

4.3.2.3.3. Pixel Dimensions

The digital images are constructed of a series of tiny squares of light which are called pixels (short for picture element). The ground covered by a single pixel acquired form a given satellite is generally fixed because of the pre-determined

altitude. Airborne systems can fly at a variety of different altitudes, which are determined by the application ,and hence the pixel size (resolution) will vary.

Generally the area on the ground to be covered by each pixel is decided on prior to the flight. The amount of data that is going to be recorded and what specifically is to be identified have to be considered when selecting the pixel size for the imagery. If the object of interest is generally small (i.e. individual trees) then the pixel size needs to be relatively small, whereas if the object of interest is large (i.e. a cropfield) then the pixel size can be correspondingly larger. It also has to be noted that with the decrease in pixel size there is a distinct increase in the total amount of data collected. With every halving of the pixel dimensions the amount of data required to cover a given areas increases fourfold, as indicated on table 4.3.

Flying Height	Pixel Size	Amount of data per km²
1000m	2.5m	160000 bytes
2000m	5.0m	40000 bytes
3000m	7.5m	17777.8 bytes
4000m	10.0m	10000 bytes

Table 4.3. Comparison of data storage needs with respect to pixel size and flying height for digital airborne imagery.

Once the pixel size has been selected and hence the flying height, there are two more parameters that need to be determined before the flight can take place: aircraft velocity and scan rate.

To obtain a good image for final analysis each portion of the ground covered by the flight should only be scanned once. This is governed by the aircraft velocity. If the aircraft flies too slowly the scanned lies overlap and the final image will look elongated as illustrated on figure 4.15. If the aircraft flies to quickly not all of the ground will be covered and the final image will look compressed as shown on figure 4.16.
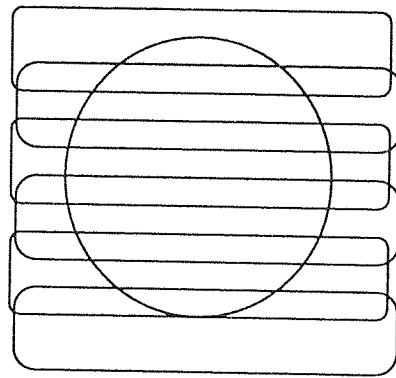
6 overlapping scanned lines
on the ground
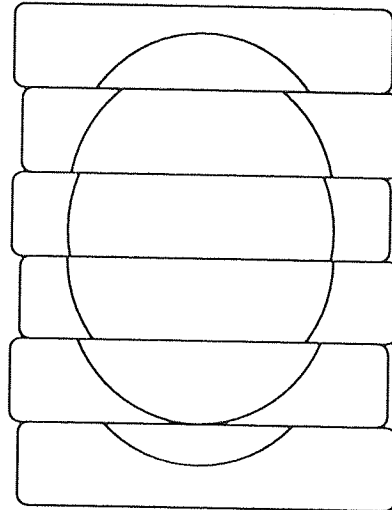
the same six scanned lines transferred to computer assuming no overlap

Figure 4.15. Example of overlapping scanned lines giving the impression of a stretched image.
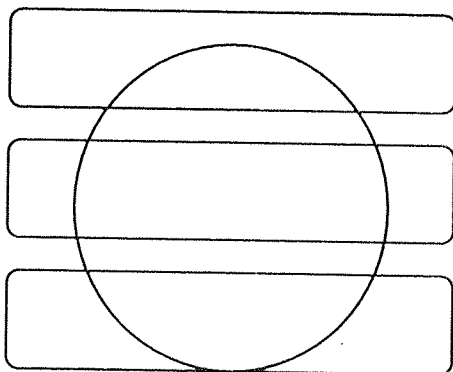
3 scanned lines on the ground
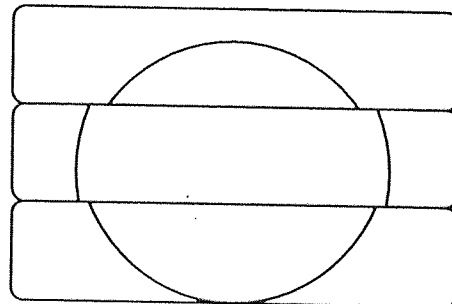
the same 3 scanned lines transferred to computer assuming complete coverage

Figure 4.16. Incomplete coverage producing the impression of a compressed image.

The scan rate (the number of lines on the ground scanned per second) is the remaining factor that has to be specified prior to a flight.

The relationship between the three flight parameters is:

$$\text{Velocity of aircraft} \propto \text{Flying Height} \times \text{Scan Rate}$$

This relationship can be expressed graphically as shown on figure 4.17.
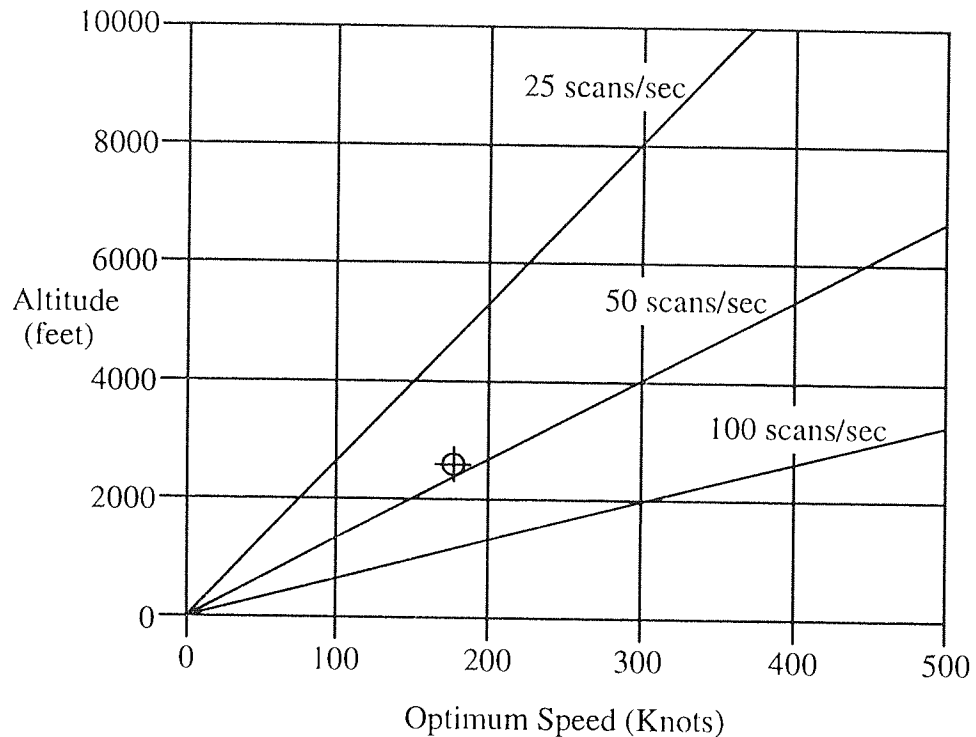
Figure 4.17. The relationship between flying height, flying speed and scan rate with the position marked (⊕) for the aircraft used in this project (adapted from Daedalus Enterprises, 1979 (see Appendix A)).

The imagery for this project was to be acquired within an urban area and required the highest resolution possible, which meant flying at the lowest practicable altitude. The minimum flying height was restricted to 800m (2625 feet), which is approximately the minimum altitude allowed for a fixed wing aircraft over a built up area. The aircraft that NERC fly the ATM in (Piper Chieftain detailed in Appendix D) has a maximum speed of 170 knots so by using figure 4.17 a scan rate of 50 scans/sec is the most appropriate of the three available rates and this position has been marked on figure 4.17. Theoretically this combination of flight conditions should give a pixel size of approximately 2m. The full specifications of the ATM are detailed in Appendix A, which is a photocopy of the official Daedalus Enterprises leaflet which was obtained in 1994.

4.3.2.3.3.1. S-Bend Correction

The way that a line-scanner views the ground is not consistent all the way across the line. Even though the Instantaneous Field Of View (IFOV) angle of the

74

sensor is always the same the amount of ground viewed increases away from the nadir producing tangential distortion as illustrated in the upper two frames of figure 4.18.

Each scanned pixel covers the same angle

But the ground coverage alters across the image

If unaltered a straight line would appear S-shaped because each pixel is displayed as being square regardless of the ground coverage

A correction is executed to make the image appear natural
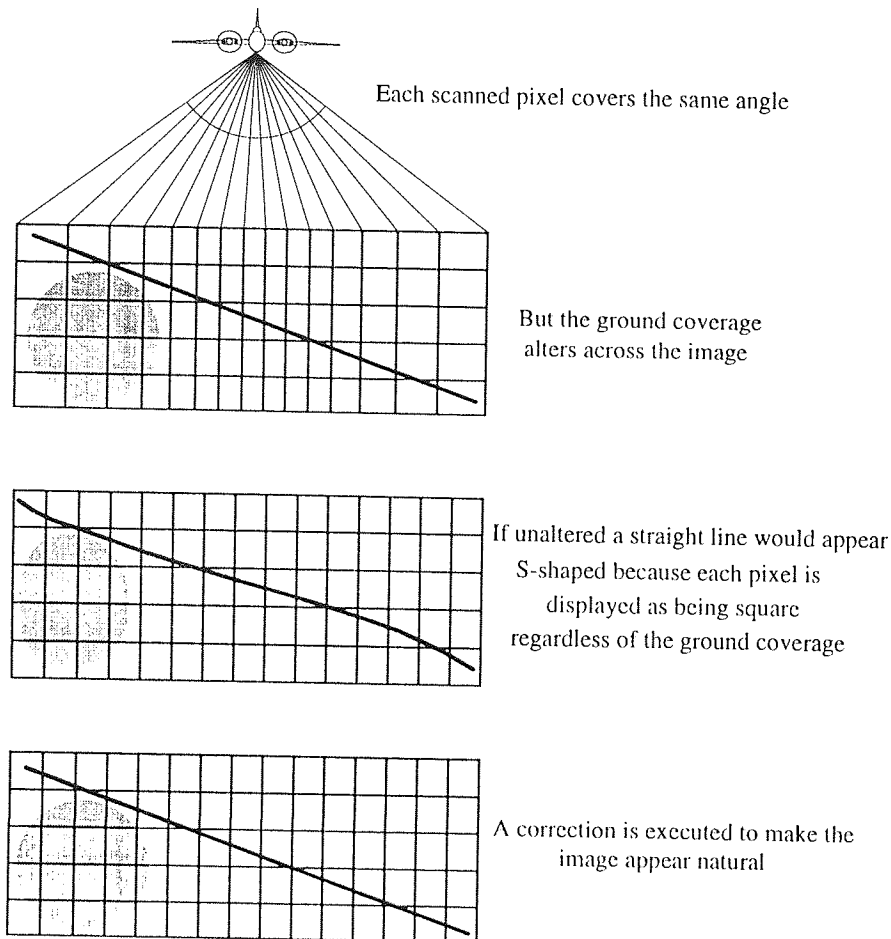
Figure 4.18. The procedure of S-bend correction.

A process termed S-bend correction is applied to the image within the sensor. If the correction were not applied a straight linear feature on the ground would appear s-shaped as in the centre frame of figure 4.18.

4.3.2.3.4. Geometric Irregularities

The geometric quality of ATM imagery suffer from the same distortion effects as aerial photography. In the case of aerial photography the various forms of distortion discussed in section 4.3.1.1 occur consistently across a single print. For ATM, though, the distortion experienced by every scanned line is unique. This makes any correction extremely difficult. Figure 4.19 shows an exaggerated example of a number of scanned lines as they might be flown and how the final image would appear. Although the features on figure 4.19 are recognisable their dimensions are irregular and a simple correction is impossible.
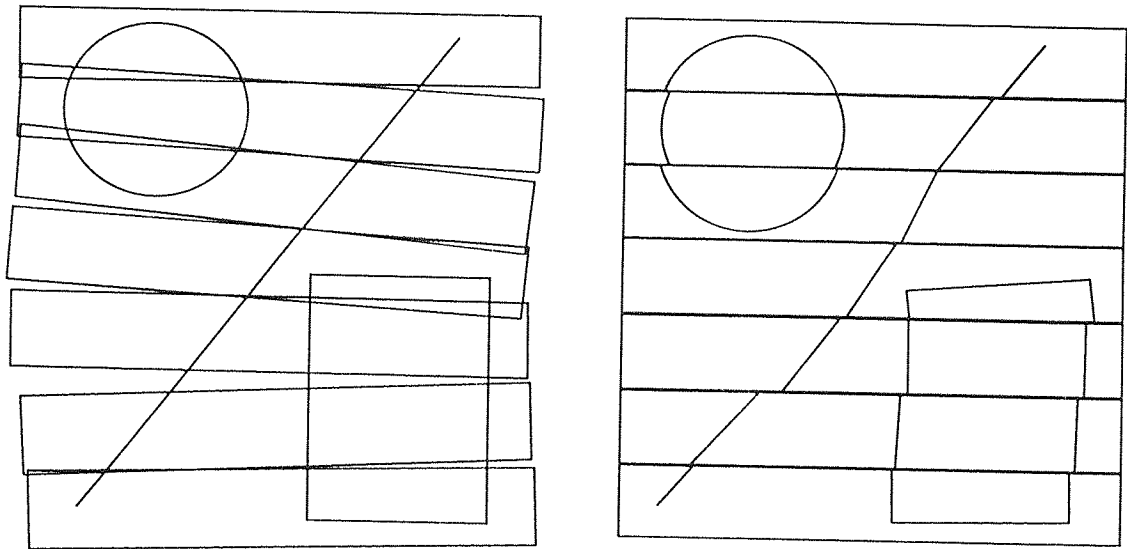
Figure 4.19. Geometric irregularities that may be experienced by ATM imagery with actual scanned lines on the ground (left) and the final image (right).

4.3.3. The Principles of a Video Camera

Video cameras are now readily available because of the reduction in size and the lowering of costs that has taken place in recent years.

The basis of a video camera is the vidicon tube, upon which a whole scene is focused and scanned every 1/25 of a second (as shown on figure 4.20). Each scene can be viewed individually as a still image, but when viewed as a continuous stream of images one after the other, displayed every 1/25 of a second as on a television, a motion picture is created.

The data obtained from the video camera is usually fed directly to video tape as analogue data (not digitally like line-scanners). Recording the information as analogue data reduces the total amount of storage. A flight taking 20 minutes may require twelve or more half-inch magnetic tapes (totalling 2-300 Mega bytes) to record the ATM data but only 20 minutes of video tape. However, as the video images are not digital they cannot be processed directly by a computer unless they are subsequently converted to digital format.

Normal video cameras record in the red, green and blue regions of the spectrum, thereby creating a normal colour picture. It is possible to create a false colour image by adjusting the sensed wavelengths in the same way as on a false colour composite photograph by using filters.

Figure 4.20. The basic workings of a video camera (Open University, 1989)

The mounting position of a video camera in the relevant platform is far more flexible than for a line-scanner due to them being much smaller and portable. The orientation of the camera in relation to the ground will not significantly affect the recognition of the objects on the final image because of the way it takes a snap-shot of a whole scene at once in the same way as a photographic camera. There are also no constraints on scan rate or aircraft velocity. Commonly, video cameras are used in oblique format (at an acute angle to the ground: in the region of 45°) and the imagery usually viewed as a motion picture.

4.3.3.1. Thermal Video Imaging

The general principles of a thermal sensing video camera is similar to conventional video cameras but the vidicon plate is replaced by a plate sensitive to radiation in the thermal region. Due to atmospheric absorption there are two separate regions of the thermal part of the spectrum that can be used for thermal sensing, 2-5µm and 8-14µm (as shown on figure 4.21).

Figure 4.21. Atmospheric absorbance in the thermal region of the spectrum showing the thermal 'windows' (Open University, 1989).

The device used during this project, the Thermovision 450, is sensitive to radiation wavelength from the 2-5μm window (the ATM is sensitive in the 8-14μm window). The more commonly used region is the 8-14μm window, which is the peak of radiation given off by a black body at 300K, and this longer wavelength window has the better signal response of the two available regions. The 2-5μm region is at the limit of solar radiation detectable within the atmosphere and the slight overlap produces some noise (see figure 4.5).

Devices sensitive in the thermal region need an artificial cooling system to reduce interference in the sensor. The Thermovision 450 was designed to detect at the shorter wavelengths of the thermal region because in this range it was possible to cool the plate by electronic means. At the time when this system was developed (1980s) any device sensitive in the longer wavelength part of the thermal region needed liquid nitrogen or helium to cool the plate. The limitations of a liquid cooled device over an electronically cooled one are clear: extra bulk, greater cost and limited time of operation due to the cooling liquid boiling off. However, there are now systems available that are electronically cooled, bypassing the problem of the containment of liquid helium and nitrogen.

4.3.4. Ground Penetrating RADAR

Ground Penetrating RADAR (GPR) is as its name suggests- the use of RADAR waves to gather information on what lies beneath the ground. It was developed during the Viet Nam war to detect buried land mines. Since then its uses have been expanded to detect buried drums/pipes, landfill debris, geological structures, voids and disturbed ground to name but a few. The information from this section was obtained from Peters et al (1994).

It operation is similar to seismic methods in that the GPR array is moved across the ground whilst continuously sending and receiving signals, the difference being the type of transmissions. GPR devices emit radiation from a few MHz to a few GHz which are sent out in pulses in the order of nanoseconds which are in turn transmitted in cycles from 60Hz to 1MHz. This process is repeated every chosen unit distance which can range from fractions of metres to metres. The traces formed are also similar to seismic testing in that they consist of black and white layered diagrams.

If the GPR traces are taken in adjacent parallel strips it is possible to build up a three dimensional picture of what is below the ground. There are main types of targets that can be detected: 1) simple planar reflectors (e.g. geological structures or water tables), 2) resonant scatterers (e.g. buried objects) and 3) non-resistant scatterers (e.g. disturbed earth. The purpose of GPR is to detect all three effects but the skill is to interpret and classify the returned signals.

GPR was not used in this project but it could help investigations of this nature. It is capable of mapping, three-dimensionally, structures below the ground making it possible to quantify the extent and volumes of landfill sites as well as other waste disposal problems such as buried drums.

4.4. Remote Sensing and Vegetation

Remote sensing has proven very useful for identifying the quantity and sometimes the quality of vegetation. Much of the following information is described in greater detail in the standard remote sensing texts cited in section 4.1.

Many plants can be differentiated from others by the way they reflect sunlight incident upon them. A generalised reflectance trace is shown in figure 4.22 for a normal healthy green leaf.
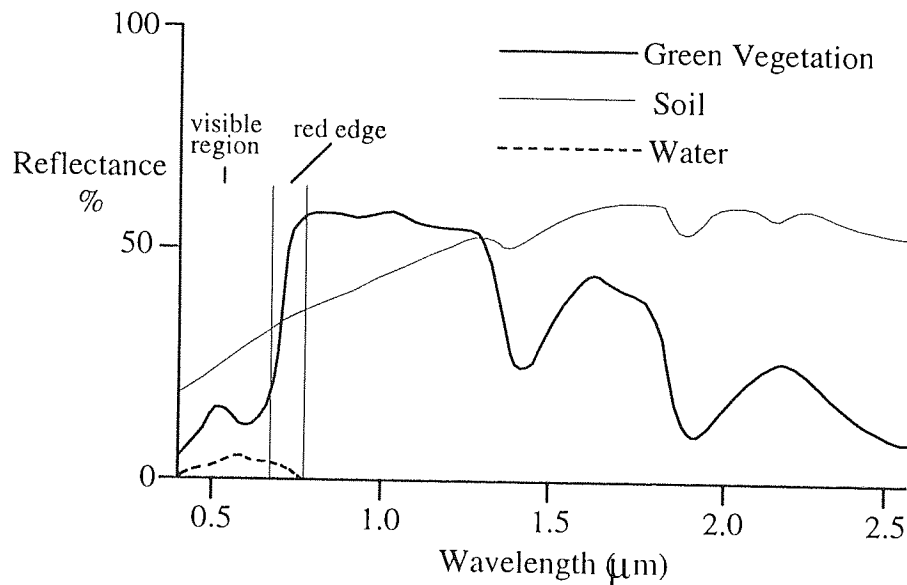
Figure 4.22. Generalised reflectance curve for a normal healthy green leaf (adapted from Lillesand and Kiefer ,1986).

The reason that plant leaves, in general, appear green is due to the absorbance properties of the photosynthesising agent, chlorophyll. Chlorophyll absorbs the sun's radiation in the visible part of the spectrum, mainly in the blue and red regions. More green light is reflected than any other part of the visible spectrum and thus to the eye the leaf takes on this colour. The conspicuous rise in the reflectance in the near infra-red region is due to the leaf's cellular structure. Incoming radiation undergoes multiple internal reflections and refractions as it passes through the leaf and as a result a large proportion returns through the membrane where it entered the leaf. Man-made objects coloured green may be mistaken for vegetation in visible light but the distinctive reflectance in the near infra-red by vegetation is unique and enables the two to be distinguished from each other.

The area of the spectrum where the visible range stops and the infra-red begins is often termed the 'red edge' (0.68-0.76μm according to Boochs et al, 1990) and it is at this point where the considerable rise in reflectance manifests itself (see figure 4.22).

Different plants have specific reflectance curves making them distinct from each other as shown in figure 4.23. In general, deciduous broad-leaved trees have a higher reflectance in the near infra-red than coniferous needle-leafed trees whilst grasses tend to reflect greater still.
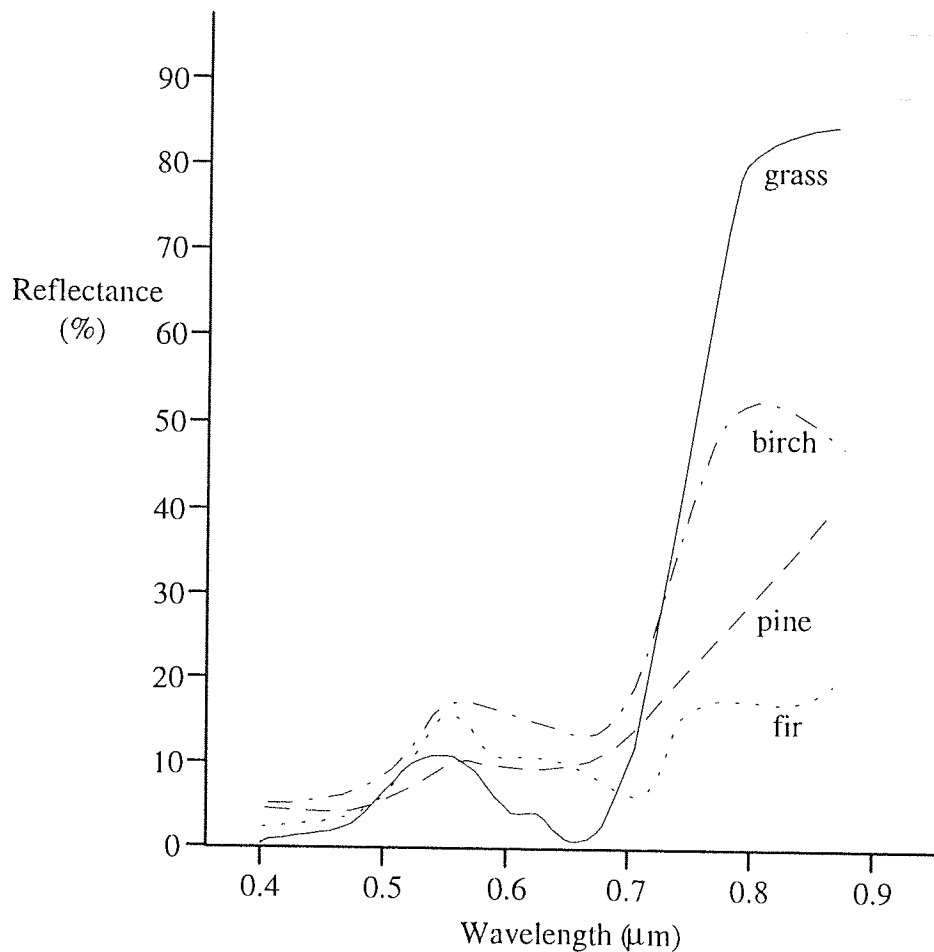
Figure 4.23. Reflectance characteristics of some plants (adapted from Open University, 1989).

Remote sensing has also been applied to detect vegetation damage. The basis for this is the colour change that occurs in leaves of plants that have become harmed or stressed. Figure 4.24 shows four idealised reflectance curves for, initially, a normal green leaf. When a plant becomes damaged or experiences undue stress or senescence the chlorophyll breaks down and the peak of the visible reflectance curve shifts towards the red region producing a yellow/red/brown coloration, and consequently an unhealthy appearance. This is usually accompanied by a distinctive drop in the near infra-red response that is due to cell wall collapse, which subsequently inhibits infra-red reflectance. The infra-red reflectance reduction is compounded by the alteration in leaf orientation (leaves drooping) and a decrease in total leaf area (leaves fall off) (Knipling, 1970). Both Jones (1991) and Groves (1989) provide a literature review on spectral differences shown by damaged, stressed or senescent vegetation.
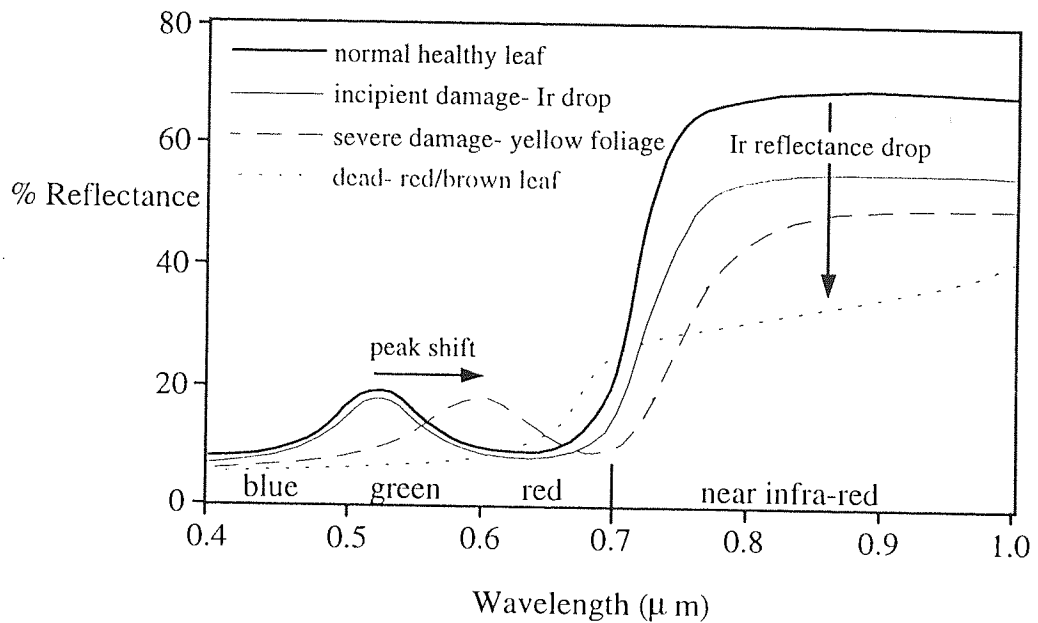
Figure 4.24. Reflectance curves for progressively damaged vegetation (adapted from Murtha, 1978).

4.4.1. Applications of Remote Sensing for Vegetation Damage Detection

The basis behind the detection of vegetation damage revolves around the change in colour of the leaves and the drop in the near infra-red reflectance as illustrated in figure 4.24.

There are three main factors that may confuse the interpreter when categorising vegetation canopies and these are (from Colwell, 1974):

- leaf transmittance (amount of light passing through the leaf),
- arrangement of leaves (dense or thin foliage),
- characteristics of ground cover (grass, soil, rock, leaf litter) - e.g. a dead tree that has healthy undergrowth may appear to have a healthy canopy (Kadro and Kuntz, 1986).

Another problem in interpretation was encountered by McCarthy et al (1982), when moss was found accumulating on dead branches and giving the false impression of a healthy tree.

The use of aerial photography and the ATM to detect vegetation damage are discussed in the following two sections. Although satellite sensors have been used extensively for this purpose they were not used in this study and therefore are not mentioned.

4.4.1.1. Aerial Photography

Aerial photography has been applied to monitor forests regularly over the last 40 years. In continental Europe many inventories of forests have been carried out to monitor the damage caused by air pollution and acid rain, a review of which can be found in Groves (1989). McCarthy et al (1982) applied 1:4800 scale normal and false colour aerial photographs to study 25 square miles of forest. The aim was to discriminate between tree-type and tree condition. Results of 80% accuracy for tree-type and 61% accuracy for tree condition (on a five damage class ranking scheme) were obtained when compared to ground truth data. Being able to rank damage in this way becomes increasingly difficult as the photographic scale decreases due to the inability to separate trees on the image.

The use of false colour composite (FCC) photographs has been often used to estimate vegetation damage because of the drop in reflectance in near infra-red radiation exhibited by unhealthy plants. The colours to look for on an FCC photograph are green/blue/cyan variations when identifying unhealthy vegetation. Weltman (1983), Vass and Van Genderen (1978) and Birkbeck and Tomlins (1985) all report examples of the application of this principle and Whitelaw (1986) was able to trace buried mine shafts by the poor vegetation covering them.

4.4.1.2. The Airborne Thematic Mapper

The ATM has, on occasion, been used to assess the damage to and defoliation of trees. Kadro and Kuntz (1986) compared multi-spectral scanner data (not ATM but a similar device: Bendix-M2S-Scanner) to FCC photographs and ground truth data for a forest damage inventory in Germany. The results obtained were favourable in distinguishing between healthy and damaged trees. Jones (1991) achieved a 68% accuracy when classifying tree damage in a wood with five damage classes. Watt (1988) and Ahern et al (1986) identified areas of forest that had lost foliage due to attack by insects. Ory (1990) showed how a Belgian forest had declined by examining imagery of the same area a year apart. These areas were differentiated using visible and infra-red bands of the ATM either individually or in combination.

Projects that set out to employ the reflecting characteristics of chlorophyll do not always involve terrestrial plants. Omar et al (1989) and George and Hewitt (1989) both calculated plankton concentrations in lakes by measuring the reflectance on band 3 (green) and bands 6 and 7 (near infra-red) respectively.

Other vegetation surveys include those of Shears (1988) and Gilvear and Watson (1993). Shears (1988) used the ATM to monitor an area of saltmarsh near a refinery in Hampshire and found the Vegetation Index (see Section 5.1.2) to be useful for distinguishing between the marsh and sediment types. Gilvear and Watson (1993)

used the ATM to estimate water table depths in a wetland marsh in Scotland. This was achieved by identifying the type of the vegetation which was found to be directly related to the water table depth which varied between 0 and 0.7 metres.

Literature relating to the detection of vegetation damage associated with landfill sites are discussed in section 4.5.

4.5. Remote Sensing and Landfill Sites

The remote sensing methods that have been applied to monitoring landfill sites have mostly been from a low altitude using sensors based in either aeroplanes, helicopters or balloons. The resolution afforded by satellite remote sensing equipment is too poor to be of use for this application.

4.5.1. General Monitoring

The common use of remote sensing in relation to landfill sites is simply for monitoring the development or the existence of sites.

4.5.1.1. Aerial Photography

Aerial photography is the major source of remotely sensed image that has been applied to monitoring landfill sites, hazardous waste sites and contaminated land. They can give information on a range of parameters associated with landfill sites including hydrology, run-off, ponding, soils and vegetation quality (Lyon, 1982).

A common method is to obtain a series of photographs that cover a long time scale (multi-temporal) and then compare them to see how sites have developed over that time (Garofalo and Wobber, 1974, Lyon, 1982, Erb et al, 1981, Finkbeiner and O'Toole, 1985, Airola and Kosson, 1989 and Bullard, 1983). Stohr et al (1987) used photographs taken many years apart to identify depressions and surface hydrology on a site. It was possible to trace ponding sufficiently to make the judgement that the cap was leaking and augmenting the leachate production. Lyon (1987) showed how it is possible to estimate the age of a disused site by the vegetation that grows upon it. Recent sites have grass and scrubby ground cover and as the age increases so does the introduction of woody plants with eventually trees dominating.

Multi-temporal data helps when making inventories of the number and types of waste disposal sites there are in a large area. Titus (1982) used old photographs and site maps to find old polluting industrial sites. Barnaba et al (1991) developed a method for making inventories known and unknown waste disposal sites in a local

government area. Van Genderen et al (1983) utilised FCC photographs to locate and monitor illegal small scale dumping in the Netherlands.

Most commonly, aerial photographs are used as a single shot study of a site. Azam (1989) applied very large scale photographs to observe some polluting sites. FCC proved very useful in identifying where polluted effluent was draining from a site into a nearby water course.

Often aerial photographs are only a part of a monitoring process, usually employed in the early stages of an investigation. Straight (1983) used FCC photographs to highlight areas suspected of containing a buried pollution hazard which were then inspected with a sensitive magnetometer to find possible locations of buried toxic containers. Wruble et al (1986) suggested a similar strategy with a three stage approach: (1) an aerial survey followed by (2) a surface inspection, finishing with (3) a sub-surface (geophysical) analysis.

4.5.1.2. Airborne Line-scanners

Airborne line-scanners have had very little use for monitoring landfill sites. One example of a flight over a contaminated site was over an area near Swansea. Coulson and Bridges (1984) classified a site and found a favourable correlation of surface cover type with heavy metal contamination.

A precursor to this project was that of Jones (1991) who used the ATM to study two rural landfill sites and the effect on the crop planted on the cap. This project is discussed in section 4.5.2.1.

4.5.2. Remote Sensing for Gas and Leachate Detection

The effects of landfill gas on vegetation are dealt with in section 3.6.4. Section 4.4 describes how damaged vegetation reflects radiation differently from healthy vegetation. Decaying refuse produces heat which can reach up to 55°C as Section 3.4.1. describes. Therefore, it is theoretically possible using remote sensors to identify migrating gas and leachate by way of vegetation damage and heat signature.

4.5.2.1. Gas Detection

Landfill gas can be harmful to vegetation directly (i.e. the toxic effects carbon dioxide) or indirectly (i.e. methane and carbon dioxide displacing oxygen in the root-zone creating adverse conditions). When a plant is harmed it may exhibit a colour change and a drop in near infra-red reflectance that is measurable by remote sensors (see section 4.4).

Curran (1986) used oblique aerial photographs on a landfill site that had been returned to agricultural use. Areas of poor vegetation and bare soil were easily identified and attributed to landfill gas at the surface. Weltman (1983) employed FCC vertical photographs taken from a radio controlled model aircraft. Areas of low reflectance were identified and attributed to landfill methane even though corresponding spike tests did not correlate at all well.

The project carried out by Jones (1991) at the University of Aston was a precursor to this study. It was centred around two rural landfill sites that were known to be producing gas. Both sites had been planted with crops but the gas migration regimes were different. The first site was producing gas that was predominately migrating upwards through the cap. By taking near-surface gas measurements the connection between the vegetation damage and the landfill gas was clear, although the precise correlation was uncertain. The confusion was associated with the differing covering soil characteristics. The gas in the second site was migrating sideways and upwards affecting both the neighbouring woodland and the crops growing on the landfill cap. Aerial photographs, aerial video and ATM data was analysed to identify vegetation and relate it to soil type with limited success. The technique is favourable when the gas concentration and vegetation damage relationship is easy to establish, i.e. in situations where there are high gas concentrations, a homogeneous vegetation cover and predictable variation in soils characteristics (Jones and Elgy, 1994).

Very little work has been undertaken to try and find gas by detecting a heat signature although Titman (1994) was able identify warm areas where gas was found to be emanating from cracks in a landfill site. An aerial thermal survey of 42 landfill sites in Wolverhampton, contracted by the local authority, was undertaken and two of the sites surveyed were found to be producing anomalous heat levels (Wolverhampton Borough Council, 1992). Both of these surveys used a thermal camera situated in a helicopter and flown at dawn.

4.5.2.2. Leachate Detection

Leachate is the liquid effluent resulting from a combination of liquid produced by the degradation of carbonaceous material found in landfill sites and water from external sources percolating through the waste (see sections 3.4 and 3.5). There are a number of ways that leachate may be detected by remote sensors; either directly by its presence (dampness, colour or heat signature) or indirectly by its toxic effects on vegetation.

Leachate is often toxic and contains many harmful elements and compounds (see Section 3.5). This can have the effect of damaging any vegetation that it comes in to contact with. Birkbeck and Tomlins (1985) found leachate migrating from a landfill

86

site using aerial photography. The polluted area appeared as grey/white on normal colour film and grey/green on FCC film. On occasion leachate can have the opposite effect. The nutrients contained within the leachate or the extra water in the vicinity can sometimes increase vegetation growth (Haynes et al, 1981 and Sangrey and Philipson, 1979).

As leachate is a liquid and usually water-based, if it reaches the surface it may exhibit itself as a damp area (Haynes et al, 1981 and Sangrey and Philipson, 1979).

Leachate often contains many metals ions, a common one of which is iron. When the iron oxidises the leachate may have a rust colour although it can also appear transparent if there is a low iron content (Sangrey and Philipson, 1979). Haynes et al (1981) identified brown staining on normal colour aerial photography that was found to be leachate. Leachate often contains organic compounds of an oily nature and when it finds its way into a surface water course it may appear as an iridescent coating (Sangrey and Philipson, 1979).

Leachate can show up warmer than its surroundings on night-time or dawn thermal imagery for two reasons (Sangrey and Philipson, 1979):

a) it is water-based and water holds its temperature well in comparison to other materials (see section 3.5.1),

b) it is warm due to refuse degradation processes (see section 3.4.1).

Haynes et al (1981) found numerous thermal anomalies near a landfill site that proved to be leachate seeps. Titman (1994) located warm leachate emerging from a slope on a landfill site. Ziloli et al (1992) used a thermal camera at ground level and observed a landfill site and two nearby lakes, one of which was receiving leachate. A 6K difference was recorded between the two lakes, the warmest being the leachate contaminated one, and a 2K difference was seen between filled and non-filled land.

5. Image Processing and GIS

The two main computer based tools applied in this project are image processing (manipulation of digital imagery) and Geographic Information Systems (manipulation of spatial and temporal data). There are a great number of procedures that can be carried out using these tools but only those that were used in this study have been described. This section has been written from the user's viewpoint to provide the non-remote sensing specialist reader with an insight into the methods used. For more technical information the reader is directed to standard texts such as Burrough (1986) for GIS and Russ (1992), Jensen (1986) and Mather (1987) for image processing.

5.1. Image Processing

Image processing is a term applied to the manipulation of digital imagery and has two basic purposes (from Russ, 1992):

a) improving the visual appearance of images to a human viewer and

b) preparing images for measurement of the features and structures present.

There is a considerable overlap between these two purposes but generally the first relates to image enhancement and the second relates to classification whilst processes such as determining the Vegetation Index are applicable to both.

The techniques of image processing are conducted on digital images, which are those which are made up of a grid of pixels, each pixel possessing a discrete numerical value. The values are usually represented on a scale of 0-255 which corresponds to one byte (8 bits) of binary data. The images are usually displayed as a 'greyscale' with each pixel taking on a brightness from black to white related to the value (i.e. a pixel with value 63 displays as 0.247 (63/255) or 24.7% of white which corresponds to a darkish grey).

5.1.1. Image Enhancement

The term enhancement is used in image processing to mean:

"...the alteration of the appearance of an image in such a way that the information contained in that image is more readily interpreted by the viewer in terms of his/her particular needs."

Mather (1987)

This section discusses how image quality is improved by increasing the contrast either by stretching or Principal Components Analysis, and by filtering.

5.1.1.1. Contrast Stretching

Contrast stretching is a method of enhancement which entails altering the pixel brightness distribution by manipulating the pixel values of the original image. This can be carried out by altering the values linearly or by way of comparison to a histogram. A linear contrast stretch is the simplest form. It entails determining low and high values of an image (either the actual low or high values or a specific quantity (i.e. 3 standard deviations) either side of the mean), transforming them to 0 and 255 respectively and balancing the other values linearly between these two extremes. Figure 5.1 illustrates this by showing how an image with low and high values of 70 and 180 would, following a linear contrast stretch, have values ranging 0 and 255. Stretches that are performed via a histogram adjust the values discriminately across the image and consequently the contrast is greater. The Gaussian stretch is described in detail below as it was the form used in this project as the author judged it to make the most use of the available data.
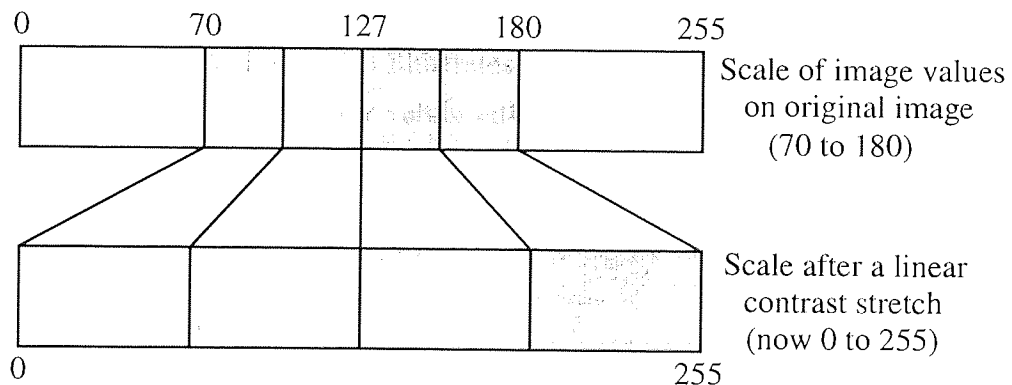
Figure 5.1. Illustration of the scale change experienced by an image undergoing a linear contrast stretch.

Figure 5.2 shows a detail of an ATM image of the green sensitive band (band 3) 116 pixels wide and 102 pixels high before and after a Gaussian contrast stretch enhancement, demonstrating the improvement.
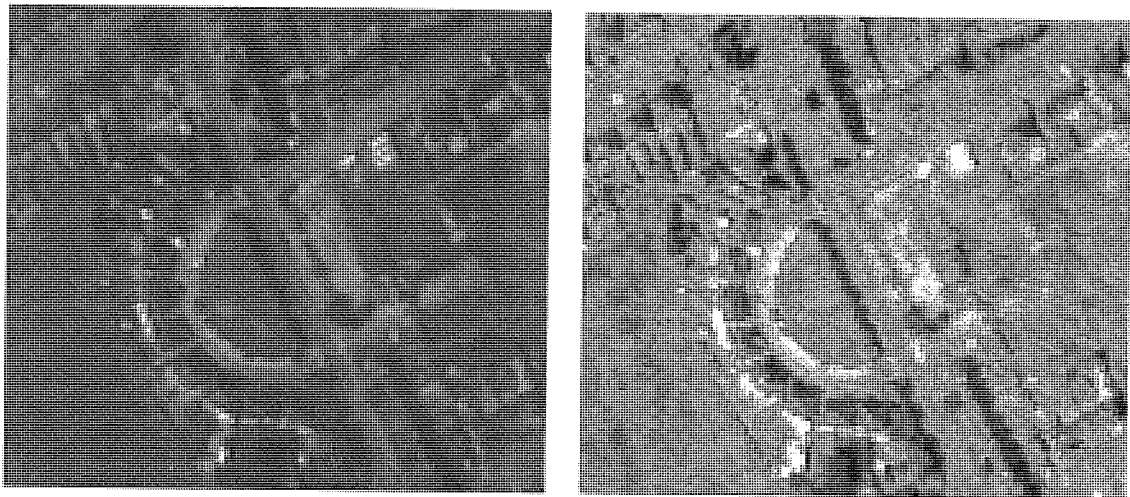
a) Unstretched   b) Stretched

Figure 5.2. An ATM extract of the green band (band 3) before and after contrast stretch enhancement.

The difference between the two is displayed in figure 5.3 by way of a histogram of each image, the statistics for which are tabulated in table 5.1. The unstretched 'raw' image is made up of values that are mostly less than half brightness and so would be displayed on a monitor as 50% intensity or less. The stretch that has been performed takes the original histogram and converts it into a normal distribution which is termed a Gaussian stretch (Mather, 1987). The stretched image now has values over a much larger range and the difference in pixel brightness is much greater, increasing the clarity. Figure 5.3 illustrates how the mean value has been modified to become the central value and the values either side have been adjusted to conform to a normal distribution.
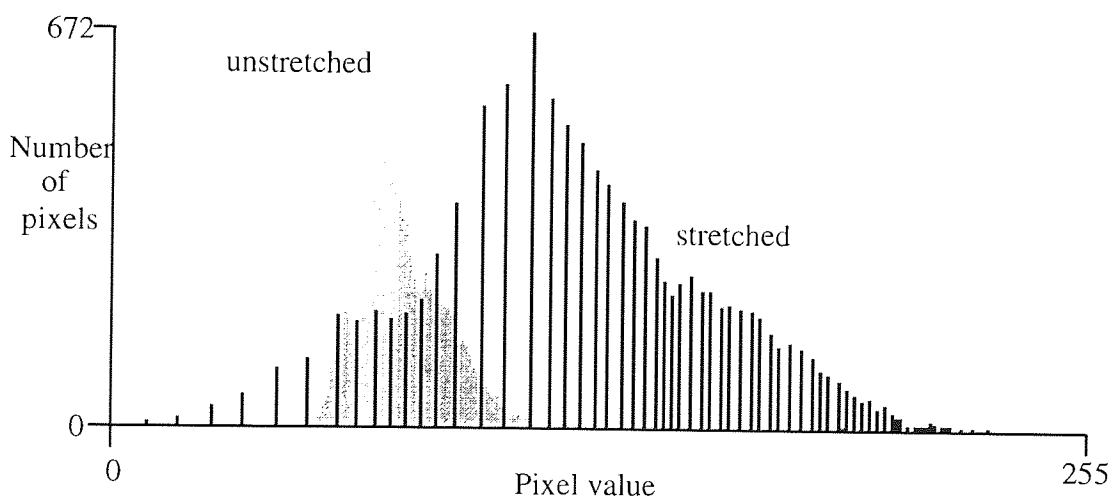
Figure 5.3. Histograms of the two images in figure 5.2 (before and after a Gaussian contrast stretch).

	Mean	full range	s.d
Unstretched	76.3	52 - 210	13.42
Stretched	128.5	0 - 255	39.03

Table 5.1. Statistics for the images from figure 5.1 and 5.2.

5.1.1.2. Filters

Image filtering (or convolution) is a method of enhancement that alters an image pixel by pixel in relation to the neighbouring pixels. There are two general types: low pass (smoothing) and high pass (sharpening) filters.

1) Low pass filters

These are also known as smoothing filters as they suppress the effect of high frequency variation and bring out low frequency changes on an image. They reduce the visual impact of edges and anomalously valued pixels in relation to their neighbours. Generally, the average (mean, mode or median) of a pixel and its neighbours is calculated and the central pixel is altered to the resulting value. The impact of the filter depends on the number of pixels used in the calculation - if a 3x3 kernel is used the central pixel and its eight neighbours are included in the calculation; if a 5x5 is used 25 pixels are included vastly increasing the smoothing effect. Figure 5.4 shows examples of the three averaging filters applied to the stretched image of figure 5.2. The mean and median filters blur the image, the latter to a lesser degree. The modal filter, on the other hand, takes the most common value in the kernel having the effect of producing clumps of like-valued pixels. This filter is very useful on classified images (and other images with large areas of pixels with similar values) as it only replaces values that already exist and discards small regions of pixels with dissimilar values. The modal filter was used in the area isolation process to remove isolated pixels following a classification (see section 7.2.3.3).

A) Mean.   b) Mode.   c) Median.
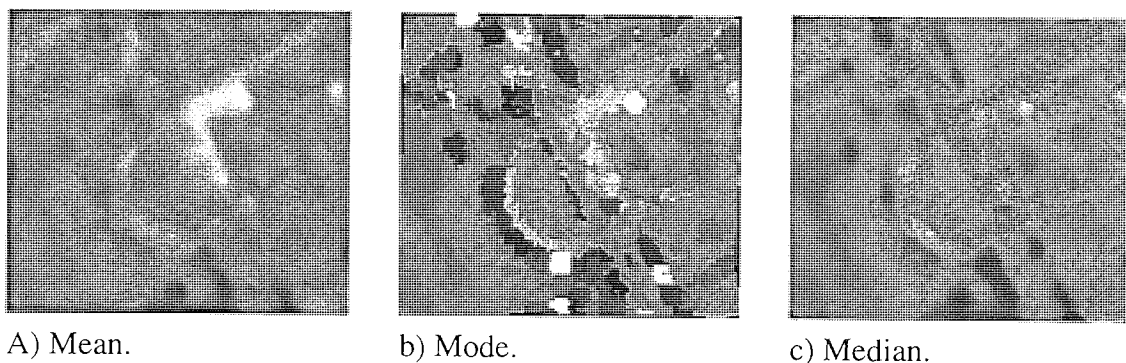
Figure 5.4. Examples of averaging filters executed on figure 5.2b.

2) **High pass filters**

These are also known as edge detecting filters and they enhance the high frequency variations on an image and increase the visual impact of edges. The central pixel of a kernel is altered according to the values of its neighbours, as with low pass filters, but it is the position of the varying values that is important not their magnitude. These filters can be designed to enhance vertical or horizontal lineations on an image as well as edges of other orientations and corners. They are not used in this project and will not be discussed further.

5.1.1.3. Principal Components Analysis

A Principal Component Analysis (PCA) is a statistical technique of reorganising data sets which can enhance imagery and often has a result reducing the effective number of images necessary without losing any information.

Many image bands convey essentially the same amount of information (i.e. bands 6, 7 and 8 of the ATM) and PCA is capable of creating a single band with greater variance than any of the original ones.
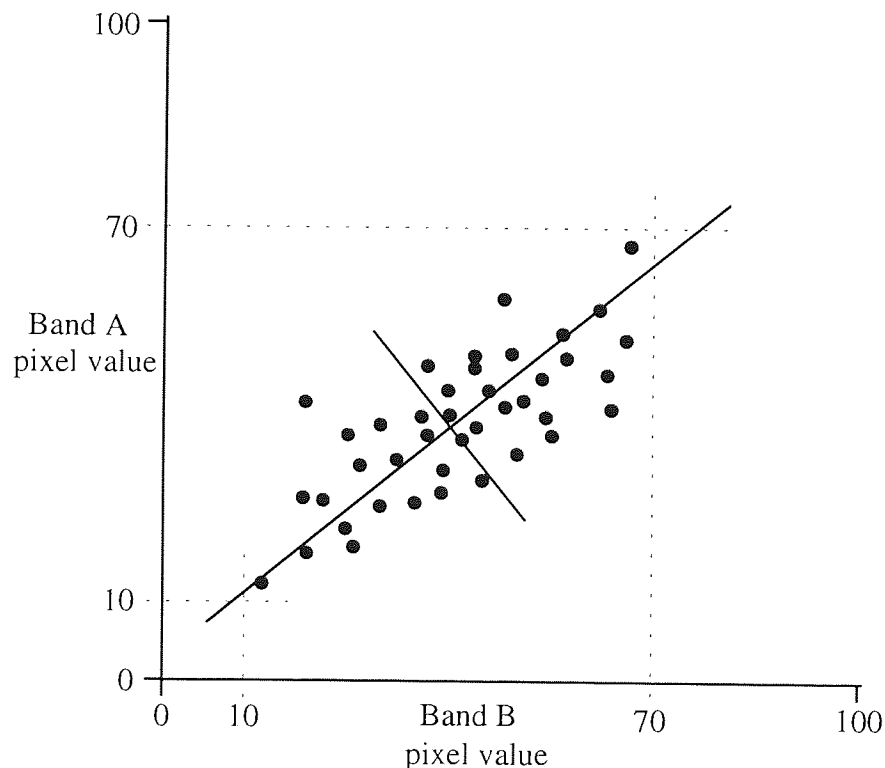
Figure 5.5. Scatter plot of two similar bands with cluster axes depicted.

The process of PCA involves primarily a formation of a multi-dimensional scatter plot followed by a reorientation of the original axes. The procedure is best described regarding two bands of data as it gets increasingly difficult to visualise as the number of bands increases. Figure 5.5 shows a scatter plot of two similar bands using a scale of 0-100. Often on such a plot, the cluster is an elongated ovoid oriented at about 45°. Both of the bands have a range of 10 to 70 which is 60% of the full contrast. During a PCA the two bands' means are determined and become the new origin. The axes are then rotated until one of them possesses the maximum possible variance. This axis is termed the First Principal Component (PC1). The next Principal Component (PC2) has an axis perpendicular to PC1 and possesses the next possible highest variance. This process is repeated as many times as there are images originally used in the PCA. Figure 5.6 shows the two Principal Components with horizontal and vertical axes to illustrate the new values possessed by them and shows how the contrast of PC 1 is now almost 80% of the full scale and PC 2 is only 35%, thus indicating the exchange of data.
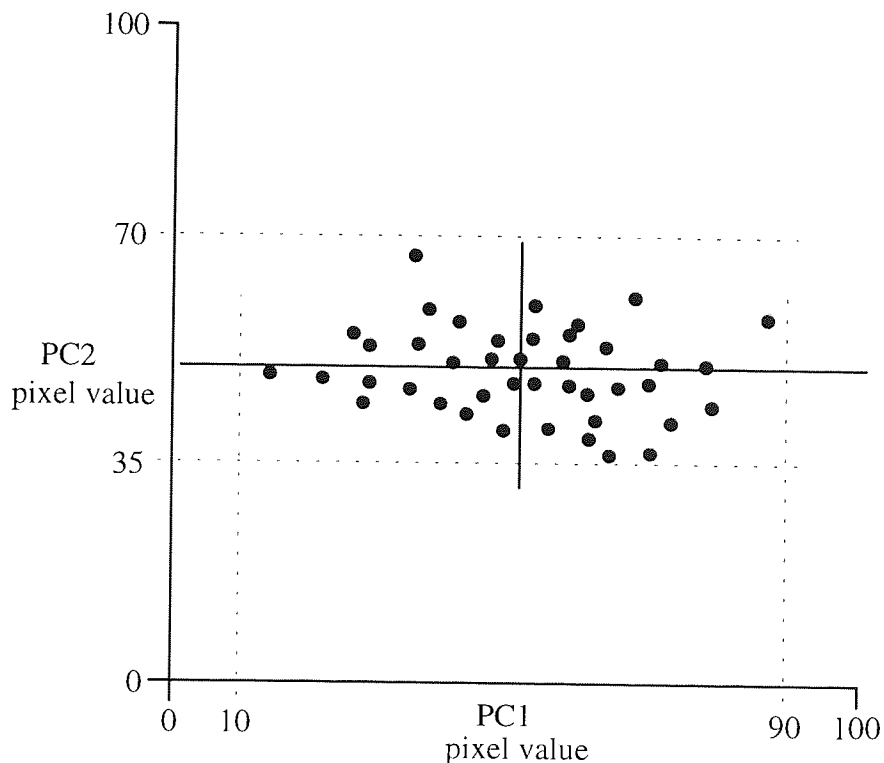
Figure 5.6. Scatter plot of the two Principal Components generated by figure 5.5.

93

The effects of undertaking a PCA are illustrated in figure 5.7 and 5.8. Figure 5.7 shows small extracts of ATM bands 6, 7 and 8 which are all near infra-red bands and have a similar spectral response. Figure 5.8 shows the three Principal Components generated from bands 6, 7 and 8 and illustrates how PC 1 now has a greater contrast than any one of the original images whilst the remaining two PCs (technically the differences between the original images) contain almost no information although there is a faint image present on PC2 of figure 5.8 which may be significant in some studies.

| band 6 | band 7 | band 8 |
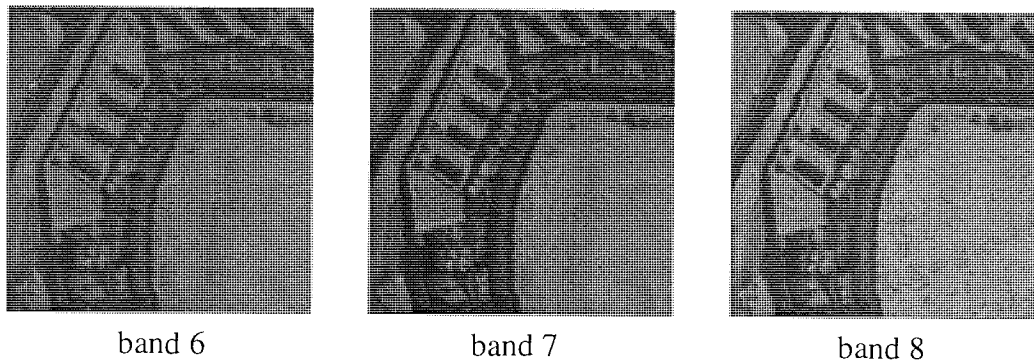
Figure 5.7. Extracts of bands 6, 7 and 8.

| PC 1 | PC 2 | PC 3 |
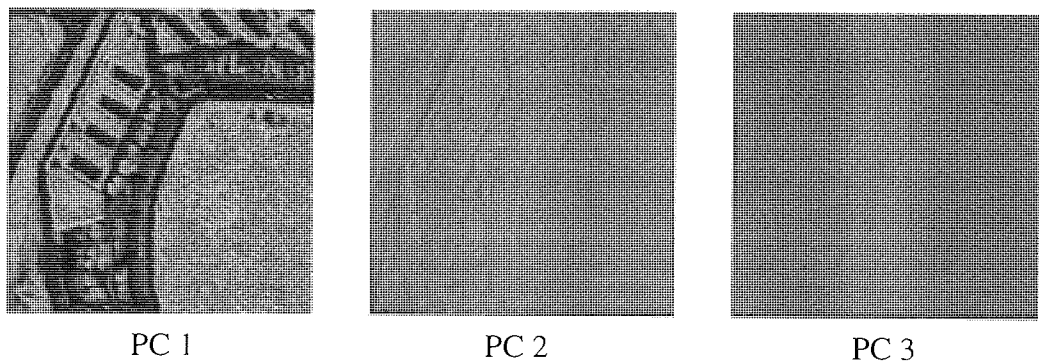
Figure 5.8. The three Principal Components generated from ATM bands 6, 7 and 8.

The calculations involved in the PCA process initiates with the calculation of a covariance matrix. From this it is possible to describe the contributions of each band to each PC from the original bands by way of Eigenvalues (the variances of the transformed space) and Eigenvectors (the direction cosines of the new axes). The Eigenvalues are an indication of the amount of information retained in each PC and those produced by figure 5.8 are given in table 5.2. Because the original bands were very similar almost all the information is now contained in PC1, a tiny fraction remaining in PC2 and PC3.

	PC1	PC2	PC3
Eigenvalues	1624.560	7.234	1.350

Table 5.2. Eigenvalues for the three Principal Components displayed in figure 5.7.

The Eigenvectors indicate how each of the original bands contribute to the new PCs. The Eigenvectors are scaled so that the sum of the squares in each row transformed component is unity. Table 5.3 illustrates that all of the original bands contribute fairly evenly to PC1 due to their similarity. Band 6 makes a large contribution to PC2 and band 7 imparts a large contribution to PC3 but as these components contain a very small amount of information (as shown by the Eigenvalues on table 5.2) these contributions are hardly, if at all, perceived in this case. If the bands had been more disparate PC1 would more likely have one main contributor.

	PC1	PC2	PC3
band 6	0.4596	0.7096	-0.5340
band 7	0.5738	0.2215	0.7884
band 8	0.6777	-0.6688	-0.3053

Table 5.3. Eigenvectors for the three Principal Components displayed in figure 5.7.

The number of bands that can be processed by PCA is limited by the image processing software (the limit of Iconoclast is five) as a computer can work in multi-dimensional space.

5.1.2. Normalised Difference Vegetation Index

The Normalised Difference Vegetation Index (NDVI) is often a simple and effective way of isolating vegetation on digital imagery produced by solar reflectance. It is a method of enhancing the vegetation on an image by taking advantage of its high reflectance in the near infra-red and the low reflectance in the red regions of the spectrum (see section 4.4). This technique is applicable to both points a) and b) from section 5.1 by a) improving the visual appearance and b) preparing the image for quantitative measurement.

The procedure conducted is a process known as band arithmetic. A Vegetation Index is generally any form of band arithmetic that enhances the vegetation. The

Normalised Difference Vegetation Index (NDVI) combines corresponding pixels from the red and near infra-red bands (i.e. from ATM bands 5 and 7 respectively) in the manner shown in equation 5.1 (Danson, 1986).

$$NDVI = \frac{near\ infra-red\ band\ -\ red\ band}{near\ infra-red\ band\ +\ red\ band} \qquad (eq.\ 5.1)$$

The NDVI accentuates the difference between the two bands with the resulting numerical values ranging from -1.0 to 1.0. To make the full scale of values fit with a standard 8-bit image they need to be re-scaled so they fall within the range 0-255 which is achieved using equation 5.2.

$$Rescaled\ pixel\ value = (NDVI * 127.0) + 127.0 \qquad (eq.\ 5.2)$$

The example shown in figure 5.9 illustrates the two bands used in the calculation with the resultant NDVI which now displays a marked difference between the lighter shades of the vegetation and darker shades of the other materials (e.g. buildings, roads and bare earth).

a) Red   b) Near infra-red   c) NDVI
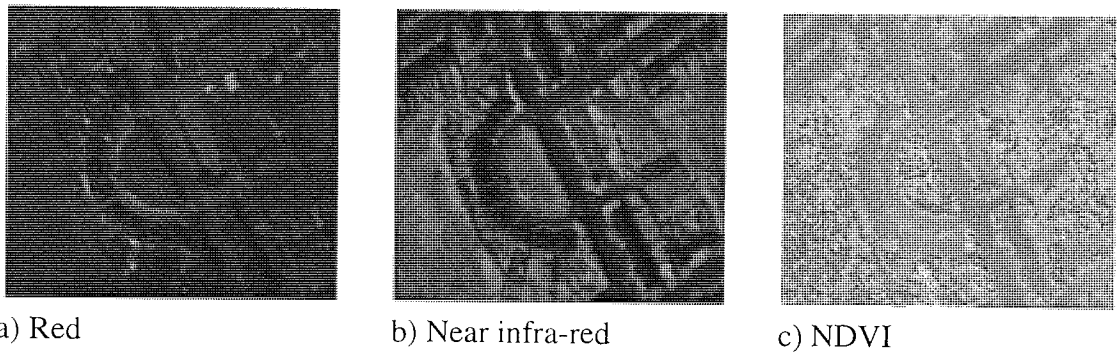
Figure 5.9. Examples of the red (ATM band 5) and near infra-red (ATM band 7) with the resultant NDVI..

5.1.3. Classification

Classification is a process performed on digital imagery that attempts to apply certain 'real world' attributes to an image and encompasses point b) from section 5.1. by preparing the image for quantitative measurement. These classified images can come in the form of dividing a grey-scale image into a multi-coloured contour type image to a categorised land cover image dependent on the reflectance properties of the objects under investigation.

5.1.3.1. Density Slicing

A density slice is a very simple classification performed on a single image, in which different colours are ascribed to prescribed pixel value ranges. Figure 5.9c shows the NDVI which consists of two basic land cover categories: vegetation and non-vegetation. It is possible to simplify this image further using a density slice into these two categories by choosing a threshold point.
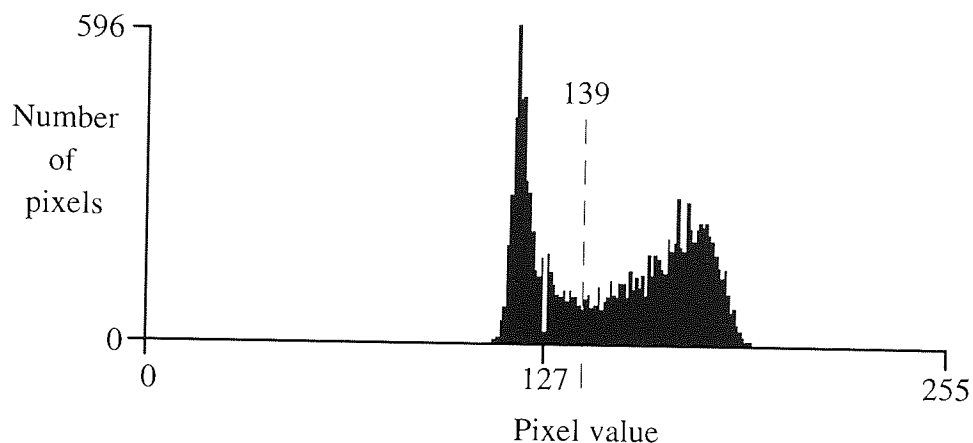
Figure 5.10. Histogram of NDVI for figure 5.9c. Threshold point chosen as 139.

Figure 5.10 shows the histogram of The NDVI from figure 5.9c clearly indicating the bimodal nature of the distribution. Taking into account that the vegetated areas have the higher pixel values, everything to the right of the midpoint (chosen as 139) is designated as vegetated. Therefore, displaying everything below 139 as black and everything above 139 as white will produce the image as shown in figure 5.11 where white areas are generally vegetated and dark areas are generally unvegetated.

Figure 5.11. Density slice of NDVI. White is vegetation, black is non-vegetation.

5.1.3.2. Unsupervised and Supervised Classification

These are methods of comparing more than one image band covering the same spatial domain and finding reflectance similarities that can be subsequently grouped in a single image. Each pixel is effectively plotted in multi-dimensional space, where each axis is the measured brightness in each of the bands used. Generally, different types of land cover occur as clusters and can be separated to produce a new image.

There are three methods of clustering the data for a classification on Iconoclast and they are illustrated in figure 5.12. To use these procedures the clusters are usually pre-determined by way of training areas by the user as in figure 5.16 and the descriptions below are assuming this. The simplest classification routine is known as min-max box method where effectively plane sided boxes are placed around each determined cluster, with the first cluster determined having precedence (see figure 5.12a). This method is very fast as it requires relatively little computation time. The minimum distance classifier is a more complex procedure and calculates the mean co-ordinate within each cluster and then draws a boundary a specific distance from the mean point, usually specified by the user. Any point then falling within each boundary is classified accordingly as shown on figure 5.12b. The maximum likelihood classifier is the most computer demanding procedure of the three and uses probability to distinguish between classes. The computer calculates the probability at each point in the multi-dimensional space in relation to each cluster and each point is placed into the class that has the highest probability. Figure 5.12c expresses this in the form of equal probability contours. For the latter two classifiers the thresholds (distance and probability) are entered by the user whilst for the min-max box method the size of the clusters determine the boundaries. As there are thresholds, some pixels may not be given a class and remain unclassified.

a) Min-max box.   b) Minimum distance.   c) Maximum likelihood.
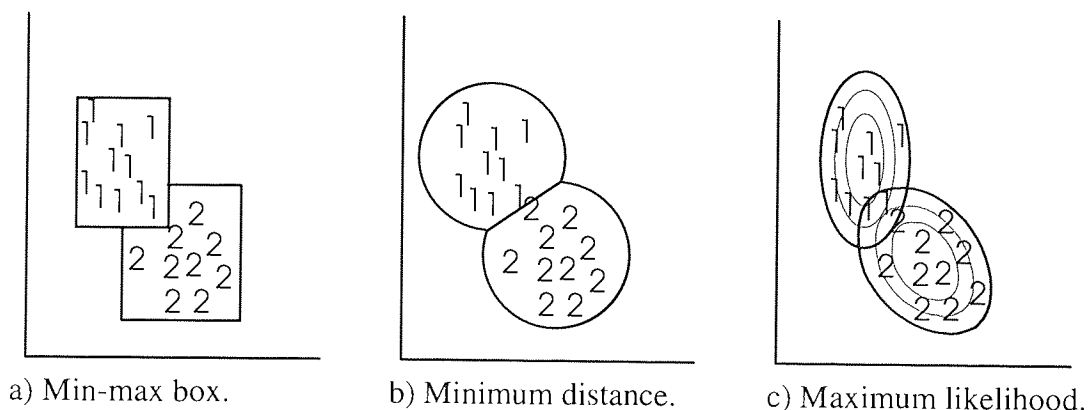
Figure 5.12. Illustrations of the three forms of clustering applied to produce a classification. (Axes correspond to pixel values of two arbitrary bands.)

Classifications can be either unsupervised, where the class statistics are determined by the computer, or supervised, where the class statistics are determined by the human operator.

5.1.3.2.1.   Unsupervised Classification

An unsupervised classification is an entirely computer based process requiring no operator input apart from choosing which bands are to be used and the number of classes required. In effect a multi-dimensional scatter plot is composed by the computer and it iteratively clusters the data into groups.

Figure 5.13 shows a scatter plot of the near infra-red band against the red band as used earlier in figure 5.9. This classification used only two bands (the red and near infra-red bands) for simplicity. Once the scatter has been analysed by the computer, it then decides where the boundaries between the classes fall depending on the number of classes specified by the user (in this case 4).
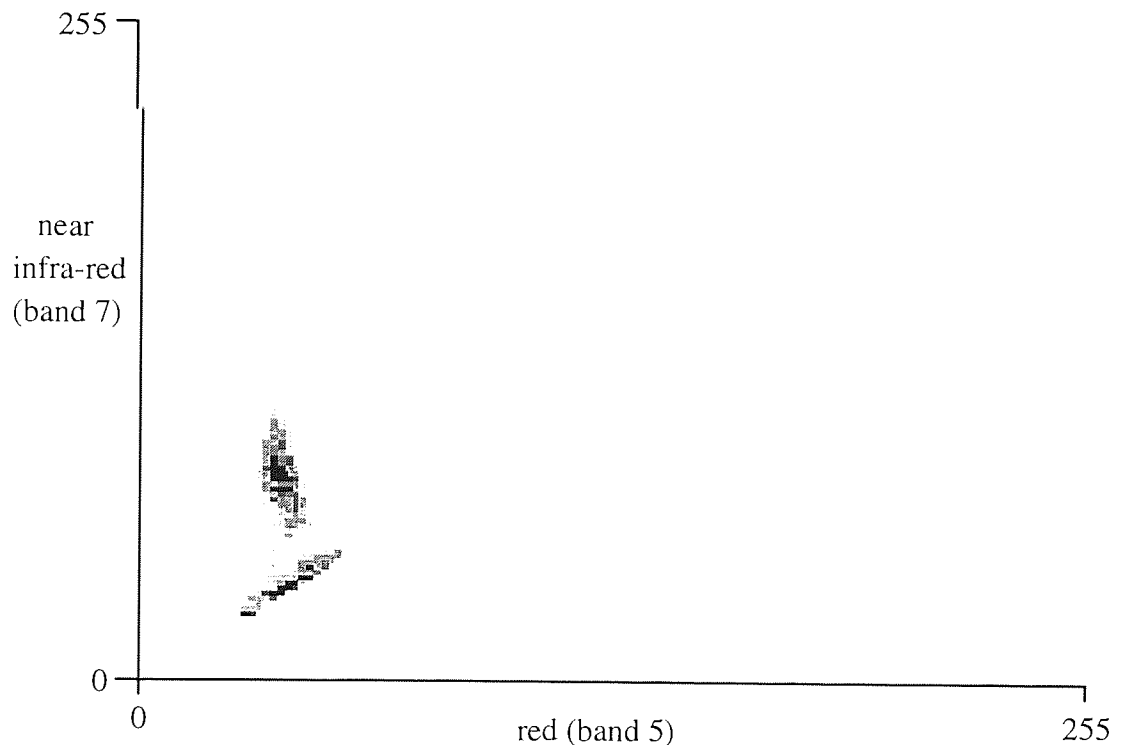
Figure 5.13. Scatter plot of near infra-red band against the red band (bands 7 and 5 respectively). Increase in frequency shown by increase in darkness.
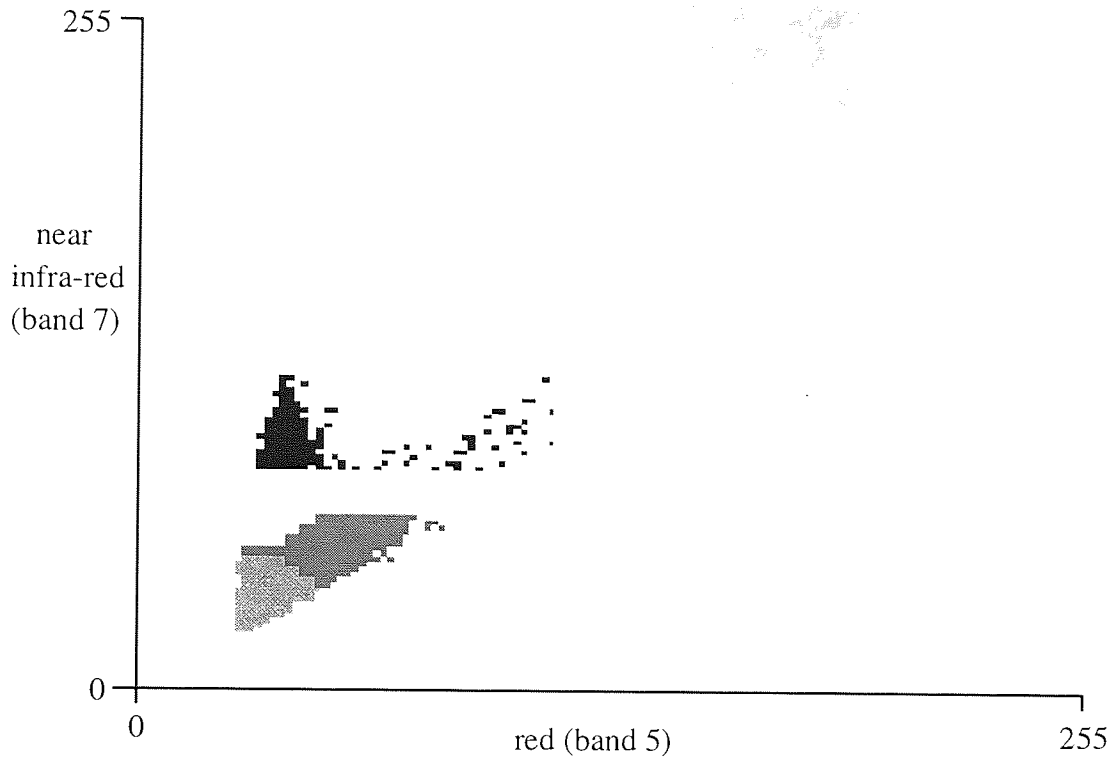
Figure 5.14. Scatter plot of the near infra-red and red bands divided into 4 clusters.

The scatter plot of figure 5.13 has been divided into 4 clusters as shown on figure 5.14 (although many more clusters are possible). These 4 areas can then be converted to an image covering the same spatial dimensions producing the image on figure 5.15. The groups, from manual observation of the original images, can be further be divided into three general classes: 1) vegetation (of which there appears to be two grades), 2) buildings and roads and 3) bare ground. The classification routine used here corresponds to a minimum distance classifier with a large threshold so all the pixels are classified. The quality of this particular classification is clearly not capable of producing a good distinction between roads and buildings hence the need of better classifying methods such as the supervised method.

Buildings and roads

Bare ground

Vegetated
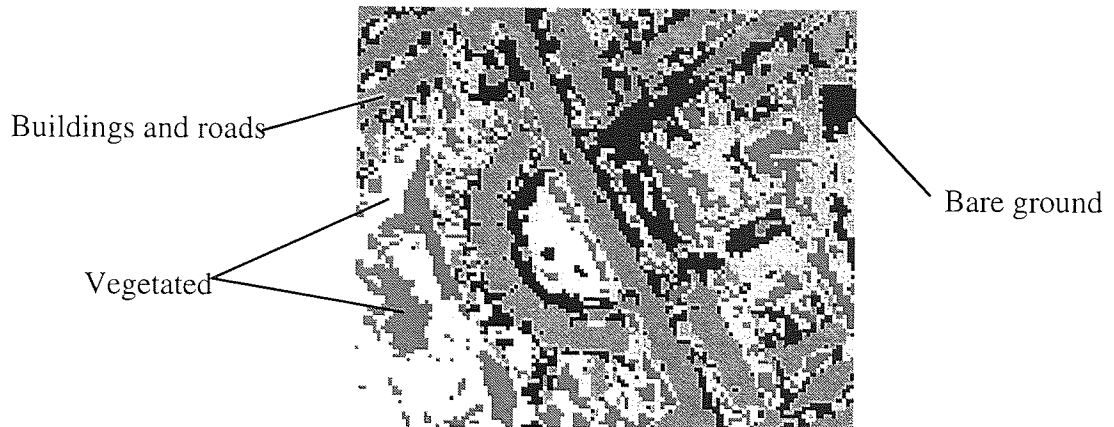
Figure 5.15. Unsupervised classification based on ATM bands 5 and 7. Colours correspond to figure 5.13.

5.1.3.2.2. Supervised Classification

A supervised classification allows the operator to specify what classes are wanted before any statistics have been produced. It is necessary to know something about the ground cover for this method to work properly as areas on the images are chosen as representative of the ground cover. Figure 5.16 shows some areas that have been chosen as classes and superimposed on to ATM band 5 for reference and these are termed 'training areas'.

houses

roads

vegetation

Figure 5.16. Training areas superimposed on ATM band 5 (which has had a contrast enhancement performed upon it).

The statistics of these areas are then calculated by the computer. The training areas are effectively predetermined clusters and have been plotted on the scatter plot shown in figure 5.17.
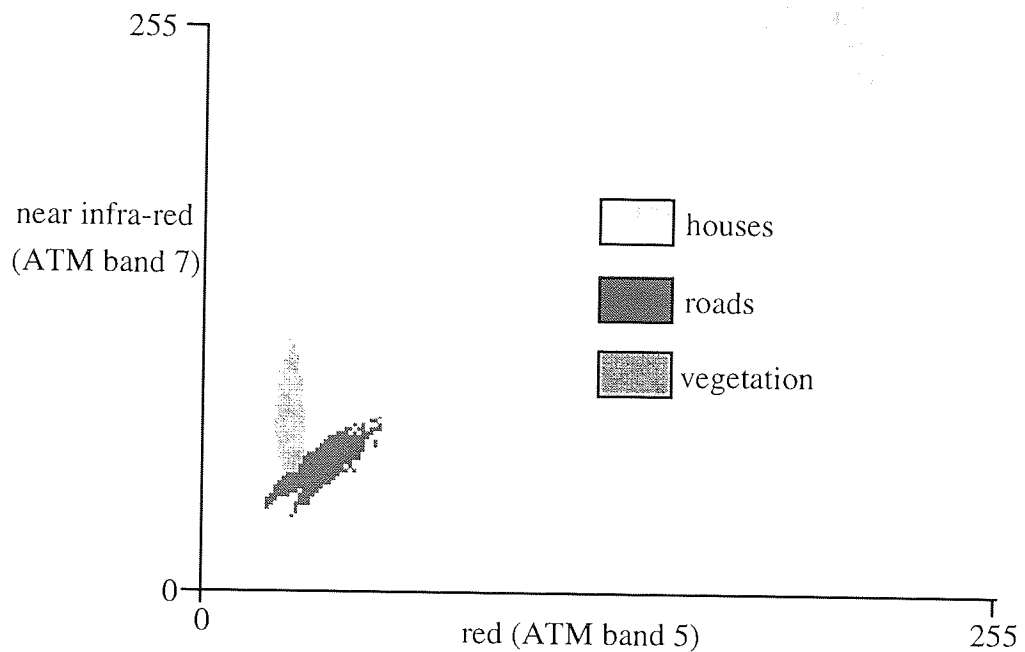
Figure 5.17. Scatter plot for the training areas used in the supervised classification.

Each pixel is then assigned to a class and a classified image is produced as shown on figure 5.18. The classification in this example was carried out using the maximum likelihood method with a threshold probability level of 95% (the pixels have a 95% chance of being classified correctly within the statistical limits of the training areas). As a consequence some of the pixels do not fall into any of the classes chosen and will therefore be unclassified (displayed as black on figure 5.18). The classification in this case is clearly superior to the unsupervised version, because the buildings and roads are more distinctly segregated, and the vegetation is grouped into one category. There is obviously some overlap between the classes but the classification routine could be improved by using more bands which would increase the contrast between the clusters. The routines used during this project employ five bands.

vegetation

roads

houses

unclassified
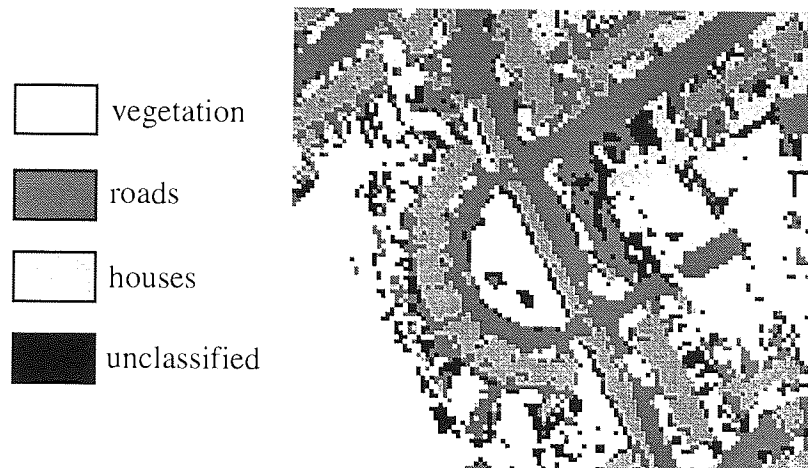
Figure 5.18. Supervised classification based on ATM bands 5 and 7.

Due to its greater flexibility, better control over the training areas and greater use of the available data the author judged that the supervised classification method using the maximum likelihood operation should be used throughout the project.

5.2. Principles of GIS

Carter (1989) defines Geographical Information Systems (GIS) as:

'An integrated system to capture, store, analyse and display information relative to concerns of a geographic nature'

GIS are a method of storing, retrieving, manipulating, and displaying digital information that has attributes that can be related in a consistent co-ordinate system. The availability of inexpensive, powerful computers has allowed the considerable expansion of the usage of GIS in recent years. Burrough (1986) gives a comprehensive overview of GIS.

The principle of GIS is that there are a number of different parameters that cover the same location. The data is therefore made up of a set of overlays covering the same region and figure 5.19 illustrates how four different maps can be viewed as separate entities, or combined revealing their interactions.
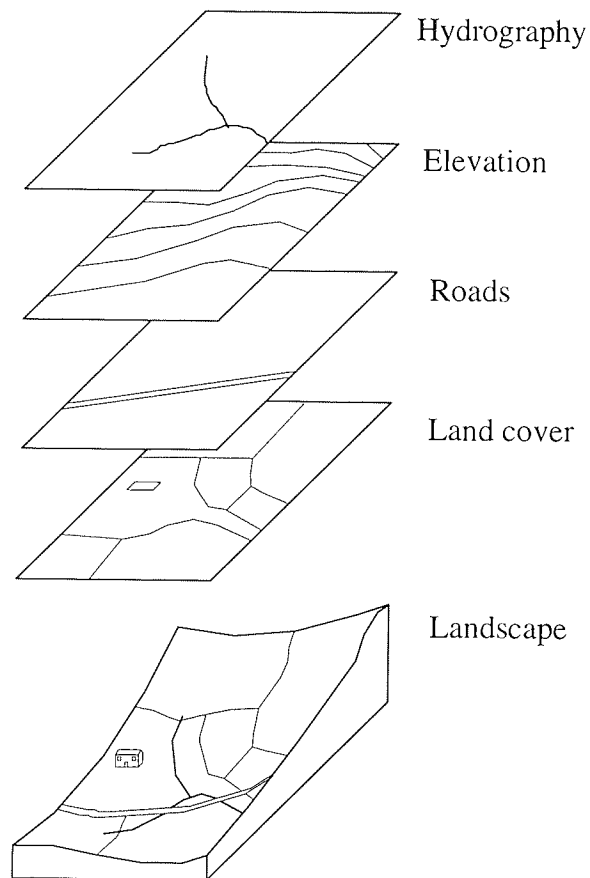
Figure 5.19. A GIS set of four overlays.

It is possible to apply many different procedures to the data that can be shaped to the users demands and these may include clumping (assigning a different class to each contiguous area), buffering (creating a zone around each chosen region of a specified distance), creating slope angle and aspect (from topographic data) or finding the least expensive path between two points (dependent on cost of traversing different cover types).

Using these and other techniques in sequence it is possible to query the database with a multi-stage problem such as: find an area 200m from a road, within 100m of a river, on a area of grassland, greater than 3 hectares and with a slope of less than 1° etc...

5.2.1. Data Types

There are two distinctive types of data used in GIS: raster and vector.

a) Raster

With raster data the images are stored as pixels on a grid with each grid location containing a value. Most digital imagery such as that produced by the ATM or satellites is stored in raster format.

b) Vector

The data in vector format is stored as co-ordinate points which may be stand alone values (as from boreholes) or a node on a line or a polygon (as in a land cover map).

1	1	1	1	1	4	4	4	4	3	3	3	3	3	3
1	1	1	1	4	4	4	4	4	4	3	3	3	3	3
1	1	1	1	4	4	4	4	4	4	4	3	3	3	3
1	1	1	4	4	4	4	4	4	4	4	2	2	2	2
1	1	4	4	4	4	4	4	4	2	2	2	2	2	2
1	1	2	2	4	4	4	2	2	2	2	2	2	2	2

Raster system

vector system
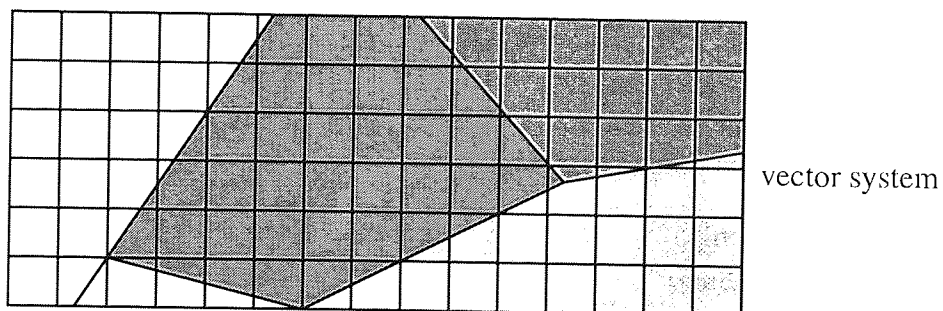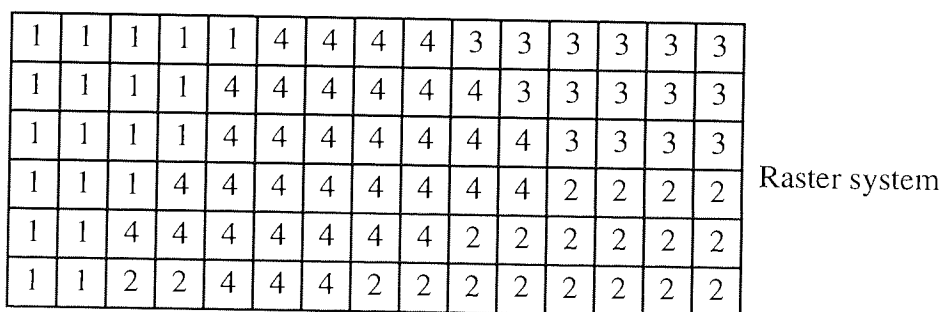
Figure 5.20. Raster and vector formats.

Figure 5.20 shows how the vector format gives a better cover for an area, the boundaries being definable regardless what angle they converge at. Raster format, on the other hand, attributes a value that represents the most common value in the pixel.

Raster format is much simpler to work with and manage when dealing with overlays such as the concept shown in figure 5.19. Vector format is advantageous when dealing with network analyses.

5.3. Geometric Correction

Most images for use within a GIS occupy space equivalent to a map co-ordinate system. Images rarely have any spatial co-ordinates when they are supplied so have to be registered on the relevant map co-ordinate system. In addition, because of the way the data is obtained there are often distortions which may need to be rectified (see sections 4.3.1.1 and 4.3.2.3.4). For instance, sun-synchronous satellites always produce a skewed image due to the earth rotating beneath it as it scans. The general term for these rectification processes is geometric correction and is achieved by registering matching points from the image onto the map and altering the image to suit as shown on figure 5.21.

○ ground control points

original image

image corrected on to
standard co-ordinate system
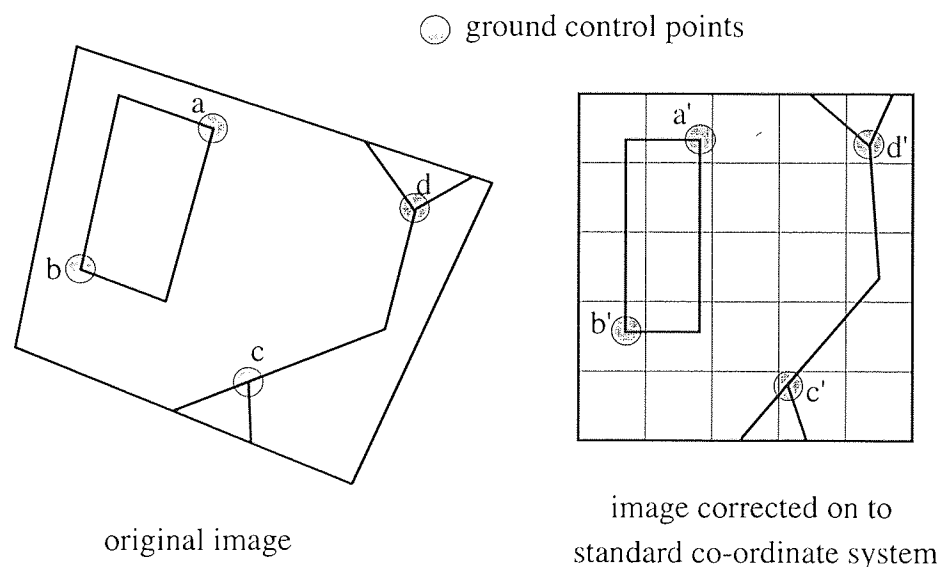
Figure 5.21. The procedure of geometric correction. Ground control points of known co-ordinates (a', b', c' and d') are identified on the original image (a, b, c, and d) and the whole image is rectified on to the standard co-ordinate system. The process is described in more detail in Colwell (1983).

The accuracy of any correction is determined by the Root Mean Square (RMS). The differences between the positions of the points of the corrected image and the positions of the points they should occupy are compared. The calculated RMS gives an indication diferences between the images in terms of distance. If the figure is less than the dimensions of about two pixels then the correction is deemed satifactory and vice versa. Throughout this project, when a correction has been performed the resulting image has only been used if it complies with the above stipulation.

5.4. Software Packages used in this Project

There are two GIS and one image processor used in this project. Idrisi and GRASS are both GIS and are mainly raster based. Both are also capable of conducting image processing procedures.

Idrisi

Idrisi is a raster based GIS written for PC compatible computers and has been developed by the Graduate School of Geography, Clark University, Massachusetts. It was written to run under DOS and uses a mouse based menu system although a Windows version is now available (Eastman, 1995).

GRASS

GRASS (Geographical Resource Analysis Support System) is a public domain GIS developed by the US Army Construction Engineering Research Laboratories. It is a raster based GIS written for a UNIX system and is run from the command line. It is possible to add modules in to the GIS and is constantly developing from a number of different sources (Shapiro, 1993).

Iconoclast

Iconoclast is the image processor used in this project. It is PC based and works off a dedicated circuit board installed into the computer which aids the speed of processing. It uses a separate monitor to display the images with a menu system on the computer monitor. It was developed at Aston university in 1987-89 by Flach (1989).

6. Data Collation and Quality Assessment

6.1. Data Acquisition

The area under study is shown on figure 6.1 and was decided upon by the sponsors and Dr. Peter Hedges of Aston University, and the flying application was submitted to NERC as part of the Airborne Remote Sensing Programme of 1992. The principal device that was to be evaluated was the ATM described in section 4.3.2.3. The research proposal highlighted two areas, the Black Country area, a considerable portion of which is 'made ground' including some completed landfill sites, and a single active landfill six miles to the east which is just on the Birmingham side of its border with Walsall.

The submission to NERC was to fly the ATM with simultaneous stereo aerial photography coverage of the study areas. The areas were flown on 25/6/92 at 9:30 in the morning even though a midday flight was requested and the actual coverage is shown on figure 6.1. The whole of the proposed area was covered with more than sufficient overlap for stereo aerial photographic coverage. The resulting photographs were approximately 1:5000 scale, each with a ground coverage of approximately 1.5km by 1.5km.
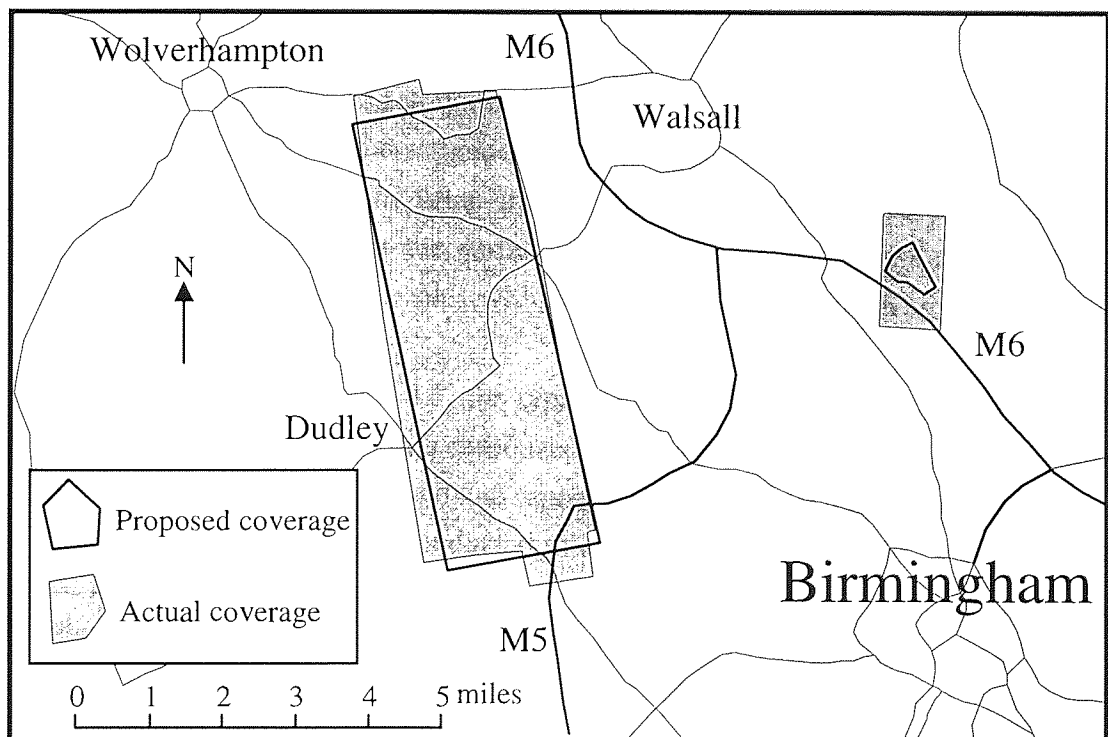
Figure 6.1. Proposed and actual coverage of the June 1992 ATM and aerial photographic data.

6.1.1. Desk Study

In studies of this nature, where circumstances of the past are under scrutiny, it is common to carry out a desk study of the available data for the area in question. Both the West Midlands Hazardous Waste Unit (HWU) and the Black Country Development Council (BCDC) hold records of sites in their areas of jurisdiction. The BCDC has records relating to sites that they own and the HWU have records of waste disposal licences that they approved from 1974 onwards.

The HWU is the regulatory body responsible for overseeing the disposal of waste in the West Midlands. Anyone wanting to dispose of any waste have a legal obligation to obtain a disposal licence from them. The HWU will then deliberate and either approve or deny a licence on the merits of the application. The licence contains details of the operating principles of the filling and aftercare procedures but, more importantly, what is allowed to be deposited (see section 3.2). All the available licences for the area were examined and their licensed fill types and quantities were collated.

The Black Country Development Corporation own much of the derelict land in the Black Country and are sanctioned to develop the area. One of the major development projects in recent years has been the Black Country Spine Road which was designed to connect the M5 at Junction 2 to Junction 10 of the M6, passing through the heavily industrialised Wednesbury and Bilston area. This road (now renamed the Black Country New Road) was officially opened in November 1995.

Before construction can commence on a project such as the Spine Road it is required that a full site investigation should be undertaken to identify potential problems. The investigations often include sinking boreholes into the ground and sampling the material below the surface. The site investigation reports for both the Spine Road project and other sites within the BCDC boundaries were examined and their contents were noted.

As stated in section 3.4.1, the types of waste that are liable to create landfill gas and leachate are those with a carbonaceous content, of which the most common is domestic refuse. The licences and site reports were examined particularly for this sort of waste. The desk study was conducted in order to gain a better understanding of the areas, test the validity of using historical records and identify suitable sites for more detailed study, which are described in section 6.5.

6.1.1.1. Monitored Gas Concentrations at sites D and Q

The BCDC and HWU provided additional sources of data in the form of monitored gas concentrations.

Since the closure of site D the boreholes outside the boundary of site are sampled for methane, carbon dioxide and oxygen on a generally weekly basis.

At site Q and extensive three month monitoring programme was undertaken from August to October 1991 using borehole levels, spike tests and Flame Ionisation Detector (FID) surveys. The locations surveyed were predominantly down the eastern side of the site as it bordered a residential area.

From the data gathered from these monitoring programmes it was intended to highlight possible areas to focus upon and in the case of the site Q data produce a rough model of the gas migration beyond the boundaries of the site.

6.1.2. Historical Aerial Photography

As part of the background study, a number of historical aerial photographs for the two areas were acquired. Details of these photographs can be found in Appendix E.

Some of the photographs were available in the remote sensing centre in the Civil Engineering Department at Aston University (the 1971 set). For this research, by far the best archive was that of the University of Cambridge, who fly the whole West Midlands area every 2 or 3 years and then supply the local authorities with the photographs.

The photographs were employed to assess their value when used for the analysis of waste disposal sites. As well as being able to tell the observer something about the ground at the time of taking, past photographs of the same area can show what has happened over time. One site was examined in detail in this manner as it was present on all of the photographic sets obtained. The analysis followed the deposition history of the site by producing overlays on acetate sheets, with the aid of a stereoscope. Areas of depression that were to be filled at a later date were outlined along with local landmarks (lakes and roads). In order to quantitatively measure the actual areas of depression the overlays were scanned into an imaging package (Picture Publisher) and the depressions were digitised on screen. The images were then read into a GIS and georectified onto National Grid co-ordinates where the physical area of each depression was ascertained.

6.1.3. Thermal Surveys

In order to test the hypothesis that leachate and landfill gas may be detected through their heat signatures, different methods of thermal remote sensing were applied. In addition to the thermal band obtained as part of the ATM daylight data, an aerial survey of two sites was carried out using a thermal video camera and a second ATM flight of the whole area was granted by NERC, but this time at dawn.

6.1.3.1. Dawn Thermal ATM

The dawn flight, using the thermal band of the ATM, took place on the 8th of April 1994 at approximately 6am. The total area covered was expanded to include sites identified by Sandwell Borough Council as being of potential interest and covered the entire region plus additional areas to the south of the original study site. Figure 6.2 shows the area covered by this thermal ATM survey. Some areas were missed which is a common problem with surveys that are carried out in very low light conditions as identifiable landmarks are difficult to locate. Fortunately, none of the actual sites of interest within the areas were missed.
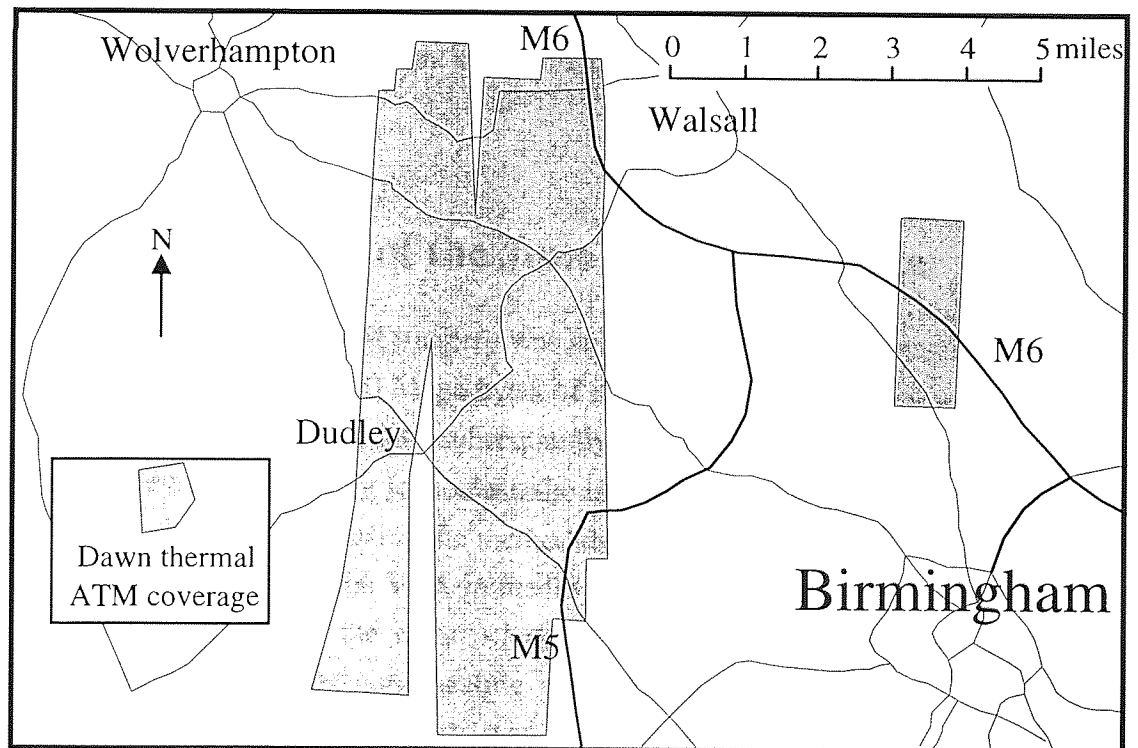
Figure 6.2. Total coverage of the dawn thermal ATM.

6.1.3.2. Aerial Thermal Video

The original intention was to undertake the flight at just after dawn, so that ground temperature would be at a minimum with all of the previous day's heat having dissipated (see section 4.2.2.1). Two landfill sites were to be surveyed, but as the particular area where they are located is prone to fog in the late autumn and winter, the flight was continually cancelled. The flight was undertaken in collaboration with TBV Stangers and was subject to their advice and time schedules. It was therefore agreed, on their advice, that the flight would be undertaken just before sunset on a day that was heavily overcast.

The flight finally took place on the 23rd November 1994 at 3:30pm under a heavily overcast sky. According to the operator of the camera if the clouds are sufficiently thick they act as a sunblock and the amount of heating due to direct solar radiation is reduced to a level through which thermal anomalies should be visible. The camera is mounted in a helicopter which flies at approximately ≈ 150m. This is the minimum flying height allowed for a twin-engined helicopter over a built up area. The method applied for this survey was to simply circle the site two or three times while pointing the camera towards the ground at about 30-45° from the horizontal. In this particular case a colour camcorder was used, in parallel with the thermal camera, to aid in feature identification during analysis. The method statement of the company that carried out the survey can be found in appendix B along with details on the camera employed.

6.2. Examination of the June 1992 ATM Data

The June 1992 ATM imagery was supplied on 9 half-inch magnetic tapes and totalled in the region of 300 Mega bytes of data. The magnetic tapes were read on to the university VAX server and subsequently downloaded onto the UNIX server. In order to view the data using Iconoclast, the interleaved ATM data had to be separated into the 12 discrete bands using the method described in section 4.3.2.3.2.

It was found that the VAX in reading the tapes was inserting additional values into the data. This had the effect of creating a non-uniform data length for each interleaved band thereby complicating what should have been a simple extraction procedure. A computer program was written by Rob Poole, the departmental computer technician, in C to enable the individual bands to be separated by searching for the end-of-line markers.

Once the data had been separated successfully it was viewed using Iconoclast. It was immediately clear that the intensity variation across the image was inconsistent.
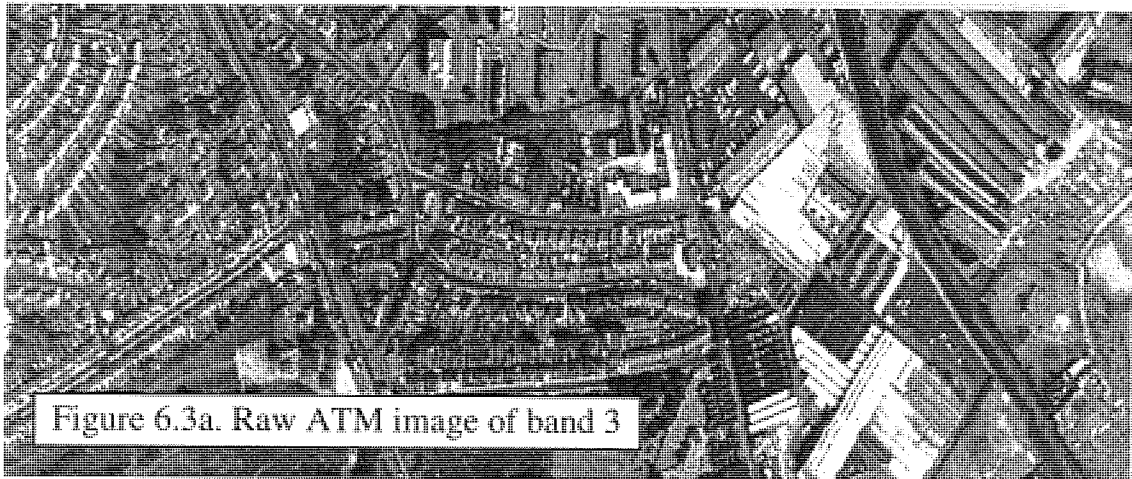
Figure 6.3a. Raw ATM image of band 3
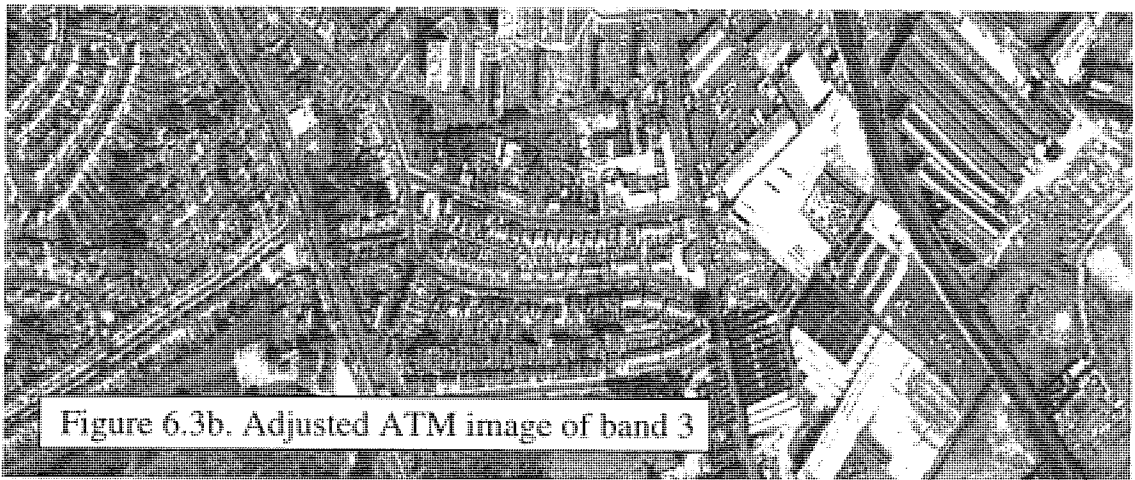
Figure 6.3b. Adjusted ATM image of band 3

Figures 6.3a and b. Extracts of ATM images of band 3 showing raw data above and the corrected image below.
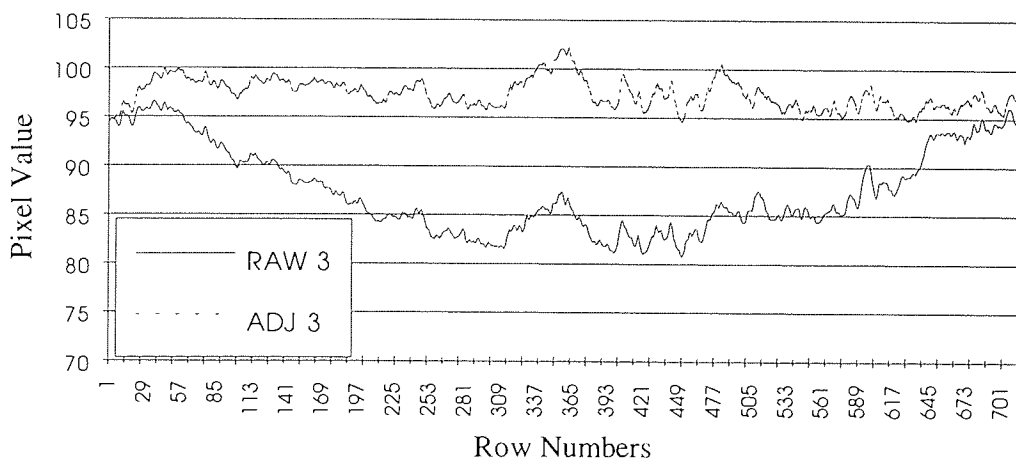
Figure 6.4. Plot of mean pixel value across the image from figure 6.3a (RAW 3) and figure 6.3b (ADJ 3).
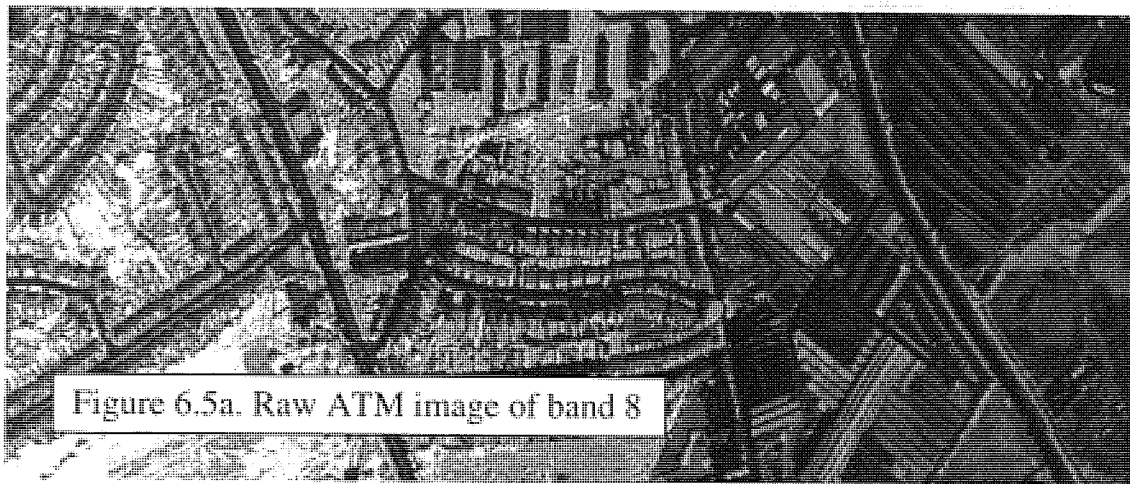
Figure 6.5a. Raw ATM image of band 8
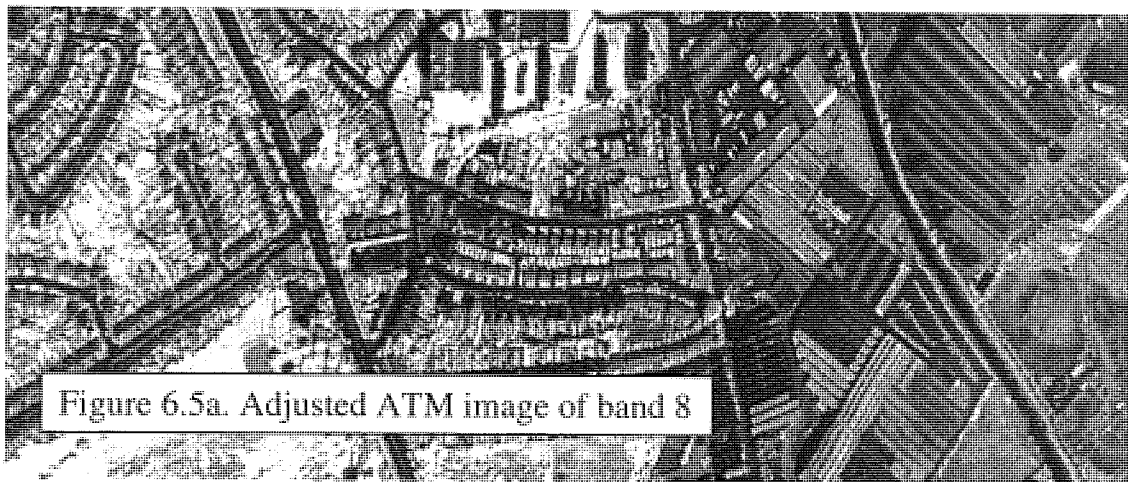
Figure 6.5a. Adjusted ATM image of band 8

Figures 6.5a and b. Extracts of ATM images of band 8 showing raw data above and the corrected image below.
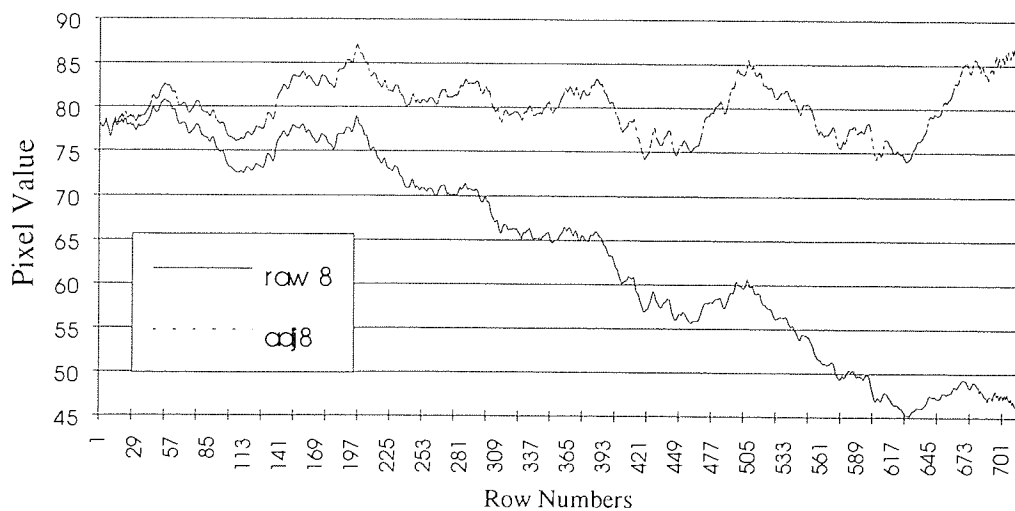
Figure 6.6. Plot of pixel value across the images from figure 6.5a (raw 8) and figure 6.5b (adj8).

Image brightness either increased towards one side or exhibited an increase/decrease down the centre of the image. This is illustrated by Figure 6.3 which shows an extract from an ATM band 3 image, with figure 6.3a being the raw data and figure 6.3b is the same image after correction.

The difference between the two images is shown more clearly by taking the mean pixel value in each of the 716 columns that make up the image and plotting them on a graph. Figure 6.4 shows clearly the reduction of mean pixel value in the central region of the image.

Figure 6.5 shows another ATM extract of band 8 for exactly the same area as on figure 6.3. On this occasion the inconsistency in the image is shown by a marked decrease in pixel value from left to right.

When plotted in the same way as figure 6.4, figure 6.6 is the result showing the raw data and the corrected data. The variation in pixel value across the image is related to the wide scan angle of the ATM often termed the 'scan angle effect' (Barnsley & Barr, 1993). This effect, according to Barnsley (1993), is due to the angular reflectance properties of earth surface materials and the anisotropic scattering of radiation within the atmosphere. The degree and characteristics of the effect are a function of the wavelength as illustrated by figures 6.4 and 6.6.

The imagery affected by 'scan angle effect' cannot be used until the disparity has been corrected. The steps of the correction process conducted are given below and illustrated in figure 6.7:

a) Calculate the mean pixel value in each of the 716 columns of a single image.
b) Fit a second order polynomial curve to the resultant values.
c) Calculate the correction needed to transform the curve down to a horizontal line.
d) Adjust the value of each individual pixel of the raw data in relation to its position to fit the horizontal line calculated in c).

The programs were written by Tom Charnock, a research student in the department, and the author in Pascal and the source codes can be found in Appendix F.
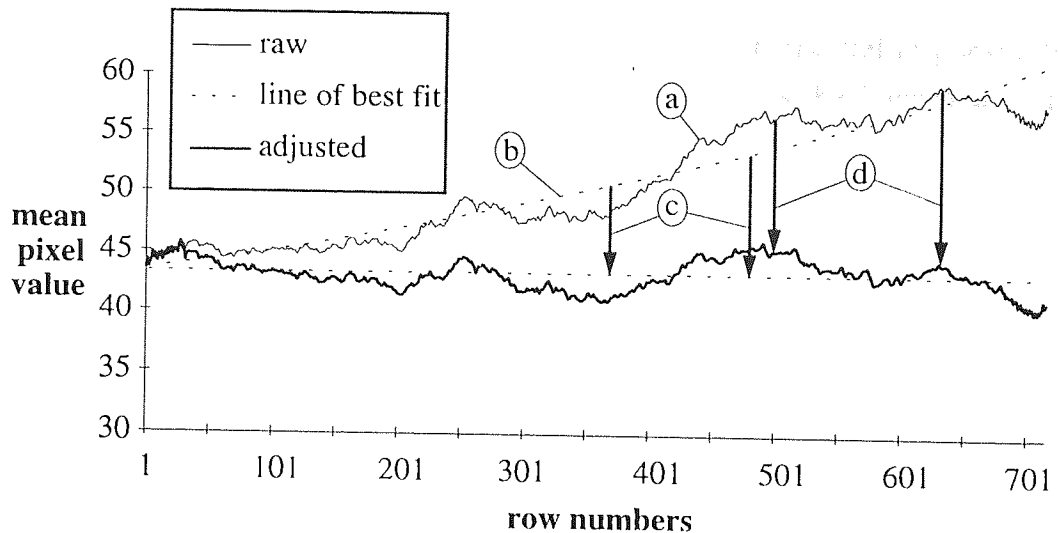
Figure 6.7. Illustration of the 'scan angle effect' correction method for ATM data. For annotations see text.

This method of correcting for 'scan angle effect' has been applied to ATM data independently on at least two other occasions (Danson, 1986 and Barnsley & Barr, 1993)

6.3. Quality of the Imagery

Each of the three sets of imagery (daylight ATM, dawn ATM and thermal video) were examined separately to ascertain its quality.

6.3.1. Daylight ATM Imagery

Each of the ATM bands was observed individually on Iconoclast to determine what general features were visible. Band 1 was extremely bad in quality appearing very noisy, a fact which has been documented before (Finch, 1993, Singh, 1988 and Groom, 1987). This band spanned the violet region (0.42μm to 0.45μm) so the noise is attributable to Rayleigh scattering (see section 4.2.1.1). The remaining visible bands (bands 2, 3, 4 and 5) were of a high quality, in general, with band 2 being slightly worse than for the others, possibly again due to Rayleigh scattering because of band 2's shorter wavelength. For all the visible bands water always appeared darkest with vegetation slightly brighter (trees darker than grass). Roads take on intermediate values whilst bare earth and buildings appear brightest of all. Any region in shadow appears very dark. The three near infra-red bands (bands 6, 7 and 8) were all of good quality with band 7 showing the greatest contrast. These three bands exhibit characteristics that appear almost inverted to the visible bands, with all vegetated areas showing up brightest whilst roads, buildings and water appear dark. Band 9

116

generally followed the very near infra-red bands with their spectral responses, but it contained a substantial amount of noise giving an overall speckled appearance. Band 10 shows similarities in spectral response with the visible bands, with water and vegetation appearing dark and man-made materials appearing brightest. Band 11 showed the greatest contrast of all the ATM bands. Buildings, roads and bare ground were the bright whilst vegetation and water appeared dark on the image. Band 12 was identical to band 11 apart from the fact that all the values were halved due to the gain setting performed by the ATM. Taking these observations into account bands 1, 9 and 12 were discarded at an early stage.

6.3.2. Dawn Thermal ATM

The appearance of the dawn thermal imagery is good and many objects on the ground are clearly identifiable. Some of the imagery was tested for 'scan angle effect' using the method described in section 6.2, but none was found and no adjustment was necessary. In general, water appears as relatively warm, vegetation shows up as an intermediate brightness and artificial materials (roads and roofs) appear cold (dark).

Geo-rectification of ATM imagery has been stated as problematic in section 5.3. Relatively small areas can be corrected on to the National Grid with a sufficiently low RMS error for it to be deemed satisfactory. An attempt was made in this project to correct the daylight ATM thermal on to the dawn ATM thermal which would have given useful information on the thermal inertia of ground surfaces and possibly eliminate the problem of masking heat sources such as water. Whereas correcting one ATM image on to a regular grid was possible for small areas, it was not possible to correct a second ATM image on to a previously corrected one as the geometric errors appear to be accentuated. Due to this problem this method was not explored further although its potential usefulness is favourable and has been noted in Chapters 9 and 10.

6.3.3. Aerial Thermal Video

The thermal video camera used in this project was the Agema Thermovision 450 which is sensitive in the shorter wavelength thermal window (2-5μm). This allows the radiation sensitive plate to be cooled electronically rather than by using extremely low temperature liquefied gasses (see section 4.3.3.1). This 'window' is susceptible to interference from solar radiation, as shown on figure 4.5, and because this survey was undertaken during the day there is considerable image quality deterioration.

Many features are recognisable in the imagery when viewed as a motion picture, but when it is paused object identification is very difficult. The small

difference between the highest and lowest temperatures on the ground (10-15°C) is only a tiny portion of the full sensitivity of the camera (−20-500°C), so it has difficulty producing a clear picture. The camera is capable of producing multi-coloured outputs and most of the survey was carried out using the 'ironbow' colour scale, favoured by the operator, which scales the colours of objects from hot to cold between white and black through yellow, orange, red, magenta and blue. Whilst this colour scheme is acceptable for normal video viewing it is not possible to transfer scenes to an image processor, because a colour picture requires the combination of three images, one of each red, green and blue light. It was possible, however, to convert the image to a greyscale using a video frame-grabber, although some contrast was lost as certain colours, whilst being different, have comparable intensities and may look similar on a monochrome image. As the video data is in analogue format the intensity of the pixels on the image displayed by the monitor are relative and can be adjusted using a saturation control. Therefore, any values measured following the grabbing operation are relative and do not refer to anything on any other quantifiable scale.

6.4. Spike Tests

In conjunction with the dawn thermal imagery a number of spike tests were conducted. A spike test is a method of obtaining a measure of soil gas levels from below the ground surface by making a hole using a ram and quickly placing a gas detector at he mouth of the hole. The device used in this case was a 12mm diameter spike that was driven approximately 30cm into the ground. Two types of gas detectors were used; a carbon dioxide meter, and a combined methane and oxygen meter. The CH_4/O_2 meter drew air in using a hand pump whilst the CO_2 meter had a motorised pump. In order for a single sampling tube to be placed in the spiked hole the meters were connected in series and the gasses were drawn through both meters using the motorised pump from the CO_2 meter.

6.5. Choice of Sites

Out of the 30 or so known sites within the two study areas, five sites were chosen for detailed study. They were selected using aerial photographs, site records and consultation with members of the HWU and BCDC on the basis that they give a good range of fill types, cover types and ages.

Site Q - Until about 1971 this site was quarried for gravel as it lies upon the Kidderminster sandstone (formerly named the Bunter Pebble Beds). When all quarrying was completed the area was filled with waste. It was operated by the local authority, and became a very important site for disposing the regions domestic waste. Filling continued until 1993 when the site was completed. As far as is known no basal or side wall liner was incorporated into the design but a synthetic liner was constructed along one side of the site and two vent trenches were excavated along two other boundaries that had houses nearby. To act in conjunction with the liner a positive pressure gas extraction system was installed. Filling officially finished in 1993, at which time another extraction system was constructed upon totally encircling the main fill area. The site was covered with clay and many areas have been planted with trees. The earliest filled areas are now accessible as public open space. A whole variety of wastes were deposited, but as previously mentioned, its prime use was for depositing domestic waste.

This site is to the east of the main study area and is the isolated area shown on figure 6.1. and lies upon the permeable Kidderminster sandstone. This sandstone and associated underlying sandstone are an important local aquifer and water abstraction has been taking place since the mid 19th Century for drinking and manufacturing (Knipe et al 1993). Even though the abstraction rates are now only a sixth of the peak rates during the 1940s the problem of leachate from site Q may still cause significant pollution of the aquifer. Unfortunately it was not possible to may any judgements of the effects of the leachate on the aquifer during this project.

Site S - This landfill site was completed in approximately 1985 and subsequently landscaped (landscaping was still under construction in July 1992 - during the first ATM flight) and opened as an urban park. It currently contains two lakes (only one of which has always been present) which are used for fishing, and are beneficial to birdlife. However, their primary use is as part of a flood alleviation scheme for the river Tame, which passes through the park. According to the site licence only "clean inert material consisting of subsoil, concrete, brick rubble and foundry sand" was supposed to be deposited, but the site is known to be producing gas.

Site S is situated on rocks of Westphalian (Upper Carboniferous) age which are designated 'no groundwater flow' rocks. Because of this any leachate the may be produced may move overland and pollute either open ground of water courses. In the case of Site S there are two lakes on the site itself and the river Tame flows through it. These are obvious possible receiving waters and will have to be carefully looked at for leachate ingress.

Site R - Site R is actually a number of sub-sites that are adjacent to each other. All the site licences for these sites allowed only inert waste (foundry sands, bricks and rubble etc.) of a non-hazardous nature, but even so landfill gas has been found coming from the site. It is located adjacent to site S on the other site of a rail and canal embankment. The river Tame passes through the site and progresses directly to Site S through a tunnel in the embankment. A residential estate has been built on a large proportion of the site.

Site R is adjacent to Site S and is located on the same rocks so the same situation with leachate migration will occur. The most likely receiving water course is the river Tame that passes through it before moving on to Site S which will be looked at carefully..

Site D - This landfill site was completed in 1991. The site is situated on the intrusive doleritic rocks in the southern part of the region and this material was quarried leaving a hole of about a million cubic metres. No lining was placed at the base or sides of the site prior to filling. The quarry was cut into a slope of about 15 ° with a flat base, so that when filling was complete forming a wedge with the depth of waste varying from 5 metres to 40 metres

The type of waste deposited was varied, but domestic waste accounted for 37% of the total weight (see appendix G for a breakdown of the waste quantities). At the base of the site there are two leachate wells which are pumped to a foul water sewer. There is a positive pressure gas extraction system in operation with 21 wells on the site. The site was not capped with an impermeable layer as would be expected so the final cover present is a mixture of inert materials such as soil and rubble. The pipes leading from the wells to the flares are supported on clay ridges and as the proper final cover has not been applied these ridges stand one metre above the surface as they were originally designed to be covered. The final topography of the site is considerably lower than before quarrying took place with the south and eastern sides of the site being up to five metres below the immediately surrounding land. There are 13 monitoring boreholes around the perimeter of the site which vary in depth but all go to at least 20m below the base of the site. There are residential buildings in close proximity to the site on all sides and some houses are a mere 20 metres from the site boundary.

On a cursory visit to the site a number of cracks were evident at the northern and eastern boundaries. Some of these cracks were clearly emanating landfill gas which revealed itself by clouds of steam as the warm moisture laden gas condensed on

meeting cooler surface air producing . For this reason this site was ear-marked as useful to the project and was the most studied of all the sites.

The igneous dolerites that Site D is situated on is very unlikely to have and groundwater flow so similarly to Sites R and S the leachate movement, if any occurs, will be overland. As this site is on a slope and higher than some of the surrounding land, with no water bodies at the lowest point the places to look for leachate migration are to the north and down the slope.

Site H - This site is situated on the same dolerite intrusion as site D and was quarried for the same purpose, and is unusual in that filling and quarrying as actually taking place at the same time. Quarrying had been undertaken for a considerable time and when it was decided that the south-eastern part of the site was no longer to be quarried filling operations commenced. The final volume for filling has been estimated at about 15Mm^3. The filled area, which is not substantial at present, has gas extraction and leachate collection systems. This site was to the south of the daylight ATM, flight but was included in the thermal camera survey and the dawn ATM flight.

Similar ground conditions occur here as at site D as they are located on the same igneous intrusion. The filled area though is on the inside wall of a large void. The lowest point locally is at the base of the void where it is bare rock and ponding often takes place regularly with site machinery usually working in the area making any leachate identification difficult.

Each of the aforementioned sites were examined using the methods described in chapters 5 and 6 where appropriate (i.e. the thermal video analysis can only be performed on sites D and H as this was the extent of the coverage). The degree of analysis performed on each site fluctuated with the quality of the results. Chapter 7 reflects this fact and provides a description of the results obtained with a considerable weighting to those sites that revealed the most information.

7. Data Analysis

7.1. Introduction

Five sites were studied in detail and are described in section 6.5. A number of procedures were performed on these sites to varying degrees and those that gave the most useful results are described in this chapter. Table 7.1 shows which procedures were carried out on which sites and whether they have been documented in this thesis. Sites S and R were found to be inert when viewed on the imagery and are only mentioned briefly. Site Q was focused on when using the aerial photography because some of the photographic sets were incomplete and only site Q was present on all of them. Site H was only included with the thermal imagery and the dawn flight as it was not present on the daylight imagery. Site D showed itself to be the most interesting from the point of view of its obvious sub-surface activity and is the most intensely studied site.

Site	Aerial photography	classification on ATM day	Day ATM thermal	dawn ATM	Thermal Video
Q	S	N	S	X	X
D	N	S	S	S	S
S	N	N	N	X	X
R	N	N	N	X	X
H	X	X	X	S	S

Table 7.1. Procedures performed on the study sites. S = studied and documented in this chapter, N = studied but not documented in this thesis and X = not studied.

7.2. Problem Site Identification and Examination

The types of wastes that pose a problem with respect to landfill gas and leachate are those that have a carbonaceous content. The most highly active waste is domestic refuse because of the relatively high complement of readily degradable organic material, such as vegetable peelings and other food type waste (see section 3.4).

Using the above reasoning, those sites that were known to contain, thought to contain and those licensed to dispose of domestic refuse were identified as having the greatest chance of being a problem.

7.2.1. Desk Study

The site disposal licences of the HWU and the site investigation reports of the BCDC were examined for the Black Country area and collated. Figure 7.1 shows all of the sites in the project area that have had a licence granted by the HWU to dispose of waste to land since the licensing system was introduced in 1974.
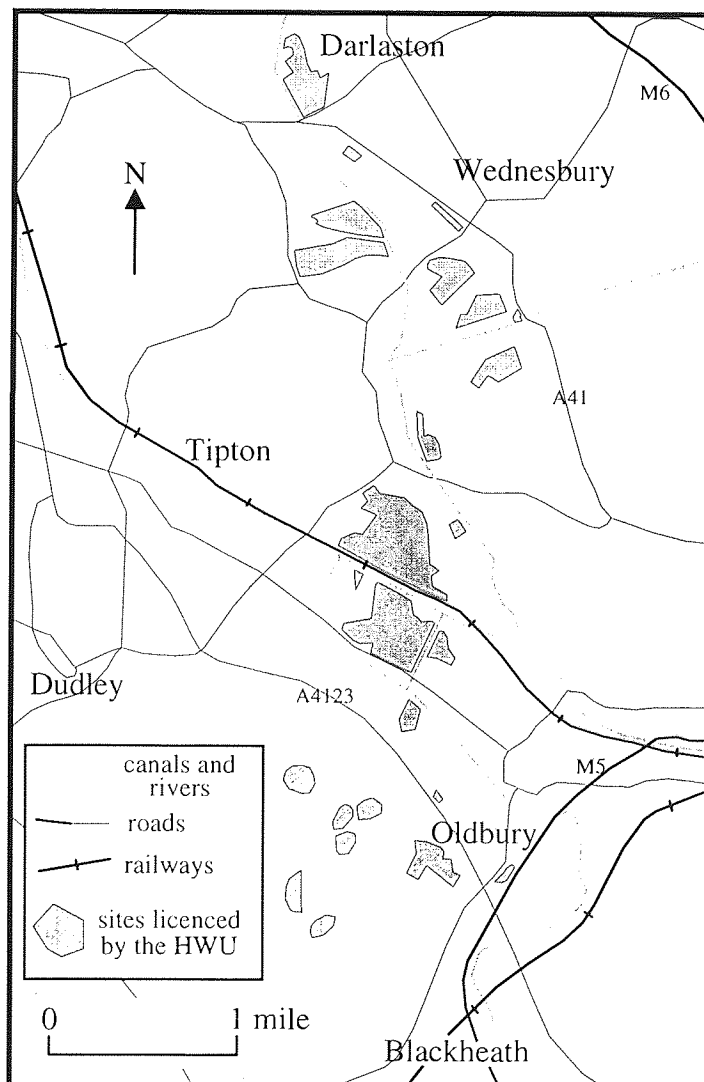
Figure 7.1. Sites that have had disposal licences granted within the Black Country study area.

Figure 7.2 illustrates all the sites under the jurisdiction of the BCDC that are known to contain fill (any non-*in situ* material used to fill a volume) by way of site investigation information. Before a project such as the Spine Road can be started it is statutory to have the sites investigated for potential problems. Investigations were undertaken for the Spine Road and for this reason much of the information about the ground condition followed the proposed route. It is significant that almost all of the sites investigated along the length of the Spine Road were found to contain fill, suggesting that a substantial amount of the region contains fill of some sort.

Of the 30 sites that had licences issued by the HWU in the Black Country area, 13 were categorised as potentially methanogenic because they were licensed to dispose of domestic refuse. 12 sites in the area are known to be producing gas, three of these, though, were not categorised as potentially methanogenic as they were only licensed for the disposal of inert material.
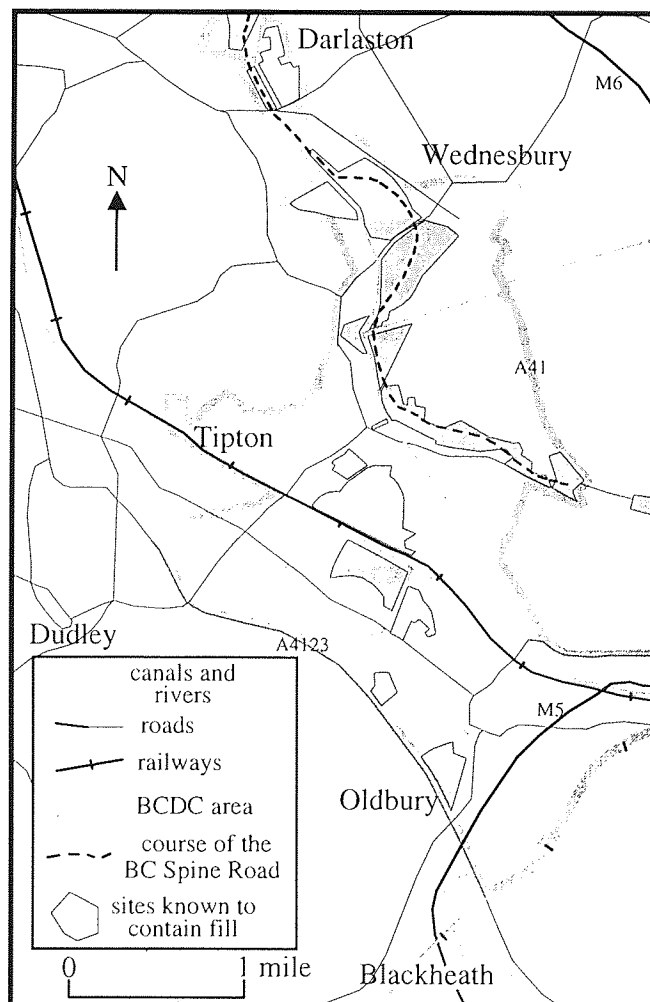
Figure 7.2. Sites within the BCDC jurisdiction area that are known to contain fill.

38 sites were identified from records produced by the BCDC as containing some sort of fill. Many are these are designated as 'sites' because they were inspected as part of the obligatory investigation of the area for the 'Black Country Spine Road' development. Consequently there is a string of sites that follow the proposed route. Of these 38 sites, 8 contain or possibly contain domestic wastes. Of these 8 sites only 5 have had a disposal licence granted by the HWU, the remaining three were probably in operation before 1974.

The indication, generally speaking, is that historical records do not tell the whole story and cannot be relied upon to determine whether a site will produce methane problems or not. There is no question that any site that contains domestic refuse will produce methane and leachate. The examples in this study, though, show that some sites licensed to dispose of inert, non-degradable and, non-potentially methanogenic, can still produce landfill gas. As some of the potentially methanogenic sites were not known to be producing gas, and the likelihood is that they are, it appears that unless there is an organised monitoring strategy or an incident occurs that requires the attention of a regulating body, any escaping pollutants will go unnoticed. There have also been examples where operators have breached the licence conditions and deposited illegal waste, a situation which is very difficult to legislate against. Even though the historical records can not give an absolutely reliable perspective on the ground situation, the utilisation of a desk study is an essential part of any investigation relating to contaminated ground as past records do provide the investigator with information unobtainable from other sources.

7.2.1.1. Monitored Gas Concentrations by BCDC and HWU

The monitored gas values from sites D and Q were examined to highlight any possible problem areas.

The borehole data from site D did not indicate any particular locations with elevated gas levels. On the basis of this and the fact that gas was clearly being produced at the site all subsequent detailed studies were conducted on the filled area.

At site Q the only significant levels of landfill gas detected during the monitoring programme were found in the boreholes immediately adjacent to the eastern site boundary. Low levels of landfill gas were found near the residential buildings which was considered worrying as gas was clearly migrating from the site.

The attempt at producing a rough model of the gas migration was shown to be impractical due to the linear placement of the sampling points covering only a small portion of the site boundary.

One interesting conclusion from the programme was related to the efficiency of the gas extraction system currently in operation down the eastern boundary. In one particular location three adjacent boreholes showed extremely high concentrations of methane ($\approx50\%$) for short periods but at most other times no gas at all. This was believed by members of the HWU to coincide at times when the gas extraction system had ceased operation emphasising what the problems that may be caused if the extraction system either failed or was absent. Since the time of the 1991 sampling programme, the site Q operators have built a passive vent trench down the eastern side of the site and the gas extraction system has been extended to cover the whole site.

7.2.2. Aerial Photography

Apart from the physical developing and printing procedures aerial photographs require no other pre-processing, making them the most readily available remote sensing imagery, and the easiest to use.

The photographs from the June 1992 flight were available for study from the start of the project. In addition to this set, photographs from 5 other flights undertaken between 1971 and 1991 were obtained from archives. The full set of photographs obtained are listed in Appendix E. Site Q was one of the few areas that appeared in all of the sets of photographs, and therefore was examined in detail.

Aerial photographs are capable of being used effectively as a monitoring tool. The direct identification and delineation of ground objects/areas is possible. The ground can be viewed in three dimensions (using a stereoscope) enabling the identification of altitudinal differences to be observed. This can be extended for temporal analysis using photographs taken on different occasions, allowing the development of an area to be observed.

Figure 7.3 is an example of a multi-temporal analysis of a single site. It was produced by creating acetate overlays drawn directly from the aerial photographs, a relatively simple process when using stereoscopic aids. To find the area of the void directly using aerial photography would involve manual measurements using a ruler, with a subsequent loss in accuracy. The area calculation in this instance entailed scanning the overlays to produce a digital image and then digitising the extent on screen. Each of the six images were then geocorrected to the National Grid co-ordinate system and, using a GIS, the calculation of the area was a simple matter and produced the values as seen on figure 7.3.

Figure 7.3 illustrates the development of site Q from 1971 to 1992. The area that was quarried out by 1971 is shown in Figure 7.3a as the fullest extent of depression. The depression then decreased over time to the rapidly diminishing hole in 1992, which was completely filled in 1993.
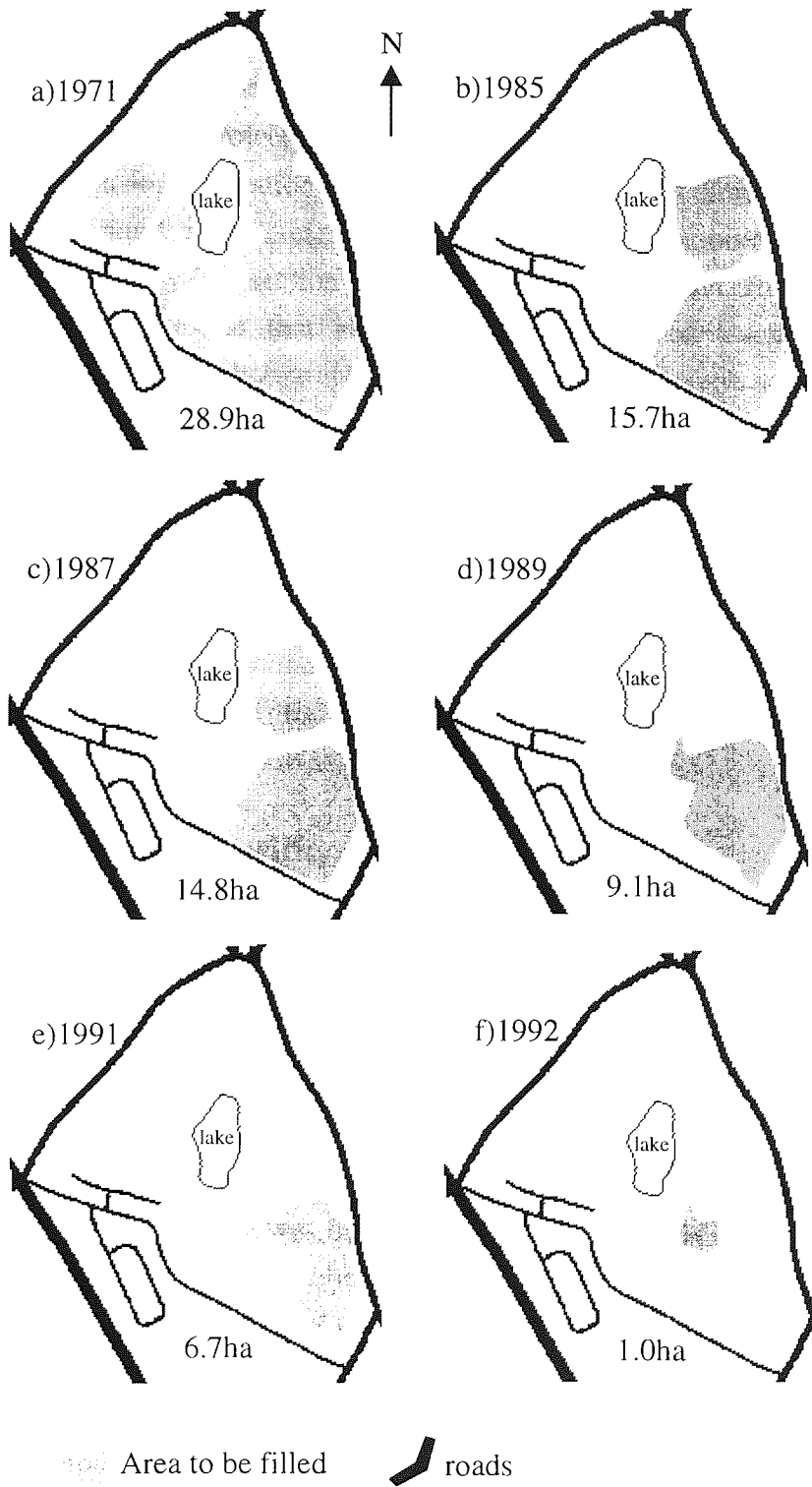
Figure 7.3. Area of depression on site Q for each of the photograph sets.

This simple analysis technique can only be applied to area and not volume. For instance, the areas in 1985 and 1987 (figures 7.3 b and c) were very similar even though filling had proceeded continuously during this period. The reason for this is that the void was being filled from the base over the whole depression thus not decreasing the area but reducing the overall volume. The calculation of a volume was not attempted in this project as the facilities and training were not available although standard photogrammetric methods such as the moving dot systems can be applied.

In respect to this project the objective was to identify the presence of landfill gas and leachate using vegetation stress or abnormal ground colorations. Of the five main sites under study many areas displayed browning vegetation and tracts of bare ground which, in theory (see section 4.4), may be indicative of the effects of migrating gas. No areas were found that showed any indication of leachate by ground discoloration using aerial photography. Following site visits some areas of escaping landfill gas were found but often there appeared to be no effect on the vegetation immediately next to the venting points. In one location only was there any vegetation stress and death. The area was confined to a few square meters on the site and the colours of the dead grasses and plantains were not distinguishable on the relevant aerial photograph. Of the other substantial regions that displayed poor vegetation or bare ground, no areas were found to be in that state because of influences from the associated landfill site. More discussion on the reasons behind why vegetation is stressed or absent can be found in section 7.2.3.1.1.

7.2.3. Image Classifications

A number of classifications were conducted on the data obtained by the ATM, either on an extracted area (≈ 250 kbytes) or on a whole tape (≈ 2-3.5 Mbytes) with additional use of Principal Components Analysis.

7.2.3.1. Single Site Classification

To highlight areas of possible contamination a classification of site D was undertaken. The classification was based on five images (bands 3, 5, 10 and 11 and the NDVI) using the maximum likelihood method with a threshold level of 90%. The images were chosen on the basis of their disparity to each other. The justification for the ground cover classes chosen was that they could be identified on aerial photographs. These classes were roads, water, car park/other road (based on the site entrance area), good vegetation (healthy, intense and usually 100% ground coverage), sparse (or patchy) vegetation (two classes of differing intensities, sparse1 being the least intense), bare ground (two classes bare1 being on-site and bare2 being off-site)

and shadow. As the areas of interest were open ground no attempt was made to classify any residential area. The resulting classification is given in figure 7.4.

Table 7.2 shows a confusion matrix for the classification demonstrated in figure 7.4. Confusion matrices are a method of assessing the accuracy of a classification. Information of the area covered by the image is acquired either by visiting the site, using observations made by aerial photographs or both in combination. This information is used as a proof (termed ground-truth) from which the classified image is compared to. Areas of known ground cover are designated on the classified image and the classification of each pixel is noted. This gives an indication of how accurate the classification was and which classes are likely to be confused with each other.

The matrix of table 7.2. is based on choosing areas of identified cover from aerial photographs and comparing them to the classified image. The two methods of determining the accuracy are shown as the final column and row on table 7.2. The last row indicates the accuracy of an object on the ground being classified correctly on the image (classification accuracy) and the final row indicates the likelihood of a pixel on a classified image being of that class on the ground (accuracy of omission and commission). Table 7.2. shows that, for instance, an area of good vegetation on the ground has a 91.1% chance of being classified correctly on the classified image and a pixel that is classified as good vegetation has a 95.7 % chance of actually being good vegetation on the ground. Also it is possible to makes statements such as that if the good vegetation is misclassified it is most likely to be a sparse class. As the method of choosing the training areas for the classification was directly from aerial photographs, with knowledge of the ground cover, the accuracy is consequently high. The only confusion was involving the sparse classes. It was difficult to discern between the sparse1 and sparse2 on the aerial photographs so they were subsequently grouped together.

From a cursory glance at the classified image, the most striking feature is that all of the site area consists of sparse vegetation or bare ground. Much of the surrounding area is classed as good vegetation, the majority of roads are correctly classed and the houses and buildings appear as a combination of roads, shadow and unclassified. From the point of view of detecting pollutants by vegetation damage, all the areas of bare ground or sparse vegetation are suspect as they are regions of unhealthy vegetation that might have been affected by landfill gas or leachate.

classified as	bare1	bare2	carpark	goodveg	roads	shadow	sparse	water	%
bare1	356	0	0	0	0	0	5	0	98.6
bare2	0	281	0	0	0	0	28	0	90.9
carpark	0	0	121	0	0	0	0	0	100
goodveg	0	5	2	728	0	5	21	0	95.7
roads	0	0	0	0	306	0	0	0	100
shadow	0	0	0	0	0	111	0	0	100
sparse1	15	4	5	40	0	0	309	0	82.8
sparse2	0	2	0	31	0	0	8	0	75.6
water	0	0	0	0	0	0	0	60	100
unclassified	0	0	6	0	0	0	0	0	0
	371	292	134	799	306	116	371	60	2449

% correctly classified	95. 6	96.2	90.3	91.1	100	95.7	83.3	100

Table 7.2. Confusion matrix for the classification of site D displayed in figure 7.4. (sparse as a selected area contains sparse 1 & 2).

7.2.3.1.1. Ground Truth Comparison

During a site visit the validity of the different ground cover classes was checked. The ground cover at each of the points 1-6 on figure 7.4 are detailed below.

Point 1 (classified as bare1).

The ground cover here consisted of generally clayey soil, often very pebbly with little vegetation (<10% cover) apart from the occasional colonising species (thistles, dandelions etc.).

Point 2 (classified as sparse1).

A variety of plants were present here and the cover is generally ruderal developing into neutral grassland with invading scrub and young trees (4-5 years old).

Point 3 (classified as a combination of shadow and unclassified).

This location is adjacent to the eastern site boundary at the base of a 5-6m, 60-70° slope, hence the classification of some of the location as shadow. About 1 or 2m from, and parallel with, the site boundary were settlement cracks releasing landfill gas. Large clusters of plantains were growing near and on the settlement cracks of which many were dead or stressed. Also dead *Poa annua* (annual meadow-grass) was present on the bank as well as other annuals.
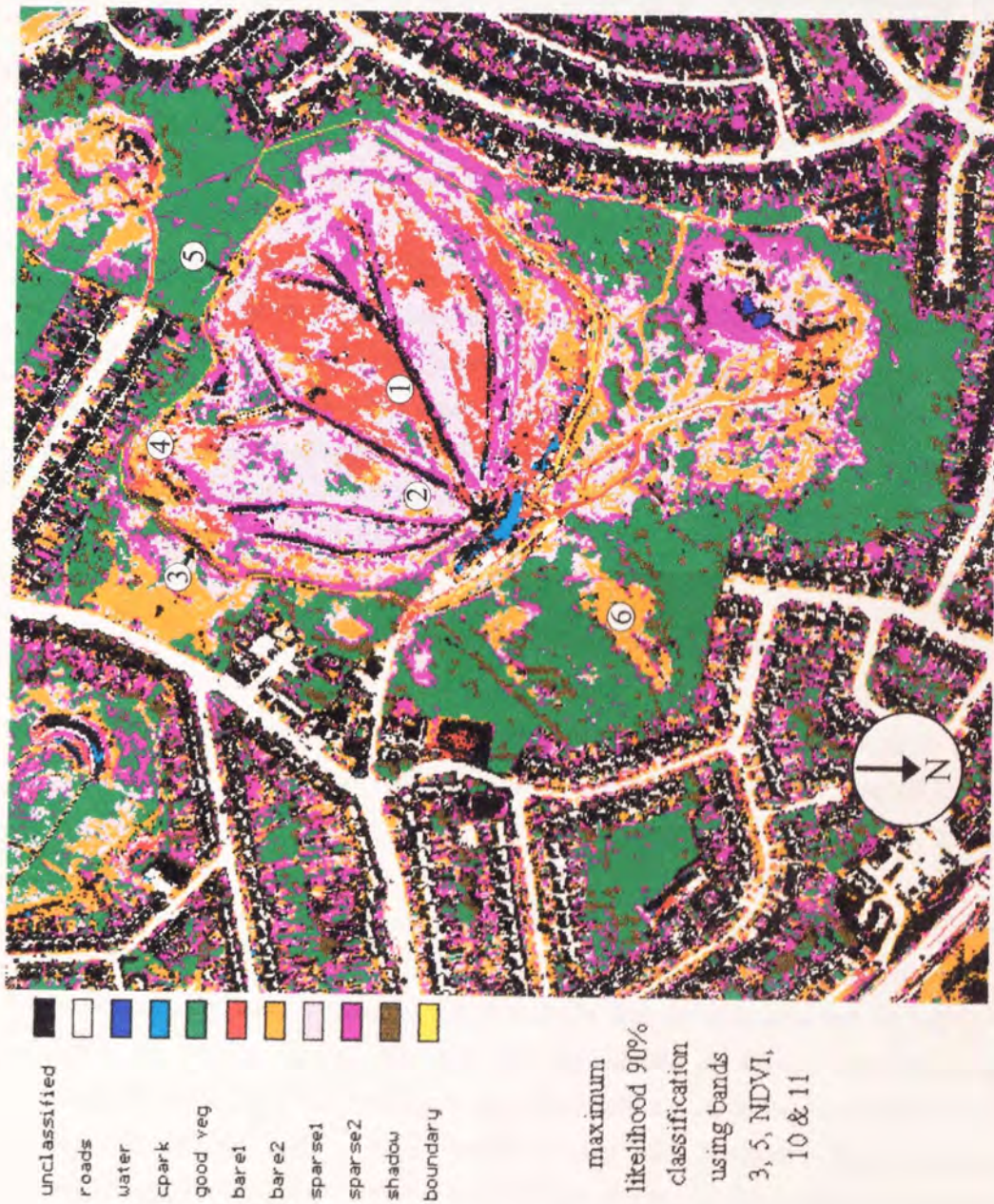
Figure 7.4. Classification of site D (refer to text for explanation of numbers.)

unclassified
roads
water
cpark
good veg
bare1
bare2
sparse1
sparse2
shadow
boundary

maximum
likelihood 90%
classification
using bands
3, 5, NDVI,
10 & 11

N

Point 4 (classified as a combination of bare1, bare2 and sparse1).

Located close to the residential area at the south-eastern corner of the site, it was very similar to point 2 but with additional garden flowering plants and various rubbish that had been thrown over the site fence (e.g. doors, furniture etc.).

Point 5 (classified as a combination of bare2 and unclassified).

This was approximately at the mid-point of the southern boundary of the site where there is a 4-5m, approximately 45° upward slope. Settlement cracks were evident parallel with the site boundary near the base of the slope, similar to point 3, with gas emanating from them. At this particular location there were two cracks about a metre apart both emitting gas but with healthy grass in between.

Point 6 (classed as bare2).

Point 6 is located on a ridge beyond the northern boundary and down hill from the site. The ground was comprised of very dry and fine orange coloured soil (presumably due to a high iron content related to the basaltic country rock), containing many angular basaltic chunks within the soil. The principal vegetation populating this ridge was 'wavy-hair' grass (*Deschampsia flexuosa*) and dark *Polytrichum piliferum* moss, both of which enjoy dry conditions.

The training data used in the site D classification was applied to site S to see if they were appropriate for any site. The vegetation on site S consisted of large areas of managed grass and was not as intense or lush as the natural growth surrounding site D. This resulted in almost the whole site being classed as either sparse1 or sparse2. An independent classification of site S would attribute much of the area as the good vegetation class.

Although most of the landfilled area of site D was covered by poor or no vegetation, this could not be attributed to landfill gas. The main reason why site D was covered thus was because of the condition that the site was left in following the cessation of filling. There was no top-soil placed down as final capping and consequently there was no seeding or attempt made at managing the vegetation, it was merely left fallow with a poor surface cover that hindered vegetation growth. Consequently, the vegetation cover is ruderal and patchy, the main constituents being early colonising species such as dandelions, thistles and annual grasses. As it was during summer when the data was obtained, many of the plants were in the seeding stage of their life cycle and appeared brown, rather than green, giving a lower reflectance response in the near infra-red and a higher response in the red. The two positions picked out that were emanating gas (points 3 and 5) were classified as a

mixture of bare, sparse vegetation, shadow and unclassified. Point 3 was comprised of some dead vegetation (plantains and annual meadow-grass) in close proximity to the venting surface cracks. Point 5 was producing gas at a comparable rate but in this case there was little or no effect on the surrounding grasses.

The regions beyond the site boundary that are poorly vegetated cannot be due to the lack of a good final cover as it has remained mostly unaltered since filling began in 1986, and probably for some time before then. The vegetation at point 6 was analysed in more detail. It was a ridge downhill from the site and appeared to be some form of slag heap deposited by a conveyor system, consisting of angular fragments (<5cm) of a basaltic rock in a matrix of orange soil; the local soil type. Although from the air it appeared to be unvegetated it was actually populated almost exclusively by *Deschampsia flexuosa* (wavy-hair grass) and *Polytrichum piliferum* moss. This combination puts the cover into the category of *Deschampsia* grassland (National Vegetation Classification category U2) by Rodwell (1992), a cover type indicative of dry, acidic, free draining ground lacking in humic soils. Consequently the ridge does not appear to be covered with healthy green (infra-red reflecting) vegetation and was classified as a bare ground cover even though it is normal and healthy for these prevailing conditions. This shows how the type of soil is a strong governing force over what vegetation grows upon it.

There are many reasons that ground many appear sparsely vegetated or bare and they are as follows:

1. varying soil characteristics which may be unsuitable soil for growth;
2. drainage characteristics of the ground - waterlogging giving wet conditions, or fast water loss creating dry conditions;
3. weather conditions - wet conditions causing flooding,
   - hot conditions causing vegetation, particularly grass, to become dry and withered.
   - excessively cold conditions causing disruption of the growth cycle or damage (i.e. creating an early autumn, a late spring, or frost damage);
4. the normal growth cycle of some vegetation involves seeding producing some withering and die off; and
5. continually trampled ground may produce receded vegetation growth.

Many of the above conditions may produce some form of vegetation stress. Vegetation stress may be evident in a number of different ways:

a) withering/loss/browning of leaves giving a lower infra-red and green and a higher visible red reflectance response,

b) reduction in leaf size with no appreciable change in reflectance response and,

c) if sufficient time has elapsed since the beginning of the stressing influence the original vegetation may have died off and been replaced by tolerant species.

The important thing to note from the points above is that stressed vegetation does not always exhibit itself as death or die-back or any change in leaf colour as indicated in figure 4.24. It therefore makes it very difficult to detect any effects from polluting influences when the effects due to the environment are so varied.

The complexity of the ground cover of the sites studied in this project provides another obstacle. A substantial number of different soils can be present as the final soil cover of landfill sites is usually imported and many have multiple sources. The process of vegetation colonisation is very haphazard and many different plants may find their way there. The vegetation population from then on is in continual flux with new and more dominant species arriving and replacing the earlier arrivals. Also, climatic/altitudinal/latitudinal influences may come to bear.

The monitoring of crops on reclaimed landfill sites on the other hand is a situation more conducive to the method applied here (Jones, 1991). The ground cover always starts as bare earth, the crops are planted at the same time and the full growth cycle is generally known in some detail, so localised abnormalities may be easier to define. Managed grassland such as sports and school fields are also more suited to monitoring because of their consistent grass covering. Difficulties are encountered, though, as they are often used substantially by the public (i.e. football pitches and pathways) producing trampled ground. In addition, these fields are mown by tractors without grass collecting attachments and the cut grass is left on the ground. The cut then will die and may give a dead vegetation reflectance response whilst obscuring the healthy grass beneath.

7.2.3.2. PCA Refined Classification

The results of the previous section suggest that each site has individual characteristics that are not always transferable onto other sites. To expand the classification technique it was decided to classify a whole tape (716 columns by 4508 rows) as opposed to analysing each site individually, thus observing a much greater area at once (10-15 times the amount of data). The classes described in section 7.2.3.1 were altered so that the categories that were causing confusion between sites in the

previous section (the sparsely vegetated classes) were discarded and two vegetated classes, along with five bare classes were used. It was decided to refine the classification by utilising Principal Components Analysis (PCA) to evaluate whether this process showed an improvement on the five original ATM bands used to produce figure 7.4. Iconoclast is capable of conducting this process on five images at a time so the five visible bands were grouped together as were the five infra-red bands. The thermal band (band 11) was deemed, by the author, sufficiently distinct from the other bands to be used separately.

The Eigenvalues for the PCA on bands 1 to 5 are given in table 7.3. and show how PC1 contains the vast majority of the information. Table 7.4 gives the Eigenvectors and shows how PC1 is contributed to fairly evenly by bands 2 to 5, with band 1 having little influence.

	PC1	PC2	PC3	PC4	PC5
Eigenvalue	827.052	17.113	14.675	5.739	1.642

Table 7.3. Eigenvalues for PCs of Bands 1 to 5.

	PC1	PC2	PC3	PC4	PC5
band 1	0.1340	0.4582	0.8733	0.0413	-0.0871
band 2	0.5337	0.6589	-0.4237	0.2703	0.1678
band 3	0.6352	-0.1838	0.0338	-0.7492	-0.0061
band 4	0.4013	-0.3041	0.0026	0.4212	-0.7543
band 5	0.3638	-0.4790	0.2378	0.4316	0.6286

Table 7.4. Eigenvectors for the PCA of bands 1 to 5.

Table 7.5 shows the Eigenvalues for the PCA of bands 6 to 10, the infra-red bands. In this instance, even though PC1 provides the majority of the information PC2 also contains a significant amount. This can be explained by the Eigenvectors shown in table 7.6. Bands 6, 7 and 8 all made a significant contribution to PC1 as the information that they contain is very similar (see section 5.1.1.3). Band 10 is almost solely responsible for PC2. PCs 3, 4 and 5 contain very little data.

	PC1	PC2	PC3	PC4	PC5
Eigenvalue	996.229	247.473	16.439	7.366	1.009

Table 7.5. Eigenvalues for PCs of Bands 6 to 10.

	PC1	PC2	PC3	PC4	PC5
band 6	0.4244	0.0186	-0.5130	-0.6431	0.3775
band 7	0.5282	-0.1959	-0.1965	0.0289	-0.8019
band 8	0.6661	-0.2138	0.2488	0.4979	0.4479
band 9	0.2691	0.3698	0.7450	-0.4721	-0.1127
band 10	0.1569	0.8824	-0.2847	0.3385	-0.0302

Table 7.6. Eigenvectors for the PCA of bands 6 to 10.

The PCA enabled the ten ATM bands to be reduced to 3. These are:

1. PC1 from bands 1 to 5 which represents all of the visible bands,
2. PC1 from bands 6 to 10 which represents the very near infra-red bands (bands 6, 7 and 8) and
3. PC2 from bands 6 to 10 which represents band 10.

In addition to these three images the NDVI and the thermal band (band 11) were used for the classification. Because of the disparity of the ground cover between different sites the classes used were also modified.

No sparse cover type was identified but two vegetation classes were used. These were: 1) vegetation that was healthy and generally unmanaged (trees and natural grassland similar to that surrounding site D); and 2) vegetation that was regularly managed (e.g. school/sports fields). Five classes of bare ground were used due to different areas with varying cover being identifiable. Water and roads were also identified. Again, no attempt was made to produce buildings and residential areas as a separate class.

The classified image is shown on figure 7.5. Using simple manual observation it was found that each of the areas classed as bare did adhere to their given class and most of the managed and unmanaged grassland was successfully segregated. Virtually all of the roads were correctly differentiated but a very large proportion of the buildings were classed as roads. The remaining parts of the buildings were made up of the various bare classes and some areas were classed as water. As often found, many shadowed areas were classified as water as they have almost identical reflectance characteristics, conspicuous by the absence of any reflectance at all.

Prior to the classification using the PCA, a separate classification was undertaken using bands 3, 7, 10, 11 and the NDVI - in effect the bands that the PCA suggested - and the classified image was not discernibly different. Even though using

PCA unquestionably makes use of more information, it is not necessarily an improvement because of it. The case here suggests that the five distinct unaltered bands are perfectly adequate to create a classified image without the additional time needed for the PCA.

7.2.3.3. Area Isolation using a GIS

The next test was to see if it was possible, using GIS techniques, to highlight any landfill sites in the region using the assumption that they will be large areas of undeveloped land. All of the bare and vegetated classes were considered as undeveloped and built-up areas and roads were considered developed. A figure of 5 hectares was chosen as a minimum size for an open space to be labelled a possible landfill site which was deemed large enough to eliminate areas of residential gardens and similar ground cover. As the roads seemed to be depicted very well and appeared to be very good dividers between regions they were the primary object of influence for the isolation process.

The classified image could not be rectified to a recognised co-ordinate system because of the subtle distortions experienced during the flight, but the approximate scale could be determined and this was used in the ground area calculation (see section 7.2.2). The area isolation process can be summarised as follows. Firstly, using GRASS (see section 5.4), the roads were extracted as a separate image. This image was filtered using a very coarse modal filter (11x11 kernel) to remove small areas of road that may have been misclassified. Once this process had been completed a buffer zone of 20 metres was placed around every region of road in order to bridge any gaps along a road that may be caused by vehicles, overhanging trees or other obstructions. The resultant image is an interconnecting network of roads and buildings with large gaps in between. To find the gaps greater than 5 hectares a procedure known as 'clumping' is applied to the image. Clumping involves changing each individual contiguous area into a separate category, the number of areas equalling the new number of categories. The areas of these clumps can be determined and those below the threshold size can be discarded.

Figure 7.6 shows the results of the above process. The roads class from figure 7.5 have been altered to black and everything white is excluded data. The original classification has been superimposed onto the areas of interest. Of the twelve or so areas highlighted by this process only one was a known landfill. Many of the others were recreational fields, where no disposal had taken place in the last 20 years, two were building free industrial sites and one was a cemetery, a somewhat special form of landfill.
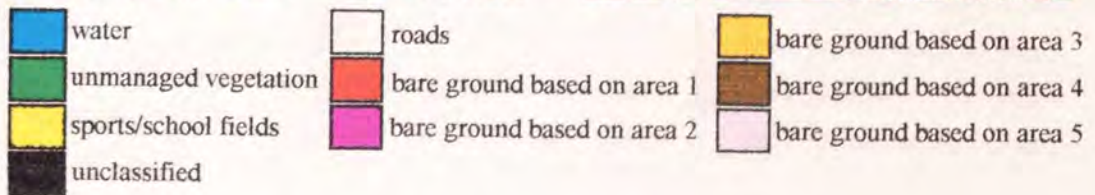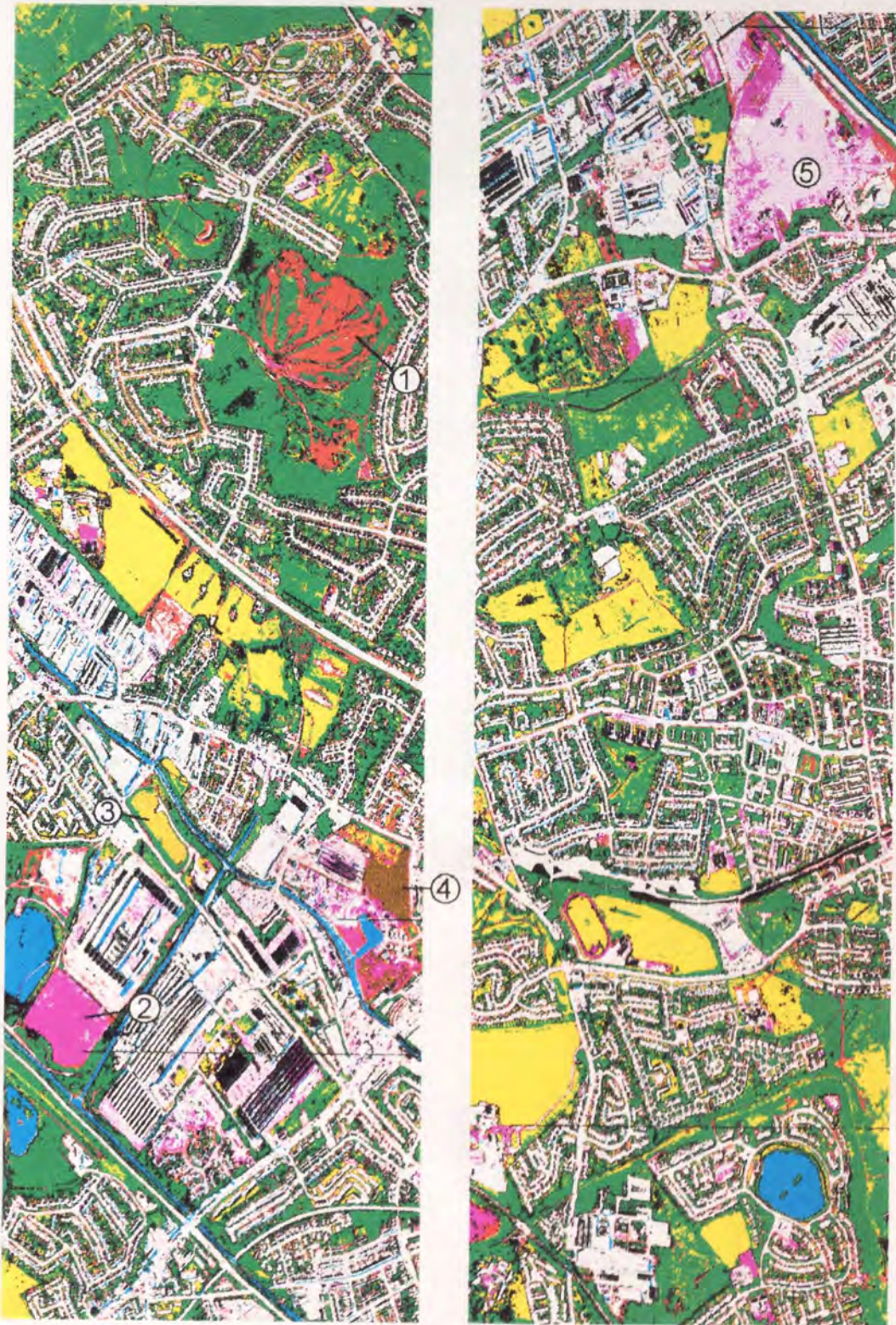
Figure 7.5. Classified image of a whole tape. (Bottom of left frame continues onto top of right frame).
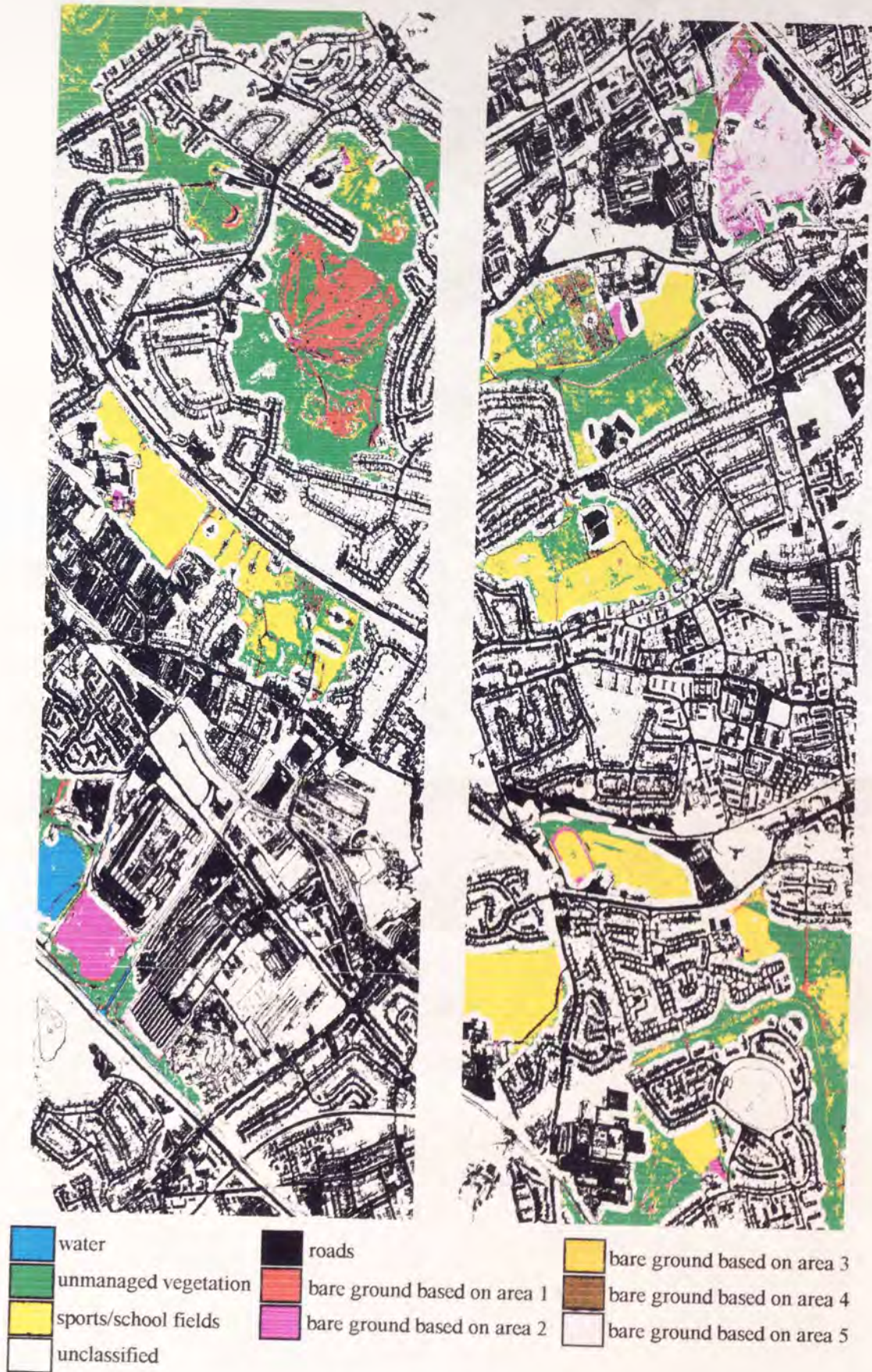
Figure 7.6. Contiguous areas of ground cover greater than 5 hectares in extent. (Bottom of left frame continues onto top of right frame).

Legend:
- water
- unmanaged vegetation
- sports/school fields
- unclassified
- roads
- bare ground based on area 1
- bare ground based on area 2
- bare ground based on area 3
- bare ground based on area 4
- bare ground based on area 5

Figure 7.7. Areas isolated by using aerial photographs and superimposed onto a map of the whole area. (Red areas are bare ground, green is unmanaged grass, yellow is managed grass and combinations are striped accordingly.

The process of area isolation using the GIS proved to be a good exercise in showing the capabilities of the manipulation of remotely sensed imagery but for the specific aim of this project was ineffectual. More use could possibly be made of this technique for town planning or general urban landscape monitoring.

7.2.3.4. Area Isolation using Aerial Photography

To compare methods the same process of isolating areas of non-development greater than 5 hectares was conducted but this time using the aerial photographs taken at the same time as the ATM. This was not restricted to the area of a single strip, it was implemented for the total area covered by the flight. The photographs were examined and relevant areas of sufficient size were drawn on to a 1:5000 map. The results of this are shown on figure 7.7. Red areas are bare, green areas are unmanaged vegetation and yellow is managed fields, with combinations marked accordingly with stripes.

The process of transferring the information on to a map is very simple and can be accomplished with relative ease. Whilst the GIS method entails a substantial amount of computer processing time where the operator is not on task, the aerial photographic method is labour intensive throughout the whole procedure. All of the areas highlighted by the computer based method were picked out by the aerial photographic method.

Generally, it shows that both methods are capable of producing essentially the same output with relative accuracy but whilst the photographic method takes by far the shorter amount of time the GIS method (when taking into account computer processing time) can produce easier to extract quantitative results (i.e. area measurement).

Regardless of the method applied, the results can only be obtained from what is present at the ground surface. No knowledge can be gained of what may lie beneath built-up areas using this method, suggesting the original premise, that large open spaces may be landfill sites, is flawed.

7.3. Analysis of Thermal Data

To test the hypotheses that warm regions could be indicative of landfill gas or leachate, data from three sources was used: the thermal band of the ATM (both dawn and daylight flights) and a thermal video camera. Each was examined separately and processed by contrast stretching and density slicing.

7.3.1.   Daylight ATM

The first thermal data obtained was band 11 from the daylight ATM imagery. Extracts of site D and site Q were isolated and examined. A three part density slice of each extract was performed. The precise density slice boundaries that were chosen were based on experimentation using the image processor with observations of ground cover, where known, to show only the warmest fraction of the image. The areas that show up warmest on the daylight thermal bands are roofs, bare ground and some roads, all due to solar heating.
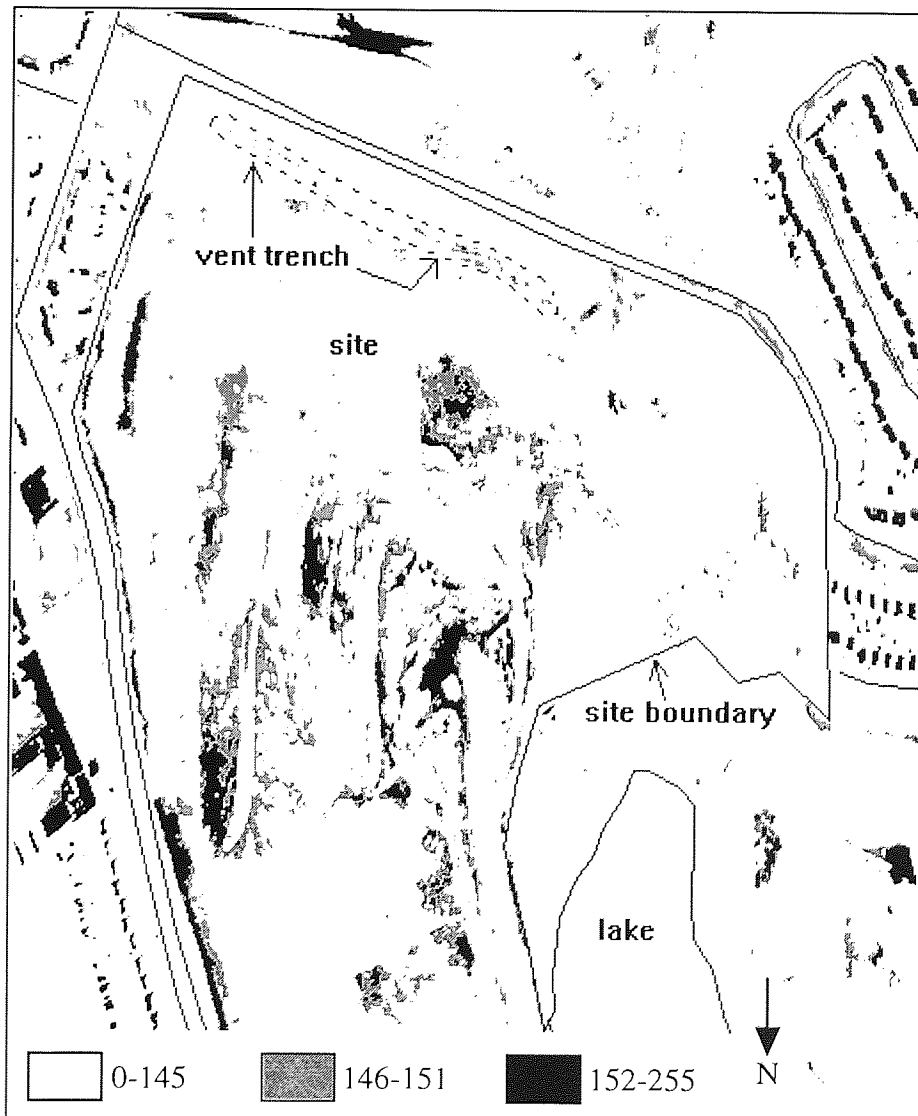
Figure 7.8. Density slice of site Q with site boundary, lake and roads (black lines) added for reference.

Figures 7.8 and 7.9 show three part density slices for site Q and site D respectively. Much of site Q appears warm due to the preponderance of bare ground as the site was still active at that time, consequently hardly any vegetation was present. On a visit to the site, the vent trench (highlighted on figure 7.8) was producing gas evident as steam as the moisture laden gas condensed on contact with the cooler atmosphere. On closer inspection the trench was producing a noticeable amount of heat that could be felt by merely placing a hand into the emerging gas. The trench that the gas was emerging from did not show up on the imagery as an ostensibly warmer area, only a few warm points appear along the line of the trench. Compared to other parts of the site which are warm due to the absorption and re-emission of solar radiation the warm points following the trench are barely discernible.
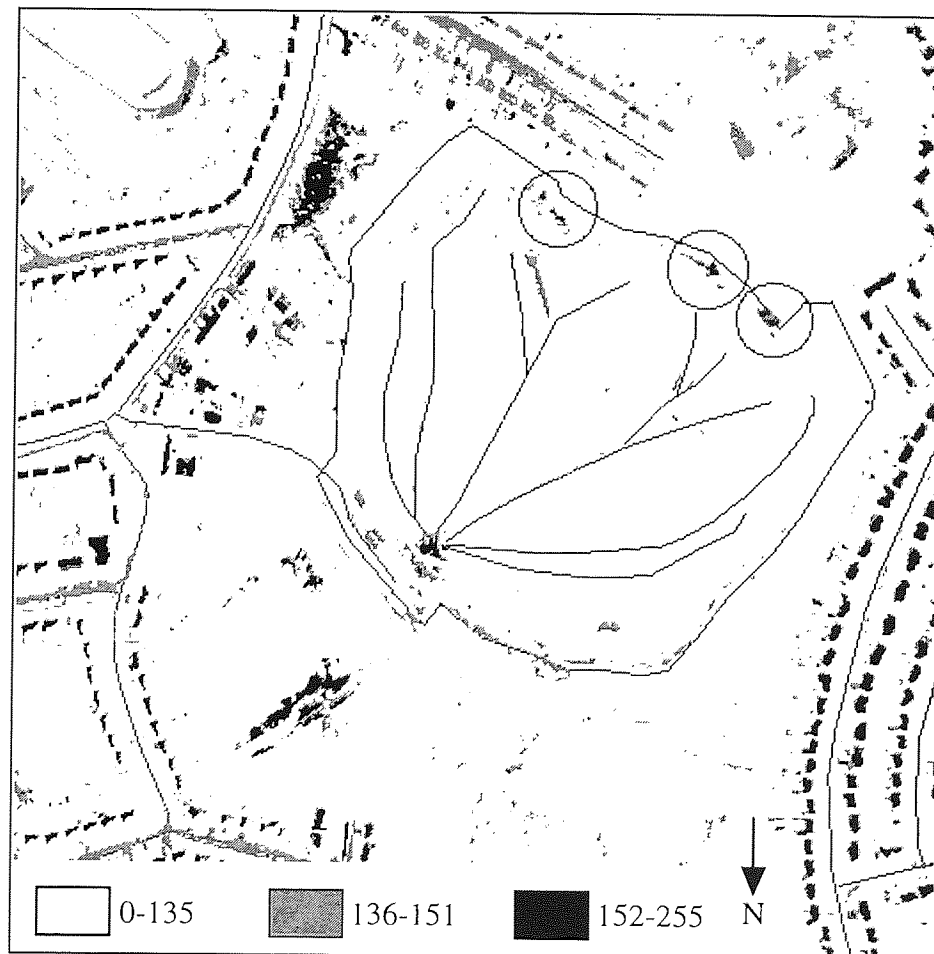
Figure 7.9. Density slice of site D with site boundary, pipe-runs and roads (black lines) added for reference. Regions circled are venting slippage cracks.

Figure 7.9 shows a three part density slice of site D based on similar experimentation, the values of the density slice boundaries decided on differing slightly from figure 7.8 . As with site Q, buildings, bare areas and some roads appear as the warmest ground cover. The warm area at the confluence of the pipe-runs is the flare stacks. In addition, some areas near the top of figure 7.9 (circled) appear abnormally warm. From a subsequent site visit these areas were found to be venting settlement cracks where gas was escaping to the atmosphere and producing sufficient heat to be discernible (points 3 and 5 from section 7.2.3.1.1 correspond to these locations).

Daylight thermal images are heavily governed by the solar absorbance properties of the materials on the ground. Substances with the lowest thermal inertia (bare soil and man-made materials) heat up quicker as evidenced by the imagery.

The areas that were emitting gas were identified and the spectral response was observed. On both sites the gassing areas were producing some heat palpable at ground level but at site Q the vent trench was barely discernible. It may be that the measured response of the vent trench was actually due to the materials that it was constructed of (bricks and rubble). Evidently, though, the heat produced by the gas was not sufficient to be noticeable at site Q.

On site D there were anomalously warm areas at the southern site boundary which corresponded to settlement cracks that were venting gas. In this case the heat produced was clearly ample to produce an anomaly. The activity at site D was relatively extreme and concentrated around deep cracks with the waste fairly close to the surface. At site Q the gas was coming from an artificially constructed vent trench and clearly not producing sufficient heat to be detected on the daylight thermal ATM. In this instance, the distinction between solar heated areas and other anomalous heat sources is very difficult without the aid of ground-truth information.

7.3.2. Dawn ATM

A dawn ATM flight was carried out in April 1994 utilising band 11. By flying at dawn the effect of the previous day's solar heating will be drastically reduced. The difference of this imagery compared to the daylight imagery was marked. The materials that were warm before (roads, buildings) were cold and those that were cold (vegetation, water) were now warm. The reasons behind this were probably a combination of each individual material's emissivity and it's rate of heat loss. Materials that lose heat at a high rate will take the shortest amount of time to reach the ambient temperature and vice versa. The emissivity may play the major part, though, as it governs how a material radiates in relation to its temperature. When the

temperatures of the different materials have equalised (as at dawn) the emissivity differences will be very noticeable. Water has both a high emissivity and a high specific heat capacity so it radiates relatively strongly and contains its heat well, altogether making it appear warm on the dawn ATM imagery. If a material heats up quickly then the total radiated output may be greater than another material, even though it may have a higher emissivity (as illustrated by bare ground and buildings on the daylight thermal ATM imagery). In general, water and some buildings (usually factories that are probably working nightshift) are emitting the most radiation.

	grass			trees		houses						roads						water			
min	67	67	68	67	39	39	36	39	24	39	33	40	41	52	40	52	49	127	133	123	177
max	83	79	85	82	90	63	74	59	61	65	67	54	51	68	67	73	69	134	144	138	133
mean	74.2	73.6	76.3	76.2	80.1	50.9	47.5	48.0	45.3	50.9	49.4	45.8	45.0	57.4	52.5	60.3	57.6	130.0	139.4	131.2	125.7
s.d.	2.86	2.52	2.3	2.8	3.22	30.7	5.8	4.43	7.26	4.99	4.98	2.6	1.9	2.46	4.43	3.85	3.32	1.20	1.45	3.06	2.89

Table 7.7. Statistics of pixel value obtained of some ground cover types from sample areas for the dawn ATM imagery.

Table 7.7 gives the means and standard deviations for some of the ground cover types, drawn from a number of arbitrary sample areas chosen from the dawn ATM imagery (high is hot), giving an idea of how they compare to each other. In general, houses and roads have the lowest value with means ranging from about 45 to 60. The grass category (managed grassland) exhibits a mean value of about 75 whilst trees appear slightly warmer with values from 76 to 80. Of all the normal ground categories, water shows the highest values from 125 to 140. Also the standard deviations of the water values are very small indicating a very restricted range.

On site Q the vent trench, referred to in section 7.3.1, was not identifiable as a heat source on the imagery so the study of the site was not continued. This may be due to atmospheric conditions suppressing the gas production (although no evidence of this was experienced at site D) or the gas extraction system that was being installed in 1993 (see section 6.5) was operational and effective.

Figure 7.10 shows a dawn thermal image of site D in black and white which has had a contrast stretch applied to it. The buildings and roads clearly appear as cold (black) and the pool near the top left of the image appears warm. Heavily vegetated areas appear warmer than most of the surrounding ground (two examples are marked with a 'T' on figure 7.10) all of which are consistent with the statistics in table 7.6.

In addition to the pool there are a number of other places on the image that exhibit relatively warm temperatures. The points marked '1' on figure 7.10 are ponds and puddles of water producing a relatively warmer temperature than the surrounding ground which is consistent with table 7.5. The region marked '2' shows the highest temperatures on the image. This is the location of the two flare stacks which are burning off the gas drawn from the site by the gas extraction system. There are two black spots within this region which are the exact positions of the flares which are producing temperatures so high that the pixels are 'burned out', giving a zero value. The gas is brought to the flares by way of a number of wells and surface pipes. Some of these pipes are visible and are marked by a 'P' on figure 7.10. They appear warm because of the warm landfill gas they are transporting. There are also a number of warm areas around the southern rim of the site marked by a '3' on figure 7.10. These areas are where warm landfill gas is emanating from the surface through settlement cracks.
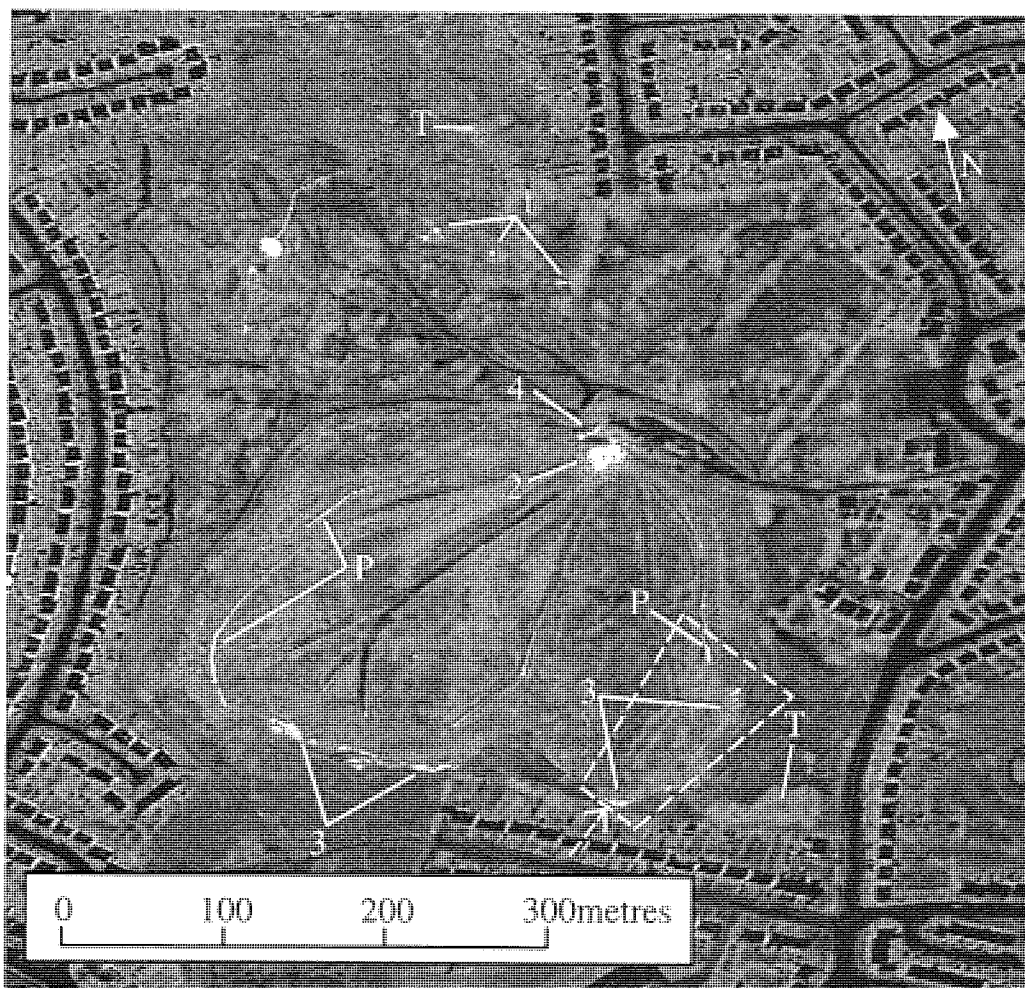
Figure 7.10. Contrast stretched dawn ATM thermal image of site D (white is warm). Dotted lines refer to figure 7.13 in section 7.3.3. (See text for annotations).

Even though the gas emitting areas are warmer than the surrounding ground, only one pixel has a value greater than the expected maximum value for water (approximately 145). Whilst this suggests that the radiated temperature is not exceptional, it also creates identification difficulties. Distinguishing between warm gassing areas and regions of standing water is not possible by a simple density slice routine, as they cover a similar pixel value range. It would be necessary to obtain either very recent ground truth or daylight imagery data to distinguish between gassing areas from water.

The only area that could technically be construed as leachate lay slightly to the north of the flare stacks and is marked with a '4' in figure 7.10. It was a puddle that occurred following heavy or persistent rain. In this case, the origin of the water is from overland flow rather than subterranean and therefore would not normally be considered as leachate.

The second site studied in detail using the dawn ATM data, site H, was approximately a kilometre due south of site D, and the thermal image of the site is shown on figure 7.11. As before, roads and buildings appear dark and water appears warm (a pool is visible in the top centre of figure 7.11). The area of the site that contains fill is inside the region outlined by an unbroken white line and has a slope of about 45° down hill from left to right. It is generally ruderal in nature with many grassland plants.

There are a number of other locations on figure 7.11 that appear warm. The region around the point marked 1 is the area where quarrying is in progress. The method of removal is by terracing and much of the area is relatively dark because of the presence of bare rock. The warmer areas to the east are pooled water on the flat terraced surfaces. The area marked by a '2' is the site works where the quarried material is broken up and prepared for transport. Judging by the heat being produced by the works and the burned out pixels it is very likely that they are in operation 24 hours a day. The filled area has leachate and gas extraction systems which are highlighted on figure 7.11 by the label '3' and '4' respectively.

In the cases of both sites D and H, many anomalously warm areas were detected. Some were merely standing water (pools and puddles) but other warm points were associated with the landfill gas production. The flares and some pipe-runs were in evidence but more importantly the locations where landfill gas was escaping were clearly depicted. Unless it was known which areas are water and which are not it makes it very difficult to make judgements on what is an anomalous heat source. Of all the pixels that were known to be landfill gas only one (which was on site D) was in

excess of that expected for water ($\approx$145) so mere magnitude cannot be a reliable measure.
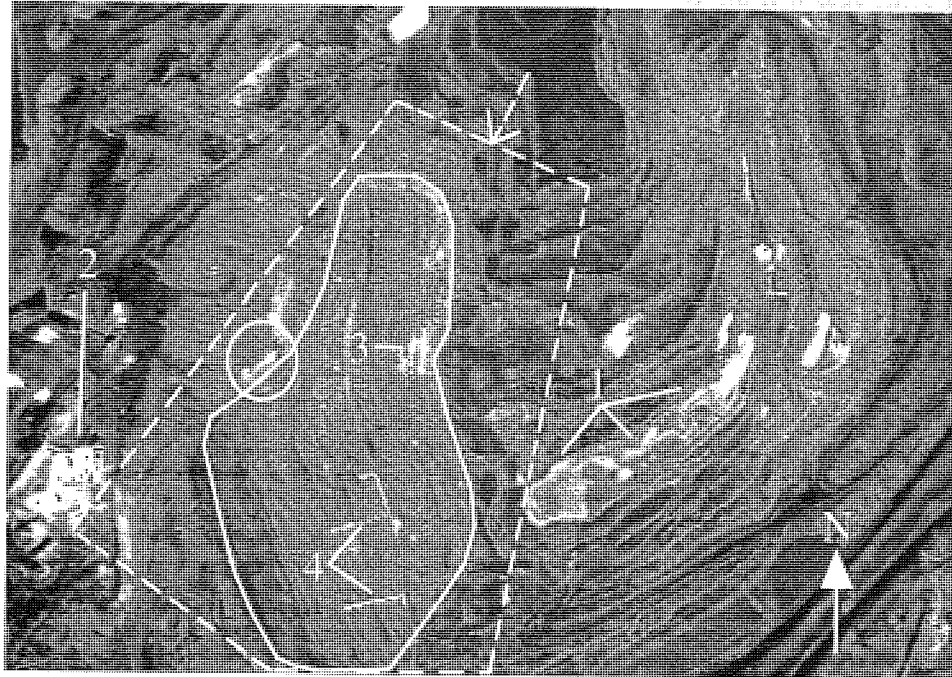
Figure 7.11. Contrast stretched dawn ATM thermal image of site H (white is warm). Dotted lines refer to figure 7.14 in section 7.3.3. (See text for annotations).

The area circled on figure 7.11 is an anomalously warm region beyond the boundary of the filled site. Following investigation this area was found to be emanating warm landfill gas.

7.3.3. Thermal Video

A thermal camera survey was carried out for comparison with the ATM. Although a dawn flight would have been preferred, the local climatic conditions and the restricted schedule of the operator made this problematic. Instead, the survey took place in November 1994 in the late afternoon, under heavily overcast weather conditions. The heavy cloud, according to the operator, would prevent any direct solar irradiation of the ground and reduce the heating effects which were experienced on the daylight thermal ATM.

Financial constraints meant that the survey was restricted to sites D and H and carried out in accordance with the method described in section 6.1.3.2 and appendix B. The image processing techniques used were performed on images that had been 'grabbed' from the video record by a PAL decoder and converted from analogue to digital format. The viewing angle of the camera was about 30° from the horizontal, so

from a height of 150 metres the field of view was fairly small (50-100 metres) and only a fraction of the site was covered in a single frame. To get the whole of site D on a single frame the helicopter was moved away from the site until it was fully in view. An example of the video screen for the whole of site D is shown in figure 7.12 (excluding the annotations 'pipe-run' and venting gas').
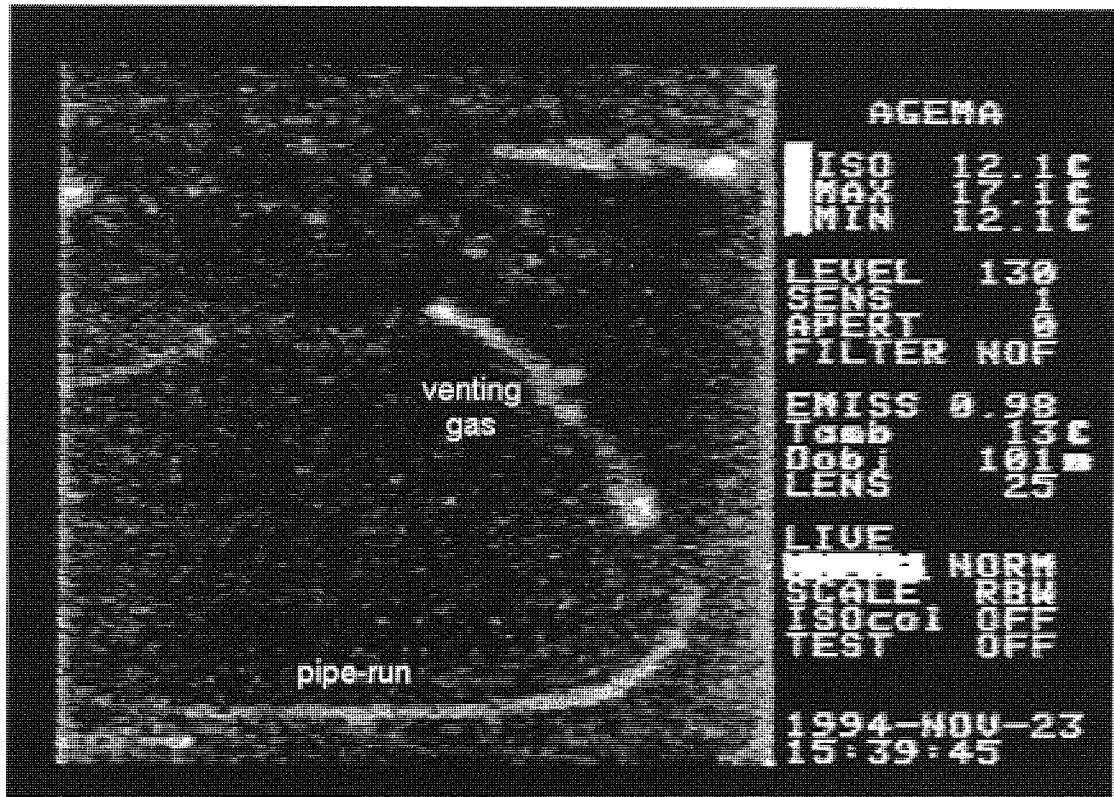
Figure 7.12. An example of the display produced by the thermal camera, most of site D is visible.

The picture quality of a paused video image produced by the camera on this survey was very poor. Figure 7.12 was particularly poor due to the increased distance between the site and the camera. There are some warm areas visible which correspond to pipe-runs and venting gas as annotated. The thick line at the top right is close to the horizon, a considerable distance from the site

Figure 7.13 shows a video image of site D taken from a lower altitude (approximately 170m) and has a number of warm areas visible. The region covered by the picture is enclosed by the dashed lines on figure 7.10 with an arrow showing direction. The warm areas on figure 7.13, as annotated, correspond to a gas extraction pipe clearly full of warm gas, a well-head at the end of a pipe-run and a significant area of venting gas.
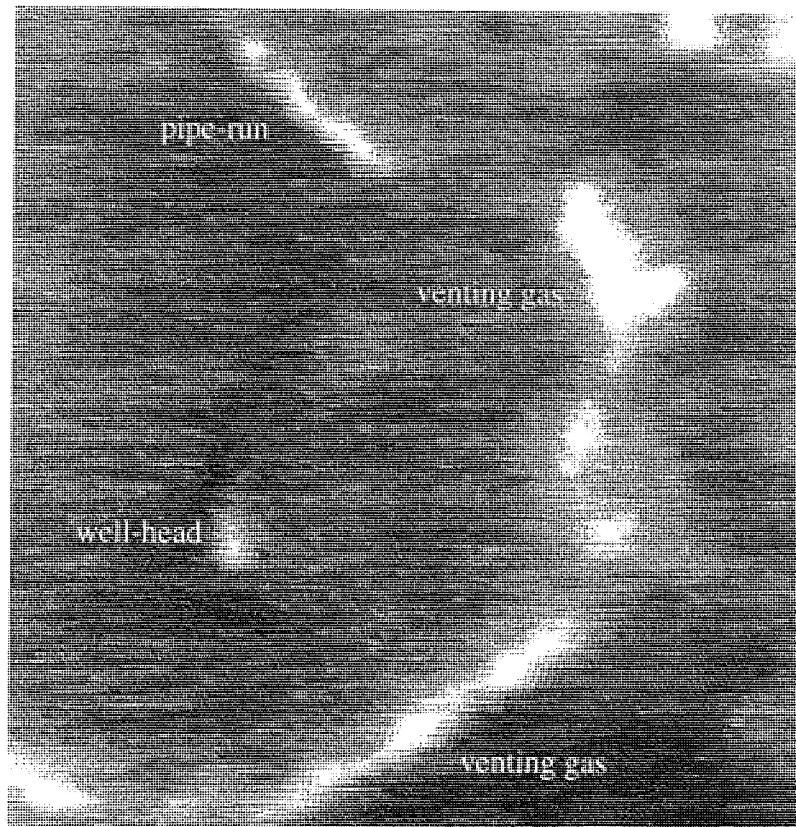
Figure 7.13. Thermal video image of a section of site D.

A video image of part of site H is shown on figure 7.14 with a number of warm areas highlighted. The region covered by figure 7.14 is enclosed by the dashed lines on figure 7.11 with an arrow showing direction. The areas marked 'P' and '1' are the pipe-runs/well-heads of the gas extraction system and the leachate collection points respectively. The area marked with a '2' is some active machinery in the quarrying part of the site. The region where gas is escaping beyond the boundary of the filled site (circled area on figure 7.11) is visible on figure 7.14 and is marked with a '3'.

The brightness values produced by the video camera are only relative as it adjusts the image intensity depending on the actual values measured. The imagery from the thermal camera was very noisy but even so, the escaping gas and the gas/leachate extraction systems were all more or less visible. The fact that houses and roads are hardly visible suggests that the cloud cover was effective in blocking out the sun.
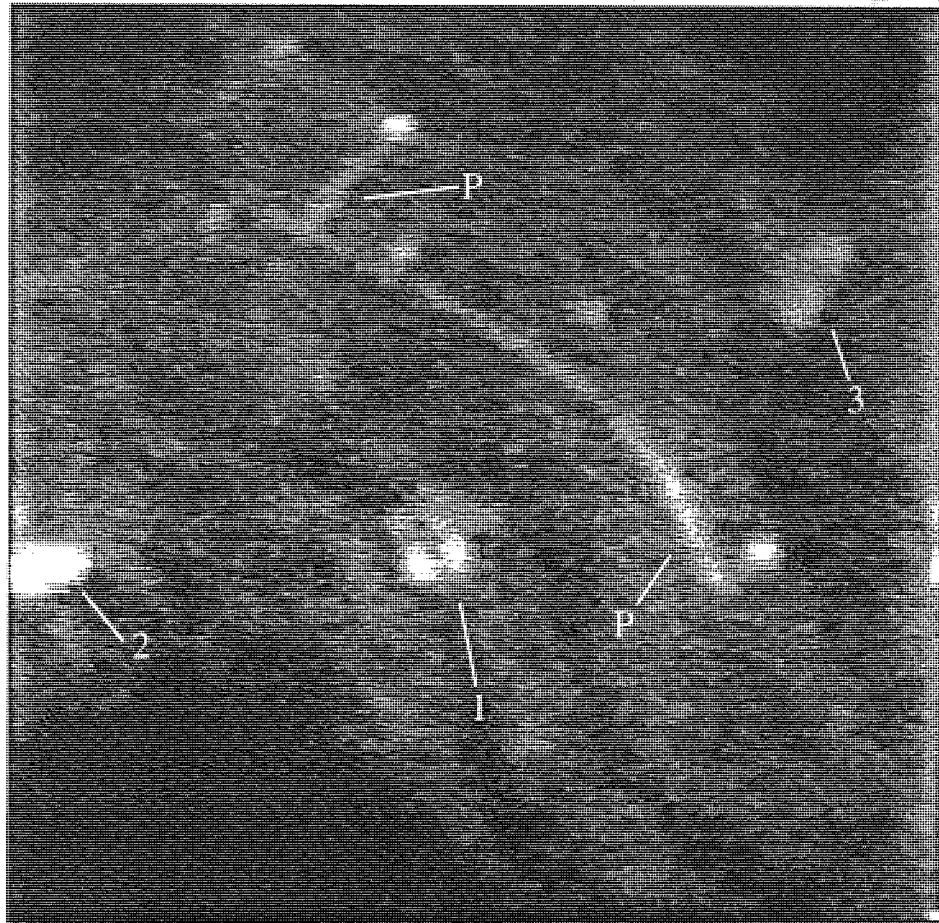
Figure 7.14. Thermal video image of part of site H. (See text for annotations).

The field of view of the camera ($\approx 30°$) means that at a sensibly low altitude the whole site can not be contained in one frame, so the site has to be viewed in small portions and, because of the method of flight, at dissimilar angles, consequently making precise location difficult when using 'grabbed' frames.

This particular thermal camera was a fairly old model. It was capable of detecting radiation in the 2-5μm region of the spectrum, more susceptible to atmospheric interference than the 8-14μm region (see section 4.3.3.1), and produced an image of approximately 100x100 pixels. More recent cameras are capable of detecting in the 8-14μm region of the spectrum without the need for liquid nitrogen cooling (see section 4.3.3.1) and have a pixel resolution of 512x512 or more. They have more control over the contrast and brightness so digital values can be obtained from the grabbed images. The newer cameras can be utilised in a similar manner to the ATM (placed vertically in a fixed-wing aircraft) to produce imagery which compares favourably with the ATM (Marsh, 1995).

7.3.4. Comparison of Video to ATM

In order to see how the ATM and video compare, the warm regions of each were drawn onto a plan of site D.

Figure 7.15 is a density slice of figure 7.10 with all pixels possessing a value of greater than 85 shown as black (table 7.6 indicates that almost everything would be expected to have a value of less than 85 apart from water or artificially warm objects). The flare (marked 'F' on figure 7.15) and some sections of the gas extraction pipes (marked 'P') are depicted. The area marked 'W' is a large puddle that develops following heavy or sustained rain, indicating that there had been considerable precipitation in the few days previous to the flight. The warm areas at the lower and lower-right edges of the site (marked with '3's on figure 7.15 - consistent with figure 7.10) are where landfill gas is escaping to the atmosphere. All other warm points evident within the site boundary are attributable to the gas or leachate extraction systems and points outside the site boundary are associated with housing.
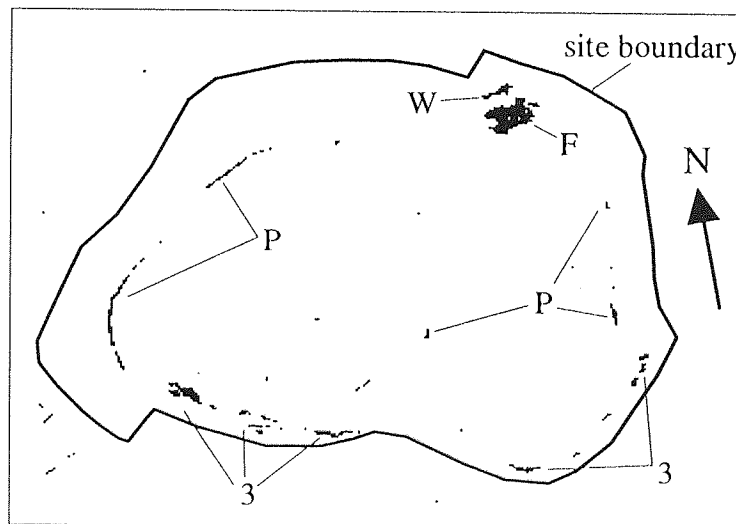
Figure 7.15. Density slice of the dawn thermal ATM. All pixels with a value of 86 or greater are displayed as black. See text for annotations.

Following examination of the thermal video imagery the warm areas were identified and manually transferred on to a plan of site D, which had been produced from an aerial photograph, as shown on figure 7.16. Again the pipe-runs were detected but some that were picked out on the ATM were not seen on the video and vice versa. The video was unable to make out the puddle (marked 'W' on figure 7.15) as water generally appears cooler than most other objects during the day. The most significant difference between figures 7.15 and 7.16 is the representation of the leachate pipe on

the video (marked by an 'L' on figure 7.16) but not the ATM. The leachate pipe is 150mm in diameter, lies on the surface and conveys warm liquid to foul water sewer. It is unlikely that the ATM thermal band would not have detected it, unless it was not in operation at that time; a common occurrence.
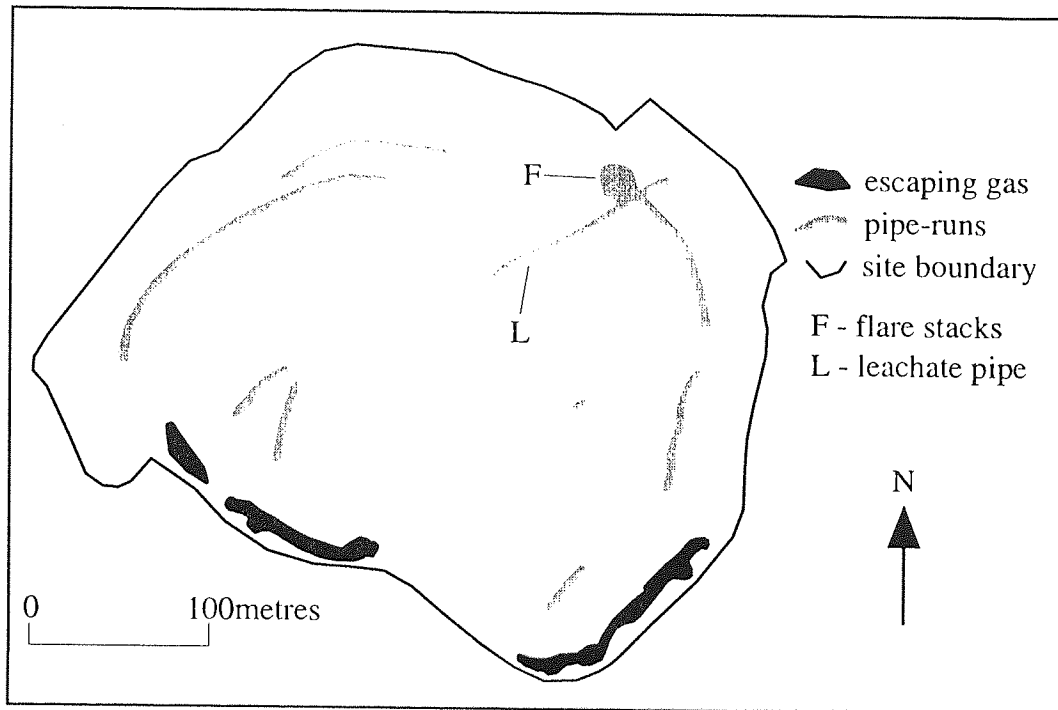
Figure 7.16. Warm areas identified by the aerial thermal video.

It is clear that warm gas is being extracted from site D at a number of separate locations indicating that below the surface over most of the site there is heat being produced. This heat is only in evidence where gas is being brought to the surface showing that the cover materials are effective as an insulator. The likelihood of there being gas passing vertically through the covering materials is very probable as shown by 'mature' landfill gas being detected 30cm below the surface by the spike tests (see section 7.4 and appendix H). If this is the case, none was detectable by heat signature. This suggests that either the gasses lose their heat before they reach the surface, or the rate of migration is not enough for sufficient heat to be imparted to the cover materials. The gas that is identifiable by heat signature is under conditions that are quite extreme, with deep cracks emitting at a substantial rate. If gas was to migrate a substantial distance from the site it is questionable whether any heat signature would be apparent considering that none can be seen on the surface of the site

7.3.5. Examination of Water Bodies for Leachate Ingress

Theoretically it should be possible to detect any elevated temperature caused by leachate using thermal imagery, although none was found in any of the study areas particularly in the case of ingress into a water body. Water generally has a very consistent temperature with a limited range of values so it is possible, using density slicing, to highlight the slightest differences using dawn ATM imagery.

Figure 7.17 shows a density slice of the dawn thermal ATM imagery of site R (south of the canal) and site S (north of the canal) over a very limited range of pixel values. All the areas in colour are water bodies and the remaining monochrome areas exhibit a pixel value of less than 120. The coldest of the bodies highlighted on figure 7.17 are the canals and the rim of the lake to the west, which are coloured in blue. The main body of the lake appears slightly warmer than the canals over a very limited range, a mere 7 increments of pixel value. The warmest water body is that of the stream passing through site R under the canal and into site S.

██ 120-132   ██ 133-138   ██ 139-255
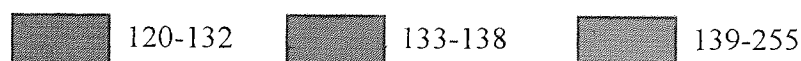
Figure 7.17. Density slice of site R highlighting the water bodies. Values less than 120 are in monochrome.

The reasons for the stream being warmer are not clear but may be related to the source of the water. The stream was traced back along its length as far as the imagery allowed, through and beyond an industrial estate adjacent to site R, and it maintained its temperature all the way giving no indication that it was receiving warm liquid from anywhere. The majority of stream water, though, originates as groundwater (Hynes, 1983) which, while in the body of the earth, is less affected by atmospheric conditions and has a more constant and undeviating temperature. This in effect makes streams warmer in winter and cooler in summer than other non-groundwater fed water bodies and may be what is happening in this instance.

120-129   130-134   135-255
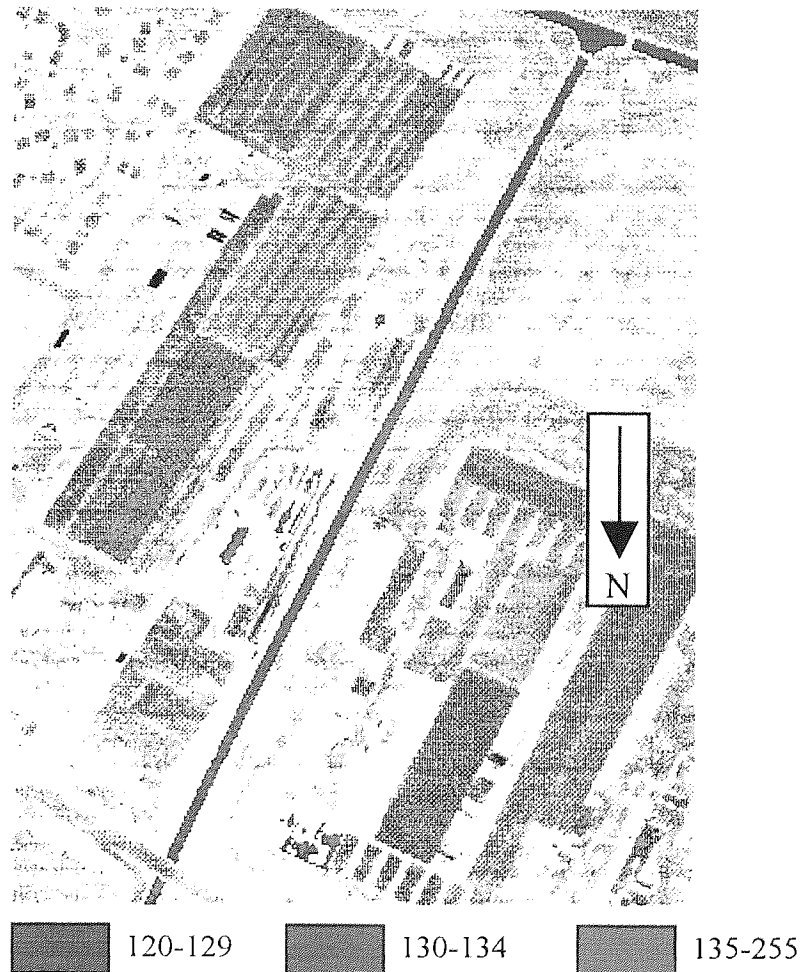
Figure 7.18. Three colour density slice superimposed on a contrast stretched dawn ATM thermal image.

Figure 7.18 is another density sliced thermal ATM image extract of an areas just to the west of site R. Again the water body (a canal) has been highlighted by the density slice on a three colour scale. This extract was chosen because there appears to be a conspicuously warmer region flanked by water of a normal cooler temperature.

The distribution of the green part of the density slice (mid temperature range) suggests that the warmer water is moving gradually out from the central (red) portion and also moving slowly down the image. The pixel values cover a very limited range but the shape and distribution of the warmer water is consistent with a discharge of warmer liquid.

The thermal imagery from the dawn ATM shows itself capable of distinguishing tiny differences in temperature in water bodies which may pinpoint where discharges to canals and streams, whether leachate or effluent, may be occurring.

7.4. Spike Test Analysis

In an attempt to relate the remotely sensed responses radiated by the ground surface to the gas values in the uppermost soil horizons, spike tests were carried out on site D ten days after the dawn ATM flight. Readings would have been taken on the day of the flight but problems were encountered with the gas detectors. At the time of the flight the barometric pressure was 1010 millibars and had risen from a 1000 millibars over the previous 18 hours. When the spike tests were obtained the barometric pressure was 1025 and had been stable for the previous 4 days. No spike tests were taken outside the boundary of the site for three reasons: 1) there was no evidence of gas being found outside the boundary of the site by the site owners (Millfield Environmental) who regularly monitor off-site boreholes, 2) gas was visible emanating from within the site boundary so more attention was placed there and 3) the site was fenced off from the public making the markers placed on a previous occasion less prone to vandalism.

The spike tests measured methane, carbon dioxide and oxygen and were taken every three metres, where possible, along two transects: approximately east-west and north-south which were between, or passed through, points with known National Grid co-ordinates obtained from a large scale map of the site supplied by the current owners. In all, readings for 179 spike tests were acquired and are detailed in Appendix H. The position of each spike test was located on the site plan and digitised into a vector file using Idrisi. The spike test transects are shown on figure 7.19.

In order to compare the spike test gas values with the pixel values from the dawn ATM, an extract of site D was geocorrected onto the National Grid, in the manner described in section 5.3, to the best of the ability of the rectification routines and the imagery. As discussed in section 4.3.2.3.4 the ATM imagery is subject to considerable distortion due to the fluctuations in the flight path and only small regions

(such as a single site) could be rectified with any confidence. The pixel value for each position was noted and a number of statistical analyses were undertaken.
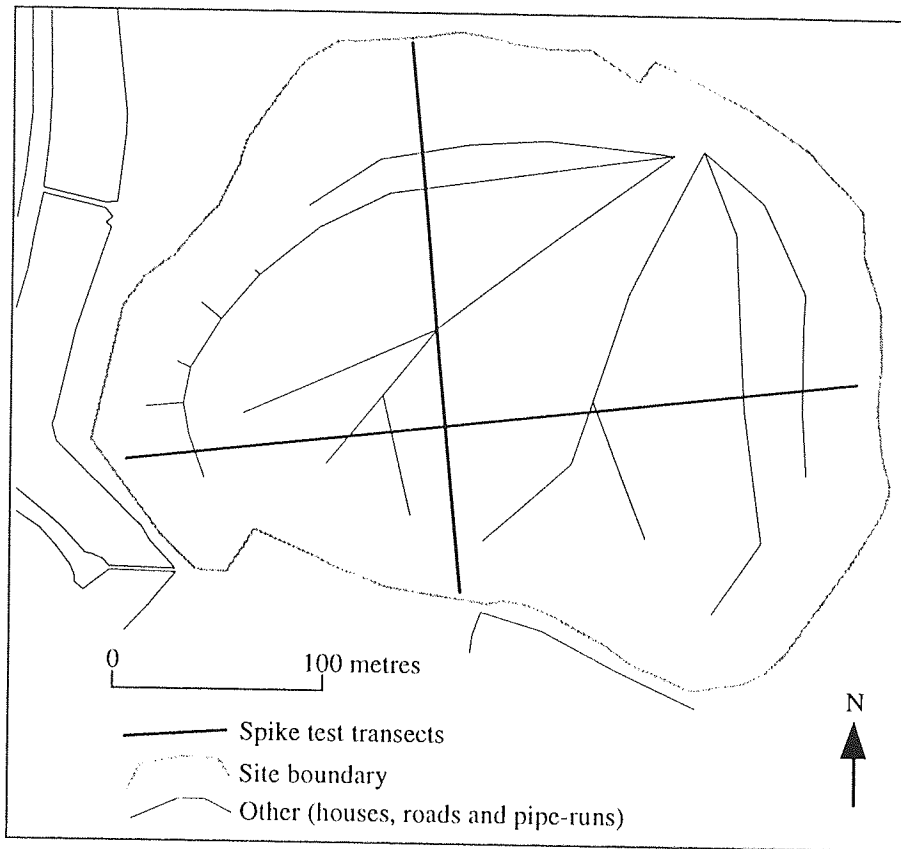
Figure 7.19. Spike test transects taken for the dawn ATM flight at site D

The estimates for fill depth were calculated by digitising topographic maps of before and after filling supplied by the owners of the site. Figure 7.20 illustrates the elevation of site D before and after filling with the physical depth of fill in the bottom frame. The total volume of fill in the site was estimated, by subtracting the final depth form the initial depth using GRASS, at approximately 1 255 000m^3.

| methane concentration (%v/v from the spike tests), |
| carbon dioxide concentration (%v/v from the spike tests), |
| oxygen concentration (%v/v from the spike tests), |
| fill depth |
| pixel value of the dawn ATM thermal |
| ground vegetation cover (evaluated at the time of the spike tests). |

Table 7.8. Parameters used in the spike test analysis.
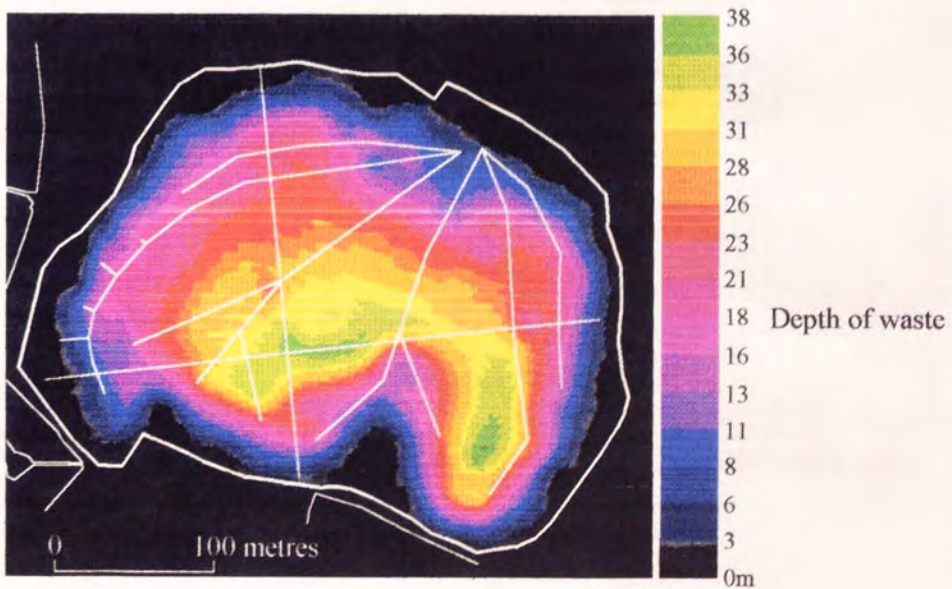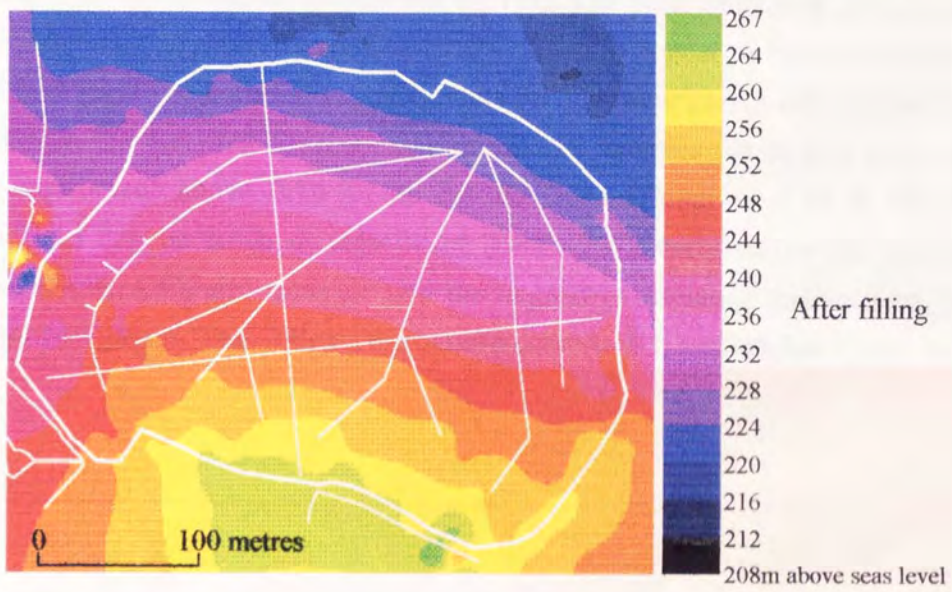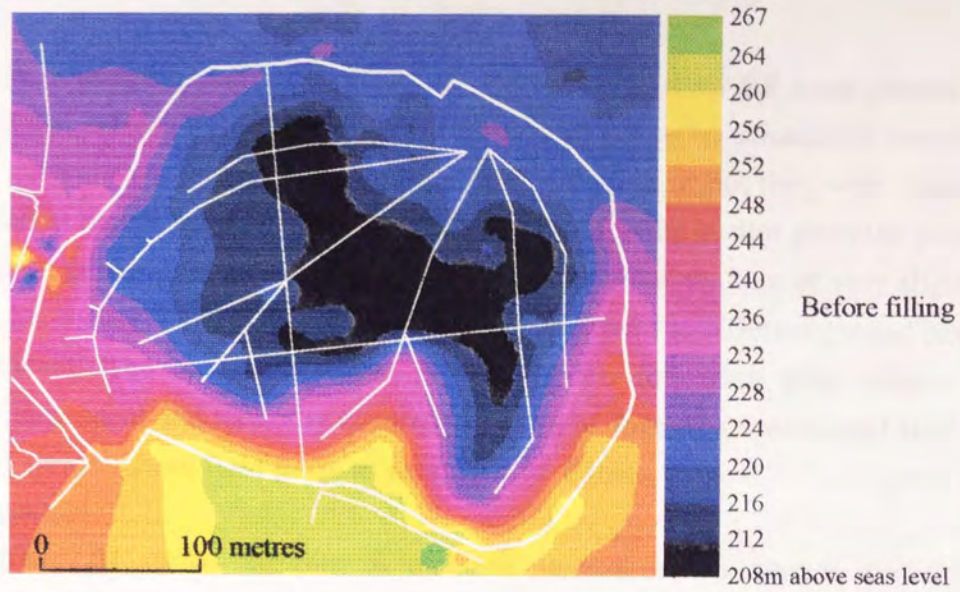
Figure 7.20. Elevation of site D before and after filling and total depth of waste.

Scatter plots for the first five parameters listed on table 7.8 were plotted to ascertain if any relationships existed. The first parameters to be considered were the measured gas values from the spike tests, to verify whether or not they were related, as suggested in sections 3.4 and 3.6. On each of the following scatter plots the points that had grass growing on them and those without grass (mainly bare or very slightly vegetated, i.e. mossy) have been plotted separately, to see if the different ground cover was significant. The term 'grass' that is used in the following plots relates to seasonally dependent and naturally occurring grasses as found on unmanaged land as opposed to sports/school field grass as classified on figures 7.5 and 7.6 and 'grass' as presented on table 7.7.

Figure 7.21 shows the plot of methane against carbon dioxide and there appears to be a positive correlation between the two. The plots of carbon dioxide and methane both against oxygen (figures 7.22 and 7.23) also appear to be correlated but this time negatively. The correlation coefficients for the three gasses are displayed in table 7.8. Given the fact that for a population of 179 samples (as in this case) any correlation coefficient above 0.14 at the 5% confidence level or 0.19 at the 1% confidence level can be taken as significant. Table 7.8 clearly shows the positive correlation between CO_2 and methane and the negative correlation between oxygen and the other two gasses. This follows the pattern described in section 3.6
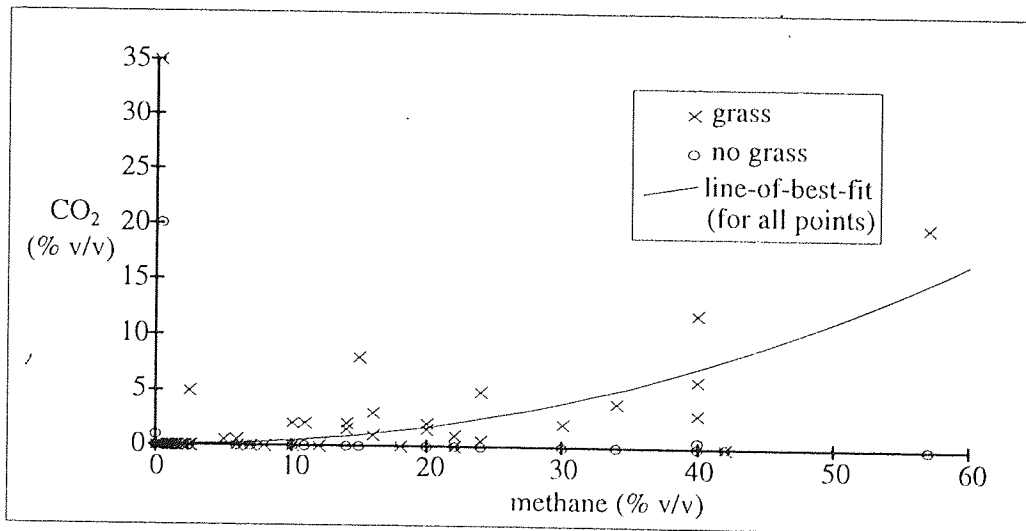
Figure 7.21. Scatter plot of methane against carbon dioxide from the spike tests.

	methane	oxygen
CO_2	0.4098	-0.6241
oxygen	-0.6923	

Table 7.9. Correlation coefficients between methane, carbon dioxide and oxygen.
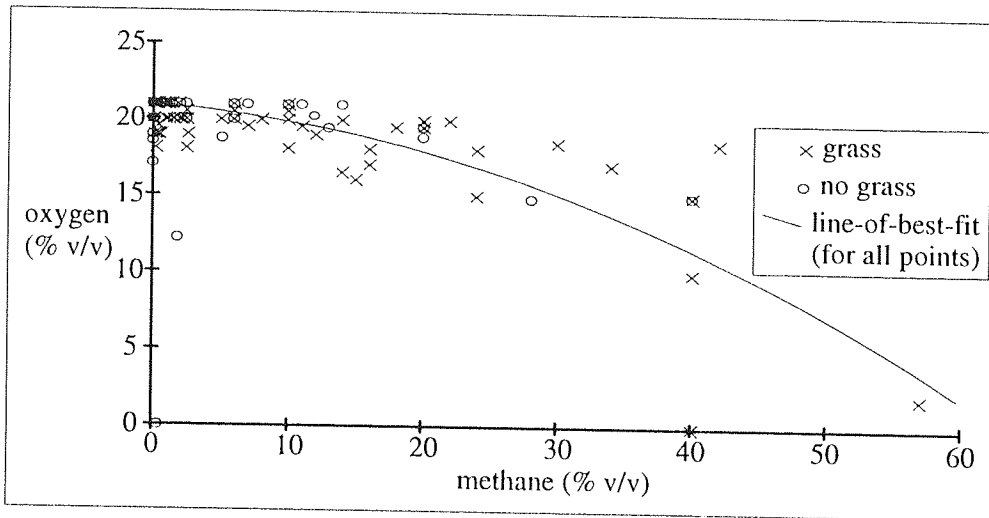
Figure 7.22. Scatter plot of methane against oxygen from the spike tests.
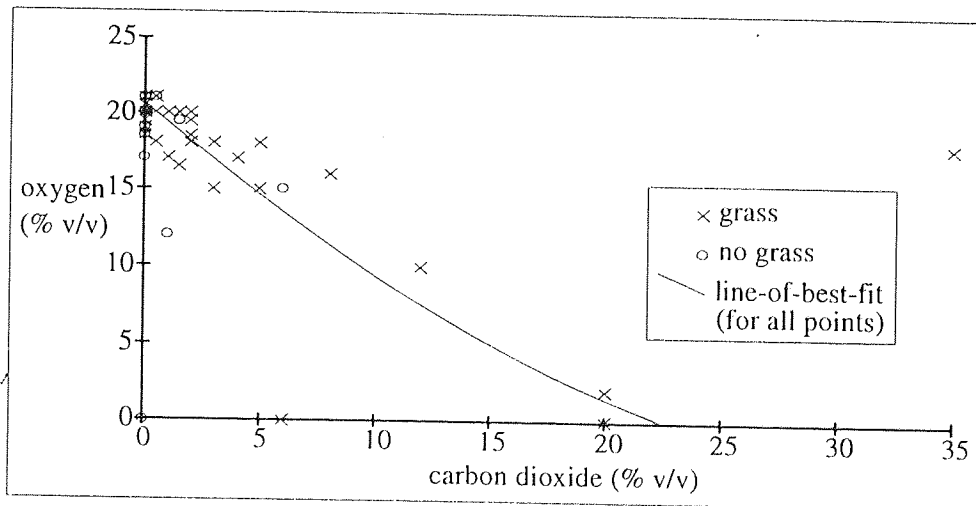
Figure 7.23. Scatter plot of carbon dioxide against oxygen from the spike tests.

One of the hypotheses, that landfill gas has detrimental effects on vegetation (see section 3.6.4) could be investigated here. In general, figures 7.21 to 7.23 indicate that locations with grass have higher methane values and lower CO_2 and oxygen levels than the ungrassed areas - the opposite of what the hypothesis suggested. The

fact that methane and CO_2 are detrimental to vegetation has been shown by Flower et al (1978 and 1981) amongst others. Most of the identified plants affected in these studies, though, were deep-rooted (trees) or artificially planted vegetation (crops). Grasses are relatively short-rooted and more air circulation occurs around the root zone, replenishing the necessary oxygen. The grass quantity and health is more likely to be influenced by the quality of the soil present which may be looser and better draining than elsewhere. Consequently these regions may be able to transport gas better than the more compacted clayey coverings where no vegetation grows and where no gas was measured at the surface either.

In order to test the significance of the relationship between the gas concentrations of grassed and non-grassed spike locations, an F test and a t test were conducted. The t test measures the significance between the means of two samples populations whilst the F test measures the significance between the variances. For the t test to be valid the two variances have to be significantly different, so the F test was carried out first to confirm if this was the case. Of the measured gasses, only methane was used in the F and t tests as it was the most significant component and had the greater breadth of values. Table 7.9 shows the means and standard deviations of methane for the grassed and non-grassed spike tests showing that they are different.

	no. samples	mean	s.d.
grass	120	5.42865	10.611
non-grass	59	3.68178	6.33

Table 7.10. Mean and standard deviations of methane concentrations for grassed and non-grassed spike test locations.

The value of F was 2.810 and the point of significance at the 1% confidence level is approximately 1.7 showing that the variances were significantly different. The value produced by the t test was 1.166. The value of significance for the t statistic is 1.658 at the 10% confidence level, showing the means are not significantly different and cannot be assumed as being from different data sets.

The other two parameters used in the statistical analysis of the spike test results were the pixel value and the depth of fill. The data sets for both were obtained by overlaying the spike test locations onto images of fill depth and pixel value using GRASS. Of the gas values, only methane was used for comparison with the pixel values and fill depth as it was correlated with the other gasses.

Figure 7.24 shows the frequency of fill depth that coincided with the spike test locations showing the predominance of deeper values.
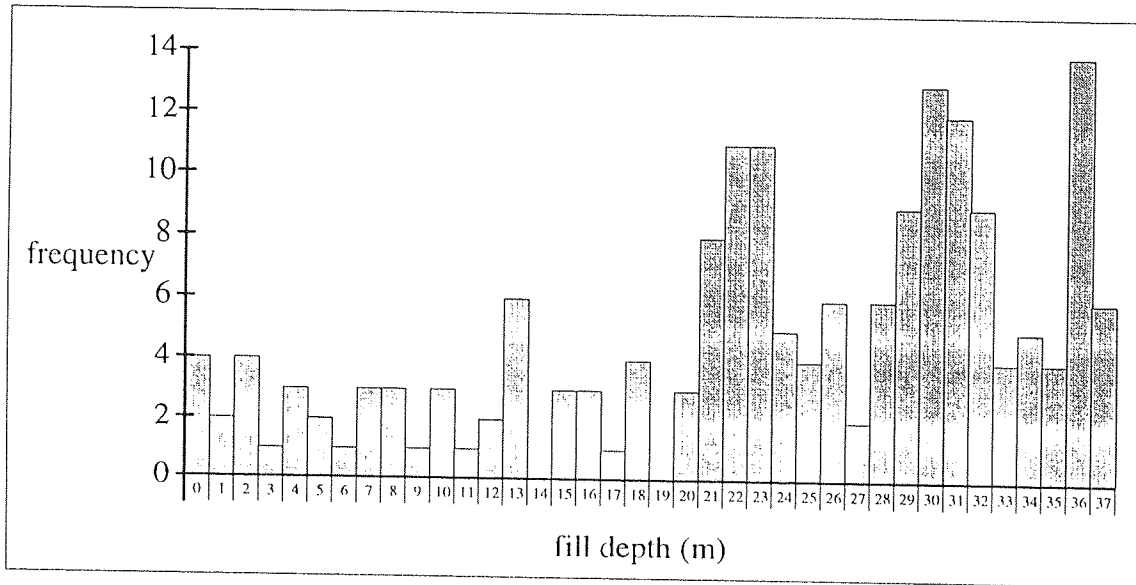
Figure 7.24. Histogram for the frequency of waste fill depth measurements.

Figure 7.25 shows a scatter plot of fill depth against methane concentration again separated into grassed and non-grassed categories. In general, higher methane values correspond with the greater depth of waste and in the majority of these instances the land cover is grass.
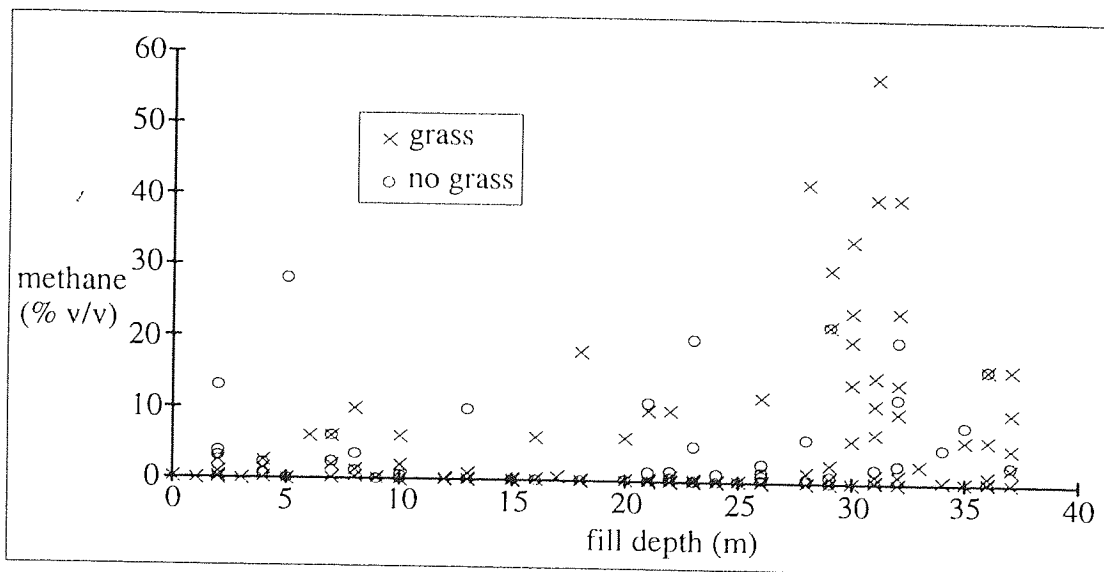
Figure 7.25. Scatter plot of fill depth of waste against methane concentration.

Arguably, the most important comparison in relation to this project is how the gas concentration varies with the pixel values from the thermal ATM, and a scatter plot of these two parameters is displayed in figure 7.26. The immediate impression is that there is a negative correlation, with the higher gas concentrations appearing to have lower pixel values.
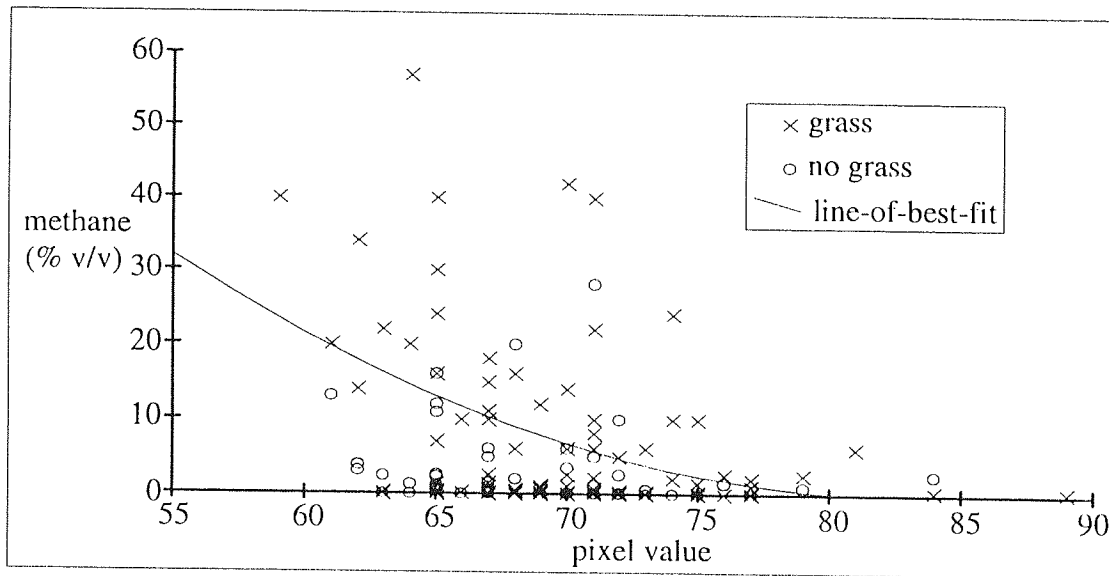
Figure 7.26. Scatter plot of pixel value against methane concentration.

Correlation coefficients between all the parameters are presented in table 7.10. Taking into consideration that the significance limits at the 5% and 1% confidence limits are 0.14 and 0.19 respectively for 177 degrees of freedom (number of samples minus number of parameters) the strongest correlations are those between the gas values as already mentioned. The pixel value shows a negative correlation with methane, a slight correlation with oxygen and none with CO_2. Only the fill depth shows a correlation with methane and none with any other parameter.

	methane	CO_2	oxygen	fill depth
pixel value	-0.2626	-0.1343	0.1691	-0.1022
fill depth	0.2607	-0.0502	-0.0646	
oxygen	-0.6923	-0.6241		
CO_2	0.4098			

Table 7.11. Correlation coefficients for all of the parameters.

Table 7.11 gives the correlation coefficients for the pixel value against methane but divided into the grassed and non-grassed categories. The negative correlation for grassed areas is stronger than as shown in table 7.10, apparently at the expense of the non-grassed values, which no longer is significant. Thus in the experience in this project the methane measured in the spike tests 30cm below the surface has little effect on vegetation on the sites investigated.

	correl coeff	no. samples	signif at 1%	signif at 5%
grassed	-0.3398605	121	±0.234	±0.151
non-grassed	-0.1124136	58	±0.330	±0.214

Table 7.12. Correlation coefficients for methane against pixel value for grassed and non-grassed areas, with significance levels.

A more visual comparison between the pixel value, fill depth and methane concentration is shown in figure 7.27 and 7.28 corresponding to the north-south and east-west transects respectively. The vertical scales of each individual parameter have been altered so the relative fluctuations can be seen more clearly.
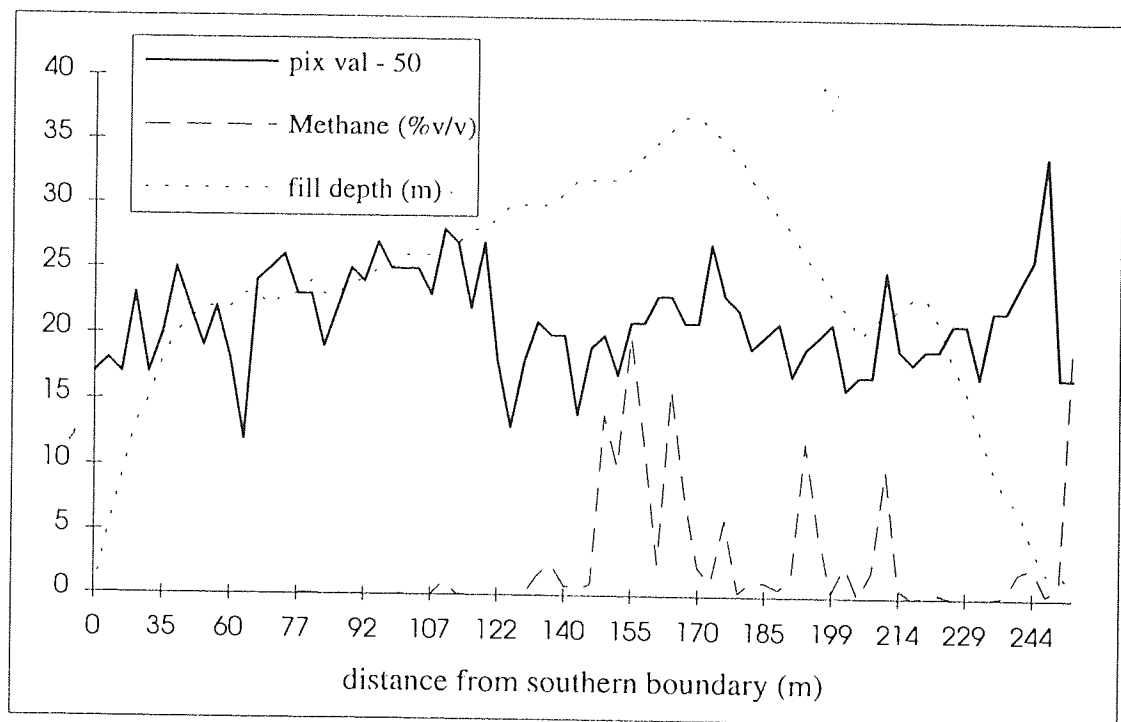
Figure 7.27. Values of methane concentration, fill depth and pixel value for an east-west transect of site D. (Pixel value is displayed 50 less than that measured, for easier comparison).

On neither of the figures 7.27 and 7.28 is there any indication that there is a relationship between the three parameters. In many instances the high values of methane are grouped in certain regions, which may be due to surface influences (i.e. cracked or more permeable capping materials).

	mean	standard deviation
grass	69.85124	4.4114645
no grass	70.576271	6.1621855
all pixels	70.100559	5.058195

Table 7.13. Mean and standard deviation for the ATM dawn thermal pixel values measured at the spike test locations.

Table 7.7 indicates that the pixel values of areas of grass should be in the region of 75. Table 7.12, on the other hand, shows that the mean pixel value for grass measured at site D was considerably lower, at less than 70. The values from table 7.7 were taken from managed sports/school fields which tend to be of a type that continually grows and is green all year round. The natural grasses that grow on site D often have a seasonal growth cycle. In April, when the readings were taken, much of this grass is in the stage where dead leaves are common and little green growth is in evidence. It is thought that vegetation appears slightly warmer than many other materials because the leaves contain water under pressure. The dead out of season grass is unlike this which may contribute to its lower than expected temperature.

The general impression is that while there is a strong correlation between the gas values, there is no relationship with the other parameters. The heat produced by the decaying refuse does not appear to be translated to the surface except where gas is physically escaping, and the methane measured at 30cm below the surface has little bearing on the vegetation or the temperature found at the surface. The spike tests and the ATM dawn flight were carried out 10 days apart under slightly differing conditions. The explosion incident at Loscoe was believed to have been augmented by a very low barometric pressure present at the time drawing out the gas (Tankard, 1986). In this project, the higher pressure at the time of the spike tests may be suppressing some of the gas in comparison to the time of the flight which may be part of the reason why the correlation between the pixel value and methane concentration was not as would be expected.
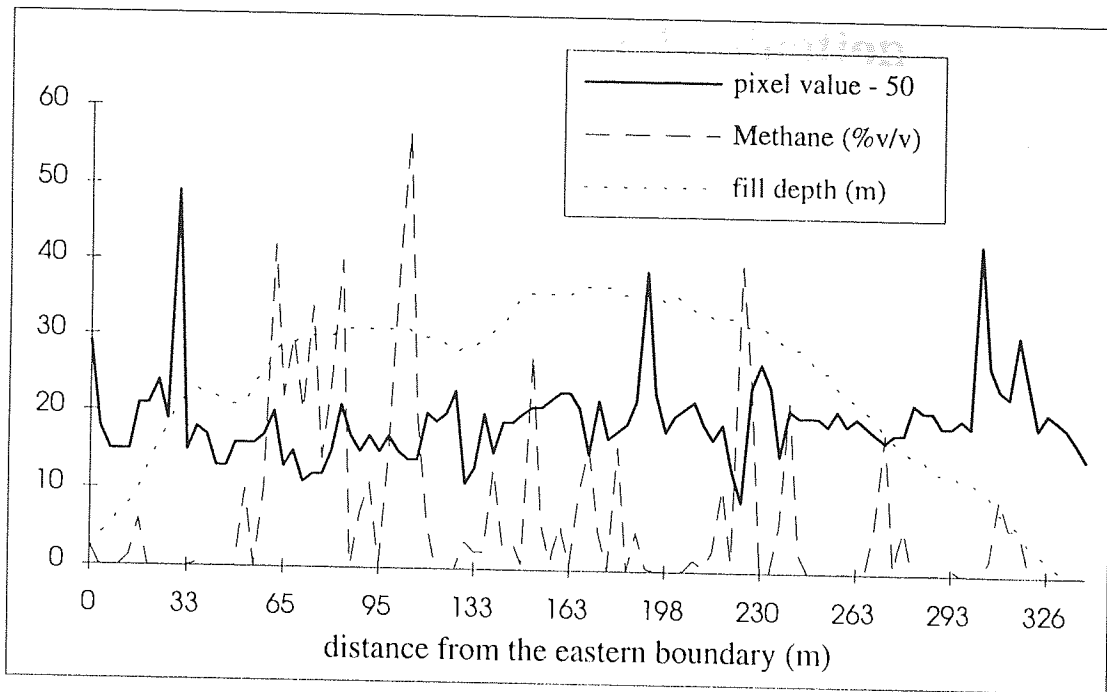
Figure 7.28. Values of methane concentration, fill depth and pixel value for an east-west transect of site D. (Pixel value is displayed 50 less than that measured for easier comparison).

8. Economic Evaluation

As the project was sponsored by parties in the public and private sector working in the field of landfill sites and environmental assessment, an economic appraisal was therefore undertaken with a view to enable decision making.

This chapter has been split into two sections: 1) the time taken to complete some of the computer and laboratory based procedures and 2) the costs of acquisition of the data with comments on the availability of the remote sensing equipment.

8.1. Timing

The times taken for most aspects of the study, from the time of the flight to the production of the final imagery, were logged. As many of the operations were new and problems were identified in an ongoing process, the times used in this project are ideal and assume no avoidable problems.

The time to undertake the main image processing and GIS based procedures for the daylight imagery are presented in table 8.1. The first row relates to the pre-processing needed to produce usable imagery including band separation and correction for 'scan angle effect' (see section 6.2). This procedure was essential as any processing would have been futile with the raw imagery supplied. The computer programs TOTAL and ADJUST (see appendix F) were used to correct the 'scan angle effect' on each of the 12 bands on each tape. The times may seem considerable but this is because all operations have to be conducted 12 times for the whole tape to be processed (once for each band).

procedure	time	comments
Pre-processing	5-6 hours	per tape including 'scan angle effect' adjustment
Classification of a single site	1 hour	for a 512 x 512 pixel image
5 band classification on whole tape	3 hours	per tape
PCA classification on whole tape	5-7 hours	per tape
Area isolation with GIS	5-7 hours	per tape
Area isolation with photos	5 hours	for the whole area

Table 8.1 Time taken to undertake the main image processing and GIS procedures for the daylight imagery (all times include computer program running time).

The second row relates to the classification of a single scene such as figure 7.4. The third row of table 8.1 refers to conducting a PCA on the bands from the whole tape and then applying a classification routine to produce an image such as figure 7.5. The processing time to complete PCA and classifications is considerable on images that are 3M bytes in size.

The fourth row of table 8.1 pertains to the production of an image such as figure 7.6 with undeveloped areas of a certain size being isolated using a GIS. This type of process can take up to 20 separate sub-processes to achieve the final image, thus requiring considerable time for the operation.

All of the computer based operations include human operator time and computer processing time (of which time the operator may be available to do other tasks). Almost all of the computer techniques contained processes that took only a few minutes to complete, often repeated 12 times, sometimes 24 times, for each tape, needing operator input in between. The exceptions were the classification processing time (used in rows three and four of Table 8.1.) and the PCA processing time (row four) which take approximately 1½ to 2 hours. Apart from these last two cases the opportunity for the operator to undertake other task would be only matters of minutes at a time disjointing any available time. There were two batches of magnetic tapes containing ATM data obtained for this project; the daylight and dawn flights. The first batch required extensive pre-processing because it needed 'scan angle effect' adjustment and it was down loaded onto a server which was adding spurious data which had to be erased using a specifically written computer program. The second set did not need any adjustment as it was a dawn flight and experienced no solar effects and was down-loaded onto a much more advanced server which created no additional problems. The data is currently delivered on CD-ROM which can be down-loaded into the relevant computer without the need for a intermediary server indicating that pre-processing time will continue to fall. Many of the procedures were undertaken on a 486 DX PC where only one task could be computed at a time. Should they have taken place on a more powerful multi-tasking computer many of the procedures could be done simultaneously reducing the amount of time taken and allowing the operator greater proportions of free time.

The last row on table 8.1 is not a computer based technique but relates to using aerial photography to highlight undeveloped areas greater than a prescribed size. The final output is a map with highlighted regions such as figure 7.7. The important difference between the aerial photographic technique and the computer based technique is the extent of ground coverage. The computer based methods are applied to a single tape at a time which corresponds to a 6x1.5km area at the altitude flown. Therefore, to produce an image such as 7.6 it takes 15-20 hours per tape. The same

procedure using the aerial photographs is conducted on the entire area (approximately 4x10km - the area covered by 8 tapes) in a fraction of the time by an operator with a reasonable amount of training by concentrating only on the areas of interest.

Not stated in table 8.1 is the density slicing procedures but they are relatively simple and can be obtained from the adjusted imagery in a matter of minutes.

Compared to the daylight imagery the thermal imagery needs considerably less time to process. It is not affected by 'scan angle effect' and as there is only one band, complex classifications are not possible. The only procedures applicable are contrast stretching and density slicing.

All of the times given in table 8.1 are for the production of an image on a monitor. Frequently it is necessary to produce a hard copy (i.e. print outs for reports and such like). Very often though, the quality of paper printouts is not as good as that displayed by a video monitor so some adjustment of the contrast and brightness is necessary. To create a printout from an Iconoclast image the file has to be converted into a different image format that can be read by graphical image manipulation programs (e.g. Picture Publisher) and adjusted accordingly. In general, images with fewer distinct colours which are of a primary or complimentary nature (cyan, yellow, magenta, red, green and blue) produce a better quality and less confusing printout. Those with numerous different shades (i.e. scanned photographs) do not generally come out with the clarity displayed by a video monitor unless the printer is of extremely high quality (i.e. photographic quality), the costs of which may be prohibitive although the prices of such items are continually getting cheaper due to technological advancements.

The image processing was carried out on a 486DX with 4M bytes of RAM and the GIS processing was carried out by a Sun ipx Sparcstation with 16M bytes of RAM linked into the university network server - faster machines will reduce the times taken.

The amount of time taken could be further reduced in a number of ways. The production of a usable image is time consuming, unavoidable but essentially simple. It is clear to the author that a person more practised in computer programming could feasibly link all of the procedures together to create a single automatic routine - i.e. calculate the mean column value, calculate the line of best fit and adjustment parameters from those values, feed it back straight into the correction routine and adjust the image accordingly.

Also, from section 7.1.3.2 the PCA classification was deemed to have no obvious advantage over the straightforward classification of 5 ATM bands. Ignoring the procedure would save time and computer storage space as the additional information created by the PCA would no longer be needed.

If the intention is merely to find large undeveloped areas and the output on a large scale map is adequate then the photographic method by far the most sensible approach. If more quantitative data is required from the area in question the computer based methods may be the best option, either by digitising the aerial photographic overlays or directly from digital imagery.

8.2. Costing

The other important economic aspect is the cost of obtaining the imagery.

The main sensor used for this project was the ATM which is operated and flown by NERC. The imagery supplied by NERC for this project was given free of charge as part of the annual Airborne Remote Sensing Campaign.

The cost for the ATM imagery has been broken down into separate sections as detailed in table 8.2 and the total cost is based on hourly rates for the equipment and personnel. The figures from table 8.2 are those quoted by NERC for commercial operations and were gathered in 1994. According to these figures, the costs of a NERC survey, to the point of the delivery of the raw data, are likely to be £1826/hour for the daylight flight (ATM and photographs) and £1702/hour for the dawn flight (ATM only). The bulk of the overhead costs, which are additional to the line-scanner hire (£594/hr), and camera hire (£124/hr), are for aircraft and personnel, which in the case of the ATM is around £1100/hour.

Rate for Piper Chieftain aircraft	£760 /hour
Rate for ATM	£594 /hour
Rate for Wild RC-8 -(photos)	£124 /hour
Navigator	£248 /hour
ATM operator	£100 /hour
Total	£1826 /hour

Table 8.2. Breakdown of costs for the ATM.

An additional consequence of hiring a rare instrument like the ATM is the difficulty of booking the device in the first place and then waiting for suitable atmospheric conditions to enable the survey to go ahead. Extra costs incurred could

include transportation to the locality (the NERC aircraft is based in Coventry so anywhere outside two hours flying time from there will necessitate the use of an additional airport and subsequent landing fees) and possibly overnight accommodation for the crew.

Table 8.3 provides the costs that may be experienced in obtaining the different forms of imagery that were used in this project. A precursor to the ATM was the AADS 1230 line-scanner that only senses in the thermal region but with the same image resolution and sensitivity. The only known AADS 1230 in Britain is owned by Clyde Surveys in Maidenhead. Their costs are £200/day when it has been leased and £200/hour when airborne. As before, if there is a delay due to atmospheric conditions the costs will increase.

Type of survey	Cost
Aerial photography	£1500 per survey
ATM daylight	£1702 per hour
ATM with photography	£1826 per hour
ATM dawn thermal	£1702 per hour
AADS 1230	£1500 per hour
Thermal video	£2500-3500 per survey

Table 8.3. Comparative costs of different forms of aerial imagery.

The airborne thermal video flown by TBV Stangers (as used in this project) has a simpler cost structure. The helicopter and pilot are organised by the owners of the camera. The typical cost for a days rental is about £2500 and it is generally regardless of the duration of flight. The equipment is hired by the day so two hours flying often costs the same as 20 minutes. Again additional costs may be incurred for overnight stays.

The camera used in this project was the AGEMA Thermovision 450 and as shown in section 7.3.3 the image quality is very poor. There are currently cameras available with considerably greater spectral and spatial resolution that can applied in the same way. One of the latest cameras is the AGEMA Thermovision 1000 which is an electronically cooled device sensitive in the 8-14µm spectral range and is similar to the systems installed in police helicopters. AGEMA themselves do not hire out their cameras so to purchase a Thermovision 1000 would cost in the region of £55000. Aspinwall & Co. have successfully hired a similar camera (a Rank Taylor Hobson,

sensitive at 8-13μm) from Geo-Services in Oxford which cost approximately £3500 for a dawn flight (Marsh 1995).

The period during which dawn thermal sensing can be carried out is very limited (usually two hours at most). This allows very little flexibility and consequently delays are more common than for daylight surveys. The costs associated with hiring aircraft based equipment may increase dramatically if the flight is delayed due to bad weather - a common occurrence in the United Kingdom.

Aerial photographs can be obtained in the same way as line-scanner or video imagery by hiring aircraft and equipment and costs in the region of £1500 for a survey are common. It is possible to obtain photographs from archives if the area of interest has been covered on a previous occasion. This is certainly the case with the West Midlands, which is flown approximately every two years by Cambridge University. These photographs are usually 1:10000 in scale and since 1989 have been taken in colour. Therefore, for stereo coverage of the area at 1:10000 scale, the size studied in this project about 20 to 30 frames are required. Each print costs about £10-20 to purchase, therefore, an outlay of £200-600 would be sufficient to cover the area with a set of prints from one particular year, without the need to charter aircraft and equipment. There are a much larger number of suppliers and operators that undertake aerial photography surveys than for airborne linescanners or thermal video cameras, which means that there is a good chance that there will be one local to the area of interest. As the aircraft may be local then windows in the weather can be exploited with greater speed and less waiting is likely. Also, as aerial photography is more common, one-off payments are more likely and 'holding' the equipment is generally unnecessary.

Table 8.4 gives a provides a general summary between the different types of imagery used in this project for a variety of aspects including image quality, image processing time, accessibility and comparative costs. The table gives a clear indication that aerial photographs are the easiest to obtain, simplest to use and require very little additional equipment. The ATM imagery, on the other hand, requires a much greater level of processing (and consequently operator skill), is very dependent on equipment and is difficult to obtain. In its favour, though is that the amount of analysis that can be conducted on the ATM imagery is extensive due to its multi-spectral sensitivity and digital data format. The thermography takes a position some where between the two as there is little or no processing needed, the interpretation needs a limited amount of understanding of the type of imagery displayed and the equipment requirements are fairly low (VCR and monitor).

Feature of the survey	Aerial photography	ATM imagery	Thermography
Platform	Piper Chieftain aircraft		Twin-engined Squirrel helicopter
Coverage	4 x 10 km	4 x 10 km	25 ha
Pre-processing	developing and printing	extensive	none
Resolution/ scale	1:5000 at 800m altitude	1.5m pixel size at 800m altitude	100x100 video display
Image quality	excellent	good	poor
Identification of sites	rapid visual interpretation	significant image processing required	impractical
Monitoring gas and leachate migration: technique	vegetation stress	i) vegetation stress through multi-spectral analysis. ii)Thermal band employed to detect temperature variation in land cover-dawn flight for best results.	Temperature variations in land cover detected-dawn flight gives best results
Monitoring gas and leachate migration: response time	rapid visual interpretation	image analysis in: ≈3 days band 11 alone, ≈7 days all bands following receipt of data.	real time or VHS tape immediately following completion of flight
Accessibility of system	no problems commissioning flights. Possibility of using archived prints	currently only one system in the UK.	Service offered by several UK consultants
Costs - this project	£1702/hr (NERC)	£1702 /hr(NERC)	£2500-3500/survey (TBV Stangers)
Costs - other organisations	≈£1500/survey (commissioned)	≈£1500/hr (AADS 1230)	£2500-3500/survey (TBV Stangers)
Geo-rectification	Not normally necessary	Very problematic	Not possible by standard software if acquired in oblique format

Table 8.4. Comparison of imagery used in this project.

9. Project Critique

There are many aspects in any project that can be improved with hindsight and this study is no exception.

In general, the study areas have proven to be fairly inert from the view of landfill gas and leachate or the ground cover was too complex for accurate judgements to be made. However, the aim of the project was to assess the validity of using remote sensing methods to detect gas and leachate specifically in an urban environment where areas are likely to be complex with few overtly active sites. As the study areas were hastily chosen by the sponsors and the project supervisor it is possible that with a more detailed preliminary investigation more suitable for study could have been selected.

Certain refinements in the methods could have been made. It was intended to carry out the spike tests immediately following the dawn ATM flight but problems with the gas detectors prohibited this and the measurements had to be taken ten days later when the atmospheric pressure may have changed. Some temperature measurements of the ground with a probe thermometer were taken at the same time as the dawn flight and would have been used in comparison with the dawn ATM readings but the locations were not adequately documented making it impossible to use them.

To run a better comparison between the different types of thermal imagery (ATM and video) it would have been preferable to have obtained the thermal video imagery at dawn as with the ATM. Due to operator schedules and local weather conditions this was not possible and it was carried out in the late afternoon. As a consequence the imagery was very noisy but the important information was obtained and gassing locations could be identified.

A major problem when identifying areas of anomalous warmth on the dawn thermal ATM imagery (which was shown to be of more use than the daylight ATM) was the confusion with other warm areas, particularly water. Table 9.1 gives the approximate ranges of pixel values of various ground cover types for the daylight and dawn thermal ATM. The areas of importance to the project are the gassing areas and table 9.1 shows that the pixel ranges overlap with vegetation, roads, buildings and bare ground on the daylight imagery and water on the dawn imagery. It is clear that if the two sets of imagery could be geo-corrected on to the same co-ordinate set then the gassing areas could be isolated using a combination of classification and band arithmetic. Unfortunately the two thermal ATM imagery sets supplied for this project could not be rectified onto each other due to the deviation of flight experienced by aircraft as described in section 4.3.2.3.4.

Ground cover	Daylight ATM	Dawn ATM
Water	75-85	120-145
Vegetation	80-100	70-90
Roads	120-135	40-60
Buildings	130-170	40-70
Bare	170-200	55-70
Gassing areas	120-190	90-140

Table 9.1. Ranges of pixel value for various ground cover sensed by the ATM (daylight and dawn).

The ATM imagery for this project was supplied in June 1992 and April 1994. Since the latter date the NERC ATM equipment has been updated and the data can now be supplied on CD-ROM. The supplied data for this project (9 tapes for the daylight survey and 21 tapes for the dawn survey), could now, for both flights, be supplied on a single CD-ROM, thereby considerably shortening downloading time.

In addition to the new data storage facility, the NERC remote sensing system now incorporates a Global Positioning System (GPS). There are four sensors on the fuselage that record the precise position of the aircraft at the end of each scanned line. The imagery can now be supplied with each line of data corrected onto a consistent set of co-ordinates producing a correctly oriented and rectified image. These improvements will allow a significant amount of the pre-processing (data transferral and band separation) to be bypassed with a subsequent time saving. Geo-rectified imagery would allow more accurate quantification (of areas etc.) and linking adjacent strips of imagery is much easier. For example, it will enable ATM imagery to be utilised more effectively for temporal studies, since it will be possible to perform band arithmetic on images of the same area but acquired at different times. This facility would have been of great benefit to this study since it may have been possible to eliminate the effects of solar warming and hence identify man induced heating effects.

These additional peripherals are likely to give the NERC airborne remote sensing system set-up greater flexibility and with the geocorrection option allow more quantifiable work to be carried out.

10. Conclusions

For the specific aim of this study - to detect gas and leachate produced by urban landfill sites by remote sensing methods (in particular the use of the ATM) - only marginal success was achieved. There were two main theories that were to be investigated. The first was concerned with detecting colour signatures on the daylight imagery. These signatures could occur either as the change in colour of stressed vegetation from green to red/yellow/brown, due to the presence of gas in the root-zone, or staining of the ground by leachate. The second theory was concerned with the detection of heat given off by gas and leachate due to the exothermic reactions of the decomposition processes.

A preliminary desk study was undertaken to select appropriate sites for study. The records examined were site licences issued by the HWU and site investigation reports conducted by the BCDC. The desk study proved very useful in giving a historical perspective on the waste disposal situation of the area by providing details of what and where waste was licensed to be disposed of and actual contents in the case of site investigation reports. The licences were found not to be entirely reliable, evidenced by the fact that some sites, which were only allowed to deposit inert, and therefore non-methanogenic, material had been found to be producing gas. Even so, historical records are an indispensable source of information as there is virtually no other way to gain an accurate viewpoint of past filling.

The first images available were the aerial photographs that were taken at the time of the daylight ATM flight. These photographs were useful when used in conjunction with the site licences to choose sites for study, based on a range of ages and coverings. In addition, a number of other sets of photographs from previous years were obtained to enable a historical record of the areas to be built up`. A single aerial photograph cannot give any indication of whether waste lies beneath the surface but it can give an indication of vegetation quality. Photographs over time can show the progression of operations on a site or sites particularly using stereo photographs. Areas where deposition took place can be accurately traced if the time period between each photo is sufficient for the changes to be noted. When used in conjunction with a GIS, values for fill area can be measured with reasonable accuracy. Actual volumes can be obtained, using suitable equipment and trained personnel, although they were not available for this project.

A number of areas of bare ground greater than 5 hectares were identified, using a GIS and aerial photographs separately, in order to test the premise that such areas were previously landfill sites. This was found to be incorrect adding to the fact

that it is not possible to make judgements on what is below the surface using appearance alone.

From the point of view of vegetation stress caused by the landfill gas and leachate, nothing detectable by the remote sensing methods was found. On both the aerial photographs and the daylight ATM (following enhancement and classification) a considerable area of ground was found that could be included in the category of vegetation stress or loss and therefore treated with suspicion. However, on the site studied in detail (site D) none of the areas of poor vegetation located on the imagery could be attributed to gas or leachate, such areas could be attributed to seasonal effects and poor soil quality. Only one small area showed any vegetation damage that could be connected to gas, but it was too small to be discernible on any of the imagery. Other areas on the site had gas escaping at the surface with healthy grass abutting the vent cracks clearly unaffected by the gas.

There are many reasons for vegetation to become or appear stressed, or die completely that can be termed natural (i.e. climatic, seasonal or poor soil quality). Most of the sites studied did not have a consistent vegetation coverage and were consequently unevenly vegetated producing areas of apparent stress. Further complications are encountered with unnatural stresses such as on areas used publicly (i.e. trampled ground). Site D was an unmanaged site with a variable soil type across the site. Consequently it was sporadically populated by colonising vegetation species producing a very uneven vegetation coverage and large areas of bare ground.

Many of the studies that proved landfill gas to be injurious to vegetation were either carried out under controlled conditions (laboratory based with regulated soil gas conditions), centred on deep-rooted plants (trees) or on artificially planted vegetation (crops). Stressed trees are of a scale that would probably be detectable by reasonably high resolution imagery (as used in this project) and as the whole or a considerable portion of the crown would be affected at the same time it would produce a characteristic signature. The situation with crops is also conducive to being used to detect stress as a field of crops is planted at the same time and the growth cycle is well known so any aberrations are likely to be noticed, even on fairly small scale imagery.

The conclusion formed is that in areas such as those chosen for this project the use of vegetation stress as an indicator of the presence of landfill gas or leachate is not appropriate. Evidence in this project suggests that:

> a) vegetation stress caused by landfill gas or leachate rarely occurs and when it does it is not on a scale detectable by the remote sensors used in this project;

b) unmanaged or public areas have a very complex soil/vegetation cover and stress experienced by the vegetation is likely to be explained in some other way.

Further proof of the fact that the landfill gas was not affecting the vegetation was provided by the spike tests on site D. In a number of cases high levels of gas were found only 30cm below the surface but the vegetation above it was perfectly healthy.

Even though the use of vegetation stress as an indicator was deemed inappropriate the classification routines were not at fault, the indicators were simply not there to be found.

The second main theory to be tested was: could the heat produced by the decay of refuse be detected in any pollutants that were escaping from the site? The daylight ATM was able to detect the heat of escaping gas from cracks around the boundary of site D, but elsewhere any anomalous readings were masked by materials heated by solar radiation (paved areas and bare ground). Due to this problem another ATM flight, as well as a thermal video flight, was commissioned which would not experience the solar heating problem.

Two sites (sites D and H) were highlighted for study using the thermal sensors (dawn ATM and thermal video camera) and both sensors yielded in essence the same results. The image quality of the ATM was far superior to the video in resolution and clarity. The warmest points on the dawn ATM thermal imagery were either buildings (factories at work), anomalous sources (escaping gas) or water. Using density slicing techniques a number of areas were found to be warm and subsequently found to be emitting gas. These areas were relatively distinct but it was not possible to differentiate them from water using the imagery alone. It was necessary to have some information on the characteristics of the site to enable the features on the thermal images to be identified.

With respect to image quality and ease of data manipulation of the final imagery the ATM was superior to the thermal video imagery. Whilst there was a considerable time delay incurred in acquiring the ATM imagery, the thermal video camera cassette was available immediately on landing. Cameras do exist now that produce imagery of a comparable quality to the ATM. They can also be oriented vertically giving a plan view and incorporate frame grabbing capabilities. This would allow comparable images to the ATM to be acquired which could then be manipulated in the same manner and be much easier to geo-rectify.

When using the density slice technique on the thermal ATM to examine water bodies for leachate ingress, it was found that different water bodies have different ambient temperatures. Streams were the warmest water bodies, followed by lakes with

canals being the coolest. It was first thought that the stream, which passed through site R, was warmer because it was receiving leachate, but it was subsequently found that the temperature was elevated before it began its course through the site. The most likely reason for this is the fact that streams are fed by groundwater, which in general has a very stable temperature and is warmer than surface water during the winter and cooler during the summer. One area of canal, though, was found to have a warm region between two cooler ones again suggesting that it was receiving input warmer than the ambient temperature of the canal.

An integral part of the project was the use of image processing to manipulate the data. Of the available techniques the main methods employed were classification, density slicing and GIS.

The five band maximum likelihood classifier used was very effective on simplifying the ATM imagery. The additional application of PCA, even though clearly more information was made available, did not show anything more than the straight five band classifier. The PCA technique has the disadvantage that it takes about twice as long to undertake as the 5 band classifier and needs double the amount of disk space.

The density slicing technique is an effective tool when used to highlight slight differences in pixel value on thermal imagery. It was successful in locating areas of landfill gas escape and a warm liquid ingress to a canal.

The use of the two GIS packages clearly showed that the imagery from the ATM could be effectively incorporated into them and manipulated. The identification of undeveloped areas of a certain size was successfully accomplished.

Regarding the time taken for processing the imagery the aerial photographs are by far the least time consuming. There is no pre-processing required and no enhancement that is necessary making them immediately available for use. Before the ATM imagery could be used it had to be corrected for the extraneous data added by the VAX server and also for 'scan angle effect'. The problem with the VAX server is no longer exists as it has been replaced but 'scan angle effect' is likely to be a problem on daylight imagery in the future and will require rectification.

The density slicing routines can be achieved in a matter of minutes but the classification procedures and the area isolation procedure using GIS were relatively time consuming, taking up to seven hours of computer and operator time to produce an image.

The economic evaluation presented in this project not only takes into account the fiscal standpoint but also addresses the time needed to undertake the procedures and the availability of the equipment, important aspects in the commercial domain.

The costs of obtaining imagery varies with the device used. All of the commissioned imagery (ATM, Thermal video and aerial photographs) and equivalent commercial imagery were in a similar cost range - between £1500-3500 - the main difference being the availability of the different forms. Aerial photographs are a very old and traditional form of image and are readily commissioned from a number of sources although false colour film can be difficult to obtain. Also, a number of archives exist where historical photographs are held and prints can be bought for usually £10-20 each. Thermal video cameras are relatively small, hand-held, and can be rented from some technical equipment hire companies. Very few operators exist that will fly these video cameras so it may be up to the user to organise the camera and aircraft (probably helicopter) rental. As far as is known there is only one ATM in the country and one AADS 1230 (thermal only) line-scanner in the UK making the acquisition of such imagery problematic unless organised well in advance. There are other multi-spectral scanning systems available such as the CASI (which is a visible and short-wave infra-red push-broom scanner) which at least two are known and owned by NERC and the Environmental Agency (EA).

The weather can play a major part in increasing the costs of acquiring imagery. Some sensors are rented by the day (AADS 1230) or have to be transported considerable distances due to their rarity (ATM) and may incur additional costs when the system is not at its home base. This problem is not usually experienced when acquiring aerial photographs as there are a large number of contractors that are likely to be local to the area of interest.

There have been a number of new additions to the NERC remote sensing system since this research began and many of the problems encountered in this project can now be avoided. The data is now supplied on CD-ROM which can hold as much as at least 10 tapes, reducing physical bulk significantly and easing processing. The data is supplied with extraction programs written to run on the SUN UNIX operating system and will transfer the data into whatever the form required by the user, including fully separated, thus avoiding the need to read it onto a server first and occupying enormous amounts of disk space.

The other significant alteration is the incorporation of a Global Positioning System (GPS). This new instrument enables the data to be rectified onto a recognised co-ordinate system allowing imagery to be mosaiced and accurate spatial measurement to be made. Accurately rectified imagery will allow rectified imagery of different scales and taken at different times to be overlaid. For instance, if imagery from a day and a dawn flight were to be subtracted some measure of thermal inertia would result. This would allow the correct classification of water which could then be

excluded from the dawn thermal imagery eliminating the confusion caused by it. Also imagery taken a year apart can be compared for similarities and diversities.

The use of airborne remote sensing methods for monitoring pollution from landfill sites may be summarised as:

- vegetation stress is not a reliable indicator of the presence of landfill gas or leachate in an urban environment when using remote sensing methods,
- heat produced in landfill sites can be detected by remote sensing techniques,
- the ATM and thermal video cameras are capable of detecting landfill gas and leachate given the right conditions
- the premise that large areas of open space may have landfill sites beneath them is flawed

References

Ahern F. J., Bennett W. J. and Kettela E. G. (1986), 'An initial evaluation of two digital airborne imagers for surveying spruce budworm defoliation.', *Photogram. Eng. & Remote Sensing.* **52**:(10), 1647-1654.

Airola T. M. and Kosson D. S. (1989), 'Digital analysis of hazardous waste site aerial photographs.' *Journal of the Water Pollution Control Federation.* **61**:(2), 180-183.

Attal A., Akunna J., Camacho P., Salmon P. and Paris I. (1992), 'Anaerobic degradation of municipal wastes in landfill.' *Water Science and Technology.* **7**, 243-253.

Avery T. E. and Berlin G. L. (1992), *Fundamentals of Remote Sensing and Airphoto Interpretation.* 5th Edition, Macmillan.

Azam J. (1989), 'The use of aerial photographs to inventory and monitor environmental pollution. *ITC Journal.* **1989**:(1), 15-20.

Bagchi A. and Carey D. (1986), 'More Effective Methane Gas Monitoring at Landfills.' *Public Works.* **117**(Dec), 44-45.

Ball S. and Bell S. (1994), *Environmental Law.* Second Edition. Blackstone Press Ltd.

Barnaba E. M., Philipson W. R. and Ingram A. W. (1991), 'The use of aerial photographs in county inventories of waste disposal sites.' *Photgram. Eng. and Remote Sensing.* **57**:(10), 1289-1296.

Barnsley M. J. (1993), 'Environmental monitoring using multiple view angle (MVA) remotely-sensed images.' *in* Curran P. J. and Foody G. (eds.) 'Global Environmental Monitoring using Remote Sensing.' Taylor and Francis, London. 181-201.

Barnsley M. J. and Barr S. L. (1993), 'Mapping urban areas using high spatial resolution remotely sensed images. 1. Data processing.' *Proc of the NERC Symp. on Airborne Remote Sensing 1993.* 20-21st Dec, Dundee. 1-13.

Barrett E. C.and Curtis L. F. (1982), *Introduction to Environmental Remote Sensing.* Third Edition. Chapman & Hall, London and New York.

Bingemer H. G. and Crutzen P. J. (1987), 'The production of methane from solid wastes. *Journal Of Geophysical Research.* **92**:(D2), 2181-2187.

Birkbeck A. E. and Tomlins G. F. (1985), Aerial photography for the detection of leachate migration from landfills.' *Water Pollution Research Journal of Canada.* **20**:(3), 92-102.

Bogner J. E. (1986), Understanding natural and induced gas migration through landfill cover materials- the basis for improving landfill gas recovery. *Proc. 21st Intersoc. Energy Conversion Engineering Conf.*, San Diego, California USA, 25th August, 1, 199-204.

Boochs F., Kupfer G., Dokter K. and Kühbauch W. (1990), 'Shape of the red edge as a vitality indicator for plants.' *Int. J. Remote Sensing.* 11:(10), 1741-1753.

Bullard R. K. (1983), *Working Paper No.8: Abandoned Land in Thurrock: An Application of Remote Sensing.* North East London Polytechnic Department of Land Surveying.

Burrough P. A. (1986), *Principle of Geographic Information Systems for Land Resources Management.* Oxford Science Publications.

Butler R. (1993), pers. comm., West Midland Hazardous Waste Unit, Walsall, UK.

Campbell D. J. V. (1989), 'The nature of landfill gas and its environmental impact.' *Wastes Management.* April, 201-208.

Campbell D. J. V. (1985), 'Production and environmental consequences of landfill gas.' *Wastes Management.* 75:(4), 166-172.

Carter (1989), 'On defining the Geographical Information System' in Ripple W. J. (ed.) 'Fundamentals of Geographical Information Systems, a Compendium'. 3-6.

Colwell J. E. (1974), 'Vegetation canopy reflectance.' *Remote Sensing of Environment.* 3, 175-183.

Colwell R. N. (1983), *Manual of Remote Sensing.* Vols 1 and 2. American Society of Photogrammetry.

Coulson M. G. and Bridges E. M. (1984), 'The remote sensing of contaminated land.' *Int. J. Remote Sensing.* 5:(4), 659-669.

Couth B. and Rumbold R. (1992), 'Leisure park keeps one step ahead.' *Waste Management.* August, 30-31.

Croft B. and Campbell D. (1992), *Characterisation of One Hundred United Kingdom Landfill Sites.* Environmental Safety Centre, Harwell, Oxon.

Crutcher A. J., Rovers F. A. and Mcbean E. A. (1982), 'Temperature as an indicator of landfill behaviour.' *Water, Air and Soil Pollution.* 17:(2), 213-223.

Curran P. J. (1986), 'Small format, oblique, colour aerial photography: an aid to the location of methane gas seepage.' *Int. J. Remote Sensing.* 7:(4), 477-479.

Curran P. J. (1985), *Principles Of Remote Sensing.* Longman.

Daedalus Enterprises Inc. (1979), *Scanner Applications...Worldwide.* Daedalus Enterprises Inc., Ann Arbor, Michigan.

Danson F. M. (1986), 'Remotely sensed red and near infra-red response to forest canopy cover.' *Proc. of the NERC 1985 Airborne Campaign Workshop.* 26th Nov, Ripton, Cambs, UK. A1-A10.

Department Of The Environment (1992a), *Waste Management Paper No. 27: Landfill Gas.* Publ. HMSO, London.

Department Of The Environment (1992b), *Planning, Pollution and Waste Management.* HMSO, London.

Department Of The Environment (1992c), *Waste Management Paper No. 26: Landfilling Wastes.* HMSO.

Department Of The Environment (1994), *Waste Management Paper No. 4: The Licencing of Waste Management Facilities.* HMSO.

Drury S. A. (1990), *A Guide To Remote Sensing - Interpreting Images Of The Earth.* Oxford. Science Publications.

Dumbleton M. J. (1983), *Air Photographs for Investigating Natural Changes, Past use and Present Condition of Engineering Sites.* TRRL Lab Report 1085. DoE, DoT, Crowthorne, Berkshire.

Eastman R. J. (1995), *Idrisi for Windows. User's Guide Version 1.0.* Clark Labs for Cartographic Technology and Geographic Analysis, Clark University, Worcester, Massachusetts, USA.

Elliot T. (1994), 'Redevelopment of derelict and contaminated land in the black country.' Presented at the '*3rd Ordinary Meeting Of The Midland Geotechnical Society.*' Haworth Building, Univ. Birmingham. 5th Dec.

Erb T. L., Philipson W. R., Teng W. L. and Liang T. (1981), 'Analysis of landfills with historic air photos.' *Photogram. Eng. and Remote Sensing.* **47**:(9), 1363-1369.

Farquar G. J. and Rovers F. A. (1973), 'Gas production during refuse decomposition.' *Water, Air and Soil Pollution.* **2**, 483-495.

Finch D. J. (1993), 'Estimating landcover in mixed urban/rural catchments for hydrological modelling.' *Proc of the NERC Symposium on Remote Sensing 1993.* 20-21 Dec, Univ. Dundee, UK. 22-36.

Finkbeiner M. A. and O' Toole M. M. (1985), 'Application of aerial photography in assessing environmental hazards and monitoring cleanup operations at hazardous waste sites.' *6th National Conf. on Management of Uncontrolled Hazardous Waste Sites.* Las Vegas, Nevada, Nov 4-6. 116-124.

Flach J. D. (1989), 'River Basin Surveillance using Remotely Sensed Data: a Water Resource Information Management System.' Ph.D. Thesis. University Of Aston In Birmingham UK.

Flower F. B., Gilman E. F. and Leone I. A. (1981), 'Landfill gas, what it does to trees and how its injurious effects may be prevented.' *Journal of Arboriculture.* 7:(1), 43-52.

Flower F. B., Leone I. A., Gilman E. F. and Arthur J. J. (1978), *A Study Of Vegetation Problems Associated With Refuse Landfills.* EPA Report No. EPA 600/2-78-094, Cincinnatti, Ohio.

Garofalo D., Wobber F. J. (1974), 'Solid waste and remote sensing.' *Photogram. Eng. and Remote Sensing.* 40:(1), 45-59.

George D. G. and Hewitt D. P. (1989), 'The trophic classification of lakes in the Windermere area.' *Proc. NERC Workshop On Airborne Remote Sensing 1989.* 23rd Nov, Inst. Freshwater Ecology, Windermere. 109-119.

Gilvear D. and Watson A. J. (1993), 'Examination of the use of ATM imagery for mapping wetland water table depths and wetland vegetation, Insh marshes, Scotland.' *Proc. NERC Symposium on Airborne Remote Sensing 1993.* 20-21st Dec, Univ. Dundee, UK. 44-49.

Graham R. and Read R. E. (1986), *Manual Of Aerial Photography.* Focal Press, Sevenoaks, Kent.

Groom S. B. and Holligan P. M. (1987), 'Remote sensing of coccolithophore blooms.' *Adv. Space Res.* 2, 73-78.

Groves M. A. (1989), 'The use of Remotely Sensed Data for Monitoring air Pollution Related Damage to Forested Areas.' Ph.D. Thesis, Aston University, Birmingham, UK.

Haynes J. E., Wood G. M., Lawrence G. and Bourque H. H. (1981), 'Remote sensing and waste management.' *Proc. 7th Canadian Symp. Of Remote Sensing.* Winnipeg, Manitoba, 8-11th Sep. 316-322.

Her Majesty's Inspectorate Of Pollution. (1991), *Waste Management Paper No. 4: The Licensing Of Waste Facilities.* HMSO, London, Fourth Impression.

Hynes H. B. N. (1983), 'Groundwater and stream ecology.' *Hydrobiologia.* 100, 93-99.

Jensen J. R. (1986), *Introductory Digital Image Processing: A Remote Sensing Perspective.* Prentice-Hall, New Jersey.

Jones H. K. (1991), 'The Investigation of Vegetation Change using Remote Sensing to Detect and Monitor Migration of Landfill Gas.' Ph.D. Thesis, University of Aston, Birmingham, UK.

Jones H. K. and Elgy J. (1994), 'Remote Sensing to assess landfill gas migration.' *Waste Management and Research.* **14**, 327-337.

Kadro A. and Kuntz S. (1986), 'Experiences in the application of multi-spectral scanner data for forest damage inventory.' *Symp. on Remote Sensing for Resources Development And Environmental Management.* Enchede, Aug. 469-472.

Kennedy J. B. and Neville A. M. (1986), *Basic Statistical Methods for Engineers and Scientists.* Third Edition, Harper & Row, New York.

Knipe C. V., Lloyd J. W., Lerner D. N. and Greswell R. (1993), *CIRIA Special Publication 92. Rising Groundwater Levels in Birmingham and the Engineering Implications.* CIRIA, London.

Knipling E. B. (1970), Physical and physiological basis for the reflectance of visible and near infra-red radiation from vegetation.' *Remote Sensing of Environment.* **1**, 155-159.

Leone I. A., Flower F. B., Arthur J. J. and Gilman E. F. (1977), 'Damage to woody species by anaerobic landfill gasses.' *Journal Of Arboriculture.* **3**:(12), 221-225.

Levitt J. (1980), *Responses of Plants to Environmental Stresses Vol 2: Water, Radiation, Salt and other Stresses.* New York, London: Academic Press.

Lillesand T. M. and Kiefer R. W. (1986), *Remote Sensing and Image Interpretation.* John Wiley & Sons.

Lyon J. G. (1987), Use of maps, aerial photographs and other remote sensor data for practical evaluation of hazardous waste sites.' *Photogram. Eng. and Remote Sensing.* **53**:(5), 515-519.

Lyon J. G. (1982), 'Use of Aerial Photography and Remote Sensing in the Management of Hazardous Wastes.' *in* Sweeny T. L., Bhatt H. G., Sykes R. M. Sproul O. J. (eds), 'Hazardous Waste Management for the 80's.' Publ. Ann Arbor Science, Michigan. ISBN 0-250-40429-X. 163-171.

Mallin K. (1991), *The Black Country.* ISBN 0 9510420 1 7.

Marsh P. (1995), pers. comm., Aspinwall & Company, Baschurch, Shrewsbury, Shropshire.

Mather P. M. (1987), *Computer Processing of Remotely-Sensed Images - an Introduction.* John Wiley & Sons.

McCarthy J., Olsen C. E. Jnr. and Witter J. A. (1982), 'Evaluation of spruce-fir forests using small format photographs.' *Photgram. Eng. and Remote Sensing.* **48**:(5), 771-778.

McRae S. G. and Hewitt A. K. J. (1986), 'Landfill gas emissions and their effects on soils and crops.' *Trans. XIII Internat. Congress Soil Sci.*, Hamburg, **4**, 1382-1383.

Murtha P. A. (1978), 'Remote sensing and vegetation damage: a theory for detection and assessment.' *Photogram. Eng. and Remote Sensing.* **44**:(9), 1147-1158.

Omar D. N., Cracknell A. P. and Codd G. A. (1989), 'Blooms of blue-green algae in lochs in Tayside and Fife.' *Proc. NERC Workshop on Airborne Remote Sensing 1989.* 23rd Nov, Inst. Freshwater Ecology, Windermere. 121-129.

Open University. (1989), *The Open University Remote Sensing Course Book.* Open Universiteit, Heerlen, The Netherlands.

Ory T. R. (1990), 'Photonics in earth sciences -protecting the environment.' *Photonics Spectra.* **24**:(9), 115-116.

Pacey J. G. and Degier J. P. (1986), 'The factors influencing landfill gas production.' *Proc. Energy from Landfill Gas Conf.* Solihull, UK. 28-31st Oct. 51-59.

Pankhurst E. S. (1973), 'The effects of natural gas on trees and other vegetation.' *Aspects of Current use and Misuse of Soil Resources.* Welsh Soils Discussion Group. 116-130.

Parsons P. J. and Smith A. J. (1986), 'The environmental impact of landfill gas.' *Proc. Energy from Landfill Gas Conf.*, 28-31st Oct, Solihull, UK 17-21.

Peters Jr L., Daniels J. J. and Young J. D. (1994), 'Ground Penetrating Radar as a subsurface Environmental Sensing Tool' *Proceeding of the IEEE.* **82**:(12), 1802-1821.

Rodwell, J. S. (1992), *The British Plant Communities. Volume 3, Grasslands and Montane Communities.* Cambridge University Press.

The Royal Institution Of Chartered Surveying. (1984), *Specifications for Vertical Air Photography.* Surveyor Publications, London. ISBN 0-85406-243-2.

Russ J. C. (1992), *The Image Processing Handbook.* CRC Press Inc., Boca Raton, Florida.

Sangrey D. A. and Philipson W. R. (1979), *Detecting Landfill Leachate Contamination Using Remote Sensors.* EPA Report No. EPA-600/4-79-060, Las Vegas, Nevada, USA.

Scott P. E. and Baldwin G. E. (1989), *Methods used to Characterise and Assess the Environmental Impact of Gaseous Emissions from Landfilled Wastes.* Waste Research Unit, Environmental Safety Centre, AEA Technology, Harwell, Oxon.

Sellers W. D. (1965), *Physical Climatology.* University of Chicago Press, Chicago and London.

Shapiro M. (1993), *Geographic Resource Analysis Support System Manual.* US Army Corps of Engineers, Construction Engineering Research Laboratories.

Shears J. R. (1988), 'The use of airborne thematic mapper imagery in monitoring saltmarsh vegetation and marsh recovery from oil refinery effluent. the case study of Fawley Saltmarsh, Hampshire.' *Proc. NERC 1987 Airborne Campaign Workshop.* 15th Dec 1988, Univ. Southampton, UK. 99-119.

Singh S. M. (1988), 'Atmospheric correction algorithm for ATM data.' *Proc of the NERC 1987 Airborne Campaign Workshop.* 15th Dec, Univ. Southampton, UK. 19-28.

Slim D. and Jones D. (1992), 'The performance of a vented void.' *Wastes Management.* August, 32-33.

Stohr C., Su W. J., Dumontelle P. D. and Griffin R. A. (1987), 'Remote sensing investigations at a hazardous waste landfill.' *Photogram. Eng. and Remote Sensing.* 53:(11), 1555-1563.

Straight L. K. (1983), 'Detecting and mapping buried hazardous waste sites.' *Technical Papers Of The American Congress Of Surveying And Mapping*, Autumn. Publ. ACSM. 563-565.

Tankard J. D. (1987), 'The plight of Loscoe, Derbyshire.' *Wastes Management.* 77:(3), 172-175.

Tankard J. D. (1986), 'The hazards associated with landfill gas production.' *Proc. Energy From Landfill Gas Conf.* 28-31st Oct, Solihull, UK. 60-69.

Titman D. J. (1994), 'Aerial thermography - a cost effective approach to landfill site surveys.' *Polluted and Marginal Land '94. Proc. of third Iternat. Conf. Re-use of Contaminated Land and Landfills.* 269-271.

Titus S. E. (1982), 'Survey and analysis of present or potential environmental impact sites in Woburn, Massachusetts.' *Proc 48th Ann. Meeting Of The American Society Of Photogrammetry.* March 19, Denver, Colorado, USA. 538-549.

Trevett W. J. (1986), *Imaging Radar For Resources Surveys.* Chapman & Hall.

Van Genderen J. L., Van De Griend J. A. and Van Stokkom H. T. C. (1983), 'An operational remote sensing methodology for the detection, inventory and environmental monitoring of waste disposal sites.' *Proc. EARSEL ESA Symp. on Remote Sensing Applications for Environmental Studies.* 26-29th April, Brussels, Belgium. 149-156.

Vass P. A. and Van Genderen J. L. (1978), 'Monitoring environmental pollution by remote sensing.' *International Archives Of Photogrammetry.* 22:(7), 2125-2142.

Watt A. D. (1988), 'Remote sensing of pine beauty moth defoliation.' *Proc. NERC 1986 Airborne Campaign Workshop.* 24th Feb. , Inst. Hydrology, Wallingford, Oxon. 31-36.

Weltman A. (1983), 'The use of aerial infra-red photography for the detection of methane from landfills.' *Ground Engineering.* **16**:(3), 22-23.

Whitelaw J. (1986), 'Mini-plane flies infra-red sorties.' *New Civil Engineer.* **685**, 39-40.

Wolverhampton Borough Council. (1992), *Aerial thermographic survey of landfill sites in Wolverhampton Metropolitan Borough.* Stangers Consultants Limited, Elstree, Herts.

Wruble D. T., Van Ee J. J. and McMillion L. G. (1986), 'Remote sensing methods for waste site subsurface investigations and monitoring.' *Hazardous and Industrial Solid Waste Testing and Disposal - Sixth Volume.*, American Society for Testing and Materials, Philadelphia. 243-253.

Ziloli E., Gomarasca M. A. and Tomasoni R. (1992), 'Application of terrestrial thermography to the detection of waste disposal sites.' *Remote Sensing Of Environment.* **40**, 153-160.

Zimmerman R. E., Goodkind M. E., Parker H. and Wilkey M. (1982), 'Environmental and safety issues of methane production from waste landfills.' *Proc. International Gas Research Conf.* Oct 1981, LA, California. Rockville, MD 1982 Gov. Inst. Inc. 1039-1047.

Appendix A

The Airborne Thematic Mapper

Leaflet supplied by Daedalus Enterprises Inc. in 1994.

Appendix B

Method Statement issued by TBV Stangers for Aerial Thermal Video Surveys and Technical Specifications of the Camera
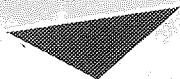
Appendix C

Emissivity

Emissivity is a ratio of a material's ability to emit radiation compared to a blackbody at equivalent temperature. It is defined as:

$$\text{Emissivity} \in (\lambda) = \frac{\text{Radiant emitance from an object at a given temperature}}{\text{Radiant emitance from a black body at a given temperature}}$$

The values of emissivity will be between 0 and 1

Material	Analysis Temperature °C	Emissivit

Aston University

Illustration removed for copyright restrictions
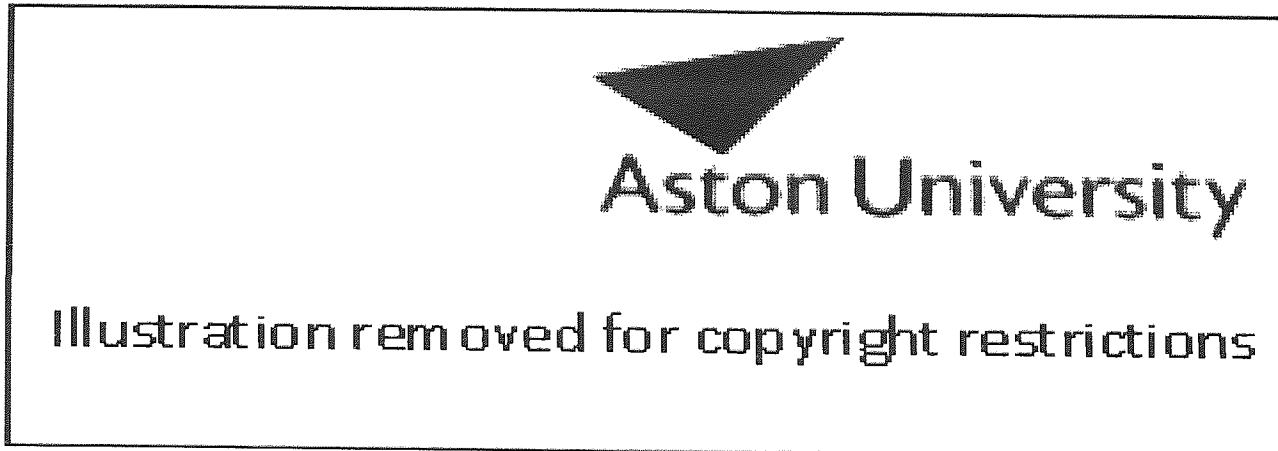
| Highly Polished Gold | 100 | 0.02 |

Table C.1. Emissivity values for a number of different materials (from Lillesand and Keefer (1992). Values measured normal to surface of object over all wavelengths. Emissivities measured at other angles and over discrete wavelength region may vary somewhat).

Appendix D

General Specification of NERC Survey Aircraft G-BBXX

Type	Piper PA31 350 Navajo Chieftan
Seating Capacity	9
Seating Capacity on task	5 maximum
Normal seating capacity on task	4
Oxygen	To all seated positions
Intercom	To 5 seat positions
Cabin size	Width 4ft 2in Height 4ft 3in Length 12ft 6in
Useful Load	2050lbs
Aircraft Power	28 volts x 60 amps
True Airspeed (transit)	150-170 knots
True Airspeed (on task)	100-170 knots
Maximum Authorised Altitude	24000 feet
Endurance (Range)	4 hours (950 nautical miles) approx, plus reserves.

Table D.1. Specifications of the NERC aircraft.

NB: Endurance (Range) varies greatly depending on True Airspeed and Altitude required for task.

Appendix E

Historical Aerial Photography

Tables B.1 and B.2 list the aerial photographs collected for this study.

Date	Type	Scale	Area	No.s	Code
8/9/71	b/w	1:12000	B'ham	015-017	134-71-
Sep '85	b/w	1:5000	B'ham	201,202,263,264	RC8-IB
Apr '87	b/w	1:5000	B'ham	178-180,228,229	RC8-IX
26/7/89	colour	1:12000	B'ham	193,194,	RC8 Kn CF
28/4/91	colour	1:10000	B'ham	112,113	RC8 Kn CU
28/6/92	colour	~1:5000	B'ham	651-654	NERC 92/18(1)

Table E.1. Photographs obtained for the project in the Queslett area.

8/9/71	b/w	1:12000	B. C.	012-021	135-71-	incomplete
2/10/71	b/w	1:12000	B. C.	094,095,214-220	137-71-	incomplete
Sep '85	b/w	1:5000	B. C.	123-126,134-138 240-242,252-256	RC8-HZ	
"	"	"	"	7-10,108-111 129-131,240-245	RC8-IB	
"	"	"	"	53-57,142-148	RC8-IC	
10/4/91	colour	1:10000	B. C.	204-207,195-198	RC8 Kn CT	
28/4/91	colour	1:10000	B. C.	26-28,66-68 70-72,122-124 144-146,182-184	RC8 Kn CU	
16/6/92	colour	~1:5000	B. C.	494-499	NERC 92/18(2)	
26/6/92	colour	~1:5000	B. C.	272-291,292-307 333-350,376-394	NERC 92/18(2)	

Table E.2. Photographs obtained for the project in the Black Country area.

Appendix F

Computer Programs

As mentioned in section 6.2 the ATM imagery had to be corrected for 'scan angle effect'. This was achieved using a combination of two programs written exclusively for the task.

The first program (TOTAL) calculated the mean pixel value in each of the 716 columns of ATM data. The data has to be in binary (1 byte per pixel) format, the 'housekeeping' data should be removed and the number of rows of data in the file must be known. The output file consists with 716 consecutive number in ascii format. This file has to be read into Cricket Graph and displayed as a graph. The resultant graph needs a second order polynomial line-of-best-fit superimposed on it and the three terms (x^2, x and constant) should be noted.

The second program (ADJUST) applies a correction factor to the original image. This is achieved by calculating the difference between the line-of-best-fit and a horizontal straight line which represents the desired trace of an unaffected line. The desired straight line crosses the vertical axis at the same point as the line-of-best-fit. The adjustment is applied as on equation f.1.

$$\text{adjusted value of pixel at column x} = \text{old value of pixel at column x} * \left[\frac{\text{constant}}{ax^2 + bx + \text{constant}} \right] \qquad \text{(eq. f.1)}$$

a = Second order component

b = First order component

Each of the programs can be altered to recieve images of varying sizes by manipulating variables. Both of the programs were written by the author and Tom Charnock, a fellow research student in the Civil Engineering Department st Aston.

TOTAL.PAS

```pascal
program Reader;



const
  WIDTH = 716;

type
  TotalArray = array[1..WIDTH] of longint;
  TotalArrayReal = array[1..WIDTH] of real;


var
  input: file of byte;
  output: text;
  FileName1, FileName2: string[20];
  NextNumber: byte;
  AvRunningTotals: TotalArrayReal;
  RunningTotals: TotalArray;
  column, row: integer;
  depth: integer;

  Begin



  writeln ('enter the number of rows');
  readln (depth);

  writeln ('enter the input file name');
  readln (Filename1);
  writeln ('enter the output file name');
  readln (Filename2);

  assign (input,FileName1);
  reset (input);
  assign (output,FileName2);
  rewrite (output);

  for column: = 1 to WIDTH do
    begin
      RunningTotals[column] := 0;
    end;

  for row: = 1 to depth do
    begin
    writeln ('row ', row);
    for column: = 1 to WIDTH do
      begin
      read (input,NextNumber);
      RunningTotals[column]:= RunningTotals[column] + NextNumber;
      end;
    end;

  for column: = 1 to WIDTH do
    begin
```

```pascal
    AvRunningTotals[column]:= (RunningTotals[column] / depth);
    end;

  for column: = 1 to WIDTH do
    begin
    writeln (output,AvRunningTotals[column]);
    end;

  close (input);
  close (output);
  Writeln ('End of program.');
end.
```

ADJUST.PAS

```pascal
program Reader;

const
  WIDTH = 716;

type
  realarray = array[1..WIDTH] of real;
  fileint = file of byte;

var
  input, output: fileint;
  FileName1, FileName2: string[20];
  NextNumber: byte;
  NewNumberInt: byte;
  NewNumberReal: real;
  column, row, Calc: longint;
  depth: integer;
  Secondx, Firstx: real;
  Constant: real;
  Maincalc: realarray;


Begin

  writeln ('enter the number of rows');
  readln (depth);

  writeln ('enter the input file name');
  readln (Filename1);
  writeln ('enter the output file name');
  readln (Filename2);

  writeln ('enter second order correction');
  readln (Secondx);
  writeln ('enter first order correction');
  readln (Firstx);
  writeln ('enter constant');
  readln (Constant);
```

```pascal
assign (input,FileName1);
reset (input);
assign (output,FileName2);
rewrite (output);

for Calc: =1 to WIDTH do
  begin
  Maincalc[Calc]: = Constant/((Secondx * (Calc * Calc)) + (Firstx * Calc) + Constant)
  end;

for row: = 1 to depth do
  begin
  writeln('row ', row);
  for column: = 1 to WIDTH do
    begin
    read (input,NextNumber);
    NewNumberReal: = NextNumber * Maincalc[column];
    NewNumberInt: = round(NewNumberReal);
    write (output,NewNumberInt);
    end;
  end;

close (input);
close (output);
Writeln ('End of program.');
end .
```

Appendix G

Waste quantities deposited at site D. All values in tonnes.

Date	waste type								Total
	domestic	incinerator ash	industrial	Notifiables	Scrap rubber	compacted	foundry sand	difficult	
Sep-86	10876	1690	19797	-----	-----	1928	668	-----	34959
Oct-86	8487	1600	14433	-----	279	2518	578	-----	27895
Nov-86	9245	1330	13510	321	408	2859	630	-----	28303
Dec-86	10052	1420	14372	886	308	3173	885	-----	31096
1986	38660	6040	62112	1207	995	10478	2761	0	122253
Jan-87	7819	1380	10773	1587	383	2243	830	-----	25015
Feb-87	7845	1360	15412	813	380	2844	938	-----	29592
Mar-87	10553	1631	17785	1773	533	3262	1148	-----	36685
Apr-87	13483	200	14298	1362	313	2857	810	-----	33323
May-87	11401	930	14244	1589	467	2587	690	-----	31908
Jun-87	16936	1870	17522	2155	53	3255	1050	-----	42841
Jul-87	14072	1160	15351	1469	19	2577	450	-----	35098
Aug-87	12760	1640	13268	1661	-----	2605	345	-----	32279
Sep-87	15540	1940	16809	2850	10	3476	270	-----	40895
Oct-87	11432	1340	11992	11665	-----	2470	135	-----	39034
Nov-87	12970	1340	9345	3312	-----	2983	180	-----	30130
Dec-87	14150	1610	8050	2995	-----	3212	272	-----	30289
1987	148961	16401	164849	33231	2158	34371	7118	0	407089
1988	No full monthly details on 1988								
1988	172800	25200	108900	26800	0	34300	0	9500	377500
Jan-89	17231	1700	21003	570	1377	2827	-----	-----	44708
Feb-89	12489	1360	17599	263	1509	2389	-----	-----	35609
Mar-89	11829	650	20694	138	1078	2189	-----	-----	36578
Apr-89	17253	1510	24721	264	1696	3027	-----	-----	48471
May-89	13537	1580	24383	68	259	1991	-----	-----	41818
Jun-89	13441	1700	22702	-----	-----	1640	-----	-----	39483
Jul-89	17140	2080	22060	-----	35	1883	-----	-----	43198
Aug-89	11179	1430	16994	-----	-----	1654	-----	-----	31257
Sep-89	5558	1690	15089	-----	-----	1379	-----	-----	23716
Oct-89	4983	2190	13149	-----	175	756	-----	-----	21253
Nov-89	6831	1720	11572	-----	-----	903	-----	-----	21026
Dec-89	4020	1660	10524	-----	-----	754	-----	-----	16958
1989	135491	19270	220490	1303	6129	21392	0	0	404075

Jan-90	810	2040	11805	-----	-----	438	-----	-----	15093
Feb-90	2	1540	968	-----	-----	74	-----	-----	2584
Mar-90	5	1770	3134	-----	-----	-----	-----	-----	4909
Apr-90	25	1050	3392	-----	-----	-----	-----	-----	4467
May-90	20	80	2068	-----	-----	-----	-----	-----	2168
1990	862	6480	21367	0	0	512	0	0	29221

	complete waste quantities								Total
	domestic	incinerator ash	industrial	Notifiables	Scrap rubber	compacted	foundry sand	difficult	
quantity	496774	73391	577718	62541	9282	101053	9879	9500	1340138
percentage of total	37.0689	5.476376	43.10884	4.666758	0.693	7.5404921	0.73716	0.709	100

Appendix H

Spike Test Values and F and *t* test Procedures

These are the values of the spike tests taken on April 18th 1994, ten days after the dawn ATM flight. Values for the gasses are percentages and fill depth is in metres.

Location spike no.	Location m from South	pixel value	Methane	CO2	Oxygen	fill depth	cover type
North South transect starting from south							
April 18th 1994 Bright, mild, light cloud.							
1	0	67	0	0	21	0	road/gravel
2	15	68	0.025	0	21	5	grassy
3	20	67	0.075	0	21	9	grassy
4	25	73	0.025	0	21	13	grassy
5	30	67	trace	0	21	15	grassy
6	35	70	0.025	0	21	18	grassy
7	40	75	0.025	0	21	20	mossy/stoney
8	45	72	0	0	21	21	grassy
9	50	69	trace	0	21	22	clay mound
10	55	72	0	0	21	22	grass
11	60	68	0	0	21	22	clay mound
12	65	62	0	0	21	23	clay mound
13	68	74	0.025	0	21	23	mossy/stoney
14	71	75	0.025	0	21	22	moss
15	74	76	trace	0	21	23	grass
16	77	73	0.1	0	21	23	grass
17	80	73	0.125	0	21	24	grass
18	83	69	trace	0	21	23	grass
19	86	72	0.075	trace	21	23	grass
20	89	75	0.025	0	20	24	grass
21	92	74	0.05	trace	17	24	mossy/stoney
22	95	77	0.05	0	20	25	grass
23	98	75	0.05	0	21	25	mossy/stoney
24	101	75	0.075	trace	19	26	grass
25	104	75	0	0	21	26	grass
26	107	73	0.025	0	20	26	grass
27	110	78	1	0	21	27	wet mossy bare patch, some stones
28	113	77	0.1	0	20	27	clay/clover damp
29	116	72	trace	0	21	28	grass
30	119	77	0	0	21	28	moss
31	122	68	0	0	21	29	grass/clay
32	126	63	0	0	21	30	clay mound
33	129	68	trace	0	21	30	clay mound
34	135	71	1.5	0	20	30	black soil? damp
35	137	70	2.5	0	21	30	stoney/bare
36	140	70	0.8	0	21	31	stoney/bare
37	143	64	0.5	0	21	32	stoney/bare light moss
38	146	69	0.9	trace	21	32	edge of grassy area
39	149	70	14	2	20	32	grass
40	152	67	10	2	18	32	grass
41	155	71	20	1	19	33	bare tarmac scalpings
42	158	71	12	trace	20	34	moss/grass
43	161	73	2.5	0	21	35	moss/stoney
44	164	73	16	0	21	36	moss
45	167	71	8	0	20	37	moss/grass
46	170	71	2.2	trace	20	37	grass

47	173	77	1	0	21	36	grass/some moss
48	176	73	6	0	21	35	grass/some moss
49	179	72	0.3	0	21	34	grass/some moss
50	182	69	1.1	0	21	32	grass/some moss
51	185	70	1.1	0	20	31	grass
52	188	71	0.6	0	19	29	grass
53	191	67	1.4	0	20	28	grass/some moss
54	194	69	12	0	19	26	grass/bare
55	196	70	5	0	20	25	bare
56	199	71	0.35	0	21	23	grass/some moss
57	202	66	2.5	0	21	22	bare/stoney
58	205	67	0.05	0	20	20	grass/clover
59	208	67	2	0	20	21	moss/bare
60	211	75	10	0	20	22	grass/moss
61	214	69	0.7	0	21	22	grass/moss
62	217	68	0	0	21	23	bare
63	220	69	0.125	0	21	23	bare/stoney
64	223	69	0.325	0	20	21	bare/stoney
65	226	71	0.05	0	21	18	grass/moss/bare
66	229	71	0.0375	0	21	16	grass
67	232	67	trace	0	21	13	grass
68	235	72	0.025	0	21	10	grass
69	238	72	0.275	0	21	8	grass
70	241	74	2	0	20	7	grass
71	244	76	2.5	0	20	4	grass
72	247	84	0.325	0	19	2	grass
73	250	67	0.9	0	20	2	grass
74	253	67	20	20	-	1	weathered rock- quarry edge

East West transect starting from East							
Location spike no.	Location m from east		Methane	CO2	Oxygen		cover type
1	0	79	2.5	5	18	2	grass
2	3	68	0.05	0	21	4	grass
3	6	65	0.025	0	21	5	grass
4	9	65	0.1	0	21	7	grass
5	12	65	1.3	0	21	8	grass
6	15	71	6	trace	21	10	light grass
7	18	71	0.0375	0	21	13	moss/stones
8	21	74	0.0125	0	21	16	moss/stones
9	24	69	0.025	0	21	18	grass
10	30	99	0	0	21	21	clay mound
11	33	65	trace	0	21	22	clay mound
12	36	68	0.4	0	19.5	23	grass
13	39	67	0.175	0	21	22	grass
14	42	63	0	0	21	22	grass
15	45	63	0.0375	0	21	21	grass
16	48	66	0.05	0	21	21	grass
17	51	66	10	0	20	21	grass
18	55	66	0	0	21	24	clay mound
19	59	67	10	0	20	25	base of clay mound
20	62	70	42	trace	18.5	28	grass
21	65	63	22	1	20	29	grass
22	68	65	30	2	18.5	29	grass
23	71	61	20	1.5	20	30	grass
24	74	62	34	4	17	30	grass
25	77	62	14	1.5	16.5	30	grass
26	80	65	24	5	15	30	grass
27	83	71	40	6	-	31	grass
28	86	67	0.2	0	21	31	grass
29	89	65	7	trace	19.5	31	grass
30	92	67	11	2	19.5	31	grass

31	95	65	0.325	0	21	31	grass
32	98	67	15	8	16	31	grass
33	101	65	40	12	10	31	grass
34	104	64	57	20	2	31	grass near daffodils
35	107	64	20	2	19.5	30	grass
36	110	70	6	0.5	21	30	grass near bush
37	113	69	0	0	21	30	grass
38	116	70	0.025	trace	21	29	grass
39	123	73	0.025	0	21	28	clay mound
40	130	61	3.5	0	20	29	gravel
41	133	63	2.3	trace	12	29	gravel/grass
42	136	70	2.25	0	21	30	gravel/moss
43	139	65	13	0	19.5	31	gravel/grass
44	142	69	3.1	0	21	32	gravel/moss
45	145	69	3.75	0	21	34	gravel/moss
46	148	70	0.7	0	21	36	gravel/grass
47	151	71	28	0.5	15	36	gravel/grass
48	154	71	6	0	21	36	gravel/grass
49	157	72	1	0	21	36	gravel/grass/moss
50	160	73	6	trace	20	36	grass
51	163	73	0.425	0	21	36	gravel
52	166	75	-	-	-	37	waterlogged
53	169	72	-	-	-	37	waterlogged
54	171	71	10	0	21	37	lush grass
55	174	65	16	3	18	37	grass
56	177	72	5	0.5	20	37	grass
57	180	67	0.05	0	21	37	grass
58	183	68	16	1	17	36	grass
59	186	69	0	0	21	36	gravel/grass
60	189	72	5	0	18.5	36	gravel/grass
61	192	89	0.35	0	21	36	short grass
62	195	73	0.075	0	21	36	grass
63	198	68	0.1	0	21	35	grass
64	201	70	0.15	0	21	36	short grass
65	204	71	0.2	0	21	35	grass/moss
66	207	72	1.5	0	21	34	moss/grass/gravel
67	210	69	0.45	0	21	34	moss/gravel
68	213	67	2.6	trace	19	33	grass
69	216	69	11	0	21	33	moss/gravel
70	220	63	1.25	0	21	33	clay mound
71	224	59	40	3	15	32	grass- wet ground
72	227	74	24	0.5	18	32	grass- wet ground
73	230	77	0	0	21	32	grass- wet ground next to clay mound
74	235	74	0	0	21	31	clay mound
75	240	65	6	0	21	30	clay/grass at base of mound
76	243	71	22	0	20	29	gravel/grass
77	246	70	2.5	0	20.5	29	grass/moss
78	249	70	0.025	0	21	28	grass
79	252	70	0.05	0	21	26	grass
80	255	69	trace	0	21	26	grass
81	258	71	0.025	0	21	24	grass
82	261	69	0.125	0	21	23	grass
83	263	70	0.025	0	21	22	grass/nettles/bushes
84	266	69	0.25	trace	21	21	grass/nettles/bushes
85	269	68	6	0.5	20	20	grass/nettles/bushes
86	272	67	18	0	19.5	18	grass/bushes
87	275	68	0.45	0	19	17	grass/moss
88	278	68	6	0	20.5	16	grass/bushes
89	281	72	0.05	0	21	15	grass/bushes
90	284	71	0.075	0	21	15	grass/bushes
91	287	71	0.05	0	21	13	grass/bushes
92	290	69	0.175	35	18	13	grass

93	293	69	0.8	0	21	13	grass
94	296	70	0.05	0	21	12	grass
95	299	69	trace	0	21	12	grass
96	304	93	0	0	21	11	clay mound
97	308	77	1.9	0	21	10	short grass
98	311	74	10	0	20.5	8	grass/gravel
99	314	73	6	0	20	7	grass
100	317	81	6	0	21	6	grass
101	320	75	1.5	0	20	4	grass
102	323	69	0.025	0	21	3	grass/bushes
103	326	71	0	0	21	2	grass/bushes
104	329	70	0	0	21	1	grass/bushes/rubble
105	332	69	0.0375	trace	21	0	grass
106	335	67	0.05	trace	21	0	grass
107	338	65	0	0	21	0	grass/brambles

The procedures for both the F and t tests were taken form Kennedy & Neville (1986).

F test

Two sets of samples from sources A and B with standard deviations s_A and s_B and number of samples n_A and n_B.

$$F = \left(\frac{s_A}{s_B}\right)^2 \qquad \text{(eq. G.1)}$$

degrees of freedom v_A and v_B defined as:

$$v_A = n_A - 1 \qquad \text{(eq. G.2)}$$

$$v_B = n_B - 1 \qquad \text{(eq. G.3)}$$

The value of F is then compared to a look-up table using the degrees of freedom.

t test

Two sets of samples from sources A and B with means x_A and x_B standard deviations s_A and s_B and number of samples n_A and n_B.

Initially we need the pooled estimate of variance s_c:

$$s_c = \frac{(n_A - 1) s_A^2 + (n_B - 1) s_B^2}{(n_A - 1) + (n_B - 1)} \qquad \text{(eq. G.4)}$$

then the calculation of t:

$$t = \frac{|x_A + x_B|}{S_c\sqrt{\dfrac{1}{n_A} + \dfrac{1}{n_B}}}$$

(eq. G.5)

and the number of degrees of freedom:

$$v = n_A + n_B - 2$$

for the values of pixel value from the thermal ATM to the corresponding methane concentration measured in the spike tests. The methane concentrations were split into two groups: significant methane values ($\geq 0.1\%$ v/v) and non-significant methane values ($< 0.1\%$ v/v) with the corresponding pixel values.

The mean and standard deviations were calculated for each group (table G.1) and then processed to find the F and t values (tables G.2 and G.3).

	mean	s.d.	no.
<0.1%CH4	70.87323944	5.598289477	71
>0.1%CH4	69.59259259	4.626290246	108

Table G.1.

F =	1.464350197
v1 =	70
v2 =	107

Table G.2.

For the calculated F value (table G.2) the differences in the standard deviations are significant at the 5% confidence level.

Sc =	5.033185482
t =	1.665332605
degrees of freedom	177

Table G.3.

For the calculated t statistic (table G.3) with 177 degrees of freedom pixel values are not significant at the 5% confidence level but would be at the 10% confidence level.

A second process using the same procedures was undertaken but this time taking the groups of grassed and not grassed and using the corresponding pixel values.

The mean ans standard deviations were first ascertained (table G.4) and then the F and *t* values were determined (tables G.5 and G.6)

	mean	s.d.	number
no grass	70.62711864	6.1529312	59
grass	69.84166667	4.4286991	120

Table G.4.

F =	1.93024207
v1 =	58
v2 =	119

Table G.5.

For the calculated F value (table G.5) the differences in the standard deviations are significant at the 1% confidence level.

S_c =	5.058856013
t =	0.976466688
degrees of freedom	177

Table G.6.

For the calculated *t* statistic (table G.6) with 177 degrees of freedom pixel values are not significant at the 5% confidence level or even the 10% confidence level.